

Multivalent Functionalized Dextran- Antibody Conjugates for Efficient Tumor Cell Killing



TECHNISCHE
UNIVERSITÄT
DARMSTADT

**Vom Fachbereich Chemie
der Technischen Universität Darmstadt**

zur Erlangung des Grades
Doctor rerum naturalium
(Dr. rer. nat)

Dissertation

von

Hendrik Peter Günter Schneider M.Sc.
aus Darmstadt

Erstgutachter: Prof. Dr. Harald Kolmar
Zweitgutachterin: Prof. Dr. Katja Schmitz

Darmstadt 2020

Schneider, Hendrik Peter Günter: Multivalent Functionalized Dextran-Antibody Conjugates for Efficient Tumor Cell Killing

Darmstadt, Technische Universität Darmstadt

Jahr der Veröffentlichung der Dissertation auf TUpriints: 2020

URN: urn:nbn:de:tuda-tuprints-115020

URL: <https://tuprints.ulb.tu-darmstadt.de/id/eprint/11502>

Tag der Einreichung: 06. Dezember 2019

Tag der mündlichen Prüfung: 10. Februar 2020

Veröffentlicht unter CC BY-NC-ND 4.0 International

<https://creativecommons.org/licenses/>

Die vorliegende Arbeit wurde unter der Leitung von Herrn Prof. Dr. Harald Kolmar am Clemens-Schöpf-Institut für Organische Chemie und Biochemie der Technischen Universität Darmstadt von Januar 2016 bis Dezember 2019 angefertigt.

Publications derived from this work

Research Articles

H. Schneider, L. Deweid, T. Pirzer, D. Yanakieva, S. Englert, B. Becker, O. Avrutina, H. Kolmar, Dextramabs: A Novel Format of Antibody-Drug Conjugates Featuring a Multivalent Polysaccharide Scaffold, *ChemistryOpen*, 8 (2019) 354-357.

H. Schneider, D. Yanakieva, A. Macarrón, L. Deweid, B. Becker, S. Englert, O. Avrutina, H. Kolmar, TRAIL-inspired multivalent dextran conjugates efficiently induce apoptosis upon DR5 receptor clustering, *ChemBioChem*, 20 (2019), 3006-3012. (Marked as Very Important Paper, Front Cover December, Issue 24) <https://doi.org/10.1002/cbic.201900251>; <https://doi.org/10.1002/cbic.201900702> (Cover Picture)

L. Deweid, L. Neureiter, S. Englert, **H. Schneider**, J. Deweid, D. Yanakieva, J. Sturm, S. Bitsch, A. Christmann, O. Avrutina, H.-L. Fuchsbauer, H. Kolmar, Directed Evolution of a Bond-Forming Enzyme: Ultrahigh-Throughput Screening of Microbial Transglutaminase Using Yeast Surface Display, *Chemistry – A European Journal*, 24 (2018) 15195-15200.

M. Baalman,* L. Neises,* S. Bitsch, **H. Schneider**, L. Deweid, N. Ilkenhans, M. Wolfring, M. J. Ziegler, P. Werther, J. Wilhelm, H. Kolmar and Richard Wombacher, A bioorthogonal click chemistry toolbox for targeted synthesis of branched and well-defined protein-protein conjugates, *Angewandte Chemie International Edition* (under review, chemRxiv. Preprint. <https://doi.org/10.26434/chemrxiv.10743344.v1>)

Review Articles

H. Schneider*, L. Deweid*, O. Avrutina and H. Kolmar, Recent progress in transglutaminase-mediated assembly of antibody-drug conjugates, *Analytical Biochemistry*, 595 (2020), 113615. <https://doi.org/10.1016/j.ab.2020.113615>

*These authors contributed equally to this work

Contributions to Conferences

Poster

H. Schneider, L. Deweid, L. Oberstraß, E. Wiegmann, O. Avrutina, H. Kolmar, Bioconjugation of antibodies and therapeutically relevant payloads on a scaffold of dextran polysaccharide (Version I). *Chemical Biology 2016, Heidelberg, Germany* (31.08-03.09.2016)

H. Schneider, L. Deweid, L. Oberstraß, E. Wiegmann, O. Avrutina, H. Kolmar, Bioconjugation of antibodies and therapeutically relevant payloads on a scaffold of dextran polysaccharide (Version I). *34th European Peptide Symposium 2016, Leipzig, Germany* (04.-09.09.2016)

H. Schneider, L. Deweid, B. Becker, S. Englert, A. Ebenig, D. Yanakieva, O. Avrutina, H. Kolmar, Bioconjugation of antibodies and therapeutically relevant payloads on a scaffold of dextran polysaccharide (Version II). *GDCh-Wissenschaftsforum Chemie 2017 – Jubiläumskongress "GDCh - 150*

Jahre, Berlin, Deutschland (10.-14.09.2017) **Poster awarded by Angewandte Chemie (Molecules of Life - Molecules in Life)**

H. Schneider, L. Deweid, B. Becker, S. Englert, A. Ebenig, D. Yanakieva, O. Avrutina, H. Kolmar, Bioconjugation of antibodies and therapeutically relevant payloads on a scaffold of dextran polysaccharide (Version II). *PEGS Europe: Protein & Antibody Engineering Summit*, Lissabon, Portugal (13.-17.11.2017)

H. Schneider, L. Deweid, A. Macarron, D. Yanakieva, S. Englert, B. Becker, O. Avrutina and H. Kolmar, Dextran as multivalence-promoting scaffold for the generation of hydrophilic high-DAR antibody-drug conjugates. *CPS 2019: 8th Chemical Protein Synthesis Meeting 2019*, Berlin, Deutschland (16.-19.06.2019) **Poster awarded by Angewandte Chemie**

Table of Content

Publications derived from this work	i
Contributions to Conferences	i
Table of Content	iii
Zusammenfassung und wissenschaftlicher Erkenntnisgewinn	iv
Scientific Novelty and Significance	viii
Individuelle Beiträge zum kumulativen Teil der Dissertation	xii
1.Introduction	1
1.1. Cancer Treatment – A Brief Introduction	1
1.2. From Innate to Adaptive Immunity	3
1.3. Antibodies	6
1.3.1. Structure and Function	6
1.4. Antibody-Drug Conjugates (ADCs)	8
1.4.1. Mechanism of Action of ADCs	8
1.4.1. ADCs: A Brief History	9
1.4.2. The Three Pillars of an ADC	11
1.4.3. Site-Specific ADCs	13
1.4.4. Transglutaminase	15
1.4.5. ADCs Assembled under mTG Catalysis	16
1.5. High-DAR ADCs	18
1.6. Dextran	22
1.7. Multivalent Binding and Death Receptor 5 Clustering	27
2.Objective	31
3.References	33
4.Cumulative Section	45
4.1. Dexamabs: A Novel Format of Antibody-Drug Conjugates Featuring a Multivalent Polysaccharide Scaffold	45
4.2. TRAIL-inspired Multivalent Dextran Conjugates Efficiently Induce Apoptosis upon DR5 Receptor Clustering	81
4.3. Recent Progress in Transglutaminase-mediated Assembly of Antibody-Drug Conjugates.	111
5.Additional Results	125
6.Danksagung	128
7.Affirmations	131

Zusammenfassung und wissenschaftlicher Erkenntnisgewinn

Trotz massiven medizinischen Fortschritts und ausgiebigen Untersuchungen in der Krebsforschung repräsentieren maligne Tumore immer noch eines der größten globalen Gesundheitsprobleme. Daher liegt das Auslösen der Apoptose von Tumorzellen seit Jahren im Fokus der Forschung. Neben den klassischen Ansätzen, wie Operationen, Strahlen- und Radiotherapie, sowie Chemotherapie wurden neue Methoden zur Behandlung von Krebs entwickelt. Hierzu zählt das Konzept der zielgerichteten Therapie, für das monoklonale Antikörper ein prominentes Beispiel darstellen. Eine zusätzliche Komponente dieses Ansatzes stellen Antikörper-Wirkstoff-Konjugate (ADCs) dar, die dem von Paul Ehrlich geprägten Konzept der „Zauberkegel“ entsprechen. Diese Klasse von Verbindungen zielen auf den ortsspezifischen Transport und die Abgabe eines Zytostatikums an Zielzellen ab, die tumorspezifische Antigene exprimieren. Diese Konstrukte kombinieren die Bindungseigenschaften eines Antikörpers mit der Toxizität eines Zytostatikums und wurden in zahlreichen Ansätzen für die Krebstherapie eingesetzt. So wurden bis heute sechs ADCs kommerziell vermarktet und über 60 werden aktuell in klinischen Studien untersucht. Trotzdem besteht weiterhin ein gewisses Verbesserungspotential dieser potenten Verbindungen hinsichtlich ihrer Toxizität, Effizienz und pharmakokinetischen Eigenschaften.

Die erste Untersuchung im Rahmen der hier vorliegenden, kumulativen Dissertation fokussierte sich auf die Generierung von ADCs, die ein hohes Wirkstoff-zu-Antikörper Verhältnis (DAR) aufweisen und deren Hydrophilie durch Anfügen von Zytotoxinen nicht beeinträchtigt wird. Da lediglich ein geringer Anteil des verabreichten ADCs tatsächlich die adressierten Zielzellen erreicht, sind entweder hochwirksame oder eine hohe Anzahl weniger potenter Zytotoxine unerlässlich, um die gewünschte Effektivität zu erzielen. In Anbetracht des hydrophoben Charakters der am häufigsten eingesetzten Zytotoxine weisen diese Konjugate jedoch häufig eine niedrige Hydrophilie auf, welche abhängig von der adressierten Konjugationsstelle, der Anzahl und dem Charakter der angewendeten Toxineinheiten ist. Folglich hat die Hydrophobizität der konjugierten Zytostatika einen großen Einfluss auf die Stabilität sowie die pharmakokinetischen Eigenschaften und bestimmt somit die Effizienz des ADCs. So wurde beispielsweise von Problemen bezüglich Aggregation, Erkennung durch *multidrug resistance* (MDR) Rezeptoren und erhöhter *Clearance* berichtet.

In dieser Arbeit sollten diese Probleme durch das Design einer neuen Klasse von Hybrid-ADCs gelöst werden, die die Hydrophobizität der im Kontext von ADCs weithin genutzten Zytostatika mindern oder sogar gänzlich kompensieren kann und zusätzlich die Möglichkeit eröffnet, eine gewünschte Menge dieser potenten Toxine pro Antikörper zur Verfügung zu stellen. Zusätzlich sollte eine zukünftige Beladung mit weniger wirksamen und folglich weniger schädlichen Toxinen ermöglicht werden, bei denen die reduzierte Toxizität durch eine erhöhte Kopienzahl kompensiert wird.

Dextran, ein von der FDA zugelassenes Polysaccharid, das aus α -1,6-verknüpften Oligoglucoseinheiten besteht, wurde in dieser Arbeit als modulares, multivalenzgenerierendes Grundgerüst für die ortsspezifische Konjugation an Antikörper und für die Beladung mit einer gewünschten Anzahl an Zytostatika verwendet. Für die Konjugation dieses Glucans an Proteine wurde berichtet, dass sie die Halbwertszeit, die thermische Stabilität sowie die pharmakokinetischen Eigenschaften dieser verbessert und deren Immunogenität verringert. Weiterhin bietet sich die Möglichkeit, chemische Modifikationen an unterschiedlichen Stellen dieses Zuckermoleküls, zur

Einführung orthogonal adressierbarer Gruppen durchzuführen. So kann sowohl eine gewünschte Anzahl an Zytostatika an den Hydroxygruppen der Glukose-Wiederholungseinheiten als auch ein Erkennungsmotiv für die enzymatische Konjugation an ein Protein an das orthogonal adressierbare Aldehyd am reduzierenden Ende angebracht werden. In dieser Arbeit wurde zudem eine Synthesestrategie entwickelt, die es ermöglicht, Dextran, beladen mit einer gewünschten Anzahl orthogonal adressierbarer chemischer Gruppen zur Toxinkonjugation, mittels Enzymkatalyse ortsspezifisch an einen Antikörper zu konjugieren und anschließend mit Toxinen auszustatten. Diese Hybridverbindung ebnete den Weg zur Generierung neuer, vielversprechender hoch hydrophiler ADCs mit hohem Wirkstoff-zu-Antikörper Verhältnis.

Synthetisch wurde hierfür eine reduktive Aminierung mit einem geschützten Diamin am reduzierenden Ende mit einer ortsspezifischen Carboxyethylierung an der C2-Position der Glukose-Wiederholungseinheiten verbunden, woraus ein Dextran mit zwei unterschiedlich adressierbaren reaktiven Gruppen resultierte. Dabei konnte eine gewünschte Anzahl der Carboxygruppen an den Glukose-Wiederholungseinheiten eingestellt werden. Anschließend wurden amintragende Azidlinker unter Bildung von Amidbindungen kovalent an den eingebauten Carboxygruppen der Glukose-Wiederholungseinheiten eingeführt, woraus ein Dextranrückgrat mit multiplen Azid-Funktionalitäten resultierte. Die Demaskierung des geschützten Amins am reduktiven Ende ergab schließlich dual adressierbare Polysaccharidgerüste mit multiplen „click“-baren Gruppen zur Konjugation der Zytostatika und einem primären Amin, mittels dessen eine enzymkatalysierte Konjugation an den Antikörper realisiert werden konnte. Trastuzumab, welcher genetisch mit einer Transglutaminase-Erkennungssequenz versehen wurde, diente hierbei als Modellantikörper. Die Konjugation des azidtragenden Dextrangerüsts an Trastuzumab unter Katalyse von mikrobieller Transglutaminase und die darauffolgende Konjugation eines potenten, sehr hydrophoben Zytoskelettinhibitors (Monomethylauristatin E (MMAE)), bildete ein neues Hybridkonstrukt. So wurde Dextran in dieser Arbeit zum ersten Mal ortsspezifisch an einen Antikörper gekoppelt und sukzessive mit einer gewünschten Anzahl an Zytostatika durch spannungskatalysierte Azid-Alkin-Cycloaddition (SPAAC) beladen. Diese neuen, als *Dextramabs* bezeichneten Hybridkonstrukte erwiesen sich nicht nur als gut löslich in wässrigen Puffern, sondern auch als mindestens ebenso hydrophil wie der nicht modifizierte Trastuzumab, selbst wenn das Polysaccharid mit elf hydrophoben MMAEs beladen wurde. Weiterhin zeigten die generierten Konstrukte unveränderte Bindungseigenschaften und keinen Stabilitätsverlust (Trastuzumab: $K_D = 4.9$ nM, *Dextramab* (DAR 8): $K_D = 5.9$ nM). In Zellviabilitätstests zeigten die entwickelten *Dextramabs* potente, subnanomolare mittlere inhibitorische Konzentration ($IC_{50} = 100$ pM) auf HER2-positiven SK-BR-3 Brustkrebszellen *in vitro*, wohingegen keine Toxizität für HER2-negative Kontrollzellen gefunden wurde. *Dextramabs* stellen eine neue Strategie für die Generierung ortsspezifisch konjugierter hoch-hydrophiler ADCs mit einem hohen DAR dar. Tierstudien werden zeigen, ob diese neue Klasse von ADCs ein vielversprechendes Konzept zur Generierung von ADCs mit hoher Wirksamkeit, geringer Immunogenität und erhöhter *in vivo*-Halbwertszeit repräsentiert.

In der zweiten Untersuchung wurde die Modularität von Dextran als Träger für Apoptose-induzierende Moleküle, die sowohl intrazelluläre als auch Ziele auf der Zelloberfläche adressieren, untersucht. Im Zuge dessen wurde, im Gegensatz zum ersten Ansatz, Dextran als eine Plattform zur Multimerisierung von krebsspezifischen Liganden untersucht. Der extrazellulär exprimierte *Death Receptor 5* (DR5) wurde hierfür als Modellziel gewählt,

welcher durch Aggregation beziehungsweise Multimerisierung aktiviert wird und eine Apoptose-induzierende Signal-Kaskade auslöst (*death-inducing signal cascade*, DISC). In dieser Arbeit wurde Dextran als Grundgerüst mit mehreren peptidischen Liganden (*death receptor 5-targeting peptide*, DR5TP) von DR5 bestückt und im Hinblick auf seine Apoptose-induzierende Wirkung untersucht. Hierbei sollte, im Gegensatz zu der ersten Untersuchung, der Zelltod durch Multimerisierung von Rezeptoren auf der Zelloberfläche induziert werden und nicht durch rezeptorvermittelte, endosomatische Aufnahme eines an den Antikörper gebundenen Zytostatikums. Hierfür wurde Dextran mit 11 respektive 13.4 DR5TP-Liganden beladen und auf seine Apoptose-induzierende Wirkung untersucht. Die resultierenden multivalenten Dextrangerüste zeigten mit zweistellig nanomolaren EC_{50} -Werten (halbmaximalen effektiven Konzentrationen) auf DR5-positiven COLO205-Kolonzellen und Jurkat T-Lymphozyten eine potente Apoptose-induzierende Wirkung *in vitro*. Eine anschließende ortsspezifische Konjugation an Glutamin 295 eines aglykosylierten kristallisierbaren Fragments (*Fragment, crystallizable, Fc*) mittels mikrobieller Transglutaminase resultierte in Protein-Polysaccharid-Konjugaten, die eine selektive DR5-Bindung in durchflusszytometrischer Analyse zeigten und die im Vergleich zu den nicht an ein Protein konjugierten DR5TP-Dextranen sogar niedrigere EC_{50} -Werte aufwiesen ($EC_{50} = 1.9 - 6.7$ nM). Interessanterweise wurde die Bindung dieser Konjugate nicht durch den Antikörper, sondern durch das mit Liganden bestückte Dextran hervorgerufen. Dies ermöglicht die zukünftige Verwendung einer zweiten Bindungseinheit im Hinblick auf bispezifisches Targeting, beispielsweise durch die Konjugation an einen Vollängen Antikörper, wodurch eventuell eine höhere Sicherheit und Effizienz realisiert werden könnte. Weiterhin ermöglichten die hergestellten Konjugate, sowohl solitär als auch gebunden an das Fc-Fragment, durch die erhöhte Flexibilität des Dextranrückgrats die beschriebene distinkte räumliche Anordnung als unumgängliche Voraussetzung für effizientes Induzieren von Apoptose zu kompensieren. Dieser Ansatz untermauert die Modularität von Dextran als Träger für unterschiedlichste Beladungen, die verschiedene Zielstrukturen zur gezielten Auslösung von Apoptose von Tumorzellen adressieren. Zukünftig könnte dieser Ansatz einen Lösungsvorschlag für die berichtete *Off-target* Toxizität von multivalenten hochaffinen proteinischen Bindern, wie TAS266, darstellen, da hierin eine höhere Anzahl an Bindern mit niedriger Affinität verwendet wird. Dies könnte zu einer geringeren Retention auf gesunden Zellen mit geringerer DR5 Expressionsdichte und somit einer höheren Verträglichkeit *in vivo* führen, die zusätzlich durch Einführung von Bispezifität erhöht werden könnte.

Der dritte Teil dieser Arbeit sollte einen detaillierten Überblick über die enzymatische Generierung von ADCs mittels Transglutaminase geben. Trotz zahlreicher Publikation von Reviews zur Generierung von ADCs fehlt bis heute ein Überblick, der die Anwendung von Transglutaminase für diese Therapeutika detailliert beschreibt. Aus diesem Grund gibt der verfasste Review einen Überblick über die an dieser Thematik forschenden Arbeitsgruppen und Firmen, als auch eine gründliche Übersicht der eingesetzten Methoden, der adressierten Konjugationsstellen oder -motive, Linkern und verwendeten Zytostatika. Dieser Review beschreibt und diskutiert zukunftsweisende Syntheserouten und -techniken, die jüngsten Fortschritte sowie verbleibende Einschränkungen der mTG-unterstützten Generierung von ADCs.

Zusätzlich wurde eine weitere Studie durchgeführt, die die Verwendung von Dextran als multivalentes Grundgerüst untermauert. Hierfür wurde eine vorläufige Studie zur Validierung von Dextran als Träger für

multiple chelatierende Komplexbildner, die Ionen für die Radiobildgebung oder -therapie komplexieren können, durchgeführt. Hierfür wurde Dextran mit einer gewünschten Anzahl an 1,4,7,10-Tetraazacyclododecan-1,4,7,10-tetraessigsäure (DOTA) beladen. In einer photometrischen Analyse von komplexierten Cu^{2+} -Ionen konnte gezeigt werden, dass die resultierenden DOTA-Dextrankonjugate 3.2 respektive 5.3 Metallionen pro Polysaccharidgerüst tragen. Zurzeit werden die hergestellten DOTA-Dextrankonjugate in Biodistributionsstudien in Mäusen untersucht. Diese Konzeptstudien werden zeigen, ob diese neuen Konstrukte für *in vivo* Anwendungen geeignet sind und ob eine Konjugation an derzeit verwendete spezielle Bindungsproteine (Affibodies), welche in radioaktiv markierter Form Probleme mit der Hydrophobizität und daher mit Solubilität, Aggregation und Präzipitation haben, vorteilhaft ist. Dieser Ansatz bestärkt die Vermutung, dass Dextran ein vielversprechendes Gerüst für die mehrwertige Befestigung und Anpassung verschiedener Liganden darstellt.

Scientific Novelty and Significance

Despite impressive progress in medical care and extensive investigation in the field of human malignancies, cancer still represents a major global health issue, and triggering apoptosis of tumor cells has been in focus of cancer research for decades. In addition to classical attempts like surgery, radiotherapy, and chemotherapy, a number of novel methodologies have recently fallen in the limelight, with monoclonal antibodies being the most prominent actors at the therapeutic scene. With their introduction, the so-called targeted therapy has finally become achievable for the treatment of malignant tumors. Having evolved from Paul Ehrlich's "Magic Bullet" concept that described directing a toxic compound exclusively to a disease-causing organism, antibody-drug conjugates (ADCs) were developed. This class of compounds is aimed at site-selective delivery of cytotoxic agents to target cells expressing a cancer-related antigen. Combining the targeting properties of an antibody with the killing properties of a potent cytotoxin, these constructs were applied in countless approaches intending to treat tumor patients. To date, six ADCs have been marketed and over 60 ones are currently in clinical trials. However, several issues still require improvement, among them toxicity, efficacy and pharmacokinetics.

The first investigation in the context of the present cumulative study was focused on the generation of highly hydrophilic ADCs characterized by a high drug-to-antibody ratio (DAR). However, since only a limited number of the administered ADCs is reported to actually reach their cellular target, either highly potent toxins or a higher number of the less-potent ones are prerequisites of these compounds to reach efficacy. Considering the hydrophobic character of most commonly applied potent cytotoxins, these conjugates often suffer from poor hydrophilicity depending on the addressed conjugation site as well as the number and character of the applied toxin units. Further, hydrophobicity of ADCs was reported to raise problems due to aggregation and recognizing by multidrug resistance (MDR) transporters, thus the number, site, and hydrophobicity of the conjugated toxin strongly influences stability, pharmacokinetic properties and the efficacy of ADCs. In this work we addressed these issues simultaneously by designing a novel class of hybrid ADCs combining ability to balance and even recompense the hydrophobicity of commonly applied highly hydrophobic cytotoxins with an option for the attachment of multiple payloads, which may further enable the application of less potent, thus less harmful for the healthy tissues, cytotoxins. To that end, we applied dextran, an FDA-approved polysaccharide, consisting mainly of α -1,6-linked oligo-D-glucose units as multivalency-generating modular scaffold for payload attachment. This glucan, reported to enhance half-life, to improve thermal stability and pharmacokinetic properties, and to reduce immunogenicity of conjugated proteins, opens certain space for chemical modifications, namely conjugation of a) a desired number of payloads to the repeating glucose units at the respective hydroxy groups, and b) at the reducing end that comprises an orthogonally addressable aldehyde. In this work, a strategy to combine an enzyme-catalyzed site-specific conjugation of the dextran scaffold, equipped with multiple reactive moieties for payload loading, to antibodies was developed, resulting in promising constructs for the generation of high-DAR ADCs.

Synthetically, a combination of reductive amination of dextran's reducing end with a protected diamine followed by site-selective carboxyethylation at the C2-position of the glucose repeating units led to dextran bearing dually

addressable reactive moieties. Notably, our synthetic procedure allowed adjustment of the number of addressable sites at the repeating glucose monomers for toxin conjugation to the desired amount of copies. Subsequent conjugation of azide-bearing aliphatic amines at the repeating units upon amidation gave a scaffold comprising multiply addressable “click” sites. Demasking of the protected amine at the reducing end yielded a multivalent scaffold combining multiple and solitaire orthogonal addressable sites. Thus, at its amine site it could be easily conjugated to the protein of interest – in this particular case, to the therapeutic antibody trastuzumab – *via* enzymatic catalysis by microbial transglutaminase (mTG). For this purpose, trastuzumab was engineered to possess an adequate mTG recognition motif at the C-terminus of the heavy chain. The azides at the sugar monomers remained for the decoration with monomethyl auristatin E (MMAE) – a highly toxic and extraordinary hydrophobic compound. To conclude, for the first-time dextran was site-specifically conjugated to a functional antibody *via* its reducing end, leaving the polysaccharide backbone intact and subsequently equipped with multiple MMAEs by strain-promoted azide-alkyne cycloaddition (SPAAC) in a desired number of copies without corrupting the polysaccharide backbone. These hybrid constructs, called *dextramabs*, were found not only readily soluble in aqueous buffers, but at least as hydrophilic as the parental antibody trastuzumab, even when conjugated with eleven highly hydrophobic MMAE counterparts.

The binding properties of all generated constructs were not affected, as demonstrated by comparable K_D values on HER2-positive SK-BR-3 cells (unmodified trastuzumab: $K_D = 4.9$ nM, dextramab (DAR 8): $K_D = 5.9$ nM). Our synthetic dextramabs showed potent subnanomolar cytotoxicity ($IC_{50} = 100$ pM) in cell proliferation assays on HER2-positive SK-BR-3 breast cancer cells and no cytotoxicity on HER2-negative control cells *in vitro*. These site-specifically assembled ADCs may combine the beneficial pharmacokinetic properties, as their protein counterparts are loaded with dextran, therefore possess higher hydrodynamic radius, with the possibility to attach a tailored number of payloads. Generally, our concept represents a promising approach for the generation of highly hydrophilic site-specific ADCs characterized by a high DAR. Follow-up animal studies will unveil if dextramabs hold promise for the novel class of ADCs with high potency, low immunogenicity and enhanced *in vivo* half-life.

In the second investigation we studied applicability of dextran polysaccharide scaffold as carrier for apoptosis-triggering payloads of diverse nature, which act by addressing distinct intra- or extracellular targets. Hence, additionally to the above-mentioned high-DAR ADCs we were focused at validating dextran as a platform for multimerization of cancer-relevant ligands.

First, death receptor 5 (DR5) was chosen as a model target expressed on the cell surface. As it is activated by oligomerization/aggregation, we aimed at constructing a flexible scaffold able to bypass the reported need for spatial ligand orientation for efficient DR5-mediated cellular cytotoxicity. Thus, we designed a molecular architecture comprising a polysaccharide scaffold carrying the desired number of DR5 peptidic binders able to efficiently trigger apoptosis upon DR5 receptor clustering. Herein, apoptosis of cancer cells was mediated by multivalent binding to and clustering of a receptor located on the cell surface, which is in fact contrary to the first approach investigated in this work, which relied on a high number of a very potent cytotoxin that only upon internalization inhibits cell division by blocking the polymerization of tubulin. Thus, dextran was loaded with on average 11 or 13.4 peptidic binders, namely death receptor 5 targeting peptides (DR5TP). The resulting

constructs were found potent apoptosis-inducing conjugates possessing double-digit nanomolar half-maximal effective concentration (EC_{50}) values on DR5-positive COLO205 colon cells and Jurkat T lymphocytes *in vitro*. Moreover, conjugation to glutamine 295 of an aglycosylated fragment crystallizable (Fc) fragment of a monoclonal antibody (mAb) by site-specific mTG-catalyzed conjugation resulted in constructs that showed selective DR5 binding upon flow cytometric analysis and further did not impair the potency of the generated multivalent scaffolds. In contrast, these protein-polysaccharide-peptide hybrids demonstrated higher potency *in vitro* (EC_{50} = 1.9 - 6.7 nM).

Notably, in this approach binding is not mediated by the protein, but rather by the ligand-bearing dextran counterpart. Thus, addition of a second targeting moiety, e.g. application of a full-length antibody, would be an interesting prospective study that opens the possibility of bispecific targeting, which may result in enhanced safety and efficacy. Furthermore, the generated DR5TP-dextran and the Fc-bound counterparts were able to circumvent the mentioned need for spatial orientation of ligands due to additional flexibility provided by dextran scaffold. Our study further underlines the modularity of dextran as carrier for different payloads addressing various targets. In addition, this approach may help overcoming the reported off-target toxicity for multimeric high-affinity protein-based constructs, e.g. TAS266, by the application of low-affinity peptidic binders. This may lead to better tolerability *in vivo*, conditioned by lower retention on healthy cells expressing minor levels of DR5, which might be additionally improved by prospective bispecific targeting.

The third part of this work was aimed at relieving the current lack of satisfactory overviews on mTG-mediated generation of homogeneous ADCs. Since most reviews dealing with ADCs cover a broad scope of topics, but usually very briefly, an in-depth comparative survey was highly required. However, a detailed overview of the factors influencing the resulting architectures in view of stability, potency, efficiency, etc. was still missing. A comprehensive summary of the reported strategies may enable tailoring of existing methods for mTG-promoted conjugation to the needs of particular research projects. On these grounds, the originated review was intended not only to enumerate the applied approaches for site-specific conjugation with respect to ADC assembly, but to map out the research groups and companies working on mTG-mediated generation of antibody-drug conjugates. Our review, gives a thorough overview of conjugation methodologies, addressed conjugation motifs or sites, applied cellular targets, linkers, and cytotoxic cargoes. Thus, it highlights pioneering routes and techniques, recent progress and remaining limitations of mTG-assisted assembly of ADCs.

Furthermore, a study aimed at assessment of possibilities offered by dextran as a multivalency-promoting framework was performed. In a preliminary proof-of-concept study dextran was applied as a vehicle for multiple attachment of metal-chelating agents able to carrier valuable ions for radio-imaging or -therapy. Thus, dextran polymer was equipped with a desired number of a widely applied metal chelator 1,4,7,10-tetraazacyclododecane-1,4,7,10-tetraacetic acid (DOTA). The assembled DOTA-dextran conjugates were able to carry 3,2 or 5,3 metal ions per polysaccharide chain, respectively, as shown by photometric analysis of the formed complexes with Cu^{2+} . *In vivo* biodistribution studies in mice are currently ongoing. This proof-of-concept study should answer the question, whether these novel molecular hybrids are suitable for *in vivo* applications and whether conjugation to commonly applied binders (affibodies) that suffer from hydrophobicity and in

consequence poor solubility, aggregation and precipitation, results in beneficial properties. This approach further strengthens the presumption that dextran represents a promising modular scaffold for multivalent attachment and tailoring of diverse payloads.

Individuelle Beiträge zum kumulativen Teil der Dissertation

1) **H. Schneider**, L. Deweid, T. Pirzer, D. Yanakieva, S. Englert, B. Becker, O. Avrutina, H. Kolmar, Dextramabs: A Novel Format of Antibody-Drug Conjugates Featuring a Multivalent Polysaccharide Scaffold, *ChemistryOpen*, 8 (2019) 354-357. <https://doi.org/10.1002/open.201900066>

Beiträge von Hendrik Schneider

- Initiale Idee und Projektplanung zusammen mit H. Kolmar.
- Durchführung des Großteils der Experimente.
- Verfassen des Manuskripts und Anfertigung aller darin enthaltenen Abbildungen.

Der Anteil von Hendrik Schneider an genanntem Projekt belief sich auf insgesamt 80%. Die verbleibenden 20% verteilen sich auf L. Deweid, T. Pirzer, D. Yanakieva für Beteiligung am Experimentalteil. Des Weiteren auf S. Englert, B. Becker und O. Avrutina für kritisches lesen und korrigieren des Manuskriptes, sowie H. Kolmar für Projektkoordination.

2) **H. Schneider**, D. Yanakieva, A. Macarrón, L. Deweid, B. Becker, S. Englert, O. Avrutina, H. Kolmar, TRAIL-inspired multivalent dextran conjugates efficiently induce apoptosis upon DR5 receptor clustering, *ChemBioChem*, 20 (2019), 3006-3012. <https://doi.org/10.1002/cbic.201900251> (Marked as Very Important Paper, will be Front Cover in December, Issue 24), <https://doi.org/10.1002/cbic.201900702> (Cover Picture)

Beiträge von Hendrik Schneider

- Initiale Idee und Projektplanung
- Literaturrecherche.
- Durchführung des Großteils der Experimente
- Schriftliche Ausarbeitung des Manuskripts und Anfertigung aller darin enthaltenen Abbildungen.
- Design und Anfertigung des Front Covers von *ChemBioChem* Ausgabe 24 (Dezember)

Der Anteil von Hendrik Schneider an genanntem Projekt belief sich auf insgesamt 80%. Die verbleibenden 20% verteilen sich auf D. Yanakieva, A. Macarrón, L. Deweid, B. Becker, S. Englert für Beteiligung am Experimentalteil, sowie O. Avrutina und H. Kolmar, die das Manuskript gelesen und konstruktiv korrigiert haben.

ChemBioChem: According to the evaluation of the referees, the results reported in your article [cbic.201900251R1](https://doi.org/10.1002/cbic.201900251R1) are of high scientific quality and your manuscript has therefore been marked as VIP (very important paper). Less than 10% of our manuscripts receive such a positive reviewer feedback. We think that the content of your article would be suitable for a front cover of the journal. Additionally, we recommend that

you tell the publicity/press department of your institute about your publication and the excellent reviews that it has received; a press release could be possible.

3) **H. Schneider***, L. Deweid*, O. Avrutina and H. Kolmar, Recent progress in transglutaminase-mediated assembly of antibody-drug conjugates, *Analytical Biochemistry*, 595 (2020), 113615. <https://doi.org/10.1016/j.ab.2020.113615>

*Diese Autoren haben gleichermaßen zu diesem Projekt beigetragen.

Beiträge von Hendrik Schneider

- Initiale Idee und Literaturrecherche.
- Schriftliche Ausarbeitung des Reviews und Anfertigung der darin enthaltenen Abbildungen.

Der Anteil von Hendrik Schneider an genanntem Projekt belief sich auf insgesamt 40%. Der Beitrag von L. Deweid als Co-Autor belief sich ebenfalls auf 40%. Die verbleibenden 20% verteilen sich auf O. Avrutina und H. Kolmar für ihre Unterstützung bei der Ausarbeitung des Manuskripts und der Anfertigung der Abbildungen. Das genannte Manuskript wird sofort nach acceptance online im Rahmen des Special Issue „Transglutaminases in Translation – Novel Tools and Methods Impacting on Diagnostics and Therapeutics“ in *Analytical Biochemistry* einer Einladung des CEO von Zedira (Ralf Pasternack) folgend veröffentlicht werden.

4) M. Baalman*, L. Neises*, S. Bitsch, **H. Schneider**, L. Deweid, N. Ilkenhans, M. Wolfring, M. J. Ziegler, P. Werther, J. Wilhelm, H. Kolmar and Richard Wombacher, A bioorthogonal click chemistry toolbox for targeted synthesis of branched and well-defined protein-protein conjugates, (under review, chemRxiv. Preprint. <https://doi.org/10.26434/chemrxiv.10743344.v1>)

Beiträge von Hendrik Schneider

- Beteiligung an der initiativen Projektidee
- Beteiligung an der Durchführung der Experimente
- Beteiligung an der schriftlichen Ausarbeitung
- Beteiligung an der Ausfertigung der Abbildungen

Der Anteil von Hendrik Schneider an genanntem Projekt belief sich auf insgesamt 15 %. Die verbleibenden 85 % verteilen sich auf M. Baalman, L. Neises, S. Bitch für ihre Beteiligung am Experimentalteil und zum Verfassen des Manuskriptes und an L. Deweid, N. Ilkenhans, M. Wolfring M. J. Ziegler, P. Werther, J. Wilhelm für ihre Beteiligung am Experimentalteil sowie H. Kolmar und R. Wombacher für Projektkoordination und Unterstützung beim Verfassen des Manuskripts.

#Diese Autoren haben gleichermaßen zu diesem Projekt beigetragen.

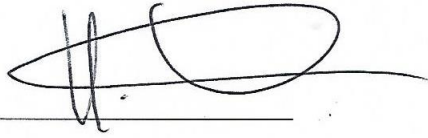
5) L. Deweid, L. Neureiter, S. Englert, **H. Schneider**, J. Deweid, D. Yanakieva, J. Sturm, S. Bitsch, A. Christmann, O. Avrutina, H.-L. Fuchsbauer, H. Kolmar, Directed Evolution of a Bond-Forming Enzyme: Ultrahigh-Throughput Screening of Microbial Transglutaminase Using Yeast Surface Display, Chemistry – A European Journal, 24 (2018) 15195-15200. <https://doi.org/10.1002/chem.201803485>

Beiträge von Hendrik Schneider

- Beteiligung an der Durchführung der Experimente

Der Anteil von Hendrik Schneider an genanntem Projekt belief sich auf insgesamt 10 %. Der Beitrag von L. Deweid für initiale Idee, Projektplanung, Durchführung des Großteils der Experimente, Verfassen des Manuskriptes und Abbildungen belief sich auf 75%. Die verbleibenden 15% verteilen sich auf L. Neureiter, S. Englert, J. Deweid, D. Yanakieva, J. Sturm, S. Bitsch und A. Christmann für ihre Beteiligung am Experimentalteil sowie O. Avrutina, H.-L. Fuchsbauer und H. Kolmar für Projektkoordination und Unterstützung beim Verfassen des Manuskripts.

Weder Referent (Prof. Dr. Harald Kolmar) noch Korreferent (Prof. Dr. Katja Schmitz) der vorliegenden kumulativen Doktorarbeit waren an der Begutachtung obenstehender Veröffentlichungen beteiligt.



Referent

(Prof. Dr. Harald Kolmar)



Korreferent

(Prof. Dr. Katja Schmitz)

Des Weiteren bestätige ich, Hendrik Peter Günter Schneider, die Richtigkeit der obenstehenden prozentualen Angaben zur Beteiligung an sämtlichen genannten Veröffentlichungen, und erkläre nicht an der Begutachtung selbiger beteiligt gewesen zu sein.

Datum:

Unterschrift:

Hendrik Peter Günter Schneider

1. Introduction

1.1. Cancer Treatment – A Brief Introduction

Cancer comprises a group of diseases characterized by abnormal cell-division and -growth thus invading surrounding tissues and spreading around the body, which results in malignant neoplasia. Despite intensive research and obvious therapeutic progress, malignancies represent a major global health issue to date. Thus, cancer is ranked as the most crucial barrier to increase the life expectancy in every single country in the 21st century.^[1] Furthermore, it represents the second leading cause of death in the United States with over 1.7 million new cases, over 600,000 new cancer-dependent deaths prognosed in 2019, and about 9.6 million deaths per year globally.^[2, 3]

In the beginning of the 1900s Paul Ehrlich introduced the concept of drugs to treat infectious diseases and the newly coined word “chemotherapy”, delineating it as the use of chemical compounds for disease treatment. Furthermore, he projected the idea of the “magic bullet” aimed at killing a harmful agent while leaving healthy tissues untouched.^[4, 5] In the 1960s, combination of surgery and radiotherapy was acknowledged as standard cancer treatment.^[4] However, only one third of treated patients were treated successfully as the applied therapies were not able to handle small metastases.^[4] At that time, new research remarkably showed that a combination of classical methods with chemotherapy can lead to full cancer remission in patients with various tumors.^[4] The first applied chemotherapeutic agents tested in humans comprised toxic nitrogen mustards, chlorambucil, and cyclophosphamide targeting DNA by alkylation (Figure 1).^[6] Further, antifolates like methotrexate were introduced as higher proliferation rates for tumors treated with folic acid were observed.^[6] Early in the following years chemotherapy became the predominant approach in tumor therapy.^[6-8] Hence, a plethora of cancer targeting compounds was designed. Today, the majority of chemotherapeutics follow a non-specific uptake through lipophilic interactions with the cell membrane of the tumor cell.^[9] Usually, these compounds promote killing of rapidly dividing cells exhibiting higher proliferations rates.^[6, 10] This is mediated by inhibiting microtubule function, DNA synthesis or protein function for example.^[11] However, not only malignant cells are affected but numerous healthy ones, for example those from the epithelium, bone marrow and gastrointestinal tract.^[6, 12] Additionally, DNA synthesis interfering nucleoside analogues (thioguanine, cytosine arabinoside), DNA interacting agents such as anthracyclines and actinomycin D, and tubulin targeting *Vinca* alkaloids derived from plants were utilized for cancer treatment (Figure 1).^[6]

Further, the combination of cytotoxins possessing different modes of action for tumor killing resulted in synergistic effects increasing the antitumoral efficacy while decreasing the overall cytotoxicity.^[7, 8, 13] Additionally, generation of highly potent cytotoxins like DNA alkylators (e.g. pyrrolobenzodiazepine dimers, CC-1065, adozelesin) and tubulin inhibitors (e.g. dolastatin 10, dolastatin 15, maytansin, cryptophycins) evolved over the years.^[6, 13] Unfortunately, these enormously potent cytotoxic agents lacked a sufficient therapeutic window conditioned by the development of resistance mechanisms and severe adverse effects caused by off-target toxicity due to the lack of selectivity.^[6, 13-15] Furthermore, the discovery of oncogenes and tumor suppresser genes triggered the introduction of novel tumor-targeting drugs.^[5, 16, 17] Being highly selective, these compounds target specific mutations originating from the cancerous cell.^[5] By inhibiting kinases

responsible for proliferation or for blocking protein interactions, these agents led to severe improvements in selectivity.^[5]

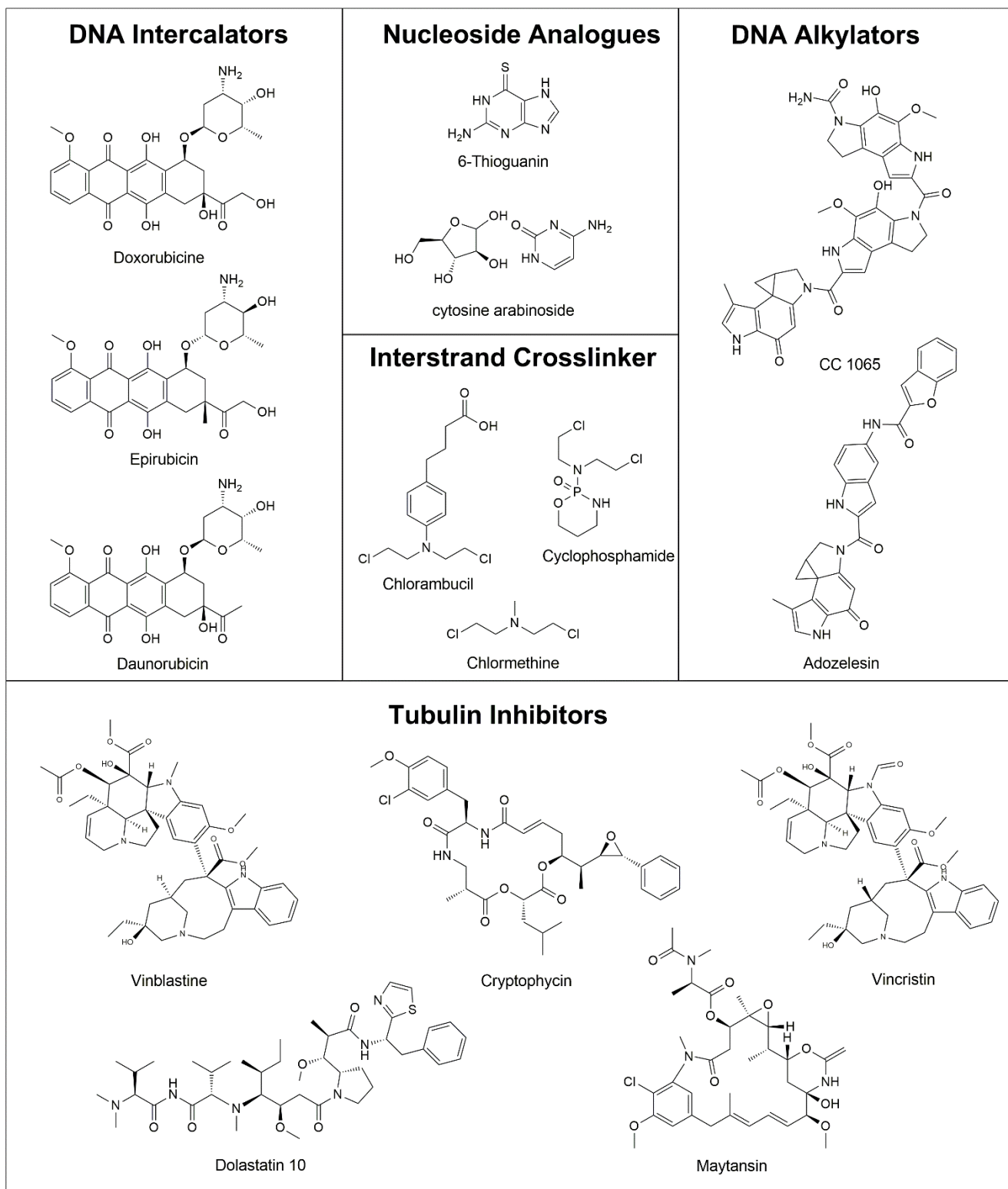


Figure 1. Overview of chemotherapeutic agents.

Additionally, highly selective therapeutic monoclonal antibodies (mAbs) have gained success for the treatment of cancer after the observation of tumor-specific antigens located on the cell surface.^[18-20] Being either overexpressed, solitarily expressed or even mutated on the surface of tumor cells,^[19] these antigens comprise e.g. cell-surface proteins, glycoproteins, or carbohydrates.^[6] High specificity of antibodies combined with their affinity to tumor antigens makes this class of molecules less off-target toxic compared to their small molecule chemotherapeutic counterparts.^[18] In the last two decades successful antibody-based therapies for the treatment of hematological malignancies and solid tumors were established.^[19] Thus, over 50 mAbs are currently undergoing evaluation in late stages of the clinical trials and at least 6-9 mAbs per year are expected to be approved, and about 70 of them are predicted to be marketed by 2020.^[21, 22] These compounds either act as agonists or antagonists when bound to surface-exposed cell receptors, though modulating receptor-mediated signaling as applied for the marketed antibodies cetuximab and trastuzumab.^[19, 23, 24] Further, these kind of biomolecules trigger Fc-mediated immune response, e.g. complement-dependent cytotoxicity (CDC), antibody-dependent cellular cytotoxicity (ADCC, rituximab) and regulation of T-cell functions,^[19, 25] as well as depletion of circulating tumor cells, antibody-dependent phagocytosis and apoptosis leading to cell death.^[6] Following the first success of this class of compounds, improvement of effector functions, pharmacokinetics and immunogenicity *via* application of chimeric, humanized and fully human antibodies has been achieved.^[19] To enhance tumor selectivity of chemotherapeutics, thus widening of the therapeutic window, the concept of antibody-drug conjugates (ADCs) evolved based on furnishing a mAb with potent cytotoxins.^[6, 26] These novel compounds combined targeting, pharmacokinetics, and suitable biodistribution properties of mAbs with the potency of the conjugated cytotoxic small molecule.^[26, 27] Following the approval of brentuximab vedotin and trastuzumab emtansin, more than 60 ADCs have currently entered clinical trials.^[27] Further, the number of mAbs in phase III clinical trials increased from 26 to 52 from 2010 to 2017; currently over 230 mAbs are in phase II clinically studies.^[22] Interestingly, only one bispecific mAb is currently investigated in phase III studies, while twelve are investigated in phase II and three are in phase I/II.^[22] The structure and functions of antibodies and ADCs will be described in the sections 1.3 and 1.4.

1.2. From Innate to Adaptive Immunity

The immune system is the host defense against different types of infectious pathogens of microbial, fungal, parasitic or viral nature constantly attacking vertebrates. Thereby, the innate or unspecific immune system acts as the first-line defense by identifying and destroying infectious pathogens.^[28] The innate immune system comprises mechanic physiological barriers, among them the skin, the gastrointestinal tract bearing gastric acid, epithelia, the blood-brain barrier, and the mucus layer. Further germline-encoded host sensors called pathogen recognition receptors (PRRs) like toll-like (TLRs), RIG-I-like (RLRs), NOD-like (NLRs) and DNA receptors play a key role by recognizing pathogen-associated molecular patterns (PAMPs), that are correlated with commonly microbial pathogens.^[29-31] Hereby, each receptor is able to bind to a variety of molecules conditioned by a broad intrinsic specificity.^[32] These PRRs are expressed on cells of the innate immune system, e.g. dendritic cells, macrophages, and neutrophils (Figure 2).^[29] The recognized bacterial PAMPs are mainly parts of the bacterial cell wall being structurally lipoproteins, lipopolysaccharides, peptidoglycans, or lipoteichoic acids, whereas viral

targets of the innate immune system are solely represented by viral nucleic acids.^[29, 30, 32] Therein, differentiation between viral, bacterial and self-DNA is possible due to chemical modifications and structural unique features of the DNA.^[30, 32] Binding of PRRs triggers several antimicrobial immune responses, like release of inflammatory cytokines, among them tumour-necrosis factor (TNF), interleukin-1 β (IL-1 β), IL-2 and IL-6, chemokines and type I interferons.^[29, 32]

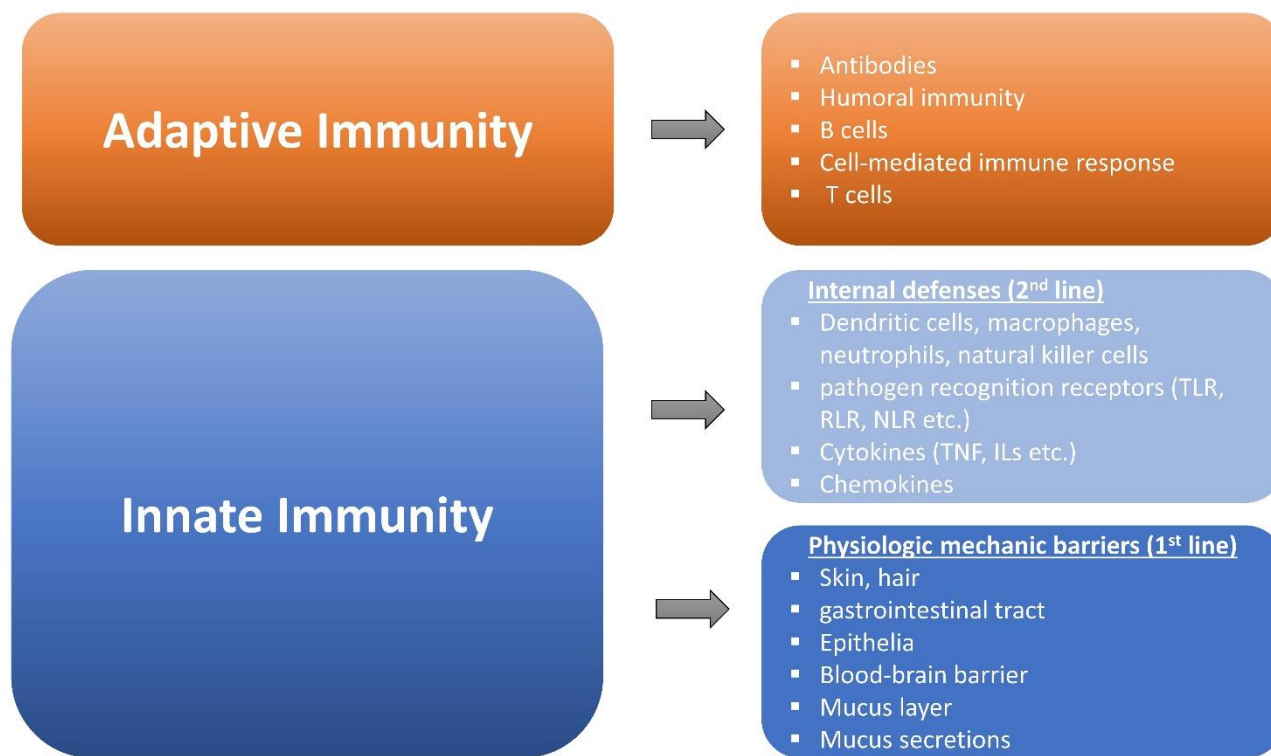


Figure 2. Hierarchy of the vertebrate immune system. The innate immune system comprises first-line mechanic barriers and second-line internal defenses. And the resulting adaptive immunity represented by highly specific immune responses, e.g. antibodies.

Furthermore, the innate immune system triggers the initiation of the adaptive immunity representing the second barrier of immunity that enables a broader and more selective response to infectious pathogens (Figure 2).^[33] Thus, generation of highly pathogen-specific B and T lymphocytes takes place, which employs antigen receptors that are not encoded in the germline.^[34] A clonally diverse repertoire of unique antigen receptors located on lymphocytes represents the main feature of the adaptive immunity.^[35] The binding diversity of these receptors is generated by somatic recombination that is mediated by the recombination-activating gene (RAG)-protein-mediated encoding genes for the variable and constant fragment.^[30, 36] Gene conversion and non-templated nucleotide addition as well as, in the case of B cells, somatic hypermutation further enhances diversity.^[30, 36]

Pathogen recognition of the adaptive immune system is achieved by multiple receptors with large soluble proteins – antibodies – among them. After activation by the respective cells, among them the dendritic ones and T lymphocytes, B cells differentiate to plasma cells and produce antibodies as humoral immunity.^[33, 37] Following receptor-mediated endocytosis and intracellular degradation, antigen peptide fragments are

presented on the surface of B lymphocytes bound to major histocompatibility complex (MHC) class II.^[32, 38] Recognition of these antigenic peptides by T-cell receptors (TCRs) of activated CD4-positive T cells leads to the secretion of cytokines that induce proliferation and differentiation of B cells to plasma cells secreting antibodies.^[32] Additionally, some microbial pathogens like microbial polysaccharides can activate B cells directly. However, somatic hypermutation and isotype switching is dependent on the interaction with CD4+ T cells resulting in a less variable repertoire of antibodies.^[32] The generated immunoglobulins, immunoglobulin M (IgM) and IgD are presented on the surface of naïve B cells.^[39] Hereby, IgM represents the first isotype produced before isotype switching.^[40] IgM builds a pentameric form comprising ten potential binding sites. It is able to recognize several phylogenetically conserved structures like proteins, nucleic acids, lipids, and carbohydrates.^[31, 41, 42] However, affinity of these naïve antibodies is rather low. Hence, stimulation with antigen results in class switching of B cells into plasma cells which enables the production of high-affinity IgG, IgA, IgE and IgD counterparts (Figure 3).^[39, 40, 43]

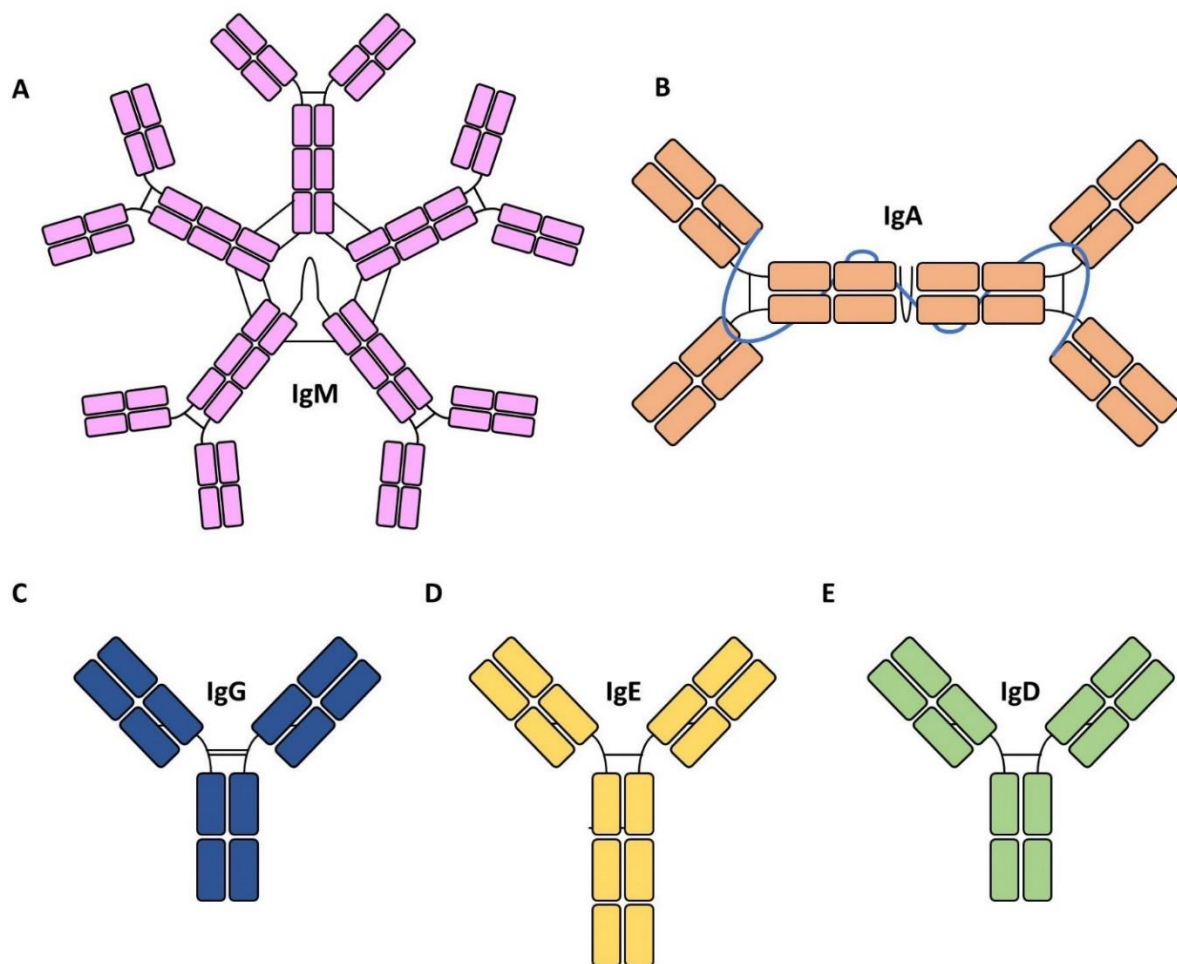


Figure 3. Antibody classes: (A) pentameric IgM, (B) dimeric IgA, (C), IgG, (D) IgE and (E) IgD. modified from News Medical Life Sciences^[44]

This switch occurs upon antigen binding by a mechanism called class switch recombination (CSR) in combination with activation-induced cytidine deaminase (AID).^[39] AID converts cytosine in the switch region to uracil resulting

in removal by DNA repair mechanisms and double strand breaks. Finally, replacement of the μ and δ heavy chain constant regions with γ , ϵ or α heavy chain constant regions occurs.^[39, 45] The structure and function of antibodies will be described in the following section.

1.3. Antibodies

1.3.1. Structure and Function

Antibodies represent a key element of the human adaptive immune system. These proteins are present either in a membrane-bound form called surface immunoglobulin and being part of the B-cell receptor or in form of a secreted protein only differing in a small part of the C-terminus of the heavy chain constant domain.^[32] Being produced as glycoproteins, these biomolecules are able to selectively bind a target antigen. The heterotrimeric glycoproteins are further divided in five classes, called IgA, IgD, IgE, IgG and IGM, which differ by the constant domain of the heavy chains (Figure 4).^[43, 46] These five classes comprise glycoproteins composed of 82-96 % protein and 4-18 % carbohydrate.^[46]

Among immunoglobulins, IgG is the most prevalent species accounting for 10-20 % of plasma proteins and subdivided in the four subclasses IgG1, IgG2, IgG3 and IgG4.^[40, 46] These subclasses possess more than 90 % sequence identity but differ in terms of antigen binding, immune complex formation, complement activation, effector cell triggering, half-life, and placental transport.^[46] IgGs are large Y-shaped molecules consisting of three equal-sized parts connected *via* a flexible linker called hinge region.^[32] These homodimeric molecules are composed of two identical light chains with a size of approximately 25 kDa, and two identical heavy chains of 55 kDa each (Figure 4).^[47] The heavy chains are linked by disulfide bonds in the flexible hinge region and by non-covalent interactions of the constant domains (C_{H3}).^[46] Further, the heavy chains are connected with the light chain by an additional disulfide bond. Each of these light chains consists of a variable domain (V_L) which is C-terminally bound to one constant domain (C_L) which can either be a λ - or κ -chain. In addition, each heavy chain of the molecule consists of one variable domain (V_H) C-terminally linked to the C_{H1} which is further connected to the C_{H2} and C_{H3} .^[46] These domains form a characteristic fold bearing two antiparallel β -sheets yielding a roughly barrel-shaped structure called β -barrel and consisting of four ~110 residue long folds.^[32] Antibody molecules can be further divided in the fragment crystallizable (Fc) consisting of two C_{H2} - C_{H3} heavy chain dimers and a structure composed of V_H , V_L , C_{H1} and C_L called fragment antibody binding (Fab) (Figure 4).^[46] Interestingly, these antibody molecules can be fragmented applying digestive proteases, e.g. papain or pepsin, especially cleaving in the flexible hinge region^[48]

The variable domains of an antibody form the paratope responsible for the binding properties, whereas the constant domains mediate the effector functions. Two identical antigen-binding sites are generated due to symmetric structure of immunoglobulins.^[32]

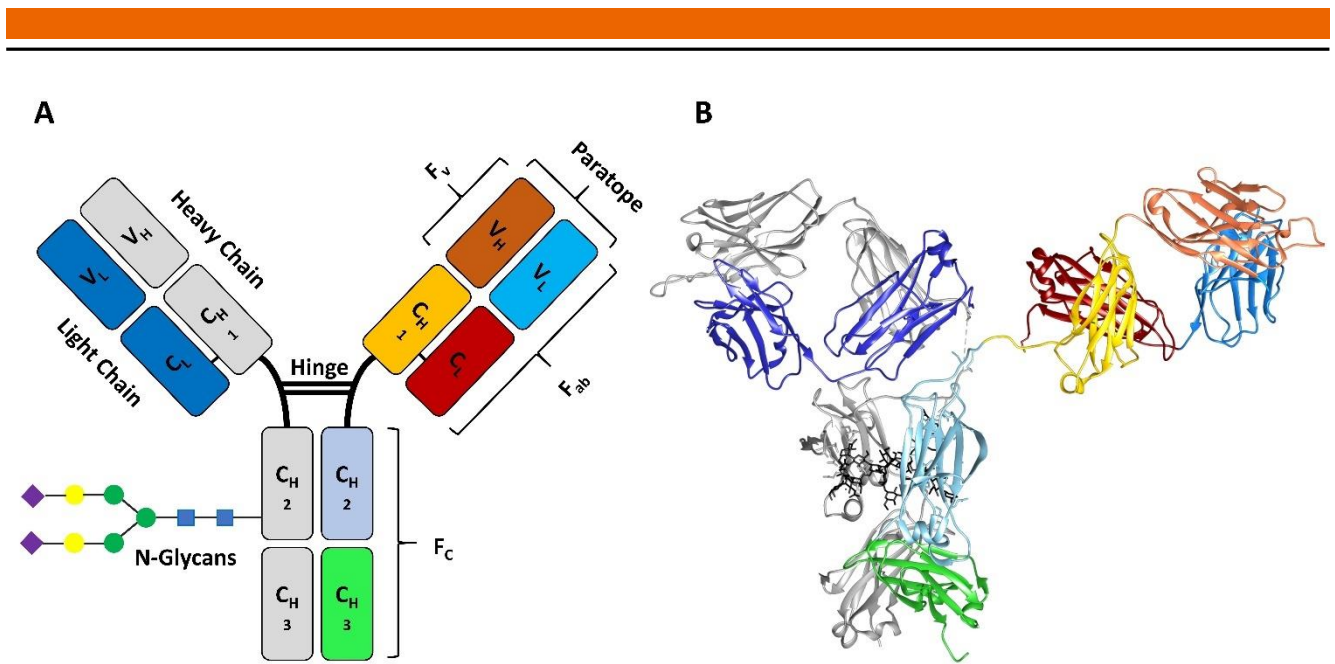


Figure 4. Schematic structure of IgG1 antibodies (A) and ribbon representation (PDB: 1HZH) (B). The homodimeric antibody consists of two identical heavy and light chains. The light chain consists of the V_L which is C-terminally connected with one constant C_L . The heavy chain consists of the V_H C-terminally linked to the C_{H1} , which is further linked to C_{H2} and C_{H3} . The molecule comprises one Fc-fragment bearing a *N*-glycosylation pattern and two F_{ab} fragments bearing the paratope facilitating antigen binding of the antibody. The V_H and the V_L together form the variable fragment F_V .

Binding is enabled by the complementarity determining regions (CDRs) located in the *N*-terminal variable domains of the heavy and light chains of the F_{ab} fragments, each possessing three hypervariable loops (CDR1, CDR2 and CDR3).^[32] The CDRs point out of the antibody framework and are neighbored by relatively rigid regions called FR1, FR2, FR3 and FR4.^[32] Notably, the antigen binding site is formed by CDRs of V_H and V_L , thus binding is mediated by a combination of heavy and light chain. Hereby, the surface formed by the CDRs of the heavy and light chains builds a site to which the complementary formed antigen can bind. Hence, small molecules bind in small pockets or junctions, whereas proteins are bound by the interfaces that involve all CDRs.^[32] The resulting non-covalent reversible binding is mediated by electrostatic forces, hydrogen bonds, Van-Der-Waals and hydrophobic interactions or the combination thereof. Diversity of CDRs is generated through differential assembly of the Variable, Diversity, and Joining gene segments, known as V(D)J-recombination accomplished by developing B lymphocytes.^[49] However, the Diversity gene segment is only assembled in V_H domain. Somatic mutations are an additional feature that further enhances diversity.^[30]

The Fc fragment formed by the lower hinge region and the C_{H2} and C_{H3} domains is responsible for the effector functions of the antibody.^[46] The Fc comprises the intrinsic binding sites for the Fcγ receptor (FcγR) and the complement-activation protein (C1q) located proximal to the hinge region in the C_{H2} domain.^[46, 50] Binding to C1q and FcγR mediates complement-dependent cytotoxicity (CDC) or antibody-dependent cytotoxicity (ADCC), respectively, representing the effector functions.^[19, 25, 46] The binding properties of FcγR and C1q are different for each IgG subclass conditioned by a varying structure of the hinge region (length and flexibility) and number of disulfide bonds.^[46] Thus, the relative binding to the IgG subclasses can be ordered as: IgG3>IgG1>IgG4>IgG2.^[46] In addition, the Fc fragment comprises a binding site for the neonatal Fc receptor (FcRn) located at the interface between C_{H2} and C_{H3} distinct from the binding sites for the FcγR and C1q located

near the hinge region in the C_{H2} domain.^[46, 51, 52] The FcRn is responsible for the recycling of IgGs extending its half-life by reducing lysosomally degradation in endothelial cells.^[51] Furthermore, it enables placental passage and the transport to mucosal surfaces.^[46] Additionally, the F_c fragment bears an *N*-glycosylation site at the interface of the C_{H2} and C_{H3} domain of the heavy chain whose glycans also play a key role in FcγR binding upon introducing changes in the quaternary structure of the antibody.^[46] Hereby, asparagine 297 (N297) of the heavy chain serves as anchor point for *N*-glycosylation.^[53] This biantennary glycan is composed of a heptasaccharide consisting of a chain of two *N*-acetylglucosamine (GlcNAc) residues as core, bound to branched mannose polysaccharides and an additional GlcNAc residue.^[53] Further, variable addition of a fucose or an additional bisecting GlcNAc and up to two galactoses or two sialic acids results in heterogeneity.^[53] Glycosylation of the Fc affects FcγR-binding as well as the stability of the Fc as the interaction of the N297 glycan with the protein backbone stabilizes the Fc.^[46, 54] Notably, core fucosylation of the IgG1-Fc *N*-glycans plays a role in FcγR IIIa-binding as non-fucosylated antibodies show higher affinity, thus compromising higher ADCC activity.^[55] These compounds possessing selective targeting properties, pharmacokinetic properties represent a promising molecular scaffold for the equipment with cytotoxic payloads. Thus, resulting ADCs are promising candidates to selectively deliver an apoptosis-inducing small molecule to a chosen cellular target. These architectures will be addressed in the following sections.

1.4. Antibody-Drug Conjugates (ADCs)

1.4.1. Mechanism of Action of ADCs

ADCs are composed of antibodies loaded with cytotoxic compounds aimed at their specific delivery to targeted cells.^[13, 56] In these architectures, the beneficial characteristics of the antibody and a cytotoxic compound are combined leading to an enhanced therapeutic window, thus safer and more patient-friendly treatment.^[7, 12, 13] To join an antibody and a cytotoxic payload, a special linker is used, either a cleavable or a non-cleavable one. Having entered the tumor tissue from the vasculature, the ADC is able to recognize and specifically bind a tumor-overexpressed antigen on the cell surface of malignant cells (Figure 5).^[18] Upon internalization following the endosome-lysosome pathway, the payload is released either *via* cleavage of the linker, or upon the antibody's degradation.^[13] Subsequently, the cytotoxic cargo diffuses into the cytoplasm to reach and interact with its target, e.g. tubulin or DNA, ultimately resulting in apoptosis of the malignant cell (Figure 5).^[13] Envisioned to overcome the shortcomings of both compound classes, this strategy allows for the selective delivery of a potent drug omitting severe dose-limiting toxicity.^[57] Further, the rather low efficacy of solitary antitumor antibodies is enhanced by addition of the cytotoxic payload.^[20] To conclude, this targeted approach results in an immense widening of the therapeutic index in comparison to commonly applied chemotherapeutics. In the following sections a brief history of ADC development will be given.

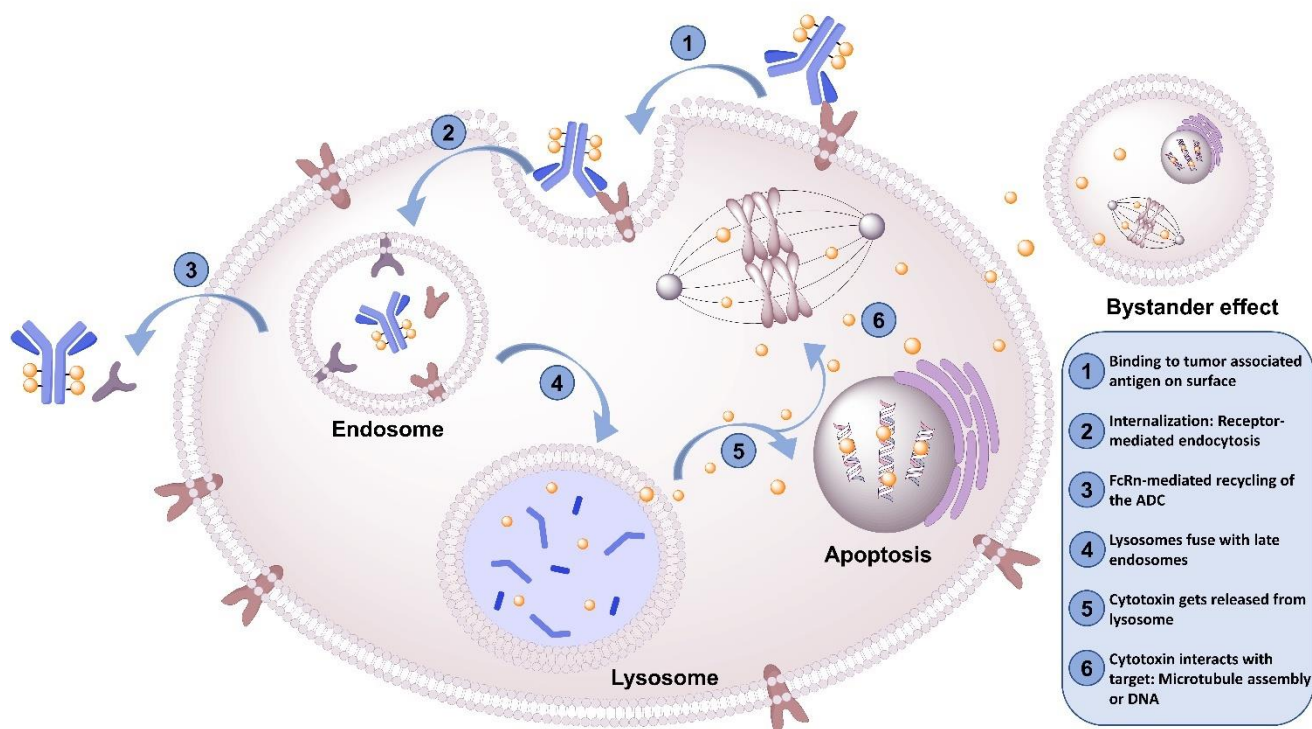


Figure 5. Mechanism of action of antibody-drug conjugates for triggering apoptosis of tumor cells. (see section 4.3)^{modified from Lambert et al.[13]}

1.4.1. ADCs: A Brief History

Chemotherapeutics kill rapidly dividing cells by inhibiting microtubule function, DNA synthesis, or protein function resulting in a dose-dependent therapeutic window (Figure 6).^[58] However, this addresses not only malignancies, but also numerous healthy cells leading to severe adverse effects. To improve the therapeutic window, a cytotoxin with higher potency can be applied resulting in a lower minimum effective dose (MED), or the selectivity of a toxic compound can be enhanced to increase the maximum tolerated dose.^[6] Thus, to bypass the narrow therapeutic window, researches turned to antibody-drug conjugates (ADCs).^[58] These evolved from Paul Ehrlich's "magic-bullet" concept^[5, 59] of a compound that selectively targets a disease-causing organism while simultaneously delivering a toxin.^[60] Thus, ADCs are part of the "targeted therapy" concept, based on specific interference with molecular targets and pathways that are important for proliferation of cancer cells.^[6]

The first ADCs arose from the need to selectively and site-specifically deliver toxins to the tumor cell.^[6] However, in the first half of the twentieth century only little progress was achieved, attributed to the difficult isolation of antibodies from animal and human serum and the fact that it was nearly impossible to produce a sufficient amount.^[61] However, in 1958 Mathé et al. reported selective antiproliferation activity of a methotrexate conjugated to an antileukemia 1210 antigen antibody on L1210 mouse lymphocytic leukemia cells.^[62] In the early 1970s covalent conjugation and the choice of ligation method were reported to play a key role for ADC activity.^[61, 63] Initially, anticancer drugs methotrexate, vinblastine, doxorubicin, and melphalan were examined.^[6]

Early clinic attempts utilized KS1/4 antibody-methotrexate conjugates against non-small cell lung cancer and BR96 antibody-doxorubicin ones against metastatic breast cancer.^[58] However, being able to localize at the tumor site, they had lack in therapeutic effectivity, obviously due to low selectivity and immunogenicity.^[58] Indeed, the targeted antigens KS1 and BR96 were expressed on both tumor cells and healthy tissues, and used antibodies were of chimeric or murine nature, which triggered immune response.^[58, 64-66]

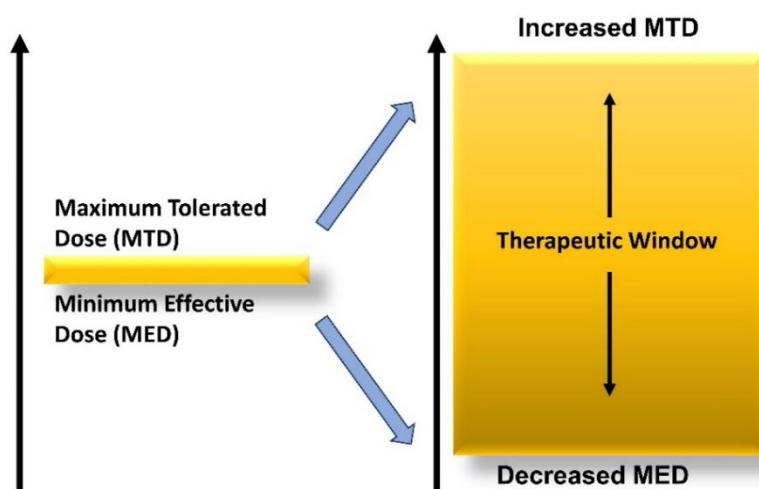


Figure 6. ADCs expand the therapeutic window. Selective delivery increases the percentage of administered toxin reaching the tumor, which lowers the medium effective Dose. Further, the targeted delivery of the cytotoxin increases the maximum tolerated dose as normal healthy tissue is reached. modified from Panowski et al.^[58]

The hybridoma technology established by Köhler and Milstein in 1975 became a major breakthrough in the field of ADC assembly as it addressed early problems in antibody production and purification.^[6, 61, 67] Furthermore, recombinant technologies for the production of chimeric and – later – humanized antibodies ensured access to ADCs with reduced immunogenicity. The identification of different biomarkers, e.g. HER2 or the vascular endothelial factor (VEGF), and understanding of protein uptake mechanisms further advanced the success of ADCs.^[61] Intracellular drug release from the protein-drug conjugate was identified as a key element for the design of effective ADCs.^[61] Thus, linkers providing different cleavage options, e.g. enzyme-catalyzed hydrolysis (by peptidases and esterases), acidolysis, or intracellular glutathione-promoted reduction evolved.^[58, 61] Fast development of these novel techniques resulted in the first marketed ADC – gemtuzumab ozogamicin (Mylotarg®) introduced by Wyeth for the treatment of acute myeloid leukemia.^[68-70] In this construct, an anti-CD33 antibody was linked to a potent calicheamicin derivative. However, in 2010 it was voluntarily withdrawn from the market due to issues regarding clinical safety and benefit.^[6, 61] Notwithstanding, in 2017 it was approved for the treatment of acute myeloid leukemia applying a different dosage.^[71]

As only a limited number of ADCs is able to reach their cellular target, second-generation ADCs were loaded with extremely potent tubulin inhibitors, e.g. monomethyl auristatin E (MMAE),^[72] monomethyl auristatin F (MMAF)^[73] and maytansinoids (DM1, DM4)^[74], or with DNA-targeting agents, like calicheamicins.^[73, 75] In addition, pyrrolobenzodiazepine^[76] and indolinobenzodiazepine^[77] were applied. Lessons learned from these

early approaches were considered upon design of the second-generation ADCs and, finally, six constructs have reached the market. These are: brentuximab vedotin (Adcetris[®], Seattle Genetics)^[78, 79], polatuzumab vedotin-piiq (Polivy[™], Genentech and Roche)^[80], trastuzumab emtansin (Kadcyla[®], Genentech and Roche)^[81, 82], inotuzumab ozogamicin and gemtuzumab ozogamicin (Besponsa[®], respectively Mylotarg[®], Pfizer)^[68, 71, 83, 84], as well as moxetumomab pasudotoxas (Lumoxiti[™], Immunotoxin, AstraZeneca)^[85] all targeting hematologic malignancies or solid tumors. In addition, more than 60 ADCs are currently in clinical trials.^[27] Most of these second generation ADCs are assembled by addressing endogenous thiols liberated by reduction of interchain disulfides, or by coupling to primary amines of lysine side chains. Obviously, heterogeneity is the feature of these compounds assembled by stochastic conjugation technologies.^[7, 13, 26, 73] For instance, Kadcyla[®] is assembled by addressing lysines of HER2-targeting antibody trastuzumab with tubulin inhibitor DM1. However, 70 out of 88 native lysines are accessible for conjugation, which results in inhomogeneity of ADC species.^[86] Contrary, Adcetris[®] is assembled by ligation to partially reduced interchain disulfides resulting in a maximal reachable DAR of eight leading to reduced heterogeneity. However, this still results in a number of species comprising different DARs.^[87]

Therefore, novel third-generation ADCs rely on site-specific conjugations resulting in homogeneous constructs. They will be discussed in section 1.4.3 in detail. To convey a better understanding of the individual components of an ADC, these will be addressed in the following section.

1.4.2. The Three Pillars of an ADC

An antibody, a linker, and a cytotoxic agent represent the three key elements of an ADC (Figure 7).^[7] The targeted antigen determines the choice of antibody that should be highly selective against it. Recently, the broad spectrum of cellular targets was delineated by a systemic database search that identified 87 ADCs against a total of 59 unique targets across 60 tumor (sub)types evaluated in clinical trials in 2017.^[57] These are, for example numerous clusters of differentiation (CD19, CD22, CD25, CD30, CD33 etc.), tyrosine-protein kinase Met (c-MET), epidermal growth factor receptor (EGFR), human epidermal growth factor receptor 2 (HER2), and tumor-associated calcium signal transducer 2 (TROP-2 known as TACSTD2).^[57] By implication, antigens highly overexpressed on malignancies but almost absent on the surface of healthy cells are favored as they result in a broader therapeutic window. However, the fact that some addressed antigens are expressed on healthy cells results in on-target, but off-tumor toxicity leading to severe adverse effects.^[88, 89] For example, the most common adverse effect of EGFR blockade is skin toxicity.^[88] Exemplarily, unwanted side-effects were observed in 80 % of patients medicated with cetuximab, among them acne-like rash, xerosis cutis, paronychia and fissuring, hair changes and mucositis.^[88] Thus, a careful adjustment of the binding properties of an antibody is a prerequisite to achieve a balance between efficacy and toxicity of an ADC, depending on the expression levels of the desired antigen on tumors and healthy cells.^[89-91]

The second key element of an ADC is a cytotoxic payload that is covalently bound to an antibody. Conditioned by the hydrophobic character of most commonly applied toxins, DAR of ADCs normally does not exceed 3-4.^[6, 7, 13] Thus, the payload needs to be highly cytotoxic to reach efficacy at the given intracellular concentrations.^[7] For instance, it is reported that about 10⁶ molecules/cell of a moderately cytotoxic compound are needed to

efficiently kill tumor cells.^[6] However, typically only 10^5 antigen molecules are present on the surface of the cell and can be recognized by an ADC. Moreover, inefficient internalization of the formed antigen-antibody complex and intracellular trafficking may additionally decrease ADCs effectiveness.^[6] Moreover, only a small portion of administered ADC was reported to reach the targeted tumor.^[6, 92]

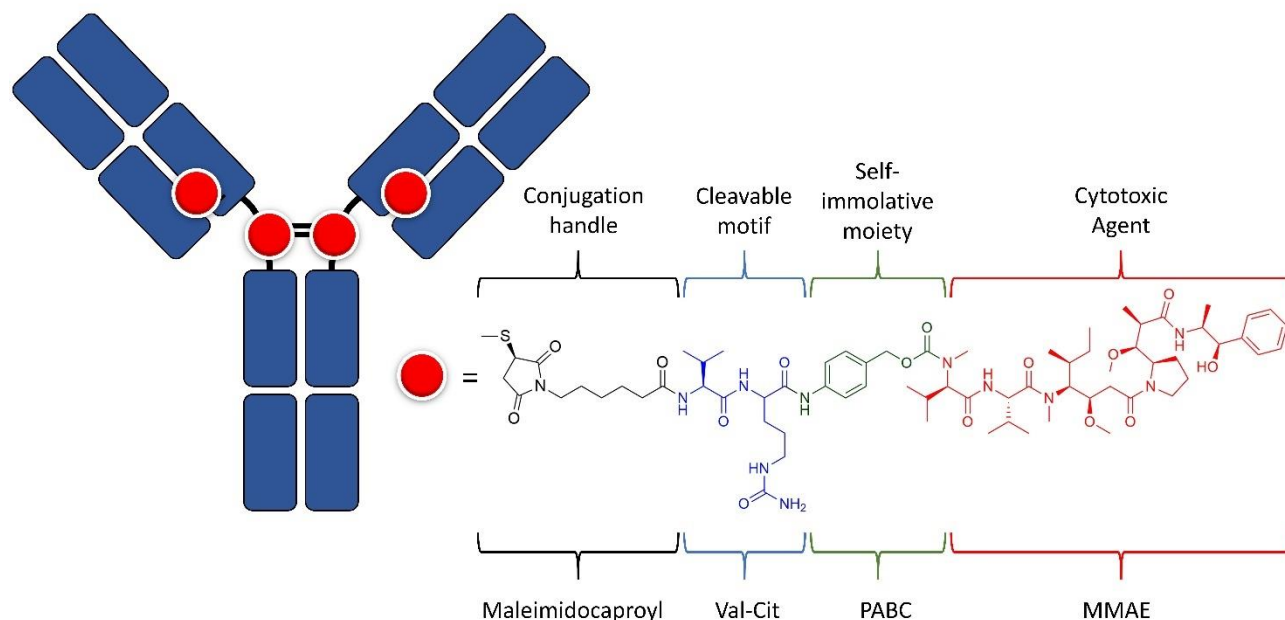


Figure 7. Representative schema of an ADC. Brentuximab vedotin (Adcetris[®]) is depicted as example. 4 linker-payloads are attached per antibody. Maleimidocaproyl is applied for attachment to reduced hinge cysteines of the brentuximab. Valine-citrulline-*p*-aminobenzyl carbamate (Val-Cit-PABC) serves as protease cleavable linker (cathepsin)^[92] and monomethyl auristatin E (MMAE) is applied as potent antineoplastic agent. ^{modified from ADC Review^[93]}

In general, the applied payload should be readily chemically modified and stable in circulation without affecting solubility. Notably, the number and hydrophobicity of the payloads have a major effect on the pharmacokinetic properties as species with high DAR may be problematic upon manufacturing and formulation due to enhanced hydrophobicity and poor solubility of the assembled ADCs.^[13, 93] Strategies aimed at overcoming this issue are discussed in section 1.4.3.

Applied toxins comprise antimetabolic drugs, e.g. maytansins and auristatins, and DNA-addressing agents, among them calicheamicins, duocarmycins, and camptothecins.^[6] Antimetabolic drugs trigger apoptosis by inhibiting tubulin polymerization. As the assembly of microtubule represents a key step during mitosis, this class of compounds preferably kills rapidly dividing cells.^[94, 95] If tubulin is bound close to the *vinca* alkaloid binding site a suppression of microtubule dynamics is provoked, thus cells are arrested in the G2/M phase ultimately leading to apoptosis.^[6] The marketed ADCs Adcetris[®] (Figure 7), Polivy[™] and Kadcyla[®] bearing vedotin, vedotin-piiq, and emtansin, respectively, comprise this class of cytotoxins. In contrast, DNA agents work by intercalating, crosslinking or by alkylation of DNA. Hence, these compounds are able to kill proliferating and non-proliferating cells. Calicheamicins, for example, bind tightly to the minor groove resulting in DNA double-strand breaks that ultimately lead to cell death.^[6, 96] In contrast, duocarmycins and indolinobenzodiazepine pseudodimers act by

alkylation of DNA, which also triggers cellular apoptosis.^[77, 97] In contrast, dimers of pyrrolobenzodiazepines (PBD) crosslink DNAs.^[76] The marketed ADCs Besponsa[®] and Mylotarg[®] are loaded with a calicheamicin derivative (ozogamicin) that primarily mediates double-strand breaks.

The third vital component of an ADC is a linker. This structural element enables covalent attachment of an antibody to the cytotoxic compound with an option to be cleaved under particular conditions and also has a certain influence on the ADCs properties. First, the linker needs to be stable in plasma to omit premature release of cytotoxin, resulting in off-target toxicity and narrowing of the therapeutic window.^[60] Second, the linker should if possible voluntarily release the payload after reaching the target cell.^[60] As mentioned above, the applied payloads are as a rule highly hydrophobic, thus a linker of the same nature could further raise problems due to aggregation and recognition by multidrug resistance (MDR) transporters.^[60]

Applied linkers can be categorized in two classes: cleavable and non-cleavable linkers. The latter hold integrity under physiological conditions, therefore payload release depends on lysosomal degradation of the whole construct.^[60, 98] As a result, an additional amino acid from the antibody is still connected with the toxin after degradation.^[60] This type of linkers is used for the assembly of marketed ADC Kadcyła[®].^[60]

The class of cleavable linkers comprises protease-, pH-, and redox-sensitive ones. For example, being overexpressed in various cancer cells, cysteine protease cathepsin B is able to readily cleave after a valine-citrulline (Val-Cit), phenylalanine-lysine (Phe-Lys), or valine-alanine (Val-Ala) motif.^[11, 99] Among the cleavable linkers, the most successful one comprises a Val-Cit motif accompanied by a self-immolative spacer, for example *p*-aminobenzyl carbamate (PABC) to enable a traceless toxin release.^[11] This linker is applied in marketed ADC Adcetris[®].^[78, 79] Additionally, β -glucuronide linkers are utilized for an ADC assembly.^[98] Hereby, β -glucuronidase present in lysosomes is responsible for toxin release. Thus, cleavage occurs by lysosomal processing followed by a 1,6-elimination of the spacer resulting in release of the free drug.^[98, 100] A major advantage of this linker is its polarity that has benefits in terms of aggregation and solubility.^[98]

Acid-labile linkers, e. g. hydrazones, are readily cleaved after internalization following the endosome-lysosome pathway as lower pH of the endosome (pH 5-6) and lysosome (pH 4.8) is sufficient for effective toxin release.^[11] This linker strategy is used for the marketed ADC Mylotarg[®].^[68-70] However, ADCs comprising this type of linkage bear the potential of undesired payload release under physiological conditions as hydrazone hydrolysis has been reported already at pH 7.4 (37 °C).^[101] In contrast, redox-sensitive linkers rely on higher cytoplasmic concentration of glutathione (up to 1000-fold) compared to the extracellular environment.^[98] Thus, a disulfide bond is incorporated at the linker that is stable in circulation, but is broken after internalization.^[60, 98]

In addition, the attachment site of the cytotoxic compound is important for the pharmacokinetic properties, e.g. half-life, stability, clearance of an ADC. This issue will be discussed in the following sections.

1.4.3. Site-Specific ADCs

Site-specific conjugation methods were introduced to overcome heterogeneity of ADCs towards an improved therapeutic window compared to the classical statistically conjugated counterparts.^[102] These methods led to more homogenous ADC, which not only simplified purification but paved the way for a better understanding of the effect of the conjugation site on overall ADC properties. Thus, most of the third-generation ADCs rely on

conjugation methods that address distinct ligation sites. These methods can be divided in two main classes, the chemical and the enzymatic ones. Numerous approaches were applied to introduce reactive moieties, among them glycoengineering,^[103-108] incorporation of additional cysteine residues (e.g. Thiomab[®], Figure 8),^[109-112] selenocysteines^[113], or non-natural amino acids,^[114-116] re-bridging of natural thiols,^[87, 117] metallopeptide-based catalysis,^[118] redox-based methionine bioconjugation^[119], as well as autocatalytic attachment of the toxin to a reactive antibody's lysine.^[120] Subsequently, the chemical handles can be addressed by different payloads following diverse procedures. For instance, the Thiomab[®] technology relies on two genetically introduced additional cysteine residues accessible for toxins equipped with a maleimide handle, thus leading to highly homogenous ADCs comprising a DAR of 2 (Figure 8).^[11, 110] Further, genetic incorporation of a non-natural amino acid was applied to introduce carbonyl or azide moieties for subsequent reactions to form oxime- or triazole conjugates, respectively.^[11]

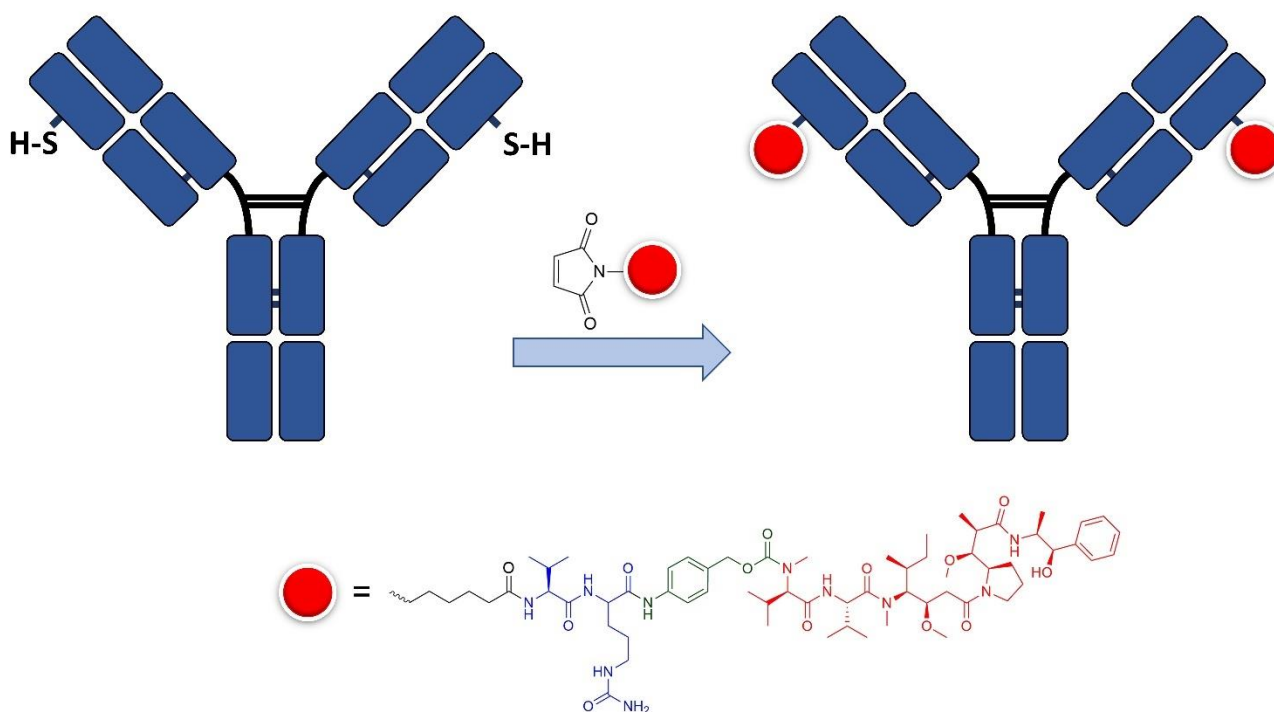


Figure 8. Scheme of Thiomab[®] ADCs. Additional genetically incorporated thiols are accessible reactive handles for conjugation of toxins equipped with maleimide moieties.

Furthermore, site-specific conjugation applying numerous enzymes were utilized to equip an antibody with a chosen payload. These enzymes comprise tubulin tyrosine ligase (TTL),^[10, 121] formylglycine-generating enzyme (FGE),^[122, 123] SpyLigase,^[124] phosphopantetheinyl transferase,^[125] sortase A,^[126-128] mushroom tyrosinase^[129] and microbial transglutaminase (mTG).^[130] The respective procedures rely on one-step enzymatic or two-step chemo-enzymatic approaches for ADC assembly. Hereby, genetically incorporated recognition motifs located at distinct sites of an antibody were site-specifically addressed by the respective enzyme of choice to introduce either a reactive handle or the cytotoxic payload directly. For instance, Sortase A is capable of catalyzing the ligation between an LPXTG recognition motif and an *N*-terminal oligoglycine substrate in the presence of calcium

ions.^[126] Hence, incorporation of a short recognition motif, exemplary at the C-terminus of the heavy chain, results in an antibody that can be easily conjugated with a payload in a site-specific manner.

All the above-mentioned approaches were successfully applied for ADC generation possess distinct advantages and certain drawbacks. Reviews delineating the current status of site-specific ADCs in detail can be found elsewhere.^[10, 131] mTG-mediated conjugation relevant for this work will be discussed in the following sections in more detail.

1.4.4. Transglutaminase

Transglutaminases (TGs) belong to the class of protein γ -glutamyltransferases found in microorganisms, plants, invertebrates, amphibians, fish, and birds.^[132] This enzyme facilitates pH-dependent formation of an isopeptide bond between a primary amine and a glutamine residue under release of ammonia resulting in γ -carboxamides (Figure 9).^[130, 133] These two counterparts can be located both in a protein or a peptide.^[132] In the first step, an active thioester is formed by reaction of the sulfhydryl group of the cysteine located in the active site of the transglutaminase and the acyl portion of the glutamine substrate. Subsequently, the acyl acceptor, which can either be water or a primary amine, reacts with the formed active thioester resulting in either deamidation or crosslinking (Crosslink I), respectively. In addition, reaction of the active thioester with a polyamine, e.g. spermine, or the ϵ -amino group of lysine generates a new primary amine bearing species that can be further crosslinked (Crosslink II) by TG.^[132] Interestingly, TGases comprise an intrinsic specificity towards the applied glutamine residue, whereas a broad variety of amine-containing acyl-donors is accepted.^[134]

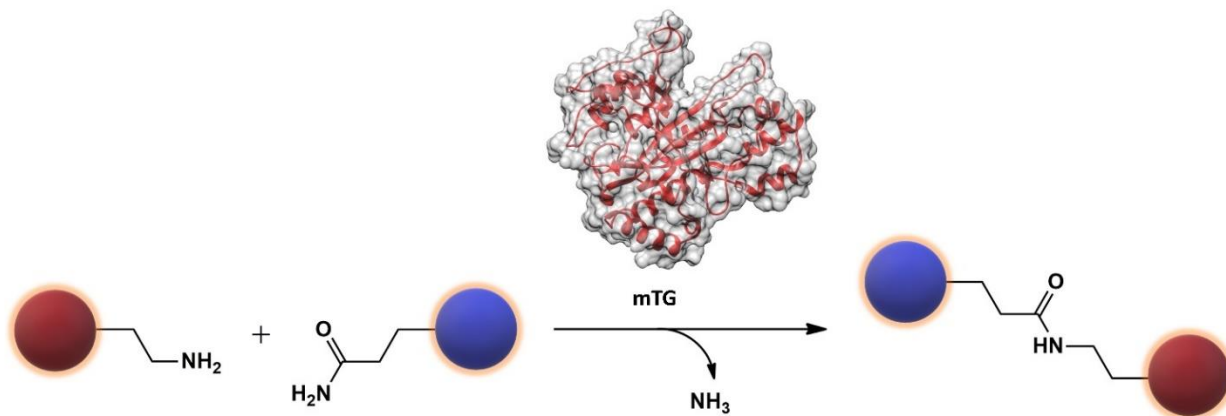


Figure 9. Mechanism of action of transglutaminases. The protein- or peptide-bond glutamine side-chain are covalently cross-linked to the lysine counterparts. The formation of an isopeptide bond is accomplished under the release of ammonia. modified from Schneider et al. see section 4.3

In nature, this mechanism is used for the conjugation of the glutamine side chain as acyl donor and the ϵ -amino group of lysine as acyl acceptor, to intra- or intermolecularly crosslink proteins.^[132] Further, in multicellular organisms the generated isopeptide bonds add strength to tissues and increase their resistance to degradation.^[130, 132] To date, different mammalian transglutaminases (TGases) are known, among them blood coagulation factor XIIIa, keratinocyte TGase, epidermal TGase, tissue TGase, prostate TGase, TGase X/Y/Z and transglutaminase 2 (TG2). TG2, for example, crosslinks proteins on the outer surface of the squamous

epithelium.^[130, 132, 133] In contrast, blood coagulation factor XIIIa catalyzes crosslinking of fibrin molecules during blood clotting.^[133, 135] Furthermore, bacterial transglutaminases (mTGs) have been discovered by thorough screening of different microorganisms.^[130] These transglutaminases catalyze the same reactions, even lacking sequential or structural homology.^[130]

However, not all of these TGases are suitable for biotechnological applications.^[133] Thus, mTG derived from the Gram-positive actinobacterium *Streptomyces mobaraensis* comprising good reactivity combined with stability represents the most applied TGase.^[133] Exemplarily, it is applied in food processing where it acts as natural glue to texture meat and dairy products, for half-life extension by PEGylation of protein drugs, surface immobilization of proteins, and to covalently attach nucleic acids to proteins (Figure 10).^[136]

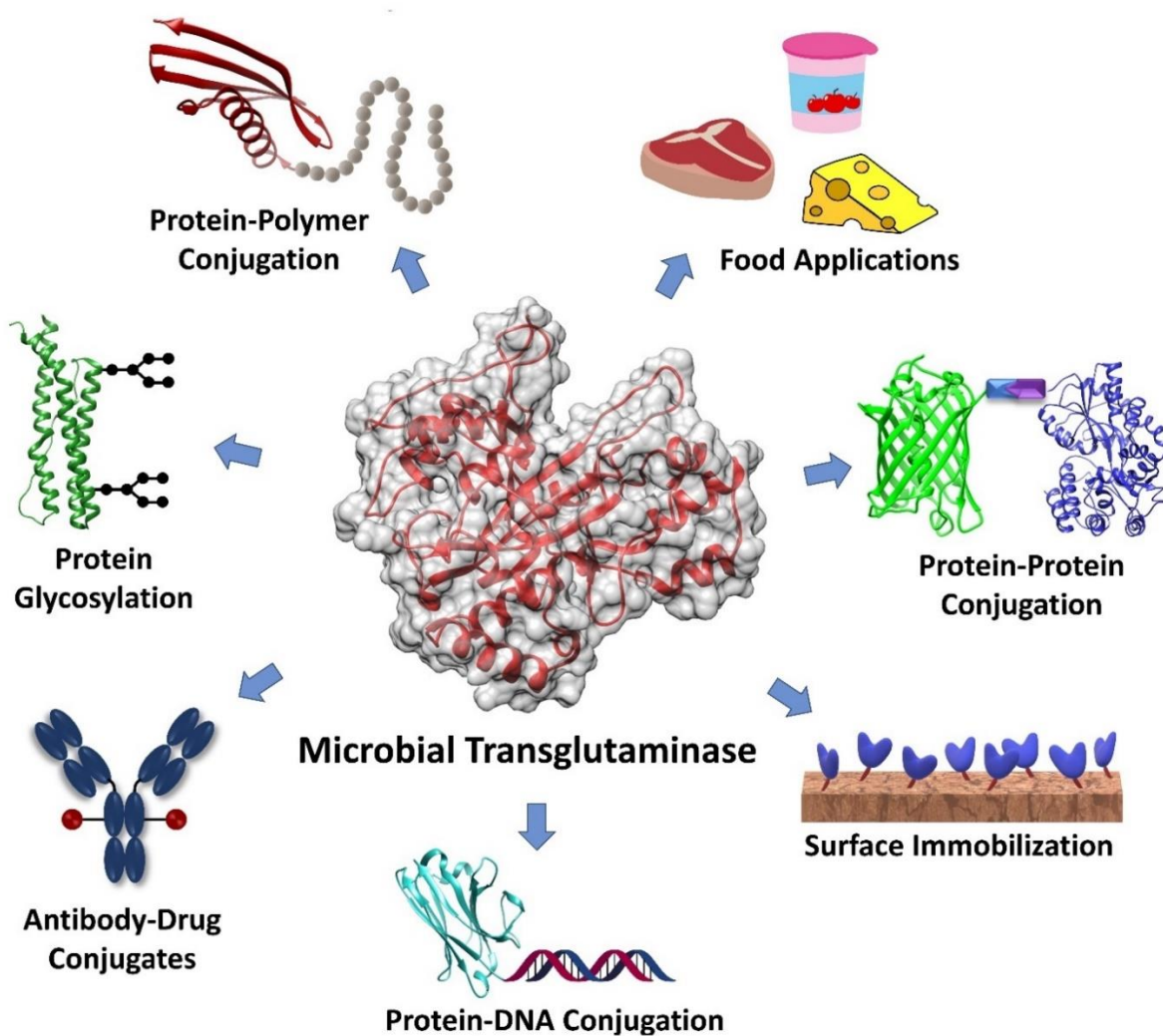


Figure 10. Overview of biotechnological and industrial applications of microbial transglutaminase. adapted from Schneider et al. see section 4.3

1.4.5. ADCs Assembled under mTG Catalysis

The need for the generation of homogenous ADCs has placed mTG in the focus of intensive research. Thus, numerous approaches towards covalent attachment of a desired payload to an antibody were carried out. First

approaches aimed at modifying native antibodies resulted in poor modification of lysine residues with glutamine-containing peptides and nearly no modification when glutamine sites were addressed.^[137] However, the observation that genetic aglycosylation significantly enhanced labeling paved the way for mTG-mediated assembly of ADCs.^[137] Consequently, in the following years either genetically aglycosylated or enzymatically deglycosylated antibodies were applied to site-specific ligate different payloads (Figure 11). A second milestone is engineering towards incorporation of glutamine-bearing motifs that are specifically recognized by mTG. In comparison to Sortase A, these motifs can also be introduced at internal positions highlighting the flexibility of mTG-based approach.^[138] Thus, the numerous internal or terminal positions were examined regarding stability, toxicity, and efficacy of the generated ADCs.^[138]

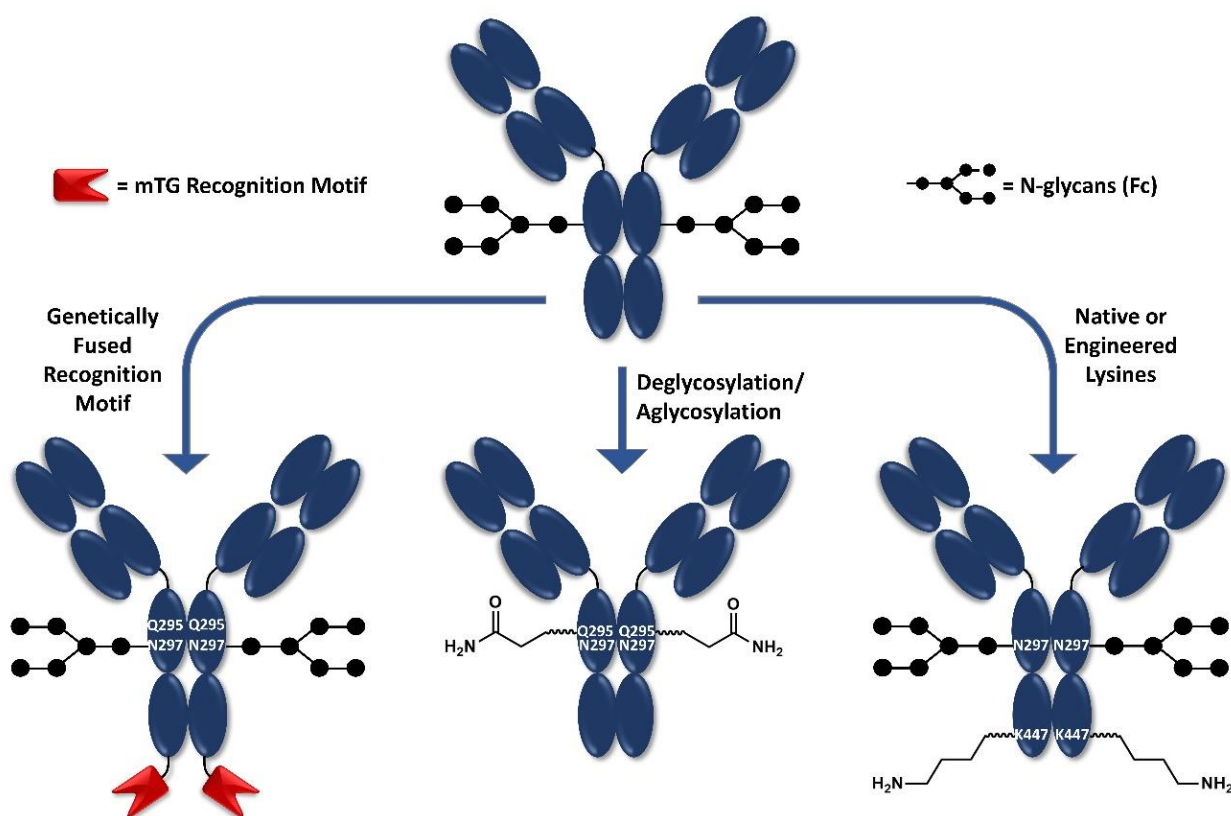


Figure 11. Transglutaminase-addressable antibodies. (top) Native, glycosylated antibodies are no substrate of mTG. (bottom) Strategies for transamidation: (left) genetic incorporation of specific recognition motif; (middle) genetic or enzymatic removal of the CH₂ glycan moiety to expose Gln295; (right) engineering of reactive lysines in surface exposed areas or addition of C-terminal residues to prevent Lys447 from intracellular processing. modified from Schneider et al. see section 4.3

Besides addressing native or engineered glutamine residues of the antibody, natural or engineered lysines were examined as conjugation site for the generation of ADCs.^[139, 140] Hence, lysine-bearing recognition motifs or solitary lysines were genetically incorporated. Further, introduction of additional amino acids at the C-terminus enabled labeling at lysine 447 by preventing its intracellular enzymatic cleavage resulting in minimal mTG recognition tags.^[139]

Besides direct conjugation with a cytotoxic compound, chemo-enzymatic two-step procedures were investigated (Figure 12). Herein, in the first step amine-bearing chemical handles, like DBCO, BCN or azides were introduced and used for payload conjugation in the second step.^[141-144] This procedure combining site-specificity

of mTG catalysis with orthogonal chemistry displays a modular and convenient method for the assembly of ADCs. These site-specific procedures not only result in homogeneous and reproducible ADCs, but also permit to examine the influence of attachment site, linker and the payload itself.^[138] Thus, numerous approaches applying ADCs assembled under mTG catalysis were reported, which were aimed at improving therapeutic properties of the generated ADCs. These are the increase of DAR, enhanced lysosomal trafficking, linker stability, and modulation of parental antibody affinity, for example. A more detailed insight into the current status of site-specific ADCs assembled under mTG catalysis can be found in the review presented in the cumulative section (section 4.3).

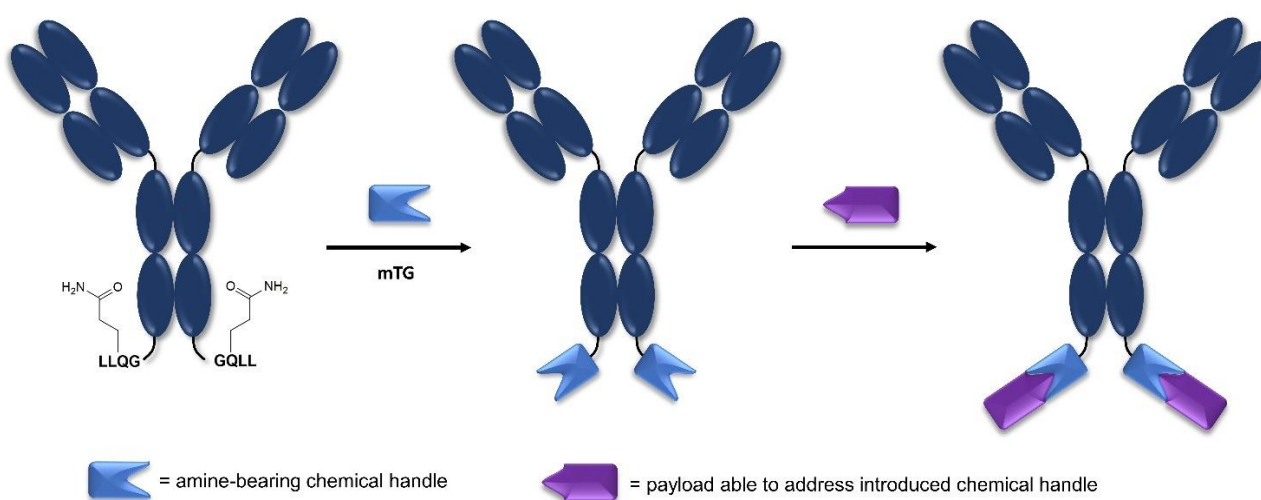


Figure 12. Exemplary chemoenzymatic two-step procedure for mTG-mediated ADC assembly. First, an amine-bearing chemical handle is introduced that is subsequently used for payload attachment.

1.5. High-DAR ADCs

As aforementioned, the applied cytotoxins in the context of ADCs need to be highly potent to be efficient at the given intracellular concentrations.^[7] Further, inefficient internalization and intracellular trafficking additionally decrease efficacy of the ADC.^[6] Thus, increasing cytotoxicity of the payload or arming the ADC with a higher number of toxins per antibody were the obvious choices to enhance efficacy of an ADC. Trial-and-error approaches over the last decade led to the conclusion that toxins with potencies in the sub-nanomolar range are required.^[145] However, the majority of applied potent cytotoxic drugs is highly hydrophobic, which may promote aggregation and enhanced recognition by MDR transporters.^[13, 60] As the number, site, and hydrophobicity of the conjugated toxin strongly influences stability, pharmacokinetic properties and efficacy of ADCs, a careful design is required to develop an effective ADC for tumor treatment.^[102, 138]

In a comparative study addressing potency and safety of conventional thiol-maleimide conjugates in dependence of their DAR, Hamblett et al. showed that a DAR 4 anti-CD30 ADC was superior to a DAR 2 and DAR 8 ADC if hydrophobic MMAE was used as a payload.^[146] The DAR 8 ADC possessed poor pharmacokinetic properties, enhanced toxicity and displayed a lower therapeutic index in mice.^[146] Thus, the authors concluded that drug loading is a key design parameter for ADCs and a drug loading of 2-4 may yield the optimal therapeutic

window. Further, Sun et al. concluded that very high-DAR, thus more hydrophobic, ADCs suffer from decreased efficacy likely due to faster liver-mediated clearance.^[147] Therefore, maytansin-based ADCs comprising a DAR of 3-4 were chosen for further clinical evaluation. However, higher-DAR ADCs were still considered for tumor antigens with low expression levels or inefficient intracellular processing.^[147] DNA alkylating agents like pyrrolobenzodiazepines (PBDs) represent another class of clinically relevant toxins, found to be even more potent, which limits the typically DAR of ADCs comprising these class toxins^[145, 148] In addition, high-DAR ADCs may enable the application of milder toxins.^[145]

Besides the obvious progress in the field of ADCs, achieving a high DAR without affecting hydrophilicity is still a major challenge. To that end, several approaches relying on more hydrophilic payloads or linkers were applied, among them e.g. a short polyethyleneglycol (PEG) chains. Using this strategy, two ADCs targeting either Trop-2 (IMMU-132) or CEACAM5 (IMMU-130) were assembled bearing the hydrophobic DNA topoisomerase inhibitor SN-38 with an average DAR of 7.6 and 7.5, respectively. Hereby, conjugation proceeded by addressing reduced cysteine thiols of antibodies by maleimide-bearing payloads.^[149, 150] Daiichi Sankyo reported an ADC where a toxic exatecan derivative was assembled with an antibody *via* an enzymatically cleavable peptide linker (GGFG) equipped with a self-immolative linker with an aminomethyl moiety and bearing at the C-terminus an additional hydrophilic group.^[151, 152] A DAR 8 ADC targeting HER2 revealed excellent tumor activity against T-DM1-insensitive and in HER2-low expression models.^[152]

Researches from Seattle Genetics applied more hydrophilic polyethylene glycol- (PEG)-bearing branched linkers to generate DAR 8 ADCs with larger therapeutic index (TI).^[153] Hereby, excess tris(2-carboxyethyl)phosphine) TCEP was applied to fully reduce hinge disulfides. This approach was further optimized by evaluating the length of different PEG chains, whereby ADCs comprising branched PEG₁₂ linker arose as lead candidates.^[154] In another approach addressing reduced interchain disulfides, Seattle Genetics developed ADCs carrying multiple payloads applying orthogonal cysteine protection and PEGylated linkers to site-specifically conjugate each drug.^[155] This approach opens avenue for the screening of dual-drug ADCs and presumably may lead to synergistic effects, thus improved activity. Furthermore, Mendelsohn et al. from Agensys introduced more hydrophilic pyridine derivatives of auristatin, called MMAPYE. These were assembled to ADCs by maleimide conjugation to reduced interchain disulfides and may enable overcome known drawbacks of hydrophobic payloads.^[156] A similar approach by Satomaa et al. made use of more hydrophilic auristatin glycoside payloads combined with conjugation to reduced interchain disulfides.^[157] Obviously, auristatin-D-glucuronide (MMAU) represents a novel promising hydrophilic payload for the application in context of ADCs.

Further, Sanofi reported PEG-containing multivalent drug linkers applying more hydrophilic MMAD (compared to MMAE) as payload to address reduced interchain disulfides resulting in potent ADCs comprising DARs of up to 10.8.^[158] In addition, a novel approach by Gupta et al. relied on platinum(II)-based linker for efficient interchain cysteine re-bridging.^[159] These linkers were found to improve stability compared to traditional maleimide-linked ADCs. Furthermore, they were equipped with PEG chains to reduce the overall hydrophobicity. Besides addressing reduced interchain disulfides, the introduction of site-specific conjugation methods enabled the decoration with payloads at a desired site of an ADC. Thus, a comparative study by researches from Pfizer/Rinat showed that high-DAR ADCs site-specifically assembled under mTG catalysis can overcome the previously reported limitations of conventionally assembled ADCs.^[102] As a high number of hydrophobic

payloads in proximity showed lower *in vivo* exposure, the authors concluded that the conjugation site is a major influential factor for *in vivo* exposure.^[102] A minimization of solvent accessibility of the hydrophobic payloads was recognized as key element in the assembly of ADCs.^[102] Notably, even though all of these approaches yielded high-DAR ADCs, none was able to fully shield the hydrophobicity of the conjugated toxin resulting in an ADC at least as hydrophilic as the unmodified parental antibody.

Moreover, numerous approaches emerged aimed at half-life extension and enhanced hydrophilicity of proteins, which apply both chemical methods and genetical engineering. PEGylation, conjugation to dextran polysaccharide or recombinant PEG mimetics like XTEN or PAS, HESylation, polysialylation, HAylation, *N*- and *O*-glycosylation, lipidation, and fusion with albumin for enhanced FcRn-mediated recycling are only a few to be mentioned.^[160] Despite the fact that not all of them were used for ADC assembly, various polymeric multivalent linker systems able to carry the desired number of payloads were introduced. In 2005, Yurkovetskiy et al. applied a degradable poly-1-hydroxymethylethylene hydroxymethyl-formal (PHF) as acyclic mimetic of polysaccharides and alternative to PEG.^[161] These polyacetals comprise pH-sensitive acetal groups stable in the extracellular environment (pH 7-7.5), but cleavable at the acidic pH of the intracellular vesicular compartment.^[161] PHF can be chemically assembled or accessed by complete lateral periodate-mediated cleavage of dextran B-512. Periodate oxidation of the 1-6 polyglycoside followed by borohydride reduction gave rise to polyals with pendant hydroxymethyl groups and vicinal glycol groups (Figure 13).^[161-163]

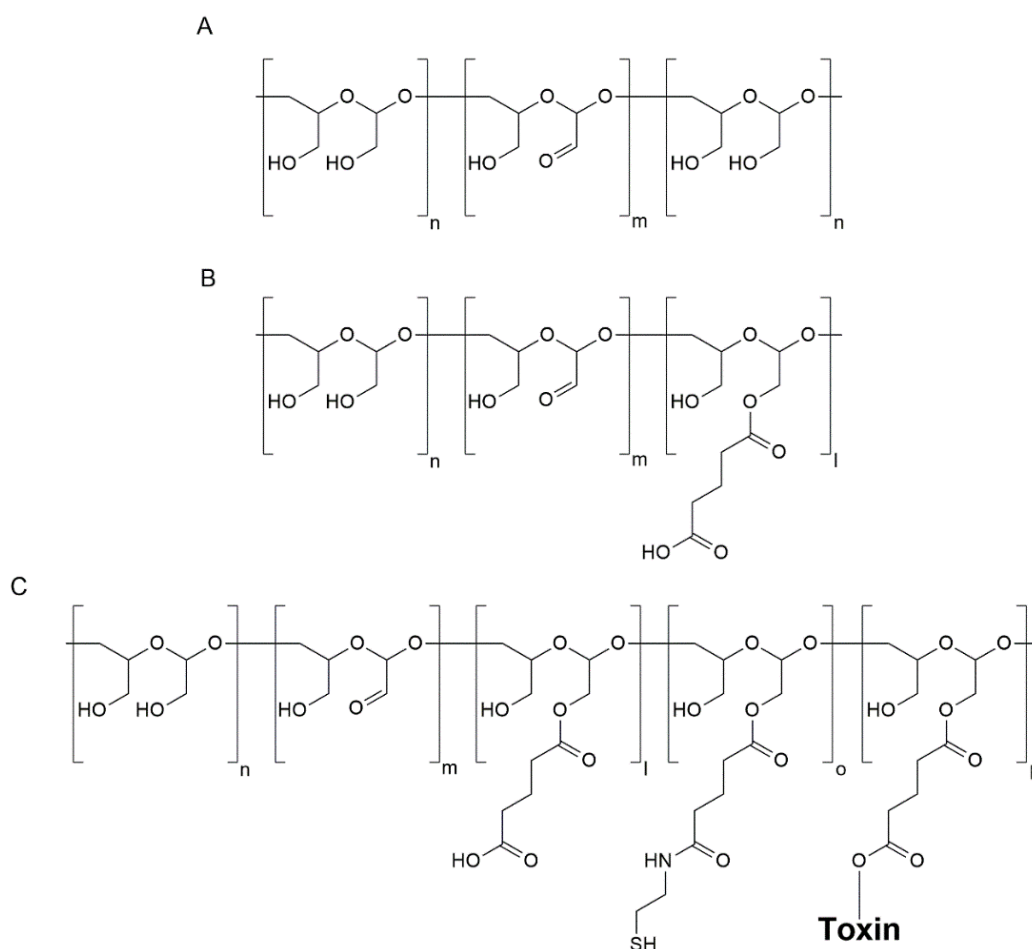


Figure 13. Fleximer®. A Schematic representation of poly-1-hydroxymethylethylene hydroxymethyl formal (PHF) (A), PHF-glutaric acid (B) and PHF equipped with toxin and thiols for antibody conjugation (C).^{modified from Yurkovetskiy et al.[163]}

Subsequently, decoration with glutaric acid through esterification gave rise to a polymer loaded with multiple moieties addressable towards amide-bond formation with the amine-bearing *N*-(3-hydroxypropyl)vinidene alanine (NH₂-Ala-HPV) and a bidentate linker bearing a protected thiol.^[163] Both moieties were coupled stoichiometrically. After deprotection of the thiol, the Fleximer[®]-toxin conjugate was stoichiometrically coupled to either a maleimide-bearing trastuzumab or rituximab assembled by standard succinimidyl 4-(*N*-maleimidomethyl)cyclohexane-1-carboxylate (SMCC) procedure. This procedure yielded ADCs comprising DARs of up to 20 and revealed single digit nanomolar IC₅₀ on different HER2-positive cell lines and effective tumor growth inhibition *in vivo* using HER2(+++) NCI-N87 human gastric cancer and BT-474 breast cancer xenograft models.^[163]

The authors concluded that the high hydrophilicity and polyvalency of the polymer enabled the generation of high-DAR ADCs without compromising the physicochemical and pharmacokinetic properties. Notably, neither SDS-PAGE nor chromatographic analysis, e.g. hydrophobic interaction chromatography (HIC) or size-exclusion chromatography (SEC), elucidating hydrophilicity was performed in this study to confirm the success of two stoichiometrically controlled reactions. Notwithstanding, potent high-DAR ADCs were achieved paving the way for the application of milder toxins in a higher number.

Furthermore, an additional improved polymer-based ADC based on Dolafelxin[®] platform was introduced by Mersana.^[164] The assembled ADCs comprised a high load of auristatin F-hydroxypropyl amide (auristatin F-HPA), a synthetic analogue of dolastin 10, linked to the Fleximer[®] scaffold conjugated to a HER2-targeting antibody. Hereby, the ADC, called XMT-1267, was assembled by addressing reduced interchain cysteines resulting in less heterogeneity. However, incorporation of thiol groups onto Fleximer[®] was still performed in a stoichiometrical manner, thus yielding heterogenous species with different numbers of toxins and Fleximers[®] conjugated per antibody. Nevertheless, this procedure revealed a polymer-dependent stabilization of the reduced antibody which is achieved by formation of interchain bridges between the polymer backbone and the antibody's thiols.^[164] Furthermore, prolonged plasma half-life and tumor specific accumulation was reported for this ADC featuring a DAR of 20. In addition, tumor growth inhibition in BT-474 xenograft models was observed applying a low dose of 2 mg/kg.^[164]

In addition, *N*-(2-hydroxypropyl)methacrylamide (HPMA) was reported as polymeric scaffold for the generation of high-DAR ADCs. For instance, an approach by Zhang et al. based on rituximab (RTX) and HPMA copolymer-epirubicin.^[165] Hereby, epirubicin was incorporated onto HPMA by a controlled living polymerization resulting in a well-defined polymer-drug conjugate bearing a single maleimide for antibody conjugation. Thus, ADCs targeting CD20 were assembled by conjugation to reduced interchain cysteines of the parental antibody. Depending on the average number of conjugated polymers (3.1 - 6.5) the DAR of the generated ADCs varied from 20.6-42.9, respectively. Interestingly, even the ADCs comprising the highest DAR were found soluble in water and no aggregation was observed. However, assembled ADCs revealed a polymer ratio-dependent decrease of affinity. Thus, a conjugate equipped with an average of 3.1 polymers retained 50 % of parental binding affinity, whereas that equipped with an average of 6.5 only retained 30 % of binding affinity. In an *in vivo* Ramos xenograft model on CD20-positive NOD SCID mice the DAR 20 ADC was found superior compared to the combinations of rituximab with HPMA-epirubicin respectively solitary epirubicin. Furthermore, a non-binding HPMA-epirubicin ADC was found non-toxic.^[165]

1.6. Dextran

Dextran is a naturally occurring polysaccharide. Today, different polymers of this class are used in biochemical applications. In recent years, numerous approaches applying polysaccharides like cellulose, starch, chitosan or dextran were developed. These natural polymers differ by the backbone sugar, linkage and the extent of branching within the polymer chain. Thus, cellulose is connected by β -D-glycosidic bonds of glucose, chitosan is composed of randomly distributed β -D-glucosamine (deacetylated unit) and *N*-acetyl-D-glucosamine, whereas dextran and starch are linked by α -D-glycosidic bonds of glucose. Due to the structure of these polysaccharides, chitosan, starch and cellulose are only poorly soluble in water. In cellulose and chitosan every sugar monomer is rotated by 180 ° with respect to its neighboring monomers promoting the formation of intra- and intermolecular hydrogen bridges and thus restricting water solubility. In contrast, starch consists of roughly 25 % of almost linear amylose and of 75 % highly branched amylopectin.^[166] Hereby, the intrinsic branching results in weak solubility in water. The mainly linear dextran polysaccharides with minimal branching ratio are good water-soluble and rather homogen.

Dextran was first studied a hundred years ago when its high viscosity caused trouble in the beet-sugar industries.^[167] This α -glucan is mainly produced by bacteria belonging to the order of *Lactobacteriaceae*, family *streptococcaceae*, genus *Leuconostoc*, species *L. mesenteroides* (*Betacoccus arabinosaceus*) and *L. dextransicum* when cultured on sucrose as carbon source.^[167-169] However, to some extent it is chemically synthesized from levoglucosan (1,6-anhydro- β -D-glucose) *via* a cationic ring-opening polymerization.^[170, 171] The enzyme polymerizes the glucose moiety of sucrose to dextran under the release of the fructose monomer.^[168, 172] The proposed mechanism for *L. mesenteroides* B-512 F is described as follows. In a first step dextransucrase bearing two sucrose binding sites and one acceptor binding site forms two covalent glucosyl-enzyme complexes (Figure 14).^[172] In the second step a nucleophilic attack of the hydroxyl group located at the non-reducing end of the acceptor to C-1 of one of the two glucosyl residues that are covalently bond to the enzyme takes place.^[172] Several sugars, like maltose or isomaltose, can inhibit dextran synthesis and yield acceptor products (Figure 14).^[172] Repetition of step two leads to the formation of dextran polysaccharide. However, a complete knowledge of the actual structure of the active site is still missing, as no experiment could give evidence that a distinct acceptor binding site exists.^[173]

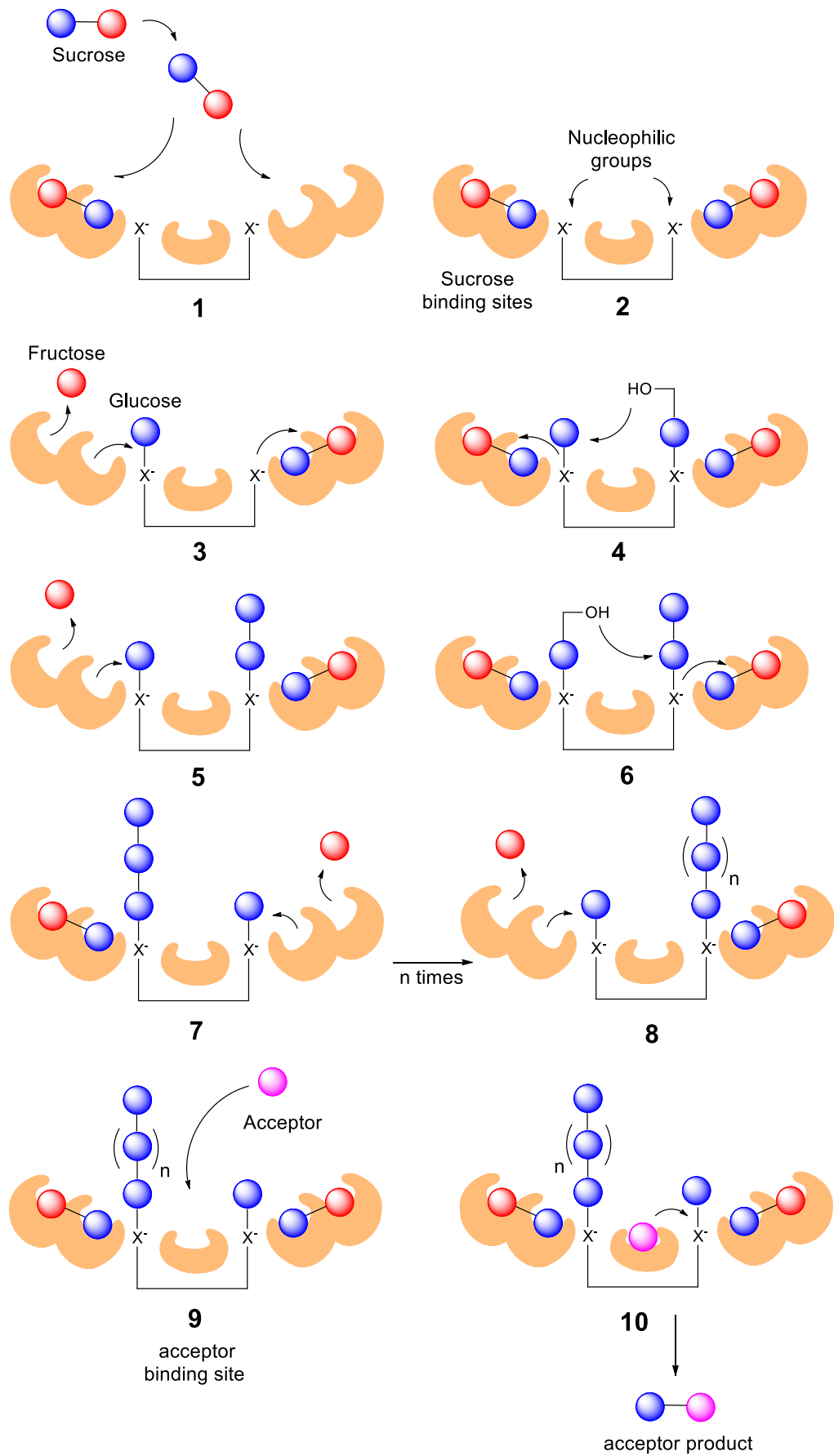


Figure 14. Proposed mechanism for the enzymatic polymerization by dextran sucrose from NRRL B.512F resulting in dextran with minimal α -1,3-branching. modified from Plou et al. [172]

The central structure of dextran consists of α -1,6-glycosidic linkage with some degree of branching.^[174] For solubility of dextran the degree of branching is a key element as higher branched dextrans are poorly water-soluble.^[175] Therefore, dextran from *Leuconostoc mesenteroides* B-512 is of special interest, as it is characterized by a content of 95 % α -1,6-glycopyranosidic linkages and only 5 % of 1,3-linkages (Figure 15).^[160, 174, 175] These 1,3-linkages are attachment points for side chains. 85% of these comprise only one or two glucose residues, whereas the remaining 15% have an average length of 33 glucose units.^[160, 174, 175] Other dextransucrases originating from different bacteria produce dextran with different percentages of branching. Exemplary, dextransucrase from *L. mesenteroides* B-1299 assembles dextran exhibiting a higher degree of branching and additional α -1,2 branching.^[172] Additionally, dextran differs in the degree of polydispersity, which has severe effects on its behaviour *in vivo*.^[175] However, today dextrans with a broad range of molecular weights and narrow polydispersity (PDI) are readily commercially available.

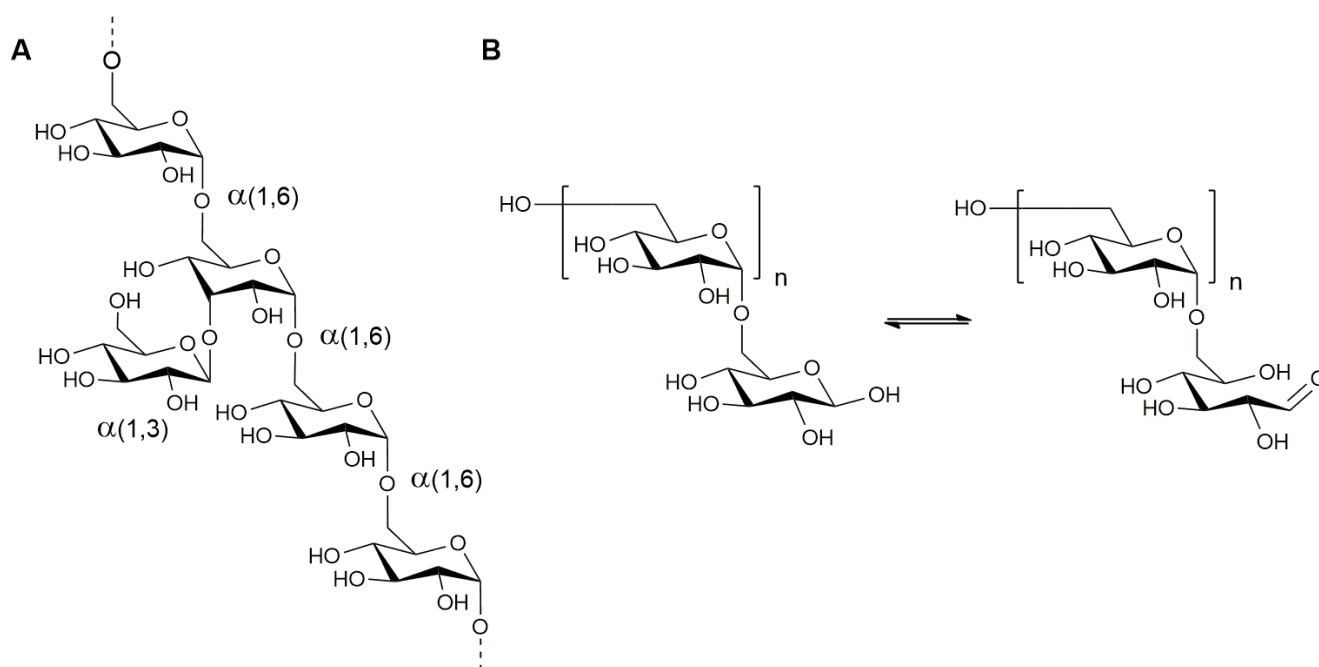


Figure 15. Structure of dextran from *Leuconostoc mesenteroides* B512. (A) The repeating glucose units are mainly connected by α -1,6-glycopyranosidic linkages with 1,3-linkages as attachment points for branching. The degree of branching is approximately 5 %. Herein, 85 % of these branches comprise only one or two glucose residues, whereas the remaining 15 % have an average length of 33 glucose units. (B) Equilibrium of the reducing end of dextran allowing for addressing the orthogonal aldehyde moiety.

The almost linear structure and its good water solubility makes dextran a promising scaffold for payload conjugation and linkage to the proteins of interest. Commercial dextran with a molecular weight of 70000 is applied in solution to restore and to maintain the blood volume for the treatment of shock, hemorrhage and burns.^[174] Further, dextran 40000 is used to improve capillary flow and for the treatment of vascular occlusion.^[174] In the United States it is clinically approved and used as 6 or 10 % aqueous solutions containing either 40000 or 70000 kDa dextran for blood-flow enhancement or as plasma-volume expander.^[175] Additionally, the FDA has granted dextran the status GRAS meaning “generally regarded as safe”.^[160]

Dextrans can be depolymerized by dextranases present in various organs of the body, among them spleen, kidney, liver, and the lower part of the gastrointestinal tract, with liver and spleen being the predominant locations.^[174, 175] However, *in vitro* studies showed that modification of dextran reduced depolymerization.^[174, 176, 177] Furthermore, biodistribution studies with fluorescein-labeled dextran revealed that its tissue disposition depends on molecular weight. Thus, low-molecular-mass dextrans are excreted unchanged in the urine, whereas dextrans with higher molecular mass show accumulation in the liver and the spleen.^[175, 178-180] It should be noted that although dextran-reactive antibodies have been involved in anaphylactoid reactions,^[181-183] and antibodies against chicken serum albumin-dextran conjugates were generated in mice,^[184] no reports of antibodies against dextran conjugates in humans have been published to date.^[160]

Offering certain space for modifications at numerous positions, dextran has come into the focus as viable carrier for diverse compounds.^[160, 175] Historically, oxidation of glucose hydroxyls was chosen to generate reactive aldehydes that were subsequently addressed by a suitable nucleophile, e.g. primary amine (Figure 16). Thus, periodate-oxidized dextran bearing numerous aldehyde moieties was reacted with a primary amine resulting in a Schiff base. Subsequent reduction yielded stable protein- or drug-dextran conjugates. In general, periodate oxidation is a standard procedure towards linkage of polysaccharides and diverse biomacromolecules.^[160, 175] For instance, soy trypsin inhibitor-^[185] and uricase-dextran^[186] conjugates were generated as well as a somatostatin-dextran conjugate with low-nanomolar binding affinity, extended PK profile and prolonged half-life in mice.^[187] A superoxide dismutase- (SOD)-dextran conjugate retained over 80 % activity when conjugated in average with 4.4 dextran units per SOD, while the anti-inflammatory activity of SOD was doubled.^[188] Additionally, the enzyme was found to be more resistant to H₂O₂-mediated inactivation and revealed a prolonged half life.^[188] The prolonged half-life was conditioned by an enlarged hydrodynamic radius combined with the increased stability of the protein-dextran conjugates.^[188] In additional studies, reduced immunogenicity of antibodies or Fabs bound to dextran scaffolds was revealed.^[189, 190] However, the presence of numerous amine moieties on most proteins led to rather heterogenous dextran-protein conjugates and crosslinking of the proteins.^[160]

Other historical conjugation methods made use of phosgene activation or cyanogen halides.^[160] However, the application of these methods has declined over the years. Moreover, carboxymethylation or the application of carbonyl diimidazole (CDI) as activating agent were used to address dextran's hydroxy groups.^[191, 192] The former methodology generates carboxymethyl dextran by utilizing bromoacetic acid under basic conditions, whereas the latter is applied to synthesize dextran equipped with multiple amine groups.^[191, 192] In a recent report, Richter et al. applied dextran for the covalent attachment of multiple BH3 peptides to effectively induce apoptosis by addressing the intracellular target Bcl-xl in a multivalent manner.^[193] In this approach uptake was achieved by nucleofection or by application of cell penetrating peptides (CPPs), that were covalently attached to the dextran backbone. To this end, carboxyethylation was performed by a Michael-type addition of acrylamide under basic conditions followed by hydrolysis of the generated amide. Interestingly, carboxyethylation was observed solitarily at the position C2, as shown by 2D-NMR analysis of the resulting constructs. Subsequently, a thiol-bearing amine linker was incorporated at the dextran backbone upon formation of an amide bond. Conjugation of thiol-bearing Bid-BH3 gave rise to potent apoptosis-inducing constructs. Multivalent binding of Bid-BH3 peptides conjugated to dextran scaffold led to the replacement of Bac-protein, which triggers the formation of membrane pores by oligomerization.^[193] In this approach either

nucleofection of the multivalent polysaccharide-peptide constructs or the application of CPPs conjugated to the scaffold both resulted in effective triggering of apoptosis.^[193]

The reducing end of dextran comprises one distinct aldehyde moiety due to equilibrium between the closed-chain (cyclic) and open-chain (acyclic) glucose forms (Figure 15). This solitary moiety opens space for modification with a primary amine by reductive amination, lactonization or oxime ligation. Thus, numerous approaches were reported to conjugate small molecules,^[174] enzymes^[194] or polymers^[195, 196] to the reducing end of dextran. For instance, Valdivia et al. combined reductive amination of a diamine with mTG-catalyzed conjugation of the resulting amine-bearing dextran to catalase.^[197] This approach yielded a more stable protein-dextran conjugate with increased catalase activity and improved pharmacokinetic properties as an increased plasma half-life and reduced total clearance in rats was observed.

Since the early 1980s dextran has been applied as a multivalent scaffold for the generation of ADCs.^[198-203] In these hybrid architectures, dextran was applied as a bridge between an antibody and cytotoxic payloads. Hurwitz et al. conjugated daunomycin and cytosine arabinoside to aldehydes of periodate-oxidized dextrans.^[198] After the drugs had been attached, the antibody was bound to the remaining aldehydes *via* its lysines.^[198] Consequently, the formed conjugates were stabilized by partial reduction either by sodium borohydride or sodium cyanoborohydride. In addition, adriamycin was conjugated by formation of a stable hydrazone between hydrazide groups located on dextran scaffolds and the keto group of the tetracycline side-chain. The antibodies were subsequently linked to this derivative *via* glutaraldehyde.

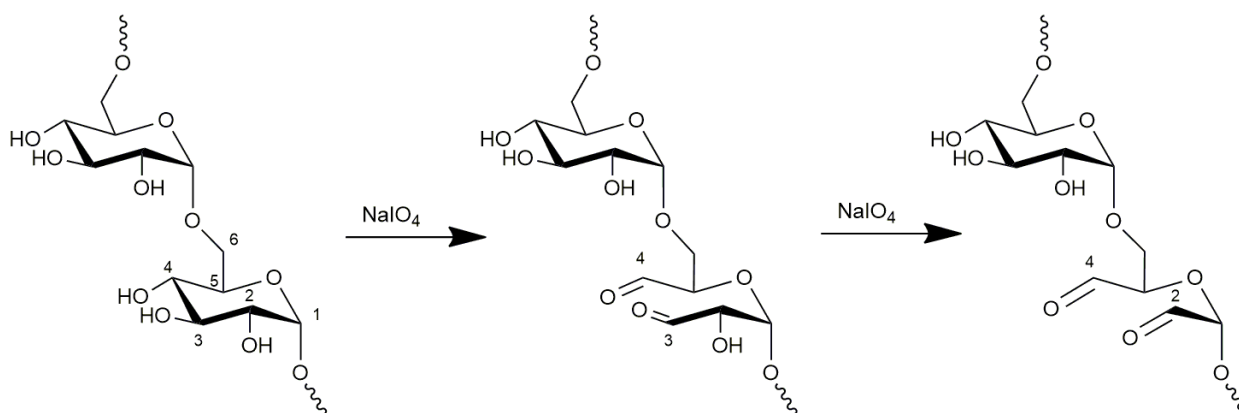


Figure 16. Periodate oxidation of dextran resulting in aldehyde moieties and a corrupted glycoside backbone. Modified from Maia et al.^[204]

Periodate-oxidized 5-fluorouridine was coupled to dextran in a similar fashion. Both approaches applied sodium cyanoborohydride to stabilize the generated compounds. The dextran-bridged ADCs maintained high drug activity and only a 50 % loss of antibody activity was observed. Furthermore, two approaches applying the above-mentioned procedure were used to couple daunomycin to monoclonal mouse or polyclonal horse antibodies targeting rat α -fetoprotein (AFP).^[201, 203] In another approach, Shih et al. conjugated methotrexate (MTX), to a monoclonal anti-carcinoembryonic antigen (CEA) antibody using an aminodextran carrier system.^[200] To that end, dextran was partially oxidized and the resulting polyaldehyde was reacted with 1,3-diamino-2-hydroxypropane yielding an amino-dextran after a reduction with sodium borohydride. MTX conjugation was attained by either utilizing *N*-hydroxysuccinimide(NHS)-activated MTX or by conjugation under

EDC activation. The MTX-dextran conjugate was linked to an oxidized IgG obtained by sodium periodate oxidation followed by a stabilizing reduction step. The generated DAR 30-50 molecules showed a significant retention of binding capacity and possessed improved pharmacokinetic properties in BALB/c mice and in hamsters. Further, these compounds demonstrated cytotoxicity against HT-29 or LoVo colon tumor cells *in vitro*. However, a lower cytotoxicity of dextran-bridged MTX-ADCs, compared to the solitary toxin, was found on LoVo cells. The authors attribute this observation to a different receptor-mediated uptake mechanism of the antibody-dextran conjugate which is dependent on efficacy of antibody internalization and receptor density. It should be noted that the extra amino groups on the dextran may confer the conjugate to non-target cells and may provoke aggregation with negatively charged antigens.^[200] Furthermore, Oseroff et al. applied dextran to conjugate multiple chlorin e₆ photosensitizer payloads to a monoclonal antibody.^[199] Periodate-oxidized dextran was conjugated with ethylenediamine and with amine-modified chlorin e₆ monoethylenediamine monoamide derivative to generate partially amine-modified dextran equipped with multiple photosensitizers. Subsequently conjugation to oxidized anti-T cell mAb anti-Leu-1 resulted in ADCs that exhibited DARs up to 36. The generated conjugates retained most of their binding activity, while the quantum efficiency of the bound chlorin e₆ was not affected. Further, these ADCs revealed a light- and target-dependent photodestruction on HPB-ALL T-cell leukemia cells *in vitro*.^[199] In general, being applied as cargoes in ADCs, photosensitizers can improve the performance of antibodies which possess certain off-target binding, as laser irradiation is needed to trigger their cytotoxicity, thus specifying and directing an application site.

However, all the above-mentioned ADCs were conjugated stoichiometrically by addressing either the antibody's lysines or the stoichiometrically generated aldehydes of an oxidized antibody, resulting in heterogenic ADCs. Furthermore, payload was conjugated to oxidized-dextran, which additionally results in heterogeneity of the corrupted polysaccharide.

1.7. Multivalent Binding and Death Receptor 5 Clustering

Multivalency is often used by nature to achieve strong interaction between different interfaces or molecules by magnification of the multiple weak forces (Figure 17).^[205] Arctium, also known as burdock, is a prominent example of this effect. Its seeds composed of thousands of miniature hooks and loops, can easily cling to and hold on fur of animals or clothes, though a single hook cannot.^[206] Velcro-type releasable fasteners are an example of bioinspired applications proposed by the swiss engineer George de Mestral after observing sticking burdock seeds.^[207] Another example obtained from nature is the wing-locking device of beetles, which utilizes densely populated microtrichia on the cuticular surface to interlock their wings to maximize lateral adhesion and prevent lateral movement.^[206, 208]

In the immune system the first-line defense also takes advantage of multivalent binding. For instance, IgM that represents the first immunoglobulin produced after exposure to an antigen is secreted either in a pentameric form connected by a joining chain or as a hexamer lacking the joining chain comprising ten or twelve antigen-binding sites, respectively.^[209] IgM antibodies exhibit rather weak binding affinities compared to affinity-maturated IgGs. However, the multivalent binding of this immunoglobulin mediates an avidity-enhanced functional binding capacity. Notably, not all ten, respectively twelve, antigen-binding sites can bind

simultaneously due to steric hindrance. Furthermore, IgA representing the major class of antibodies present in mucosal secretions and being part of first-line defence against inhaled and ingested antigens is produced in a dimeric form.^[210] Being synthesized locally at mucosal sites, it is transported across the epithelial cell boundary and out to secretion by interaction with the polymeric immunoglobulin receptor.^[210] These dimers are linked by an end-to-end connection of the heavy chains, and stabilized by disulfide bridges and a joining chain (Figure 3).^[210] Additionally, IgA has been found in serum of many species acting as second-line defense against pathogens which have breached the mucosal surface.^[210] In general, immunoglobulins possess at least two binding sites, thus demonstrating that multivalency is a useful tool to enhance binding.

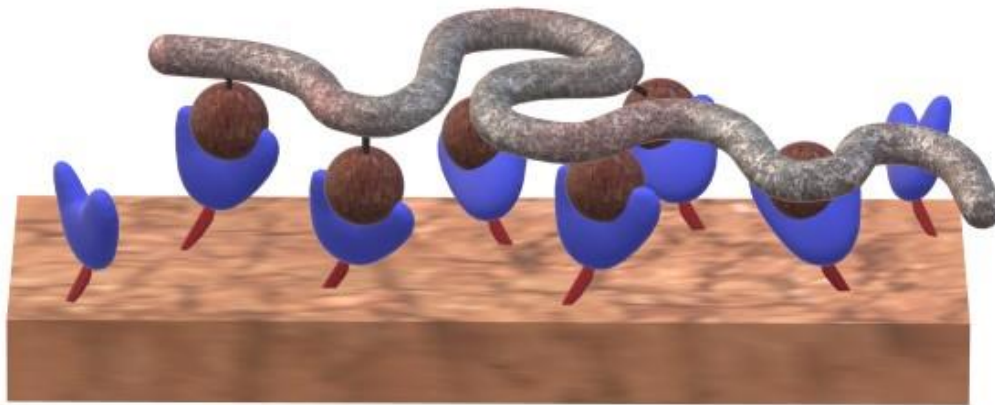


Figure 17. A multiple ligand-bearing scaffold enables multivalent binding to a cell surface.

In recent years, besides the classical chemotherapy or targeted approaches, killing of tumor cells by activation of apoptosis-triggering cascades has become a promising field for investigations.^[211] Herein, a major breakthrough was the discovery of the tumor necrosis factor (TNF) superfamily and TNF-related apoptosis-inducing ligand (TRAIL).^[211] TRAIL is a type 2 transmembrane protein naturally present as a trimer on the surface of activated immune cells (e.g. natural killer cells and CD8+ T cells).^[211] The fact that TRAIL is capable of inducing programmed cell death of a wide range of cancer cells while leaving healthy cells untouched, made it a promising anticancer agent.^[212, 213] Among the five known receptors of TRAIL, i.e. death receptor 4 (DR4), death receptor 5 (DR5), TNF-related apoptosis-inducing ligand receptor 3 (DcR1), TNF-related apoptosis-inducing ligand receptor 4 (DcR2), and osteoprotegerin (OPG), only DR4 and DR5 possess a functional ~90 amino acids stretch called death domain (DD) which is a prerequisite for efficient signaling leading to apoptosis.^[211] Notably, OPG harbours a complete DD, but as it is expressed as soluble receptor, it is not able to trigger apoptosis.^[211] Furthermore, DcR2 possesses an intracellular domain but only a truncated DD.^[211] Binding of trimeric TRAIL leads to the oligomerization/aggregation of bound receptors, which is the first critical step for programmed cell death upon formation of the so-called death-inducing signaling complex (DISC) (Figure 18).^[211] Subsequently, this binding allows for the recruitment of adapter Fas-associated protein with death domain (FADD) also possessing a DD, which constitutes the DISC. Further, recruitment of pro-caspase-8 and/or -10 and its interaction within the DISC complex allows for their activation and release in the cytosol resulting in apoptosis mediated by cleaving of

effector caspase-3 and/or-7.^[213] An additional backup pathway proceeding *via* mitochondria is initiated by the cleavage of Bid. Subsequently, truncated Bid (tBid) translocates to mitochondria to induce the activation of Bax and/or Bak resulting in the release of cytochrome c, which triggers apoptosis by the activation of caspase-9.^[213]

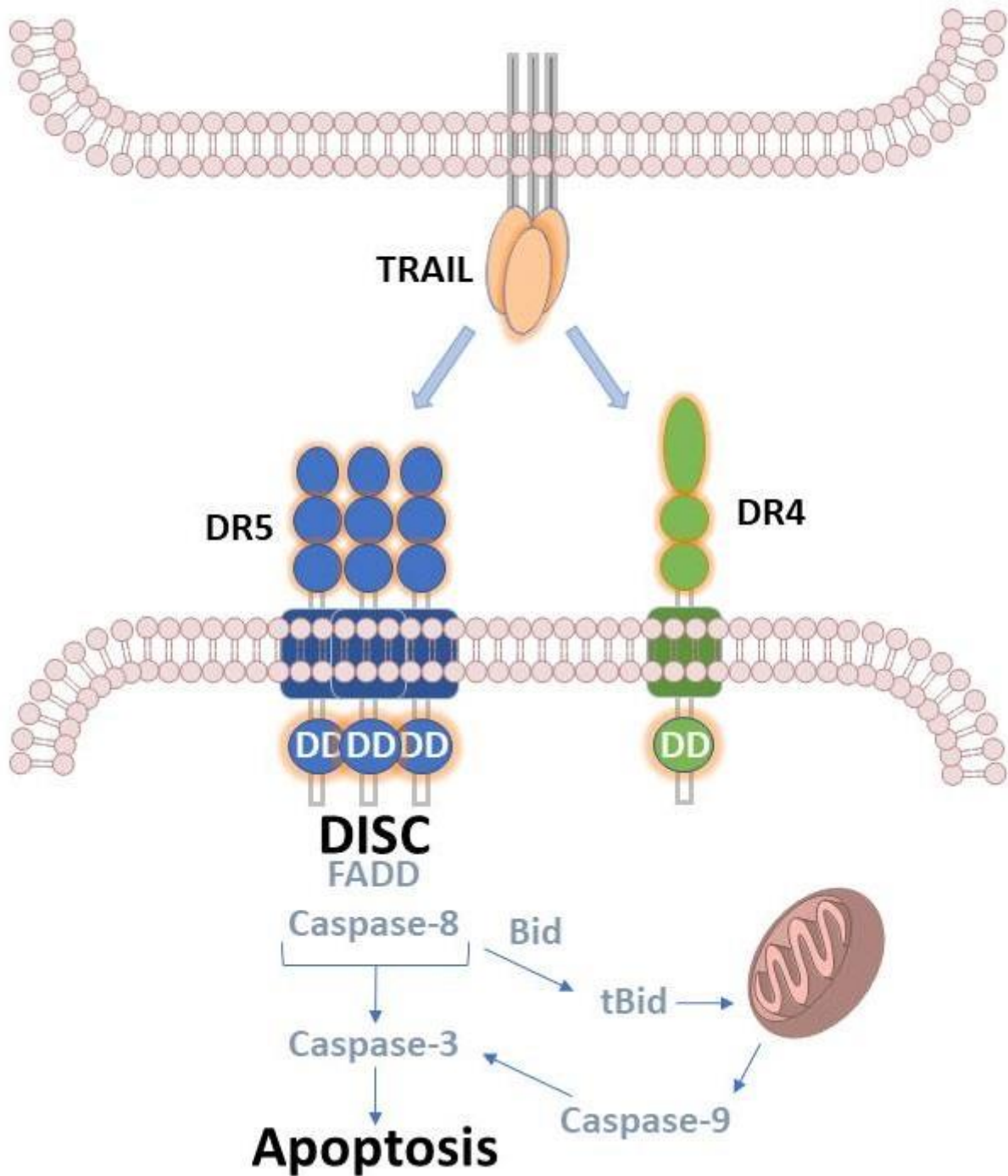


Figure 18. Proposed mechanism for apoptosis triggering upon DR5 receptor-clustering. modified from Dubuisson et al. [211]

DR4 and DR5 are often co-expressed on the same cell. However, DR5 seems to be more important for induction of apoptosis.^[214] It is proposed that DR5 forms large clusters (~300-500 nm) within the membrane upon ligand binding, which are not the co-localizations in cholesterol-rich membrane domains as was believed for a long time.^[215] Further, highly structured networks held together by receptor dimers were found, underlining that the formed clusters are not random aggregates of the receptors^[215] However, the relationship of trans-membrane helix dimerization, receptor activity and membrane cholesterol is still too complex to be fully understood.^[215] Therefore, it is not clear if the membrane itself plays an active role in these processes.^[215]

Due to their ability to trigger apoptosis, DR4 and DR5 became promising targets for tumor treatment. However, in clinical trials both soluble TRAIL and agonist antibodies targeting either DR4 or DR5 failed to demonstrate the desired efficacy.^[213] Indeed, dulcanermin developed by Genentech, a recombinant protein that encodes TRAIL from amino acid 114-281, did not show sufficient therapeutic activity.^[216, 217] Additionally, TRAIL was found to suffer from resistance induced by decoy receptors and is likely to promote cell migration and metastasis.^[218, 219] Furthermore, TRAIL-targeting antibodies, like mapatumumab^[220] that combines selectivity with effector functions of the Fc of an antibody, were developed. However, though being well-tolerated, they often lack efficacy due to their bivalent architecture compared to trivalent natural TRAIL.^[211] Novel TRAIL versions aimed at improved stability and half-life, relied on genetic fusion towards TRAIL single-chain trimers. The same genetic approach is used to fuse it with single-chain variable fragments (scFvs) and Fc fragments. In addition, conjugation with chemical drugs or nanoparticles and expression on the cell surface of delivery cells have been reported.^[211] For instance, circularly permuted TRAIL (CPT),^[221, 222] a recombinant mutant of human TRAIL introduced by Beijing Sunbio Biotech Co. Ltd., represents the best and most promising TRAIL derivative so far.^[211] CPT exhibited better stability, half-life, and stronger antitumor activity compared to dulcanermin and was found well-tolerated in early phase II clinical studies.^[211, 221, 222] However, CPT is, like parent TRAIL, supposed to suffer from decoy receptors and is believed to promote migration and metastasis.^[211]

Considering the drawbacks of the mentioned compounds, researchers around the globe investigated novel TRAIL-inspired approaches that rely on multivalent derivatives of antibodies or peptidic binders, among them multimerization of small binding mimetics of antibodies, e.g. scFvs^[223] or single-domain antibodies from sharks or camelids^[224] (V_{NAR} or V_{HH}). Further, oligovalent binders based on IgM, frameworks relying on either adamantane^[225, 226] or C4b-binding protein (C4BP)^[227] have been currently reported. Interestingly, TAS266, a tetrameric nanobody linked by three 35 amino acid peptides each representing one of these highly potent binders, was found hepatotoxic, which may be attributed to its high potency, immunogenicity, and possibly increased DR5 expression on hepatocytes.^[224]

The peptide-based approaches rely on the death receptor 5 targeting peptide (DR5TP)^[228] that solitarily was not capable of inducing apoptosis. However, upon multimerization on the mentioned scaffolds effective programmed cell-death was observed. Notably, the authors depicted a certain spatial orientation of the ligands as indispensable element for efficacy.^[225, 227] A review giving a deeper insight into the current status of DR4 and DR5 targeting antibodies and derivatives can be found elsewhere.^[211]

2. Objective

This doctoral research was focused on application of dextran polysaccharide to tailor-made next-generation antibody-drug conjugates and other hybrid architectures. To that end, addressing several crucial issues for ADCs regarding their water solubility and multivalent applications should expand the scope of these biomolecules. In particular, the ultimate goal of this work was the development of a highly hydrophilic, modular and multivalent scaffold based on dextran polymer, that allows not only for multivalent presentation of desired payloads in a controlled fashion, but site-specific, orthogonal conjugation with a biomolecule of choice.

The first part of this thesis was aimed at the generation of potent antibody-drug conjugates (ADCs) comprising a high drug-to-antibody ratio (DAR) and retaining a preferred hydrophilic profile. ADCs are multicomponent biomolecules that combine the targeting properties of an immunoglobulin with the cytotoxic potency of a covalently attached cargo. Since only a limited number of the administered ADCs is able to reach their cellular target, the cytotoxic payload they carry needs to be highly potent. That can be achieved by improving its potency or applying higher numbers of copies, thus making use of a multivalent organization. However, considering the fact that the majority of commonly used toxins are strongly hydrophobic compounds, highly loaded ADCs often suffer from poor solubility and unexpected aggregation, which can become crucial regarding pharmacokinetics, immunogenicity, and efficacy. Therefore, these architectures require careful design in terms of conjugation site and number of attached payloads. Indeed, the average DAR of most ADCs does not exceed 3-4, and generation of high-DAR hydrophilic ADCs is an important and challenging task.

In the present work, this issue should be addressed by introducing a hydrophilic, modular scaffold enabling equipment of an antibody of choice with a potent cytotoxin in a desired number of copies. To that end, dextran should be used. It is an FDA-approved biocompatible polymer reported to enhance half-life, improve the thermal stability and pharmacokinetics, and reduce immunogenicity of conjugated proteins. Due to its structure comprising repeated sugar units, dextran bears multiply addressable functional groups. It should be investigated as modular hydrophilic carrier system. To that end, a viable synthetic approach to novel dextran-ADC constructs should be established providing a possibility for the tailoring of toxin loading. Subsequently, the question should be answered, if and how the polarity of a dextran scaffold is influenced upon loading with cargoes and conjugation to an antibody. For that purpose, dextran polysaccharide should be ligated with a commonly applied antibody site-specifically and subsequently equipped with multiple units of a highly potent hydrophobic payload. The resulting high-DAR ADC should be validated regarding its hydrophilic properties, binding capacity of the parental antibody and toxicity of a payload *in vitro*.

In the second part of this doctoral study, the modularity of the novel multimerization scaffold should be validated by attaching multiple peptidic ligands. Death receptor 5-targeting peptide (DR5TP) should be applied as ligand for this proof-of-concept study. These ligands are known to trigger apoptosis of malignant tumor cells in the case when they adopt a special orientation. Hence, it should be investigated if the dextran backbone is suitable to provide enough variability to effectively bind and finally cluster death receptor 5 (DR5) which is known to trigger apoptosis when bound in a multivalent manner by tumor necrosis factor related apoptosis

ligand (TRAIL). This concept should overcome the need of spatial orientation as prerequisite for efficient multivalent receptor clustering that was previously reported. To that end, DR5TP should be attached to dextran backbone in multiple copies. On that account, the potential to trigger apoptosis should be visualized by cell proliferation assays on DR5-overexpressing cells *in vitro*. Furthermore, it should be elucidated if site-selective enzymatic conjugation to a protein of choice affects binding and/or potency of the generated hybrid compounds. Thus, dextran scaffold should be site-specifically conjugated to a fraction crystallizable (Fc) fragment of an antibody that is solitary not to able to target DR5-positive cells and the potency should be assessed in respective biologic assays *in vitro*

Furthermore, an additional approach which substantiates the modularity of dextran as multivalent scaffold for payloads of diverse nature was performed. To that point dextran should be examined as a vehicle for multiple attachment of metal-chelating agents able to carry ions valuable for radio-imaging or -therapy. Therefore, dextran should be decorated with 1,4,7,10-tetraazacyclododecane-1,4,7,10-tetraacetic acid (DOTA) which is a widely applied metal chelator. Furthermore, it should be validated if DOTA-loaded dextran is able to complex a non-radioactive metal as test substance. Furthermore, the biodistribution of DOTA-dextran compound should be investigated in a preliminary *in vivo* study. This study should answer the question if dextran represents a promising carrier for radio-imaging and -therapy.

The third part of the thesis should delineate a detailed overview of ADC assembly applying microbial transglutaminase (mTG), as to date, notwithstanding numerous reviews of the field, a comprehensive view of application of transglutaminase for generation of therapeutics is missing. Thus, it intends to give a comparative survey that describes conjugation sites, motifs and procedures, as well as cellular targets, and applied linkers and toxins. Furthermore, this review should provide a thorough overview of research groups and companies working on ADCs assembled under mTG catalysis.

3. References

- [1] F. Bray, J. Ferlay, I. Soerjomataram, R.L. Siegel, L.A. Torre, A. Jemal, *Global cancer statistics 2018: GLOBOCAN estimates of incidence and mortality worldwide for 36 cancers in 185 countries*, CA: A Cancer Journal for Clinicians, 68, (2018), 394-424.
- [2] WHO, *Cancer: Key Facts*, (2018). Available online: <https://www.who.int/en/news-room/fact-sheets/detail/cancer> (accessed on 20 October 2019)
- [3] R.L. Siegel, K.D. Miller, A. Jemal, *Cancer statistics, 2019*, CA: A Cancer Journal for Clinicians, 69, (2019), 7-34.
- [4] V.T. DeVita, E. Chu, *A History of Cancer Chemotherapy*, Cancer Research, 68, (2008), 8643.
- [5] K. Strebhardt, A. Ullrich, *Paul Ehrlich's magic bullet concept: 100 years of progress*, Nature Reviews Cancer, 8, (2008), 473-480.
- [6] R.V.J. Chari, M.L. Miller, W.C. Widdison, *Antibody–Drug Conjugates: An Emerging Concept in Cancer Therapy*, Angewandte Chemie International Edition, 53, (2014), 3796-3827.
- [7] J.M. Lambert, C.Q. Morris, *Antibody–Drug Conjugates (ADCs) for Personalized Treatment of Solid Tumors: A Review*, Advances in Therapy, 34, (2017), 1015-1035.
- [8] E. Frei, *Combination Cancer Therapy: Presidential Address*, Cancer Research, 32, (1972), 2593.
- [9] A.I. Minchinton, I.F. Tannock, *Drug penetration in solid tumours*, Nature Reviews Cancer, 6, (2006), 583-592.
- [10] D. Schumacher, C.P.R. Hackenberger, H. Leonhardt, J. Helma, *Current Status: Site-Specific Antibody Drug Conjugates*, Journal of Clinical Immunology, 36, (2016), 100-107.
- [11] K. Tsuchikama, Z. An, *Antibody-drug conjugates: recent advances in conjugation and linker chemistries*, Protein & Cell, 9, (2018), 33-46.
- [12] C.R. Behrens, B. Liu, *Methods for site-specific drug conjugation to antibodies*, mAbs, 6, (2014), 46-53.
- [13] J.M. Lambert, A. Berkenblit, *Antibody–Drug Conjugates for Cancer Treatment*, Annual Review of Medicine, 69, (2018), 191-207.
- [14] M. Cristofanilli, W.J. Bryan, L.L. Miller, A.Y. Chang, W.J. Gradishar, D.W. Kufe, G.N. Hortobagyi, *Phase II study of adozelesin in untreated metastatic breast cancer*, Anti-cancer drugs, 9, (1998), 779-782.
- [15] B.F. Issell, S.T. Crooke, *Maytansine*, Cancer Treatment Reviews, 5, (1978), 199-207.
- [16] D. Hanahan, R.A. Weinberg, *The Hallmarks of Cancer*, Cell, 100, (2000), 57-70.
- [17] B. Vogelstein, K.W. Kinzler, *Cancer genes and the pathways they control*, Nature Medicine, 10, (2004), 789-799.
- [18] Q. Zhou, *Site-Specific Antibody Conjugation for ADC and Beyond*, Biomedicines, 5, (2017), 64.
- [19] A.M. Scott, J.D. Wolchok, L.J. Old, *Antibody therapy of cancer*, Nature Reviews Cancer, 12, (2012), 278-287.
- [20] K.C. Nicolaou, S. Rigol, *The Role of Organic Synthesis in the Emergence and Development of Antibody–Drug Conjugates as Targeted Cancer Therapies*, Angewandte Chemie International Edition, 58, (2019), 11206-11241.
- [21] D.M. Ecker, S.D. Jones, H.L. Levine, *The therapeutic monoclonal antibody market*, mAbs, 7, (2015), 9-14.
- [22] J.M. Reichert, *Antibodies to watch in 2017*, mAbs, 9, (2017), 167-181.
- [23] K. McKeage, C.M. Perry, *Trastuzumab*, Drugs, 62, (2002), 209-243.
- [24] P. Kirkpatrick, J. Graham, M. Muhsin, *Cetuximab*, Nature Reviews Drug Discovery, 3, (2004), 549-550.
- [25] G.J. Weiner, *Rituximab: Mechanism of Action*, Seminars in Hematology, 47, (2010), 115-123.
- [26] T. Kline, A.R. Steiner, K. Penta, A.K. Sato, T.J. Hallam, G. Yin, *Methods to Make Homogenous Antibody Drug Conjugates*, Pharmaceutical Research, 32, (2015), 3480-3493.
- [27] A. Beck, L. Goetsch, C. Dumontet, N. Corvaia, *Strategies and challenges for the next generation of antibody–drug conjugates*, Nature Reviews Drug Discovery, 16, (2017), 315.
- [28] M. Riera Romo, D. Pérez-Martínez, C. Castillo Ferrer, *Innate immunity in vertebrates: an overview*, Immunology, 148, (2016), 125-139.
- [29] H. Kumar, T. Kawai, S. Akira, *Pathogen Recognition by the Innate Immune System*, International Reviews of Immunology, 30, (2011), 16-34.
- [30] R. Medzhitov, *Recognition of microorganisms and activation of the immune response*, Nature, 449, (2007), 819-826.
- [31] C.A. Janeway, R. Medzhitov, *Innate Immune Recognition*, Annual Review of Immunology, 20, (2002), 197-216.

- [32] C.A. Janeway, P. Travers, M. Walport, M.J. Shlomchik, *Immunobiology 5: The immune system in health and disease*, Garland Science, New York, (2001).
- [33] F.A. Bonilla, H.C. Oettgen, *Adaptive immunity*, *Journal of Allergy and Clinical Immunology*, 125, (2010), 33-40.
- [34] A. Iwasaki, R. Medzhitov, *Regulation of Adaptive Immunity by the Innate Immune System*, *Science*, 327, (2010), 291.
- [35] M.D. Cooper, M.N. Alder, *The Evolution of Adaptive Immune Systems*, *Cell*, 124, (2006), 815-822.
- [36] D.G. Schatz, M.A. Oettinger, M.S. Schlissel, *V(D)J Recombination: Molecular Biology and Regulation*, *Annual Review of Immunology*, 10, (1992), 359-383.
- [37] *Chapter 14 - B Cell Memory and Plasma Cell Development*, in: F.W. Alt, T. Honjo, A. Radbruch, M. Reth (Eds.) *Molecular Biology of B Cells (Second Edition)*, Academic Press, London, (2015), pp. 227-249.
- [38] D.C. Parker, *T Cell-Dependent B Cell Activation*, *Annual Review of Immunology*, 11, (1993), 331-360.
- [39] J. Stavnezer, C.E. Schrader, *IgH chain class switch recombination: mechanism and regulation*, *Journal of immunology (Baltimore, Md. : 1950)*, 193, (2014), 5370-5378.
- [40] S. Panda, J.L. Ding, *Natural Antibodies Bridge Innate and Adaptive Immunity*, *The Journal of Immunology*, 194, (2015), 13-20.
- [41] D.M. Czajkowsky, Z. Shao, *The human IgM pentamer is a mushroom-shaped molecule with a flexural bias*, *Proceedings of the National Academy of Sciences*, 106, (2009), 14960-14965.
- [42] M.R. Ehrenstein, C.A. Notley, *The importance of natural IgM: scavenger, protector and regulator*, *Nature Reviews Immunology*, 10, (2010), 778-786.
- [43] J. Stavnezer, J.E.J. Guikema, C.E. Schrader, *Mechanism and regulation of class switch recombination*, *Annual review of immunology*, 26, (2008), 261-292.
- [44] FDA, *NEWS MEDICAL LIFE SCIENCES, Types of Antibodies*, (2019). Available online: <https://www.news-medical.net/life-sciences/Types-of-Antibodies.aspx> (accessed 21.11.2019)
- [45] M.R. Lieber, K. Yu, S.C. Raghavan, *Roles of nonhomologous DNA end joining, V(D)J recombination, and class switch recombination in chromosomal translocations*, *DNA Repair*, 5, (2006), 1234-1245.
- [46] G. Vidarsson, G. Dekkers, T. Rispens, *IgG Subclasses and Allotypes: From Structure to Effector Functions*, 5, (2014).
- [47] H.W. Schroeder, L. Cavacini, *Structure and function of immunoglobulins*, *Journal of Allergy and Clinical Immunology*, 125, (2010), 41-52.
- [48] M. Waller, N. Curry, J. Mallory, *Immunochemical and serological studies of enzymatically fractionated human IgG globulins—I: Hydrolysis with pepsin, papain, ficin and bromelin*, *Immunochemistry*, 5, (1968), 577-583.
- [49] E. Market, F.N. Papavasiliou, *V(D)J Recombination and the Evolution of the Adaptive Immune System*, *PLOS Biology*, 1, (2003), e16.
- [50] E.E. Idusogie, L.G. Presta, H. Gazzano-Santoro, K. Totpal, P.Y. Wong, M. Ultsch, Y.G. Meng, M.G. Mulkerrin, *Mapping of the C1q Binding Site on Rituxan, a Chimeric Antibody with a Human IgG1 Fc*, *The Journal of Immunology*, 164, (2000), 4178-4184.
- [51] D.C. Roopenian, S. Akilesh, *FcRn: the neonatal Fc receptor comes of age*, *Nature Reviews Immunology*, 7, (2007), 715-725.
- [52] W.L. Martin, A.P. West, L. Gan, P.J. Bjorkman, *Crystal Structure at 2.8 Å of an FcRn/Heterodimeric Fc Complex: Mechanism of pH-Dependent Binding*, *Molecular Cell*, 7, (2001), 867-877.
- [53] G. Alter, T.H.M. Ottenhoff, S.A. Joosten, *Antibody glycosylation in inflammation, disease and vaccination*, *Seminars in Immunology*, 39, (2018), 102-110.
- [54] T.A. Bowden, K. Baruah, C.H. Coles, D.J. Harvey, X. Yu, B.-D. Song, D.I. Stuart, A.R. Aricescu, C.N. Scanlan, E.Y. Jones, M. Crispin, *Chemical and Structural Analysis of an Antibody Folding Intermediate Trapped during Glycan Biosynthesis*, *Journal of the American Chemical Society*, 134, (2012), 17554-17563.
- [55] Y. Sakae, T. Satoh, H. Yagi, S. Yanaka, T. Yamaguchi, Y. Isoda, S. Iida, Y. Okamoto, K. Kato, *Conformational effects of N-glycan core fucosylation of immunoglobulin G Fc region on its interaction with Fcγ receptor IIIa*, *Scientific Reports*, 7, (2017), 13780.
- [56] D.Y. Jackson, *Processes for Constructing Homogeneous Antibody Drug Conjugates*, *Organic Process Research & Development*, 20, (2016), 852-866.

- [57] K.L. Moek, D.J.A. de Groot, E.G.E. de Vries, R.S.N. Fehrmann, *The antibody–drug conjugate target landscape across a broad range of tumour types*, *Annals of Oncology*, 28, (2017), 3083-3091.
- [58] S. Panowski, S. Bhakta, H. Raab, P. Polakis, J.R. Junutula, *Site-specific antibody drug conjugates for cancer therapy*, *mAbs*, 6, (2014), 34-45.
- [59] R.S. Schwartz, *Paul Ehrlich's Magic Bullets*, *New England Journal of Medicine*, 350, (2004), 1079-1080.
- [60] N. Jain, S.W. Smith, S. Ghone, B. Tomczuk, *Current ADC Linker Chemistry*, *Pharmaceutical Research*, 32, (2015), 3526-3540.
- [61] W.-C. Shen, *Antibody-Drug Conjugates: A Historical Review*, in: J. Wang, W.-C. Shen, J.L. Zaro (Eds.) *Antibody-Drug Conjugates: The 21st Century Magic Bullets for Cancer*, Springer International Publishing, Cham, (2015), pp. 3-7.
- [62] G. Mathe, L.O. Tran Ba, J. Bernard, *[Effect on mouse leukemia 1210 of a combination by diazo-reaction of amethopterin and gamma-globulins from hamsters inoculated with such leukemia by heterografts.]*, *Comptes rendus hebdomadaires des seances de l'Academie des sciences*, 246, (1958), 1626-1628.
- [63] E. Hurwitz, R. Levy, R. Maron, M. Wilchek, R. Arnon, M. Sela, *The Covalent Binding of Daunomycin and Adriamycin to Antibodies, with Retention of Both Drug and Antibody Activities*, *Cancer Research*, 35, (1975), 1175-1181.
- [64] D.J. Elias, L. Hirschowitz, L.E. Kline, J.F. Kroener, R.O. Dillman, L.E. Walker, J.A. Robb, R.M. Timms, *Phase I Clinical Comparative Study of Monoclonal Antibody KS1/4 and KS1/4-Methotrexate Immunconjugate in Patients with Non-Small Cell Lung Carcinoma*, *Cancer Research*, 50, (1990), 4154-4159.
- [65] M.N. Saleh, S. Sugarman, J. Murray, J.B. Ostroff, D. Healey, D. Jones, C.R. Daniel, D. LeBherz, H. Brewer, N. Onetto, A.F. LoBuglio, *Phase I Trial of the Anti–Lewis Y Drug Immunconjugate BR96-Doxorubicin in Patients With Lewis Y–Expressing Epithelial Tumors*, *Journal of Clinical Oncology*, 18, (2000), 2282-2292.
- [66] A.W. Tolcher, S. Sugarman, K.A. Gelmon, R. Cohen, M. Saleh, C. Isaacs, L. Young, D. Healey, N. Onetto, W. Slichenmyer, *Randomized Phase II Study of BR96-Doxorubicin Conjugate in Patients With Metastatic Breast Cancer*, *Journal of Clinical Oncology*, 17, (1999), 478-478.
- [67] G. KÖHler, C. Milstein, *Continuous cultures of fused cells secreting antibody of predefined specificity*, *Nature*, 256, (1975), 495-497.
- [68] F.R. Appelbaum, I.D. Bernstein, *Gemtuzumab ozogamicin for acute myeloid leukemia*, *Blood*, 130, (2017), 2373-2376.
- [69] J.K. Lamba, L. Chauhan, M. Shin, M.R. Loken, J.A. Pollard, Y.-C. Wang, R.E. Ries, R. Aplenc, B.A. Hirsch, S.C. Raimondi, R.B. Walter, I.D. Bernstein, A.S. Gamis, T.A. Alonzo, S. Meshinchi, *CD33 Splicing Polymorphism Determines Gemtuzumab Ozogamicin Response in De Novo Acute Myeloid Leukemia: Report From Randomized Phase III Children's Oncology Group Trial AAML0531*, *Journal of clinical oncology : official journal of the American Society of Clinical Oncology*, 35, (2017), 2674-2682.
- [70] P.F. Bross, J. Beitz, G. Chen, X.H. Chen, E. Duffy, L. Kieffer, S. Roy, R. Sridhara, A. Rahman, G. Williams, R. Pazdur, *Approval Summary: gemtuzumab ozogamicin in relapsed acute myeloid leukemia*, *Clinical Cancer Research*, 7, (2001), 1490-1496.
- [71] FDA, (2017). Available online: <https://www.fda.gov/news-events/press-announcements/fda-approves-myotarg-treatment-acute-myeloid-leukemia> (accessed on 22.11.2019)
- [72] S.O. Doronina, B.E. Toki, M.Y. Torgov, B.A. Mendelsohn, C.G. Cervený, D.F. Chace, R.L. DeBlanc, R.P. Gearing, T.D. Bovee, C.B. Siegall, J.A. Francisco, A.F. Wahl, D.L. Meyer, P.D. Senter, *Development of potent monoclonal antibody auristatin conjugates for cancer therapy*, *Nature Biotechnology*, 21, (2003), 778-784.
- [73] M. Vankemmelbeke, L. Durrant, *Third-generation antibody drug conjugates for cancer therapy – a balancing act*, *Therapeutic Delivery*, 7, (2016), 141-144.
- [74] W.C. Widdison, S.D. Wilhelm, E.E. Cavanagh, K.R. Whiteman, B.A. Leece, Y. Kovtun, V.S. Goldmacher, H. Xie, R.M. Steeves, R.J. Lutz, R. Zhao, L. Wang, W.A. Blättler, R.V.J. Chari, *Semisynthetic Maytansine Analogues for the Targeted Treatment of Cancer*, *Journal of Medicinal Chemistry*, 49, (2006), 4392-4408.
- [75] A.L. Smith, K.C. Nicolaou, *The Enediynes Antibiotics*, *Journal of Medicinal Chemistry*, 39, (1996), 2103-2117.
- [76] M.S. Kung Sutherland, R.B. Walter, S.C. Jeffrey, P.J. Burke, C. Yu, H. Kostner, I. Stone, M.C. Ryan, D. Sussman, R.P. Lyon, W. Zeng, K.H. Harrington, K. Klussman, L. Westendorf, D. Meyer, I.D. Bernstein, P.D. Senter, D.R. Benjamin, J.G. Drachman, J.A. McEarchern, *SGN-CD33A: a novel CD33-targeting antibody–drug conjugate using a pyrrolobenzodiazepine dimer is active in models of drug-resistant AML*, *Blood*, 122, (2013), 1455-1463.

- [77] M.L. Miller, N.E. Fishkin, W. Li, K.R. Whiteman, Y. Kovtun, E.E. Reid, K.E. Archer, E.K. Maloney, C.A. Audette, M.F. Mayo, A. Wilhelm, H.A. Modafferi, R. Singh, J. Pinkas, V. Goldmacher, J.M. Lambert, R.V.J. Chari, *A New Class of Antibody–Drug Conjugates with Potent DNA Alkylating Activity*, *Molecular Cancer Therapeutics*, 15, (2016), 1870-1878.
- [78] P.D. Senter, E.L. Sievers, *The discovery and development of brentuximab vedotin for use in relapsed Hodgkin lymphoma and systemic anaplastic large cell lymphoma*, *Nature Biotechnology*, 30, (2012), 631-637.
- [79] J.H. Yi, S.J. Kim, W.S. Kim, *Brentuximab vedotin: clinical updates and practical guidance*, *Blood Res*, 52, (2017), 243-253.
- [80] E.D. Deeks, *Polatuzumab Vedotin: First Global Approval*, *Drugs*, 79, (2019), 1467-1475.
- [81] P.M. LoRusso, D. Weiss, E. Guardino, S. Girish, M.X. Sliwkowski, *Trastuzumab Emtansine: A Unique Antibody–Drug Conjugate in Development for Human Epidermal Growth Factor Receptor 2–Positive Cancer*, *Clinical Cancer Research*, 17, (2011), 6437-6447.
- [82] I. Niculescu-Duvaz, *Trastuzumab emtansine, an antibody-drug conjugate for the treatment of HER2+ metastatic breast cancer*, *Current opinion in molecular therapeutics*, 12, (2010), 350-360.
- [83] Y.N. Lamb, *Inotuzumab Ozogamicin: First Global Approval*, *Drugs*, 77, (2017), 1603-1610.
- [84] B. Shor, H.-P. Gerber, P. Sapro, *Preclinical and clinical development of inotuzumab-ozogamicin in hematological malignancies*, *Molecular Immunology*, 67, (2015), 107-116.
- [85] R.J. Kreitman, C. Dearden, P.L. Zinzani, J. Delgado, L. Karlin, T. Robak, D.E. Gladstone, P. le Coutre, S. Dietrich, M. Gotic, L. Larratt, F. Offner, G. Schiller, R. Swords, L. Bacon, M. Bocchia, K. Bouabdallah, D.A. Breems, A. Cortelezzi, S. Dinner, M. Doubek, B.T. Gjertsen, M. Gobbi, A. Hellmann, S. Lepretre, F. Maloisel, F. Ravandi, P. Rousselot, M. Rummel, T. Siddiqi, T. Tadmor, X. Troussard, C.A. Yi, G. Saglio, G.J. Roboz, K. Balic, N. Standifer, P. He, S. Marshall, W. Wilson, I. Pastan, N.-S. Yao, F. Giles, *Moxetumomab pasudotox in relapsed/refractory hairy cell leukemia*, *Leukemia*, 32, (2018), 1768-1777.
- [86] M.T. Kim, Y. Chen, J. Marhoul, F. Jacobson, *Statistical Modeling of the Drug Load Distribution on Trastuzumab Emtansine (Kadcyla), a Lysine-Linked Antibody Drug Conjugate*, *Bioconjugate Chemistry*, 25, (2014), 1223-1232.
- [87] C.R. Behrens, E.H. Ha, L.L. Chinn, S. Bowers, G. Probst, M. Fitch-Bruhns, J. Monteon, A. Valdiosera, A. Bermudez, S. Liao-Chan, T. Wong, J. Melnick, J.-W. Theunissen, M.R. Flory, D. Houser, K. Venstrom, Z. Levashova, P. Sauer, T.-S. Migone, E.H. van der Horst, R.L. Halcomb, D.Y. Jackson, *Antibody–Drug Conjugates (ADCs) Derived from Interchain Cysteine Cross-Linking Demonstrate Improved Homogeneity and Other Pharmacological Properties over Conventional Heterogeneous ADCs*, *Molecular Pharmaceutics*, 12, (2015), 3986-3998.
- [88] G. Spallone, E. Botti, A.J.C. Costanzo, *Targeted therapy in nonmelanoma skin cancers*, 3, (2011), 2255-2273.
- [89] P. Strop, T.-T. Tran, M. Dorywalska, K. Delaria, R. Dushin, O.K. Wong, W.-H. Ho, D. Zhou, A. Wu, E. Kraynov, L. Aschenbrenner, B. Han, C.J. Donnell, J. Pons, A. Rajpal, D.L. Shelton, S.-H. Liu, *RN927C, a Site-Specific Trop-2 Antibody–Drug Conjugate (ADC) with Enhanced Stability, Is Highly Efficacious in Preclinical Solid Tumor Models*, *Molecular Cancer Therapeutics*, 15, (2016), 2698-2708.
- [90] M.J. Costa, J. Kudravalli, J.-T. Ma, W.-H. Ho, K. Delaria, C. Holz, A. Stauffer, A.G. Chunyk, Q. Zong, E. Blasi, B. Buetow, T.-T. Tran, K. Lindquist, M. Dorywalska, A. Rajpal, D.L. Shelton, P. Strop, S.-H. Liu, *Optimal design, anti-tumour efficacy and tolerability of anti-CXCR4 antibody drug conjugates*, *Scientific Reports*, 9, (2019), 2443.
- [91] O.K. Wong, T.-T. Tran, W.-H. Ho, M.G. Casas, M. Au, M. Bateman, K.C. Lindquist, A. Rajpal, D.L. Shelton, P. Strop, S.-H. Liu, *RN765C, a low affinity EGFR antibody drug conjugate with potent anti-tumor activity in preclinical solid tumor models*, *Oncotarget*, 9, (2018), 33446-33458.
- [92] H.H. Sedlacek, G. Seemann, D. Hoffmann, J. Czech, P. Lorenz, C. Kolar, K. Bosslet, *Antibodies as carriers of cytotoxicity*, Karger Basel(1992).
- [93] J.M. Lambert, *Typical antibody–drug conjugates*, in: S.A.H. Kenneth J. Olivier Jr. (Ed.) *Antibody-Drug Conjugates: Fundamentals, Drug Development, and Clinical Outcomes to Target Cancer*(2016), pp. 1-32.
- [94] H.L. Perez, P.M. Cardarelli, S. Deshpande, S. Gangwar, G.M. Schroeder, G.D. Vite, R.M. Borzilleri, *Antibody–drug conjugates: current status and future directions*, *Drug Discovery Today*, 19, (2014), 869-881.
- [95] A.B. Waight, K. Bargsten, S. Doronina, M.O. Steinmetz, D. Sussman, A.E. Prota, *Structural Basis of Microtubule Destabilization by Potent Auristatin Anti-Mitotics*, *PLOS ONE*, 11, (2016), e0160890.
- [96] M.D. Lee, G.A. Ellestad, D.B. Borders, *Calicheamicins: discovery, structure, chemistry, and interaction with DNA*, *Accounts of Chemical Research*, 24, (1991), 235-243.

- [97] D.L. Boger, *The Duocarmycins: Synthetic and Mechanistic Studies*, Accounts of Chemical Research, 28, (1995), 20-29.
- [98] J. Lu, F. Jiang, A. Lu, G. Zhang, *Linkers Having a Crucial Role in Antibody-Drug Conjugates*, International journal of molecular sciences, 17, (2016), 561-561.
- [99] A. Dal Corso, S. Cazzamalli, R. Gébleux, M. Mattarella, D. Neri, *Protease-Cleavable Linkers Modulate the Anticancer Activity of Noninternalizing Antibody-Drug Conjugates*, Bioconjugate chemistry, 28, (2017), 1826-1833.
- [100] G. Michelle de, B. Epie, W.S. Hans, J.H. Hidde, M.P. Herbert, *Beta-Glucuronidase-Mediated Drug Release*, Current Pharmaceutical Design, 8, (2002), 1391-1403.
- [101] B.C. Laguzza, C.L. Nichols, S.L. Briggs, G.J. Cullinan, D.A. Johnson, J.J. Starling, A.L. Baker, T.F. Bumol, J.R.F. Corvalan, *New antitumor monoclonal antibody-vinca conjugates LY203725 and related compounds: design, preparation, and representative in vivo activity*, Journal of Medicinal Chemistry, 32, (1989), 548-555.
- [102] P. Strop, K. Delaria, D. Foletti, J.M. Witt, A. Hasa-Moreno, K. Poulsen, M.G. Casas, M. Dorywalska, S. Farias, A. Pios, V. Lui, R. Dushin, D. Zhou, T. Navaratnam, T.-T. Tran, J. Sutton, K.C. Lindquist, B. Han, S.-H. Liu, D.L. Shelton, J. Pons, A. Rajpal, *Site-specific conjugation improves therapeutic index of antibody drug conjugates with high drug loading*, Nature Biotechnology, 33, (2015), 694-696.
- [103] X. Li, T. Fang, G.-J. Boons, *Preparation of Well-Defined Antibody-Drug Conjugates through Glycan Remodeling and Strain-Promoted Azide-Alkyne Cycloadditions*, Angewandte Chemie International Edition, 53, (2014), 7179-7182.
- [104] P.K. Qasba, *Glycans of Antibodies as a Specific Site for Drug Conjugation Using Glycosyltransferases*, Bioconjugate Chemistry, 26, (2015), 2170-2175.
- [105] B. Ramakrishnan, E. Boeggeman, P.K. Qasba, *Applications of glycosyltransferases in the site-specific conjugation of biomolecules and the development of a targeted drug delivery system and contrast agents for MRI*, Expert Opinion on Drug Delivery, 5, (2008), 149-153.
- [106] R. van Geel, M.A. Wijdeven, R. Heesbeen, J.M.M. Verkade, A.A. Wasiel, S.S. van Berkel, F.L. van Delft, *Chemoenzymatic Conjugation of Toxic Payloads to the Globally Conserved N-Glycan of Native mAbs Provides Homogeneous and Highly Efficacious Antibody-Drug Conjugates*, Bioconjugate Chemistry, 26, (2015), 2233-2242.
- [107] Q. Zhou, J.E. Stefano, C. Manning, J. Kyazike, B. Chen, D.A. Gianolio, A. Park, M. Busch, J. Bird, X. Zheng, H. Simonds-Mannes, J. Kim, R.C. Gregory, R.J. Miller, W.H. Brondyk, P.K. Dhal, C.Q. Pan, *Site-Specific Antibody-Drug Conjugation through Glycoengineering*, Bioconjugate Chemistry, 25, (2014), 510-520.
- [108] Z. Zhu, B. Ramakrishnan, J. Li, Y. Wang, Y. Feng, P. Prabakaran, S. Colantonio, M.A. Dyba, P.K. Qasba, D.S. Dimitrov, *Site-specific antibody-drug conjugation through an engineered glycotransferase and a chemically reactive sugar*, mAbs, 6, (2014), 1190-1200.
- [109] N. Dimasi, R. Fleming, H. Zhong, B. Bezabeh, K. Kinneer, R.J. Christie, C. Fazenbaker, H. Wu, C. Gao, *Efficient Preparation of Site-Specific Antibody-Drug Conjugates Using Cysteine Insertion*, Molecular Pharmaceutics, 14, (2017), 1501-1516.
- [110] J.R. Junutula, H. Raab, S. Clark, S. Bhakta, D.D. Leipold, S. Weir, Y. Chen, M. Simpson, S.P. Tsai, M.S. Dennis, Y. Lu, Y.G. Meng, C. Ng, J. Yang, C.C. Lee, E. Duenas, J. Gorrell, V. Katta, A. Kim, K. McDorman, K. Flagella, R. Venook, S. Ross, S.D. Spencer, W. Lee Wong, H.B. Lowman, R. Vandlen, M.X. Sliwkowski, R.H. Scheller, P. Polakis, W. Mallet, *Site-specific conjugation of a cytotoxic drug to an antibody improves the therapeutic index*, Nature Biotechnology, 26, (2008), 925-932.
- [111] B.-Q. Shen, K. Xu, L. Liu, H. Raab, S. Bhakta, M. Kenrick, K.L. Parsons-Reponte, J. Tien, S.-F. Yu, E. Mai, D. Li, J. Tibbitts, J. Baudys, O.M. Saad, S.J. Scales, P.J. McDonald, P.E. Hass, C. Eigenbrot, T. Nguyen, W.A. Solis, R.N. Fuji, K.M. Flagella, D. Patel, S.D. Spencer, L.A. Khawli, A. Ebens, W.L. Wong, R. Vandlen, S. Kaur, M.X. Sliwkowski, R.H. Scheller, P. Polakis, J.R. Junutula, *Conjugation site modulates the in vivo stability and therapeutic activity of antibody-drug conjugates*, Nature Biotechnology, 30, (2012), 184-189.
- [112] D. Shinmi, E. Taguchi, J. Iwano, T. Yamaguchi, K. Masuda, J. Enokizono, Y. Shiraishi, *One-Step Conjugation Method for Site-Specific Antibody-Drug Conjugates through Reactive Cysteine-Engineered Antibodies*, Bioconjugate Chemistry, 27, (2016), 1324-1331.
- [113] X. Li, C.G. Nelson, R.R. Nair, L. Hazlehurst, T. Moroni, P. Martinez-Acedo, A.R. Nanna, D. Hymel, T.R. Burke, C. Rader, *Stable and Potent Selenomab-Drug Conjugates*, Cell Chemical Biology, 24, (2017), 433-442.e436.

- [114] J.Y. Axup, K.M. Bajjuri, M. Ritland, B.M. Hutchins, C.H. Kim, S.A. Kazane, R. Halder, J.S. Forsyth, A.F. Santidrian, K. Stafin, Y. Lu, H. Tran, A.J. Seller, S.L. Biroc, A. Szydlak, J.K. Pinkstaff, F. Tian, S.C. Sinha, B. Felding-Habermann, V.V. Smider, P.G. Schultz, *Synthesis of site-specific antibody-drug conjugates using unnatural amino acids*, Proceedings of the National Academy of Sciences, 109, (2012), 16101-16106.
- [115] M.P. VanBrunt, K. Shanebeck, Z. Caldwell, J. Johnson, P. Thompson, T. Martin, H. Dong, G. Li, H. Xu, F. D'Hooge, L. Masterson, P. Bariola, A. Tiberghien, E. Ezeadi, D.G. Williams, J.A. Hartley, P.W. Howard, K.H. Grabstein, M.A. Bowen, M. Marelli, *Genetically Encoded Azide Containing Amino Acid in Mammalian Cells Enables Site-Specific Antibody-Drug Conjugates Using Click Cycloaddition Chemistry*, Bioconjugate Chemistry, 26, (2015), 2249-2260.
- [116] E.S. Zimmerman, T.H. Heibeck, A. Gill, X. Li, C.J. Murray, M.R. Madlansacay, C. Tran, N.T. Uter, G. Yin, P.J. Rivers, A.Y. Yam, W.D. Wang, A.R. Steiner, S.U. Bajad, K. Penta, W. Yang, T.J. Hallam, C.D. Thanos, A.K. Sato, *Production of Site-Specific Antibody-Drug Conjugates Using Optimized Non-Natural Amino Acids in a Cell-Free Expression System*, Bioconjugate Chemistry, 25, (2014), 351-361.
- [117] P. Bryant, M. Pabst, G. Badescu, M. Bird, W. McDowell, E. Jamieson, J. Swierkosz, K. Jurlewicz, R. Tommasi, K. Henseleit, X. Sheng, N. Camper, A. Manin, K. Kozakowska, K. Peciak, E. Laurine, R. Grygorash, A. Kyle, D. Morris, V. Parekh, A. Abhilash, J.-w. Choi, J. Edwards, M. Frigerio, M.P. Baker, A. Godwin, *In Vitro and In Vivo Evaluation of Cysteine Rebridged Trastuzumab-MMAE Antibody Drug Conjugates with Defined Drug-to-Antibody Ratios*, Molecular Pharmaceutics, 12, (2015), 1872-1879.
- [118] J. Ohata, Z.T. Ball, *A Hexa-rhodium Metallopeptide Catalyst for Site-Specific Functionalization of Natural Antibodies*, Journal of the American Chemical Society, 139, (2017), 12617-12622.
- [119] S. Lin, X. Yang, S. Jia, A.M. Weeks, M. Hornsby, P.S. Lee, R.V. Nichiporuk, A.T. Iavarone, J.A. Wells, F.D. Toste, C.J. Chang, *Redox-based reagents for chemoselective methionine bioconjugation*, Science, 355, (2017), 597-602.
- [120] A.R. Nanna, X. Li, E. Walseng, L. Pedzisa, R.S. Goydel, D. Hymel, T.R. Burke Jr, W.R. Roush, C. Rader, *Harnessing a catalytic lysine residue for the one-step preparation of homogeneous antibody-drug conjugates*, Nature Communications, 8, (2017), 1112.
- [121] D. Schumacher, J. Helma, F.A. Mann, G. Pichler, F. Natale, E. Krause, M.C. Cardoso, C.P.R. Hackenberger, H. Leonhardt, *Versatile and Efficient Site-Specific Protein Functionalization by Tubulin Tyrosine Ligase*, Angewandte Chemie International Edition, 54, (2015), 13787-13791.
- [122] P.M. Drake, A.E. Albers, J. Baker, S. Banas, R.M. Barfield, A.S. Bhat, G.W. de Hart, A.W. Garofalo, P. Holder, L.C. Jones, R. Kudirka, J. McFarland, W. Zmolek, D. Rabuka, *Aldehyde Tag Coupled with HIPS Chemistry Enables the Production of ADCs Conjugated Site-Specifically to Different Antibody Regions with Distinct in Vivo Efficacy and PK Outcomes*, Bioconjugate Chemistry, 25, (2014), 1331-1341.
- [123] T. Krüger, S. Weiland, G. Falck, M. Gerlach, M. Boschanski, S. Alam, K.M. Müller, T. Dierks, N. Sewald, *Two-fold Bioorthogonal Derivatization by Different Formylglycine-Generating Enzymes*, Angewandte Chemie International Edition, 57, (2018), 7245-7249.
- [124] V. Siegmund, B. Piater, B. Zakeri, T. Eichhorn, F. Fischer, C. Deutsch, S. Becker, L. Toleikis, B. Hock, U.A.K. Betz, H. Kolmar, *Spontaneous Isopeptide Bond Formation as a Powerful Tool for Engineering Site-Specific Antibody-Drug Conjugates*, Scientific Reports, 6, (2016), 39291.
- [125] J. Grünwald, H.E. Klock, S.E. Cellitti, B. Bursulaya, D. McMullan, D.H. Jones, H.-P. Chiu, X. Wang, P. Patterson, H. Zhou, J. Vance, E. Nigoghossian, H. Tong, D. Daniel, W. Mallet, W. Ou, T. Uno, A. Brock, S.A. Lesley, B.H. Geierstanger, *Efficient Preparation of Site-Specific Antibody-Drug Conjugates Using Phosphopantetheinyl Transferases*, Bioconjugate Chemistry, 26, (2015), 2554-2562.
- [126] R.R. Beerli, T. Hell, A.S. Merkel, U. Grawunder, *Sortase Enzyme-Mediated Generation of Site-Specifically Conjugated Antibody Drug Conjugates with High In Vitro and In Vivo Potency*, PLOS ONE, 10, (2015), e0131177.
- [127] L. Chen, J. Cohen, X. Song, A. Zhao, Z. Ye, C.J. Feulner, P. Doonan, W. Somers, L. Lin, P.R. Chen, *Improved variants of SrtA for site-specific conjugation on antibodies and proteins with high efficiency*, Scientific Reports, 6, (2016), 31899.
- [128] Y. Xu, S. Jin, W. Zhao, W. Liu, D. Ding, J. Zhou, S. Chen, *A Versatile Chemo-Enzymatic Conjugation Approach Yields Homogeneous and Highly Potent Antibody-Drug Conjugates*, International Journal of Molecular Sciences, 18, (2017), 2284.

- [129] J.J. Bruins, A.H. Westphal, B. Albada, K. Wagner, L. Bartels, H. Spits, W.J.H. van Berkel, F.L. van Delft, *Inducible, Site-Specific Protein Labeling by Tyrosine Oxidation–Strain-Promoted (4 + 2) Cycloaddition*, *Bioconjugate Chemistry*, 28, (2017), 1189-1193.
- [130] P. Strop, *Versatility of Microbial Transglutaminase*, *Bioconjugate Chemistry*, 25, (2014), 855-862.
- [131] K. Yamada, Y. Ito, *Recent Chemical Approaches for Site-Specific Conjugation of Native Antibodies: Technologies toward Next-Generation Antibody–Drug Conjugates*, *ChemBioChem*, 20, (2019), 2729-2737.
- [132] M. Griffin, R. Casadio, C.M. Bergamini, *Transglutaminases: nature's biological glues*, *The Biochemical Journal*, 368, (2002), 377-396.
- [133] M.J. Arrizubieta, *Transglutaminases*, in: J. Polaina, A.P. MacCabe (Eds.) *Industrial Enzymes: Structure, Function and Applications*, Springer Netherlands, Dordrecht, (2007), pp. 567-581.
- [134] G. Falck, K.M.J.A. Müller, *Enzyme-based labeling strategies for antibody–drug conjugates and antibody mimetics*, 7, (2018), 4.
- [135] A. Ichinose, R.E. Bottenus, E.W. Davie, *Structure of transglutaminases*, *Journal of Biological Chemistry*, 265, (1990), 13411-13414.
- [136] L. Deweid, O. Avrutina, H. Kolmar, *Microbial transglutaminase for biotechnological and biomedical engineering*, *Biol Chem*, 400, (2019), 257-274.
- [137] T.L. Mindt, V. Jungi, S. Wyss, A. Friedli, G. Pla, I. Novak-Hofer, J. Grünberg, R. Schibli, *Modification of Different IgG1 Antibodies via Glutamine and Lysine using Bacterial and Human Tissue Transglutaminase*, *Bioconjugate Chemistry*, 19, (2008), 271-278.
- [138] P. Strop, S.-H. Liu, M. Dorywalska, K. Delaria, Russell G. Dushin, T.-T. Tran, W.-H. Ho, S. Farias, Meritxell G. Casas, Y. Abdiche, D. Zhou, R. Chandrasekaran, C. Samain, C. Loo, A. Rossi, M. Rickert, S. Krimm, T. Wong, Sherman M. Chin, J. Yu, J. Dilley, J. Chaparro-Riggers, Gary F. Filzen, Christopher J. O'Donnell, F. Wang, Jeremy S. Myers, J. Pons, David L. Shelton, A. Rajpal, *Location Matters: Site of Conjugation Modulates Stability and Pharmacokinetics of Antibody Drug Conjugates*, *Chemistry & Biology*, 20, (2013), 161-167.
- [139] J.L. Spidel, B. Vaessen, E.F. Albone, X. Cheng, A. Verdi, J.B. Kline, *Site-Specific Conjugation to Native and Engineered Lysines in Human Immunoglobulins by Microbial Transglutaminase*, *Bioconjugate Chemistry*, 28, (2017), 2471-2484.
- [140] P.R. Spycher, C.A. Amann, J.E. Wehrmüller, D.R. Hurwitz, O. Kreis, D. Messmer, A. Ritler, A. Kuchler, A. Blanc, M. Béhé, P. Walde, R. Schibli, *Dual, Site-Specific Modification of Antibodies by Using Solid-Phase Immobilized Microbial Transglutaminase*, *ChemBioChem*, 18, (2017), 1923-1927.
- [141] Y. Anami, W. Xiong, X. Gui, M. Deng, C.C. Zhang, N. Zhang, Z. An, K. Tsuchikama, *Enzymatic conjugation using branched linkers for constructing homogeneous antibody–drug conjugates with high potency*, *Organic & Biomolecular Chemistry*, 15, (2017), 5635-5642.
- [142] Y. Anami, C.M. Yamazaki, W. Xiong, X. Gui, N. Zhang, Z. An, K. Tsuchikama, *Glutamic acid–valine–citrulline linkers ensure stability and efficacy of antibody–drug conjugates in mice*, *Nature Communications*, 9, (2018), 2512.
- [143] P. Dennler, A. Chiotellis, E. Fischer, D. Brégeon, C. Belmant, L. Gauthier, F. Lhospice, F. Romagne, R. Schibli, *Transglutaminase-Based Chemo-Enzymatic Conjugation Approach Yields Homogeneous Antibody–Drug Conjugates*, *Bioconjugate Chemistry*, 25, (2014), 569-578.
- [144] S. Puthenveetil, S. Musto, F. Loganzo, L.N. Tumej, C.J. O'Donnell, E. Graziani, *Development of Solid-Phase Site-Specific Conjugation and Its Application toward Generation of Dual Labeled Antibody and Fab Drug Conjugates*, *Bioconjugate Chemistry*, 27, (2016), 1030-1039.
- [145] N. Bodyak, A.V. Yurkovetskiy, *Delivering More Payload (High DAR ADCs)*, in: M. Damelin (Ed.) *Innovations for Next-Generation Antibody-Drug Conjugates*, Springer International Publishing, Cham, (2018), pp. 215-240.
- [146] K.J. Hamblett, P.D. Senter, D.F. Chace, M.M.C. Sun, J. Lenox, C.G. Cervený, K.M. Kissler, S.X. Bernhardt, A.K. Kopcha, R.F. Zabinski, D.L. Meyer, J.A. Francisco, *Effects of Drug Loading on the Antitumor Activity of a Monoclonal Antibody Drug Conjugate*, *Clinical Cancer Research*, 10, (2004), 7063-7070.
- [147] X. Sun, J.F. Ponte, N.C. Yoder, R. Laleau, J. Coccia, L. Lanieri, Q. Qiu, R. Wu, E. Hong, M. Bogalhas, L. Wang, L. Dong, Y. Setiady, E.K. Maloney, O. Ab, X. Zhang, J. Pinkas, T.A. Keating, R. Chari, H.K. Erickson, J.M. Lambert, *Effects of Drug–Antibody Ratio on Pharmacokinetics, Biodistribution, Efficacy, and Tolerability of Antibody–Maytansinoid Conjugates*, *Bioconjugate Chemistry*, 28, (2017), 1371-1381.

- [148] J. Mantaj, P.J.M. Jackson, K.M. Rahman, D.E. Thurston, *From Anthramycin to Pyrrolobenzodiazepine (PBD)-Containing Antibody-Drug Conjugates (ADCs)*, *Angewandte Chemie (International ed. in English)*, 56, (2017), 462-488.
- [149] D.M. Goldenberg, T.M. Cardillo, S.V. Govindan, E.A. Rossi, R.M. Sharkey, *Trop-2 is a novel target for solid cancer therapy with sacituzumab govitecan (IMMU-132), an antibody-drug conjugate (ADC)*, *Oncotarget*, 6, (2015), 22496-22512.
- [150] S.V. Govindan, T.M. Cardillo, E.A. Rossi, P. Trisal, W.J. McBride, R.M. Sharkey, D.M. Goldenberg, *Improving the Therapeutic Index in Cancer Therapy by Using Antibody-Drug Conjugates Designed with a Moderately Cytotoxic Drug*, *Molecular Pharmaceutics*, 12, (2015), 1836-1847.
- [151] T. Nakada, T. Masuda, H. Naito, M. Yoshida, S. Ashida, K. Morita, H. Miyazaki, Y. Kasuya, Y. Ogitani, J. Yamaguchi, Y. Abe, T. Honda, *Novel antibody drug conjugates containing exatecan derivative-based cytotoxic payloads*, *Bioorganic & Medicinal Chemistry Letters*, 26, (2016), 1542-1545.
- [152] Y. Ogitani, T. Aida, K. Hagihara, J. Yamaguchi, C. Ishii, N. Harada, M. Soma, H. Okamoto, M. Oitate, S. Arakawa, T. Hirai, R. Atsumi, T. Nakada, I. Hayakawa, Y. Abe, T. Agatsuma, *DS-8201a, A Novel HER2-Targeting ADC with a Novel DNA Topoisomerase I Inhibitor, Demonstrates a Promising Antitumor Efficacy with Differentiation from T-DM1*, *Clinical Cancer Research*, 22, (2016), 5097-5108.
- [153] R.P. Lyon, T.D. Bovee, S.O. Doronina, P.J. Burke, J.H. Hunter, H.D. Neff-LaFord, M. Jonas, M.E. Anderson, J.R. Setter, P.D. Senter, *Reducing hydrophobicity of homogeneous antibody-drug conjugates improves pharmacokinetics and therapeutic index*, *Nature Biotechnology*, 33, (2015), 733-735.
- [154] P.J. Burke, J.Z. Hamilton, S.C. Jeffrey, J.H. Hunter, S.O. Doronina, N.M. Okeley, J.B. Miyamoto, M.E. Anderson, I.J. Stone, M.L. Ulrich, J.K. Simmons, E.E. McKinney, P.D. Senter, R.P. Lyon, *Optimization of a PEGylated Glucuronide-Monomethylauristatin E Linker for Antibody-Drug Conjugates*, *Molecular Cancer Therapeutics*, 16, (2017), 116-123.
- [155] M.R. Levensgood, X. Zhang, J.H. Hunter, K.K. Emmerton, J.B. Miyamoto, T.S. Lewis, P.D. Senter, *Orthogonal Cysteine Protection Enables Homogeneous Multi-Drug Antibody-Drug Conjugates*, *Angewandte Chemie (International ed. in English)*, 56, (2017), 733-737.
- [156] B.A. Mendelsohn, S.D. Barnscher, J.T. Snyder, Z. An, J.M. Dodd, J. Dugal-Tessier, *Investigation of Hydrophilic Auristatin Derivatives for Use in Antibody Drug Conjugates*, *Bioconjugate Chemistry*, 28, (2017), 371-381.
- [157] T. Satomaa, H. Pynnonen, A. Vilkmann, T. Kotiranta, V. Pitkanen, A. Heiskanen, B. Herpers, L.S. Price, J. Helin, J. Saarinen, *Hydrophilic Auristatin Glycoside Payload Enables Improved Antibody-Drug Conjugate Efficacy and Biocompatibility*, *Antibodies*, 7, (2018).
- [158] B. Chen, D.A. Gianolio, J.E. Stefano, C.M. Manning, R.C. Gregory, M.M. Busch, W.H. Brondyk, R.J. Miller, P.K. Dhal, *Design, Synthesis, and in vitro Evaluation of Multivalent Drug Linkers for High-Drug-Load Antibody-Drug Conjugates*, *ChemMedChem*, 13, (2018), 790-794.
- [159] N. Gupta, J. Kancharla, S. Kaushik, A. Ansari, S. Hossain, R. Goyal, M. Pandey, J. Sivaccumar, S. Hussain, A. Sarkar, A. Sengupta, S.K. Mandal, M. Roy, S. Sengupta, *Development of a facile antibody-drug conjugate platform for increased stability and homogeneity*, *Chemical science*, 8, (2017), 2387-2395.
- [160] S.B. van Witteloostuijn, S.L. Pedersen, K.J. Jensen, *Half-Life Extension of Biopharmaceuticals using Chemical Methods: Alternatives to PEGylation*, *ChemMedChem*, 11, (2016), 2474-2495.
- [161] A. Yurkovetskiy, S. Choi, A. Hiller, M. Yin, C. McCusker, S. Syed, A.J. Fischman, M.I. Papisov, *Fully degradable hydrophilic polyals for protein modification*, *Biomacromolecules*, 6, (2005), 2648-2658.
- [162] M.I. Papisov, A. Hiller, A. Yurkovetskiy, M. Yin, M. Barzana, S. Hillier, A.J. Fischman, *Semisynthetic Hydrophilic Polyals*, *Biomacromolecules*, 6, (2005), 2659-2670.
- [163] A.V. Yurkovetskiy, M. Yin, N. Bodyak, C.A. Stevenson, J.D. Thomas, C.E. Hammond, L. Qin, B. Zhu, D.R. Gumerov, E. Ter-Ovanesyan, A. Uttard, T.B. Lowinger, *A Polymer-Based Antibody-Vinca Drug Conjugate Platform: Characterization and Preclinical Efficacy*, *Cancer Research*, 75, (2015), 3365.
- [164] A. Yurkovetskiy, N. Bodyak, M. Yin, J. Thomas, P. Conlon, C. Stevenson, A. Uttard, L. Qin, D. Gumerov, E. Ter-Ovanesyan, *Advantages of polyacetal polymer-based antibody drug conjugates employing cysteine bioconjugation*, *Proceedings of the 104th annual meeting of the American Association for Cancer Research*, (2013),
- [165] L. Zhang, Y. Fang, J. Kopeček, J. Yang, *A new construct of antibody-drug conjugates for treatment of B-cell non-Hodgkin's lymphomas*, *European Journal of Pharmaceutical Sciences*, 103, (2017), 36-46.

- [166] C. Olsson, G.J.C.-F.A. Westman, *Direct dissolution of cellulose: background, means and applications*, Cellulose - Fundamental Aspects(2013), pp. 521-44.
- [167] W.B. Neely, *Dextran: Structure and Synthesis*, in: M.L. Wolfrom, R.S. Tipson (Eds.) *Advances in Carbohydrate Chemistry*, Academic Press(1961), pp. 341-369.
- [168] W. Soetaert, D. Schwengers, K. Buchholz, E.J. Vandamme, *A wide range of carbohydrate modifications by a single micro-organism: leuconostoc mesenteroides*, in: S.B. Petersen, B. Svensson, S. Pedersen (Eds.) *Progress in Biotechnology*, Elsevier(1995), pp. 351-358.
- [169] A. Jeanes, S. Hassan, A. Groner, F. Huebner, J. Bietz, J. Wall, *2626101. Dextans and pullulans: industrially significant alpha D glucans*, ACS Symp Ser, (1977), pp. 284-298
- [170] M. Nasrollahzadeh, M. Sajjadi, S.M. Sajadi, Z. Issaabadi, *Chapter 5 - Green Nanotechnology*, Interface Science and Technology, Elsevier(2019), pp. 145-198.
- [171] C. Naveen, N.R. Shastri, *12 - Polysaccharide nanomicelles as drug carriers*, in: S. Maiti, S. Jana (Eds.) *Polysaccharide Carriers for Drug Delivery*, Woodhead Publishing(2019), pp. 339-363.
- [172] F.J. Plou, M.T. Martín, A.G. de Segura, M. Alcalde, A.J.C.J.o.C. Ballesteros, *Glucosyltransferases acting on starch or sucrose for the synthesis of oligosaccharides*, 80, (2002), 743-752.
- [173] V. Monchois, R.-M. Willemot, P. Monsan, *Glucansucrases: mechanism of action and structure–function relationships*, FEMS Microbiology Reviews, 23, (1999), 131-151.
- [174] C. Larsen, *Dextran prodrugs — structure and stability in relation to therapeutic activity*, Advanced Drug Delivery Reviews, 3, (1989), 103-154.
- [175] R. Mehvar, *Dextrans for targeted and sustained delivery of therapeutic and imaging agents*, Journal of Controlled Release, 69, (2000), 1-25.
- [176] E. Schacht, R. Vercauteren, S.J.J.o.b. Vansteenkiste, c. polymers, *Some aspects of the application of dextran in prodrug design*, 3, (1988), 72-80.
- [177] R. Vercauteren, D. Bruneel, E. Schacht, R. Duncan, *Effect of the Chemical Modification of Dextran on the Degradation by Dextranase*, Journal of Bioactive and Compatible Polymers, 5, (1990), 4-15.
- [178] Y. Kaneo, T. Uemura, T. Tanaka, S. Kanoh, *Polysaccharides as Drug Carriers : Biodisposition of Fluorescein-Labeled Dextrans in Mice*, Biological & Pharmaceutical Bulletin, 20, (1997), 181-187.
- [179] R. Mehvar, M.A. Robinson, J.M. Reynolds, *Molecular Weight Dependent Tissue Accumulation of Dextrans: In Vivo Studies in Rats*, Journal of Pharmaceutical Sciences, 83, (1994), 1495-1499.
- [180] T. Yamaoka, Y. Tabata, Y. Ikada, *Body distribution profile of polysaccharides after intravenous administration*, Drug Delivery, 1, (1993), 75-82.
- [181] E.M. Berg, S. Fasting, O.F.M. Sellevold, *Serious complications with dextran-70 despite hapten prophylaxis*, Anaesthesia, 46, (1991), 1033-1035.
- [182] H. Hedin, W. Richter, J. Ring, *Dextran-induced Anaphylactoid Reactions in Man*, International Archives of Allergy and Immunology, 52, (1976), 145-159.
- [183] D. Kraft, H. Hedin, W. Richter, O. Scheiner, H. Rumpold, M.E. Devey, *Immunoglobulin Class and Subclass Distribution of Dextran-Reactive Antibodies in Human Reactors and Non Reactors to Clinical Dextran*, Allergy, 37, (1982), 481-489.
- [184] I. Seppälä, J. Pelkonen, O. Mäkelä, *Isotypes of antibodies induced by plain dextran or a dextran-protein conjugate*, European Journal of Immunology, 15, (1985), 827-833.
- [185] Y. Takakura, Y. Kaneko, T. Fujita, M. Hashida, H. Maeda, H. Sezaki, *Control of Pharmaceutical Properties of Soybean Trypsin Inhibitor by Conjugation with Dextran I: Synthesis and Characterization*, Journal of Pharmaceutical Sciences, 78, (1989), 117-121.
- [186] Y. YASUDA, T. FUJITA, Y. TAKAKURA, M. HASHIDA, H.J.C. SEZAKI, P. Bulletin, *Biochemical and biopharmaceutical properties of macromolecular conjugates of uricase with dextran and polyethylene glycol*, 38, (1990), 2053-2056.
- [187] M. Behe, J. Du, W. Becker, T. Behr, C. Angerstein, M. Márquez, J. Hiltunen, S. Nilsson, A.R. Holmberg, *Biodistribution, blood half-life, and receptor binding of a somatostatin-dextran conjugate*, Medical Oncology, 18, (2001), 59-64.
- [188] Y. Perez, A. Valdivia, L. Gomez, B.K. Simpson, R. Villalonga, *Glycosidation of Cu,Zn-Superoxide Dismutase with End-Group Aminated Dextran. Pharmacological and Pharmacokinetics Properties*, Macromolecular Bioscience, 5, (2005), 1220-1225.

- [189] R. Fagnani, M.S. Hagan, R.J.C.r. Bartholomew, *Reduction of immunogenicity by covalent modification of murine and rabbit immunoglobulins with oxidized dextrans of low molecular weight*, *Cancer Research*, 50, (1990), 3638-3645.
- [190] R. Fagnani, S. Halpern, M.J.N.m.c. Hagan, *Altered pharmacokinetic and tumour localization properties of Fab'fragments of a murine monoclonal anti-CEA antibody by covalent modification with low molecular weight dextran*, 16, (1995), 362-369.
- [191] K.M. McLean, G. Johnson, R.C. Chatelier, G.J. Beumer, J.G. Steele, H.J. Griesser, *Method of immobilization of carboxymethyl-dextran affects resistance to tissue and cell colonization*, *Colloids and Surfaces B: Biointerfaces*, 18, (2000), 221-234.
- [192] J. Morimoto, M. Sarkar, S. Kenrick, T. Kodadek, *Dextran as a generally applicable multivalent scaffold for improving immunoglobulin-binding affinities of peptide and peptidomimetic ligands*, *Bioconjugate chemistry*, 25, (2014), 1479-1491.
- [193] M. Richter, A. Chakrabarti, I.R. Ruttekkolk, B. Wiesner, M. Beyermann, R. Brock, J. Rademann, *Multivalent Design of Apoptosis-Inducing Bid-BH3 Peptide–Oligosaccharides Boosts the Intracellular Activity at Identical Overall Peptide Concentrations*, *Chemistry – A European Journal*, 18, (2012), 16708-16715.
- [194] R. Villalonga, A. Valdivia, Y. Pérez, B. Chongo, *Improved pharmacokinetics and stability properties of catalase by chemical glycosidation with end-group activated dextran*, *Journal of Applied Polymer Science*, 102, (2006), 4573-4576.
- [195] M. Aliboland, F. Alabdollah, F. Sadeghi, M. Mohammadi, K. Abnous, M. Ramezani, F. Hadizadeh, *Dextran-b-poly(lactide-co-glycolide) polymersome for oral delivery of insulin: In vitro and in vivo evaluation*, *Journal of Controlled Release*, 227, (2016), 58-70.
- [196] Y.-I. Jeong, D.-G. Kim, D.-H.J.J.o.C. Kang, *Synthesis of dextran/methoxy poly (ethylene glycol) block copolymer*, *Journal of Chemistry*, Volume 2013, (2013), Article ID 414185.
- [197] A. Valdivia, R. Villalonga, P.D. Pierro, Y. Pérez, L. Mariniello, L. Gómez, R. Porta, *Transglutaminase-catalyzed site-specific glycosidation of catalase with aminated dextran*, *Journal of Biotechnology*, 122, (2006), 326-333.
- [198] E. Hurwitz, *Specific and nonspecific macromolecule–drug conjugates for the improvement of cancer chemotherapy*, *Biopolymers*, 22, (1983), 557-567.
- [199] A.R. Oseroff, D. Ohuoha, T. Hasan, J.C. Bommer, M.L. Yarmush, *Antibody-targeted photolysis: selective photodestruction of human T-cell leukemia cells using monoclonal antibody-chlorin e6 conjugates*, *Proceedings of the National Academy of Sciences*, 83, (1986), 8744-8748.
- [200] L.B. Shih, R.M. Sharkey, F.J. Primus, D.M. Goldenberg, *Site-specific linkage of methotrexate to monoclonal antibodies using an intermediate carrier*, *International Journal of Cancer*, 41, (1988), 832-839.
- [201] Y. Tsukada, K. Ohkawa, N.J.C.r. Hibi, *Therapeutic effect of treatment with polyclonal or monoclonal antibodies to α -fetoprotein that have been conjugated to daunomycin via a dextran bridge: studies with an α -fetoprotein-producing rat hepatoma tumor model*, 47, (1987), 4293-4295.
- [202] E. Hurwitz, R. Maron, A. Bernstein, M. Sela, R. Arnon, M. Wilchek, *The effect in vivo of chemotherapeutic drug–antibody conjugates in two murine experimental tumor systems*, *International Journal of Cancer*, 21, (1978), 747-755.
- [203] Y. Tsukada, E. Hurwitz, R. Kashi, M. Sela, N. Hibi, A. Hara, H. Hirai, *Effect of a conjugate of daunomycin and purified polyclonal or monoclonal antibodies to rat α -fetoprotein on the growth of α -fetoprotein-producing tumor cells*, *Annals of the New York Academy of Sciences*, 417, (1983), 262-269.
- [204] J. Maia, L. Ferreira, R. Carvalho, M.A. Ramos, M.H.J.P. Gil, *Synthesis and characterization of new injectable and degradable dextran-based hydrogels*, 46, (2005), 9604-9614.
- [205] C. Fasting, C.A. Schalley, M. Weber, O. Seitz, S. Hecht, B. Kokschi, J. Dervede, C. Graf, E.-W. Knapp, R. Haag, *Multivalency as a Chemical Organization and Action Principle*, *Angewandte Chemie International Edition*, 51, (2012), 10472-10498.
- [206] C. Pang, T.-i. Kim, W.G. Bae, D. Kang, S.M. Kim, K.-Y. Suh, *Bioinspired Reversible Interlocker Using Regularly Arrayed High Aspect-Ratio Polymer Fibers*, *Advanced Materials*, 24, (2012), 475-479.
- [207] D. Vokoun, P. Sedláč, M. Frost, J. Pilch, D. Majtás, P. Šittner, *Velcro-like fasteners based on NiTi micro-hook arrays*, *Smart Materials and Structures*, 20, (2011), 085027.
- [208] J. Sun, B. Bhushan, *Structure and mechanical properties of beetle wings: a review*, *RSC Advances*, 2, (2012), 12606-12623.

- [209] L. Erlandsson, P. Akerblad, C. Vingsbo-Lundberg, E. Kallberg, N. Lycke, T. Leanderson, *Joining chain-expressing and -nonexpressing B cell populations in the mouse*, *The Journal of experimental medicine*, 194, (2001), 557-570.
- [210] J.M. Woof, M.A. Kerr, *IgA function--variations on a theme*, *Immunology*, 113, (2004), 175-177.
- [211] A. Dubuisson, O.J.A. Micheau, *Antibodies and derivatives targeting DR4 and DR5 for cancer therapy*, 6, (2017), 16.
- [212] A. Ashkenazi, R.C. Pai, S. Fong, S. Leung, D.A. Lawrence, S.A. Marsters, C. Blackie, L. Chang, A.E. McMurtrey, A. Hebert, L. DeForge, I.L. Koumenis, D. Lewis, L. Harris, J. Bussiere, H. Koeppen, Z. Shahrokh, R.H. Schwall, *Safety and antitumor activity of recombinant soluble Apo2 ligand*, *The Journal of Clinical Investigation*, 104, (1999), 155-162.
- [213] H. Belkahla, G. Herlem, F. Picaud, T. Gharbi, M. Hemadi, S. Ammar, O.J.N. Micheau, *TRAIL-NP hybrids for cancer therapy: a review*, 9, (2017), 5755-5768.
- [214] W. Schneider-Brachert, U. Heigl, M.J.I.j.o.m.s. Ehrenschwender, *Membrane trafficking of death receptors: implications on signalling*, 14, (2013), 14475-14503.
- [215] A.K. Lewis, C.C. Valley, S.L. Peery, B. Brummel, A.R. Braun, C.B. Karim, J.N. Sachs, *Death Receptor 5 Networks Require Membrane Cholesterol for Proper Structure and Function*, *Journal of Molecular Biology*, 428, (2016), 4843-4855.
- [216] J.-C. Soria, E. Smit, D. Khayat, B. Besse, X. Yang, C.-P. Hsu, D. Reese, J. Wiezorek, F. Blackhall, *Phase 1b Study of Dulanermin (recombinant human Apo2L/TRAIL) in Combination With Paclitaxel, Carboplatin, and Bevacizumab in Patients With Advanced Non-Squamous Non-Small-Cell Lung Cancer*, *Journal of Clinical Oncology*, 28, (2010), 1527-1533.
- [217] M. Kozloff, W.A. Messersmith, A.V. Kapp, A. Ashkenazi, S. Royer-Joo, C.C. Portera, Z.A. Wainberg, *Phase Ib study of dulanermin combined with first-line FOLFOX plus bevacizumab (BV) in patients (Pts) with metastatic colorectal cancer (mCRC)*, *Journal of Clinical Oncology*, 30, (2012), 3552-3552.
- [218] N. Ishimura, H. Isomoto, S.F. Bronk, G.J. Gores, *Trail induces cell migration and invasion in apoptosis-resistant cholangiocarcinoma cells*, *American Journal of Physiology-Gastrointestinal and Liver Physiology*, 290, (2006), G129-G136.
- [219] P. Secchiero, C. Zerbinati, E. Rimondi, F. Corallini, D. Milani, V. Grill, G. Forti, S. Capitani, G. Zauli, *TRAIL promotes the survival, migration and proliferation of vascular smooth muscle cells*, *Cellular and Molecular Life Sciences*, 61, (2004), 1965-1974.
- [220] L. Pukac, P. Kanakaraj, R. Humphreys, R. Alderson, M. Bloom, C. Sung, T. Riccobene, R. Johnson, M. Fiscella, A. Mahoney, J. Carrell, E. Boyd, X.T. Yao, L. Zhang, L. Zhong, A. von Kerczek, L. Shepard, T. Vaughan, B. Edwards, C. Dobson, T. Salcedo, V. Albert, *HGS-ETR1, a fully human TRAIL-receptor 1 monoclonal antibody, induces cell death in multiple tumour types in vitro and in vivo*, *British Journal of Cancer*, 92, (2005), 1430-1441.
- [221] C. Geng, J. Hou, Y. Zhao, X. Ke, Z. Wang, L. Qiu, H. Xi, F. Wang, N. Wei, Y. Liu, S. Yang, P. Wei, X. Zheng, Z. Huang, B. Zhu, W.-M. Chen, *A multicenter, open-label phase II study of recombinant CPT (Circularly Permuted TRAIL) plus thalidomide in patients with relapsed and refractory multiple myeloma*, *American Journal of Hematology*, 89, (2014), 1037-1042.
- [222] Y. Leng, J. Hou, J. Jin, M. Zhang, X. Ke, B. Jiang, L. Pan, L. Yang, F. Zhou, J. Wang, Z. Wang, L. Liu, W. Li, Z. Shen, L. Qiu, N. Chang, J. Li, J. Liu, H. Pang, H. Meng, P. Wei, H. Jiang, Y. Liu, X. Zheng, S. Yang, W. Chen, *Circularly permuted TRAIL plus thalidomide and dexamethasone versus thalidomide and dexamethasone for relapsed/refractory multiple myeloma: a phase 2 study*, *Cancer Chemotherapy and Pharmacology*, 79, (2017), 1141-1149.
- [223] F. Liu, Y. Si, G. Liu, S. Li, J. Zhang, Y. Ma, *The tetravalent anti-DR5 antibody without cross-linking direct induces apoptosis of cancer cells*, *Biomedicine & Pharmacotherapy*, 70, (2015), 41-45.
- [224] K.P. Papadopoulos, R. Isaacs, S. Bilic, K. Kentsch, H.A. Huet, M. Hofmann, D. Rasco, N. Kundamal, Z. Tang, J. Cooksey, A. Mahipal, *Unexpected hepatotoxicity in a phase I study of TAS266, a novel tetravalent agonistic Nanobody® targeting the DR5 receptor*, *Cancer Chemotherapy and Pharmacology*, 75, (2015), 887-895.
- [225] V. Pavet, J. Beyrath, C. Pardin, A. Morizot, M.-C. Lechner, J.-P. Briand, M. Wendland, W. Maison, S. Fournel, O. Micheau, G. Guichard, H. Gronemeyer, *Multivalent DR5 Peptides Activate the TRAIL Death Pathway and Exert Tumoricidal Activity*, *Cancer Research*, 70, (2010), 1101-1110.

-
- [226] G. Lamanna, C.R. Smulski, N. Chekkat, K. Estieu-Gionnet, G. Guichard, S. Fournel, A. Bianco, *Multimerization of an Apoptogenic TRAIL-Mimicking Peptide by Using Adamantane-Based Dendrons*, *Chemistry – A European Journal*, 19, (2013), 1762-1768.
- [227] B. Valldorf, H. Fittler, L. Deweid, A. Ebenig, S. Dickgiesser, C. Sellmann, J. Becker, S. Zielonka, M. Empting, O. Avrutina, H. Kolmar, *An Apoptosis-Inducing Peptidic Heptad That Efficiently Clusters Death Receptor 5*, *Angewandte Chemie International Edition*, 55, (2016), 5085-5089.
- [228] Y.M. Angell, A. Bhandari, M.N.D. Francisco, B.T. Frederick, J.M. Green, K. Leu, K. Leuther, R. Sana, P.J. Schatz, E.A. Whitehorn, K. Wright, C.P. Holmes, *Discovery and Optimization of a TRAIL R2 Agonist for Cancer Therapy*, in: S.D. Valle, E. Escher, W.D. Lubell (Eds.) *Peptides for Youth*, Springer New York, New York, NY, (2009), pp. 101-103

4. Cumulative Section

4.1. Dextramabs: A Novel Format of Antibody-Drug Conjugates Featuring a Multivalent Polysaccharide Scaffold

Title:

Dextramabs: A Novel Format of Antibody-Drug Conjugates Featuring a Multivalent Polysaccharide Scaffold

Authors:

H. Schneider, L. Deweid, T. Pirzer, D. Yanakieva, S. Englert, B. Becker, O. Avrutina, H. Kolmar

Bibliographic data:

ChemistryOpen

Volume 8, Pages 354-357

Article first published online: 28th Mar 2019

DOI: <https://doi.org/10.1002/open.201900066>

Open Access Article

Available under the terms of the Creative Commons Attribution Non-Commercial No Derivatives License

CC BY-NC-ND

Contributions by Hendrik Schneider:

- Initial idea and project management together with H. Kolmar
- Performed the majority of experiments
- Preparation of the manuscript and all included graphical material
- Revised the manuscript

Dextramabs: A Novel Format of Antibody-Drug Conjugates Featuring a Multivalent Polysaccharide Scaffold

Hendrik Schneider, Lukas Deweid, Thomas Pirzer, Desislava Yanakieva, Simon Englert, Bastian Becker, Olga Avrutina, and Harald Kolmar*^[a]

Antibody-drug conjugates (ADCs) are multicomponent biomolecules that have emerged as a powerful tool for targeted tumor therapy. Combining specific binding of an immunoglobulin with toxic properties of a payload, they however often suffer from poor hydrophilicity when loaded with a high amount of toxins. To address these issues simultaneously, we developed dextramabs, a novel class of hybrid antibody-drug conjugates. In these architectures, the therapeutic antibody trastuzumab is equipped with a multivalent dextran polysaccharide that enables efficient loading with a potent toxin in a controllable fashion. Our modular chemoenzymatic approach provides an access to synthetic dextramabs bearing monomethyl auristatin as releasable cytotoxic cargo. They possess high drug-to-antibody ratios, remarkable hydrophilicity, and high toxicity *in vitro*.

Having evolved from Paul Ehrlich's "magic bullet" concept, antibody-drug conjugates (ADCs) are aimed at achieving a site-specific delivery of cytotoxic agents to target cells, usually those expressing tumour-associated antigens.^[1] A three-component ADC format comprises a monoclonal antibody armed with a cytotoxic payload *via* a special, in an ideal case biodegradable, linker making use of a vast bioconjugation arsenal.^[1a,c] To date, chemistry of surface-exposed lysines or reduced cysteines at the hinge region is used to access covalent attachment of a cytotoxic counterpart. However, the lack of specificity leads to formation of heterogeneous products, which is a serious drawback regarding efficacy, immunogenicity and pharmacokinetic issues.^[1a,b,2] To overcome these deficiencies site-specific routes have been proposed, among them cysteine^[3] and glycoengineering,^[2c,4] non-natural amino acid formats^[1b] or enzyme-mediated ligations applying transglutaminase,^[5]

sortase^[6] and formylglycine-generating enzyme,^[7] as well as the tub-tag technology.^[8]

Despite obvious progress in the field of ADCs, it is still a challenge to achieve high drug-to-antibody ratio (DAR) while maintaining hydrophilicity. Indeed, since the hydrophobic character of commonly used highly potent toxins compromises the ADC's biophysical properties, first of all solubility and aggregation, the DAR values usually do not exceed 3–4.^[1b,d,3b,9] Moreover, highly toxin-loaded ADCs possess faster clearance due to enhanced hydrophobicity.^[10] Therefore, tailoring their polarity might simultaneously enhance DAR and increase circulation time, thus modulating both efficiency and pharmacokinetics.^[11] Different approaches to address these challenges have been recently reported. Thus, Mendelsohn et al.,^[12] Lyon et al.^[11] and Santomaa et al.^[13] engineered toxic auristatin payloads towards enhanced hydrophilicity. Chen et al.^[3b] made use of thiol-ene ligation applying less hydrophobic multidrug linkers. To enhance polarity of their ADCs, Mersana Therapeutic Inc. decorated an antibody with a polymeric polyol-scaffold Fleximer[®] *via* hinge-region cysteines.^[14] By means of enzymatic catalysis Anami et al.^[5a] equipped a therapeutic antibody with branched PEG chains bearing numerous orthogonally addressable sites that enabled attachment of a toxic cargo in multiple copies.

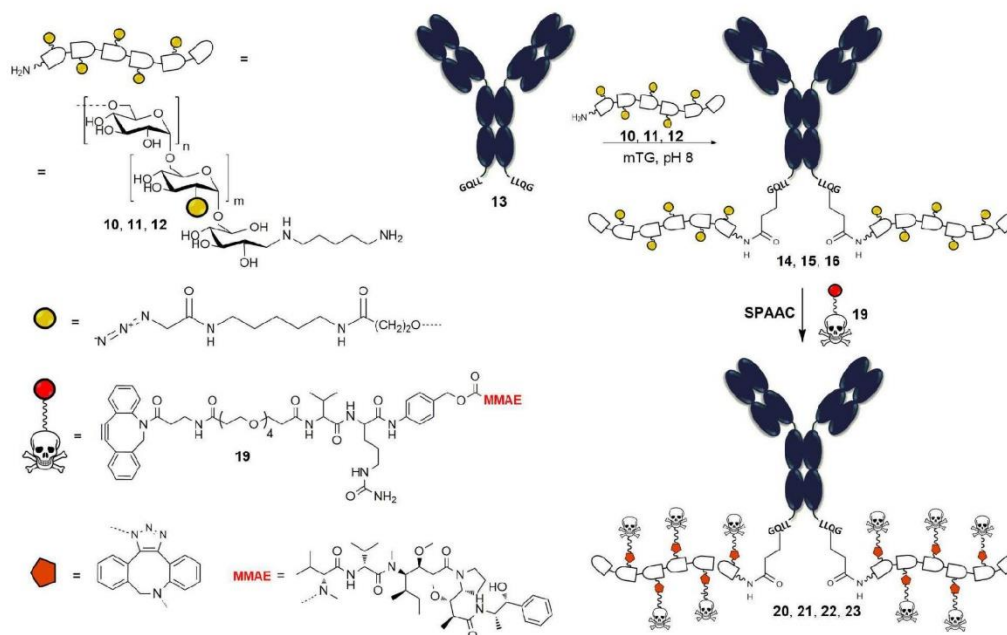
Encouraged by these achievements, we designed dextramabs, a novel ADC format comprising a therapeutic antibody as a highly specific delivery module and a hydrophilic polysaccharide scaffold carrying a releasable toxic payload in desired number of copies (Scheme 1). To enable conjugation of functional counterparts, we developed a set of efficient chemoenzymatic transformations (Scheme 1).

Dextran polysaccharide (M_w 10.000 g mol⁻¹) was chosen as a DAR- and polarity-enhancing scaffold. This biocompatible, clinically and FDA-approved glucan consisting of repeating α -(1-6)-linked oligo-D-glucose units is an accredited blood-flow enhancer and plasma volume expander.^[15] Offering certain space for chemical modifications at numerous positions, this polymer has been thoroughly investigated as a carrier for agents of diverse nature.^[15-16] A number of studies reported that conjugation to dextran positively influenced the properties of involved biomolecules.^[15,17] For example, site-specific ligation of dextran to catalase mediated by microbial transglutaminase (mTG) resulted in hybrid constructs with improved thermal stability and pharmacokinetics.^[17e] Reduced immunogenicity was demonstrated by several antibodies or Fabs when bound to dextran scaffolds.^[15,17a,b]

[a] H. Schneider, L. Deweid, T. Pirzer, D. Yanakieva, S. Englert, B. Becker, Dr. O. Avrutina, Prof. Dr. H. Kolmar
Clemens-Schöpfung-Institut für Organische Chemie und Biochemie
Technische Universität Darmstadt, Alarich-Weiss-Straße 4,
64287 Darmstadt (Germany)
E-mail: Kolmar@biochemie-tud.de

Supporting information for this article is available on the WWW under <https://doi.org/10.1002/open.201900066>

© 2019 The Authors. Published by Wiley-VCH Verlag GmbH & Co. KGaA.
This is an open access article under the terms of the Creative Commons Attribution Non-Commercial NoDerivs License, which permits use and distribution in any medium, provided the original work is properly cited, the use is non-commercial and no modifications or adaptations are made.

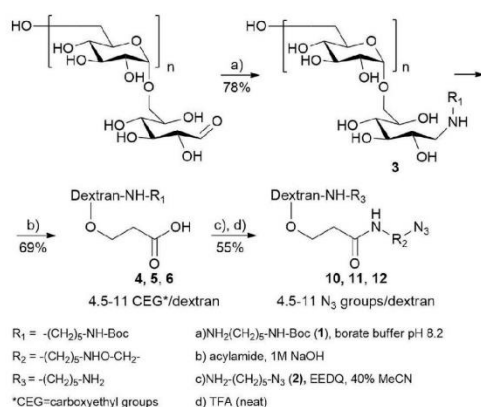


Scheme 1. General scheme for the generation of dextramabs. SPAAC: strain-promoted azide-alkyne cycloaddition. MMAE: monomethyl auristatin E.

Dextran polymer provides several possibilities for chemical modification, with oxidation of its glucose hydroxyls towards reactive aldehydes followed by coupling of a suitable nucleophile being the obvious choice.^[15,17a,d] Lacking selectivity, this strategy often yields conjugates with unpredicted properties, especially in view of immunoreactivity.^[15,17a,b] Therefore we decided to omit oxidation of hydroxyls making use of dextran's orthogonal addressability at its reducing end^[18] and at the glucose repeating units^[9] (Scheme 2). Thus, its sugar backbone was assigned for the

covalent immobilization of a toxic cargo, and the red-end for the enzyme-catalyzed conjugation to an antibody.

The reducing end of dextran was decorated with Boc-protected cadaverine **1** upon reductive amination, giving derivative **3** (Scheme 2) bearing a masked site for enzymatic conjugation. Afterwards, the cytotoxic payload was attached to the dextran polysaccharide backbone. The required synthetic module comprised monomethyl auristatin E (MMAE),^[20] a traceless linker (Val-Cit-PAB, Scheme 1) ensuring endosomal release of a cargo after cellular uptake, and an addressable site for the strain-promoted azide-alkyne cycloaddition (SPAAC) (Scheme 1 <xscr1). MMAE was chosen as a hydrophobic payload^[20] as it can allow to easily assess whether coupling to the dextran polymer provides advantages in terms of overall hydrophilicity. The polysaccharide scaffold was prepared for toxin attachment *via* SPAAC by decoration with an azide group, while a dibenzocyclooctyne (DBCO) moiety was introduced into the linker-toxin construct. Carboxyethylation at the C2 position of the glucose units followed by hydrolysis of the formed amide resulted in carboxydextran **4**, **5**, and **6** which differed in carboxyl density (Scheme 2). The amount of carboxylic groups per dextran was controlled stoichiometrically and assessed by ¹H-NMR analysis (Section S1.1.5, ESI). We maintained this level at 4.5–11 carboxylates per dextran. The carboxyls of modified dextran **4**, **5**, and **6** were then addressed by an amine end of the bifunctional linker **2** (Scheme 2) using EEDQ activation resulting in azide-bearing constructs **7**, **8**, and **9**. Successive removal of the Boc protecting group at the dextran reducing end yielded cadaverine-modified dextran



Scheme 2. Synthetic route to SPAAC- and mTG-addressable dextran scaffold. EEDQ: N-ethoxycarbonyl-2-ethoxy-1,2-dihydroquinoline.

11, and 12 suitable for both SPAAC and transglutaminase-mediated chemoenzymatic bioconjugation and providing up to 11 addressable positions for the cytotoxic payload (confirmed by $^1\text{H-NMR}$ and IR, Section S1.1.6, ESI).

As a targeting/delivery module we used the monoclonal antibody trastuzumab. This immunoglobulin targets HER2-overexpressing cancer cells and is a constitutive element of the FDA-approved ADC Adcetris®.^[1b] Trastuzumab was engineered to possess an mTG recognition tag LLQG 13 at the C-termini of its heavy chains.^[21] Transglutaminase-catalysed condensation with cadaverine-dextran towards dextran-modified antibodies 14, 15, and 16 proceeded smoothly in aqueous buffer overnight (Scheme 1, Section S1.2.1, ESI). Then the desired fluorescent/cytotoxic payload was coupled using SPAAC (Scheme 2). To that end, the cargo molecules were modified to carry a click-reactive DBCO motif (Section S1.2.2, ESI). Hydrophobic interaction chromatography (HIC) and SDS-PAGE analysis of conjugates 14, 15 and 16 revealed a dextran-to-antibody coupling efficiency between 1 and 2 (2 is the highest achievable number) indicating that every protein molecule was decorated with at least one dextran scaffold. No efforts were made yet to further enhance coupling efficiency by e.g. suppression of observed minor enzyme-mediated antibody multimerization presumably due to a reactive lysine of trastuzumab 13 (Section S1.1.8, ESI).

Following generation of dextran-trastuzumab hybrids, the toxic cargo was attached at the polysaccharide site in multiple copies. First, the fluorogenic probe DBCO-Cy5 17 was "clicked" to the azide-bearing construct 15 to yield conjugate 18 (Section S1.2.2, ESI). The completeness of SPAAC was confirmed by photometric analysis (Section S1.1.15, ESI). A well-established drug module in the context of ADC development, DBCO-PEG₃-ValCit-PAB-MMAE 19 (Scheme 1), was chosen as a payload to be "clicked" to conjugates 14, 15, and 16. Depending on the scaffold-to-payload ratio that was stoichiometrically controlled, dextramabs 20, 21, 22, and 23 were generated that differed in their DAR estimated as 2, 4, 8.5, and 11 per construct, respectively (Table S4, ESI).

To examine how the conjugation with a hydrophobic toxin influenced the polarity of synthetic dextramabs, HIC analysis was performed (Figure 1). Compared to the ADC composed of trastuzumab 25 bearing two MMAEs and lacking a polarity-enhancing dextran moiety, all dextramabs (with DAR 2–11)

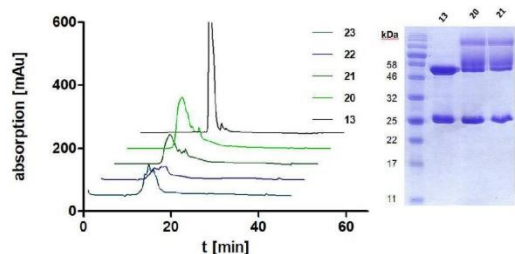


Figure 1. Left panel: HIC analysis of dextramabs 20–23 compared to the parent unmodified trastuzumab 13. Right panel: SDS PAGE of dextramabs 20 and 21 compared to solitary antibody 13 (HC: heavy chain, LC: light chain).

showed an enormous hydrophilic shift (Section S1.1.8, ESI) indicating that the dextran hydrophilicity compensated toxin hydrophobicity even at high DAR, making these hybrid antibody-coupled dextran-toxin architectures at least as hydrophilic as the unmodified trastuzumab 13 (Figure 1).

Binding properties of synthetic dextramabs were assessed using fluorescence-activated cell sorting (FACS) on HER2-overexpressing SK-BR-3 cells. Both fluorophore- and toxin-bearing dextramabs with FAR=4 (fluorophore-to-antibody ratio) and DARs=4–8, respectively, showed binding similar to an unmodified trastuzumab. To substantiate these findings, dissociation constants (K_D) were determined by flow cytometry (Section S1.1.13–14, ESI). A K_D of 4.9 nM for the unmodified mAb 13 and a K_D of 5.9 nM for MMAE-dextramab 22 (DAR=8) was determined. Thermal shift assays of dextramabs displayed identical melting points compared to unmodified trastuzumab and therefore no loss in stability was found (S1.1.12, ESI).

The potency of four different cytotoxic dextramabs was determined *in vitro* by cell proliferation assays. The HER2-positive breast cancer cell line SK-BR-3 was chosen and CHO cells, lacking HER2, served as negative control (Figure 2, S1.1.16, ESI). A DAR-

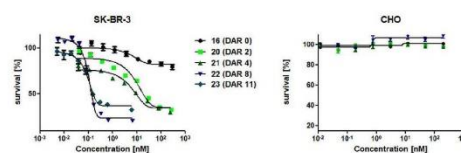


Figure 2. Cell proliferation assays. Left panel: HER 2-positive cells treated with respective dextramabs. Right panel: HER 2-negative cells treated with dextramabs. Details in text.

dependent cell killing was revealed for all examined dextramabs (20–23) on SK-BR-3 cells while no toxicity against HER2-negative cells was observed, indicating a HER2-dependent cellular uptake. Constructs 20 and 21 (DAR 2–4) showed IC_{50} values at the double-digit nanomolar range, whereas the constructs 22 and 23 (DAR 8–11) demonstrated subnanomolar inhibitory activity (IC_{50} =0.10 nM). As expected, dextramabs with no toxin warheads were found innocuous for cancer cells. Indeed, no toxicity against SK-BR-3 was observed for construct 16 (Figure 2) that lacked MMAE but possessed the highest density of enthetic azide groups. Dextramabs 22 and 23 were found more potent than a classical DAR 2 ADC 25, while possessing a highly hydrophilic character (Section S1.1.8. and S1.1.16 ESI). Nevertheless further investigations in the field of endosomal uptake of dextramabs and cathepsin-mediated cleavage of the releasable payload in dextran-bound state are needed for complete understanding of the observed cytotoxic profile.

In conclusion, we have developed a strategy towards a novel class of hybrid antibody-drug conjugates, dextramabs, which possess high toxin loading without compromising binding, stability, and solubility under physiologic conditions. In these architectures, a monoclonal antibody ensures selective binding and transport, and a polysaccharide scaffold allows for multiple, controllable attachment of a cargo. Our modular

approach includes dextran modifications at the backbone and the red-end towards site-directed enzyme-mediated monovalent conjugation with an engineered immunoglobulin of choice, followed by highly efficient SPAAC to attach a cytotoxin.

To the best of our knowledge, for the first time dextran framework was conjugated to a functional antibody site-specifically *via* its reducing end, leaving the sugar backbone intact. This has an obvious advantage compared to the common procedure that relies on random oxidation of the backbone hydroxyls with subsequent reductive amination. Though all the transformations used are rather efficient, the space for improvements still remains with respect to mTG catalysis. Engineering of improved transglutaminase recognition sites is currently ongoing in our lab.

Synthetic cytotoxic dextramabs surpass the respective ADCs in frames of hydrophilicity while possessing a high DAR, thus highlighting the potential of dextran as carrier for hydrophobic toxins. They selectively target and kill HER2-positive SK-BR-3 cells at subnanomolar concentrations showing that the dextran pendants do not affect selectivity. In a perspective, the dextramab format should allow loading of milder toxins at higher density, thus opening novel avenues to tailor-made ADCs for therapeutic applications. Follow-up animal studies will reveal, whether dextramabs with high DAR hold promise for ADCs with high potency, long *in vivo* half-life and low immunogenicity.

Acknowledgements

This work was supported by the Deutsche Forschungsgemeinschaft through grant SPP 1623.

Conflict of Interest

The authors declare no conflict of interest.

Keywords: ADC · bioconjugation · dextran modification · cancer · drug discovery

- [1] a) D. Y. Jackson, *Org. Process Res. Dev.* **2016**, *20*, 852–866; b) J. M. Lambert, A. Berkenblit, *Annu. Rev. Med.* **2018**, *69*; c) Q. Zhou, *Biomedicine* **2017**, *5*, 64; d) J. M. Lambert, C. Q. Morris, *Adv. Ther.* **2017**, *34*, 1015–1035.
- [2] a) K. J. Hamblett, P. D. Senter, D. F. Chace, M. M. Sun, J. Lenox, C. G. Cerveny, K. M. Kissler, S. X. Bernhardt, A. K. Kopcha, R. F. Zabinski, *Clin. Cancer Res.* **2004**, *10*, 7063–7070; b) L. Wang, G. Amphlett, W. A. Blättler, J. M. Lambert, W. Zhang, *Protein Sci.* **2005**, *14*, 2436–2446; c) Q. Zhou, J. E. Stefano, C. Manning, J. Kyazike, B. Chen, D. A. Gianolio, A. Park, M. Busch, J. Bird, X. Zheng, H. Simonds-Mannes, J. Kim, R. C. Gregory, R. J. Miller, W. H. Brondyk, P. K. Dhal, C. Q. Pan, *Bioconjugate Chem.* **2014**, *25*, 510–520.
- [3] a) P. Bryant, M. Pabst, G. Badescu, M. Bird, W. McDowell, E. Jamieson, J. Swierkosz, K. Jurlewicz, R. Tommasi, K. Henseleit, *Mol. Pharm.* **2015**, *12*, 1872–1879; b) B. Chen, D. A. Gianolio, J. E. Stefano, C. M. Manning, R. C. Gregory, M. M. Busch, W. H. Brondyk, R. J. Miller, P. K. Dhal, *ChemMedChem* **2018**, *13*, 790–794; c) J. R. Junutula, H. Raab, S. Clark, S. Bhakta, D. D. Leopold, S. Weir, Y. Chen, M. Simpson, S. P. Tsai, M. S. Dennis, *Nature Biotechnol.* **2008**, *26*, 925.
- [4] a) P. K. Qasba, *Bioconjugate Chem.* **2015**, *26*, 2170–2175; b) X. Li, T. Fang, G. J. Boons, *Angew. Chem.* **2014**, *126*, 7307–7310; *Angew. Chem. Int. Ed.* **2014**, *53*, 7179–7182; c) B. Ramakrishnan, E. Boeggeman, P. K. Qasba, *Exp. Opin. Drug Del.* **2008**, *5*, 149–153; d) Z. Zhu, B. Ramakrishnan, J. Li, Y. Wang, Y. Feng, P. Prabhakaran, S. Colantonio, M. A. Dyba, P. K. Qasba, D. S. Dimitrov, *mAbs* **2014**, *6*, 1190–2000; e) R. van Geel, M. A. Wijdeven, R. Heesbeen, J. M. Verkade, A. A. Wasiel, S. S. van Berkel, F. L. van Delft, *Bioconjugate Chem.* **2015**, *26*, 2233–2242.
- [5] a) Y. Anami, W. Xiong, X. Gui, M. Deng, C. C. Zhang, N. Zhang, Z. An, K. Tsuchikama, *Org. Biomol. Chem.* **2017**, *15*, 5635–5642; b) P. Denner, A. Chiotellis, E. Fischer, D. Brégeon, C. Belmant, L. Gauthier, F. Lhospice, F. o. Romagne, R. Schibli, *Bioconjugate Chem.* **2014**, *25*, 569–578; c) P. R. Spycher, C. A. Amann, J. E. Wehrmüller, D. R. Hurwitz, O. Kreis, D. Messmer, A. Rittler, A. Küchler, A. Blanc, M. Béhé, *ChemBioChem* **2017**, *18*, 1923–1927; d) P. Strop, S.-H. Liu, M. Dorywalska, K. Delaria, R. G. Dushin, T.-T. Tran, W.-H. Ho, S. Farias, M. G. Casas, Y. Abdiche, *Chem. Biol.* **2013**, *20*, 161–167.
- [6] R. R. Beerli, T. Hell, A. S. Merkel, U. Grawunder, *PLoS One* **2015**, *10*, e0131177.
- [7] a) P. M. Drake, A. E. Albers, J. Baker, S. Banas, R. M. Barfield, A. S. Bhat, G. W. de Hart, A. W. Garofalo, P. Holder, L. C. Jones, *Bioconjugate Chem.* **2014**, *25*, 1331–1341; b) P. Wu, W. Shui, B. L. Carlson, N. Hu, D. Rabuka, J. Lee, C. R. Bertozzi, *PNAS* **2009**, *106*, 3000–3005.
- [8] a) D. Schumacher, C. P. Hackenberger, H. Leonhardt, J. Helma, *J. Clin. Immunol.* **2016**, *36*, 100–107; b) D. Schumacher, J. Helma, F. A. Mann, G. Pichler, F. Natale, E. Krause, M. C. Cardoso, C. P. Hackenberger, H. Leonhardt, *Angew. Chem. Int. Ed.* **2015**, *54*, 13787–13791; *Angew. Chem.* **2015**, *127*, 13992–13996.
- [9] a) R. V. Chari, M. L. Miller, W. C. Widdison, *Angew. Chem. Int. Ed.* **2014**, *53*, 3796–3827; *Angew. Chem.* **2014**, *126*, 3872–3904; b) E. E. Hong, H. Erickson, R. J. Lutz, K. R. Whiteman, G. Jones, Y. Kovtun, V. Blanc, J. M. Lambert, *Mol. Pharm.* **2015**, *12*, 1703–1716.
- [10] Y. T. Adem, K. A. Schwarz, E. Duenas, T. W. Patapoff, W. J. Galush, O. Esue, *Bioconjugate Chem.* **2014**, *25*, 656–664.
- [11] R. P. Lyon, T. D. Bovee, S. O. Doronina, P. J. Burke, J. H. Hunter, H. D. Neff-LaFord, M. Jonas, M. E. Anderson, J. R. Setter, P. D. Senter, *Nat. Biotechnol.* **2015**, *33*, 733.
- [12] B. A. Mendelsohn, S. D. Barnscher, J. T. Snyder, Z. An, J. M. Dodd, J. Dugal-Tessier, *Bioconjugate Chem.* **2017**, *28*, 371–381.
- [13] T. Satomaa, H. Pynnönen, A. Vilkmann, T. Kotiranta, V. Pitkänen, A. Heiskanen, B. Herpers, L. S. Price, J. Helin, J. Saarinen, *Antibodies* **2018**, *7*, 15.
- [14] A. V. Yurkovetskiy, M. Yin, N. Bodyak, C. A. Stevenson, J. D. Thomas, C. E. Hammond, L. Qin, B. Zhu, D. R. Gumerov, E. Ter-Ovanesyan, *Cancer Res.* **2015**, *canres. 0129.2015*.
- [15] R. Mehvar, *J. Controlled Release* **2000**, *69*, 1–25.
- [16] S. B. van Witteloostuijn, S. L. Pedersen, K. J. Jensen, *ChemMedChem* **2016**, *11*, 2474–2495.
- [17] a) R. Fagnani, M. S. Hagan, R. Bartholomew, *Cancer Res.* **1990**, *50*, 3638–3645; b) R. Fagnani, S. Halpern, M. Hagan, *Nucl. Med. Commun.* **1995**, *16*, 362–369; c) R. Melton, C. Wiblin, R. Foster, R. Sherwood, *Biochem. Pharmacol.* **1987**, *36*, 105–112; d) T. E. Wileman, R. L. Foster, P. N. Elliott, *J. Pharm. Pharmacol.* **1986**, *38*, 264–271; e) A. Valdivia, R. Villalonga, P. Di Pierro, Y. Pérez, L. Mariniello, L. Gómez, R. Porta, *J. Biotechnol.* **2006**, *122*, 326–333.
- [18] M. Yalpani, D. E. Brooks, *J. Polym. Sci. Polym. Chem. Ed.* **1985**, *23*, 1395–1405.
- [19] M. Richter, A. Chakrabarti, I. R. Ruttekkol, B. Wiesner, M. Beyermann, R. Brock, J. Rademann, *Chem. Eur. J.* **2012**, *18*, 16708–16715.
- [20] H. Chen, Z. Lin, K. E. Arnst, D. D. Miller, W. Li, *Molecules* **2017**, *22*, 1281.
- [21] a) V. Siegmund, S. Schmelz, S. Dickgiesser, J. Beck, A. Ebenig, H. Fittler, H. Frauendorf, B. Piater, U. A. K. Betz, O. Avrutina, A. Scrima, H.-L. Fuchsbaauer, H. Kolmar, *Angew. Chem. Int. Ed.* **2015**, *54*, 13420–13424; *Angew. Chem.* **2015**, *127*, 13618–13623; b) L. Deweid, L. Neureiter, S. Englert, H. Schneider, J. Deweid, D. Yanakieva, J. Sturm, S. Bitsch, A. Christmann, O. Avrutina, *Chem. Eur. J.* **2018**, *24*, 15195–15200; c) P. Strop, *Bioconjugate Chem.* **2014**, *25*, 855–862; d) L. Deweid, O. Avrutina, H. Kolmar, *Biol. Chem.* **2018**.

Manuscript received: February 19, 2019

Supporting Information

© Copyright Wiley-VCH Verlag GmbH & Co. KGaA, 69451 Weinheim, 2019

Dextramabs: A Novel Format of Antibody-Drug Conjugates Featuring a Multivalent Polysaccharide Scaffold

Hendrik Schneider, Lukas Deweid, Thomas Pirzer, Desislava Yanakieva, Simon Englert, Bastian Becker, Olga Avrutina, and Harald Kolmar*© 2019 The Authors. Published by Wiley-VCH Verlag GmbH & Co. KGaA.

This is an open access article under the terms of the Creative Commons Attribution Non-Commercial NoDerivs License, which permits use and distribution in any medium, provided the original work is properly cited, the use is non-commercial and no modifications or adaptations are made.

1 Experimental	1
1.1 General	1
1.1.1 Materials	1
1.1.2 Mass spectrometry	1
1.1.3 NMR spectroscopy	1
1.1.4 IR spectroscopy.....	1
1.1.5 Quantification of carboxyethyl groups per dextran using ¹ H-NMR.....	2
1.1.6 Detection of N ₃ -groups via IR spectroscopy and quantification using NMR spectroscopy ...	5
1.1.7 Liquid chromatography	6
1.1.8 Hydrophobic interaction chromatography (HIC)	7
1.1.9 Cell culture.....	7
1.1.10 Protein expression and purification	7
1.1.11 Activation of pro-microbial transglutaminase.....	8
1.1.12 Thermal shift assay.....	8
1.1.13 Cellular binding.....	8
1.1.14 Determination of K _D by flow cytometry.....	9
1.1.15 Photometric control of strain-promoted azide-alkyne cycloaddition (SPAAC) and determination of fluorophore-to-antibody ratio (FAR)	10
1.1.16 Cytotoxicity assay.....	11
1.2 Conjugation protocols	13
1.2.1 Microbial transglutaminase-mediated bioconjugation of trastuzumab	13
1.2.2 Strain-promoted azide-alkyne cycloaddition (SPAAC) of dextramab or <i>N</i> -(5-aminopentyl)- 2-azidoacetamide-modified trastuzumab.....	15
1.3 Synthesis of compounds	18
1.3.1 General remarks.....	18
1.3.2 Synthesis of <i>N</i> -Boc-cadaverine 1	20
1.3.3 Synthesis of protected azide linker 2	21
1.3.4 Synthesis of dextran- <i>N</i> -Boc-cadaverine 3.....	22
1.3.5 Synthesis of 2-CED- <i>N</i> -Boc-cadaverine 4, 5, 6.....	24
1.3.6 Synthesis of N ₃ -Dex- <i>N</i> -Boc-cadaverine 7, 8, 9 and N ₃ -Dex-cadaverine 10, 11, 12.....	27
References	29

1 Experimental

1.1 General

1.1.1 Materials

All reagents were used as supplied by Iris Biotech, Agilent Technologies, Sigma Aldrich, Roth or Fisher Scientific without further purification. DBCO-PEG₃-PAB-MMAE and azadibenzocyclooctyne-Cy5 (DBCO-Cy5) were kindly provided by Merck KGaA (Darmstadt, Germany). Cadaverine, dextran from *leuconostoc mesenteroides* (average Mol. Wt. 9000-11000), *N*-Ethoxycarbonyl-2-ethoxy-1,2-dihydroquinoline (EEDQ), SYPRO Orange and 2-azidoacetic acid were purchased from Sigma-Aldrich. Di-*tert*-butyl dicarbonate was purchased from Carbolutions (St. Ingbert, Germany), and dispase – from Cellsystems (Troisdorf, Germany). For immune-staining Alexa-Fluor® 488 AffiniPure Fab Fragment specific for human IgG (H+L) was obtained from Jackson ImmunoResearch, and goat anti-human IgG Fc PE eBioscience™ – from Fisher Scientific (Hampton, USA).

1.1.2 Mass spectrometry

Electrospray ionization mass spectrometry (ESI-MS) spectra were obtained using a *Shimadzu LCMS-2020* mass spectrometer equipped with a *Phenomenex Synergy 4 u Fusion-RP 80* (C-18, 250 × 4.6 mm, 2 μm, 80 Å). The eluent system consisted of 0.1% (v/v) aq. formic acid (LC-MS grade, Fisher Scientific (Hampton, USA) (eluent A) and acetonitrile containing 0.1% (v/v) formic acid (LC-MS grade, Fisher Scientific (Hampton, USA) (eluent B).

1.1.3 NMR spectroscopy

NMR measurements were recorded on an Avance III or an Avance II NMR Spectrometer at 300 MHz (Bruker BioSpin GmbH, Rheinstetten, Germany). Samples were dissolved in chloroform-*d* or deuterium oxide from Sigma Aldrich Chemie GmbH (Munich, Germany, now Merck KGaA, Darmstadt, Germany).

1.1.4 IR spectroscopy

IR measurements were performed using homogenous potassium bromide pellet on a FTIR-Spectrometer Spectrum Two (PerkinElmer, Rodgau, Germany). Spectra were obtained by PerkinElmer Spectrum following instructions of manufacturer. Wave number area: 8.300-350 cm⁻¹, spectral resolution 0.5 cm⁻¹; wave number

accuracy better than 0,01 cm⁻¹ at 3.000 cm⁻¹; wave number correctness: 0,1 cm⁻¹ at 3.000 cm⁻¹; signal-to-noise-ratio: 9.300 : 1 Peak to Peak, 5 s and 32.000 : 1 Peak to Peak, 1 min.

1.1.5 Quantification of carboxyethyl groups per dextran using ¹H-NMR

Quantification of carboxyethyl (CE) groups per Dextran was determined as previously described.^[1] A quantification using titration was not performed, since NMR analysis showed similar results.^[1] Briefly: The ratio of integrals corresponding to the anomeric proton of glucose repeating units to the signals corresponding to the C2-position of the carboxyethyl group (CE-group) was used to determine the number of CE groups per dextran *via* ¹H-NMR.^[1] Richter et al. showed by 2D-NMR analysis, that carboxyethylation following the procedure used in this work only took place at C2 position of the glucose of repeating units.^[1] An example for quantification is shown in Figure S1 (for further NMR data see Section 1.3.5). Signal 1 corresponds to anomeric protons of glucose repeating units, whereas signal 2 corresponds to the two protons at the C2 of the integrated carboxyethyl groups.

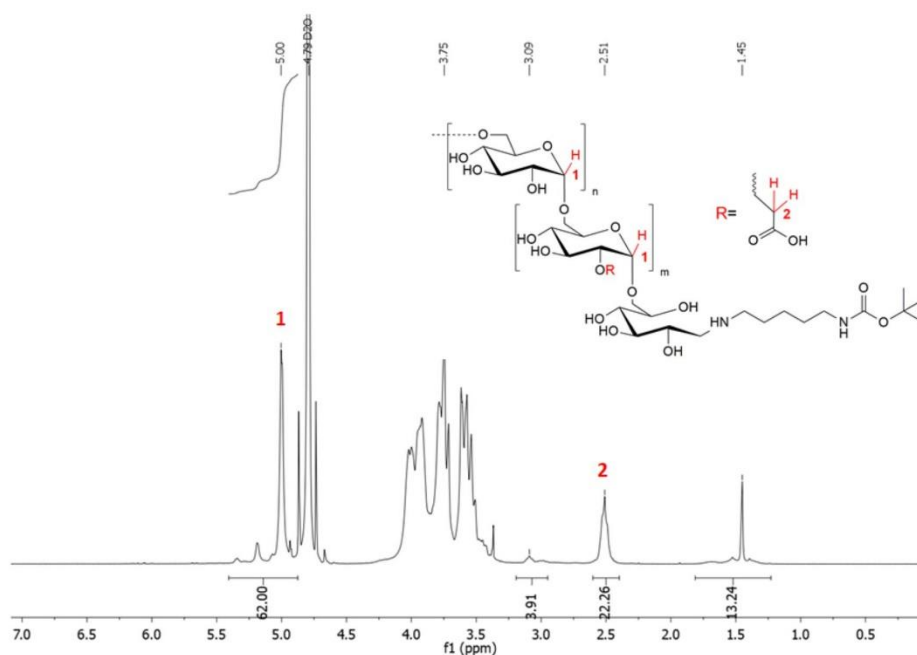


Figure S1: Quantification of carboxyl groups per Dextran using ¹H-NMR: 10 kDa Dextran contains an average of 62 glucose repeating units (1). The number of CE-groups was calculated by using the corresponding signal (2).

The ratio of CE-groups per dextran was calculated using formula (1)

$$CE - groups/dextran = \frac{integral(signal\ 2)}{2} \quad (1)$$

Adjustment of the amount of acrylamide changed the degree of substitution as shown in Figure S2. A substitution of 4.5, 8.5 and 11 CE groups per dextran was found for compound **4**, **5**, and **6**. The degree of substitution was adjusted from 4.5 to 25 (data not shown). About 40 % of the applied acrylamide was conjugated to the glucose repeating units in all experiments (Table S1). A higher density of CE groups per dextran was achieved using a smaller dextran ($M_w = 5000$) with only 31 glucose repeating units (24 CE groups/dextran, Figure S2).

Table S1: Quantification of CE-groups per dextran.

	4	5	6
CE groups/ dextran	4.5	8.5	11
acrylamide/ dextran	12.7	20.4	24.7
bound CE groups/ applied acrylamide	0.35	0.42	0.45

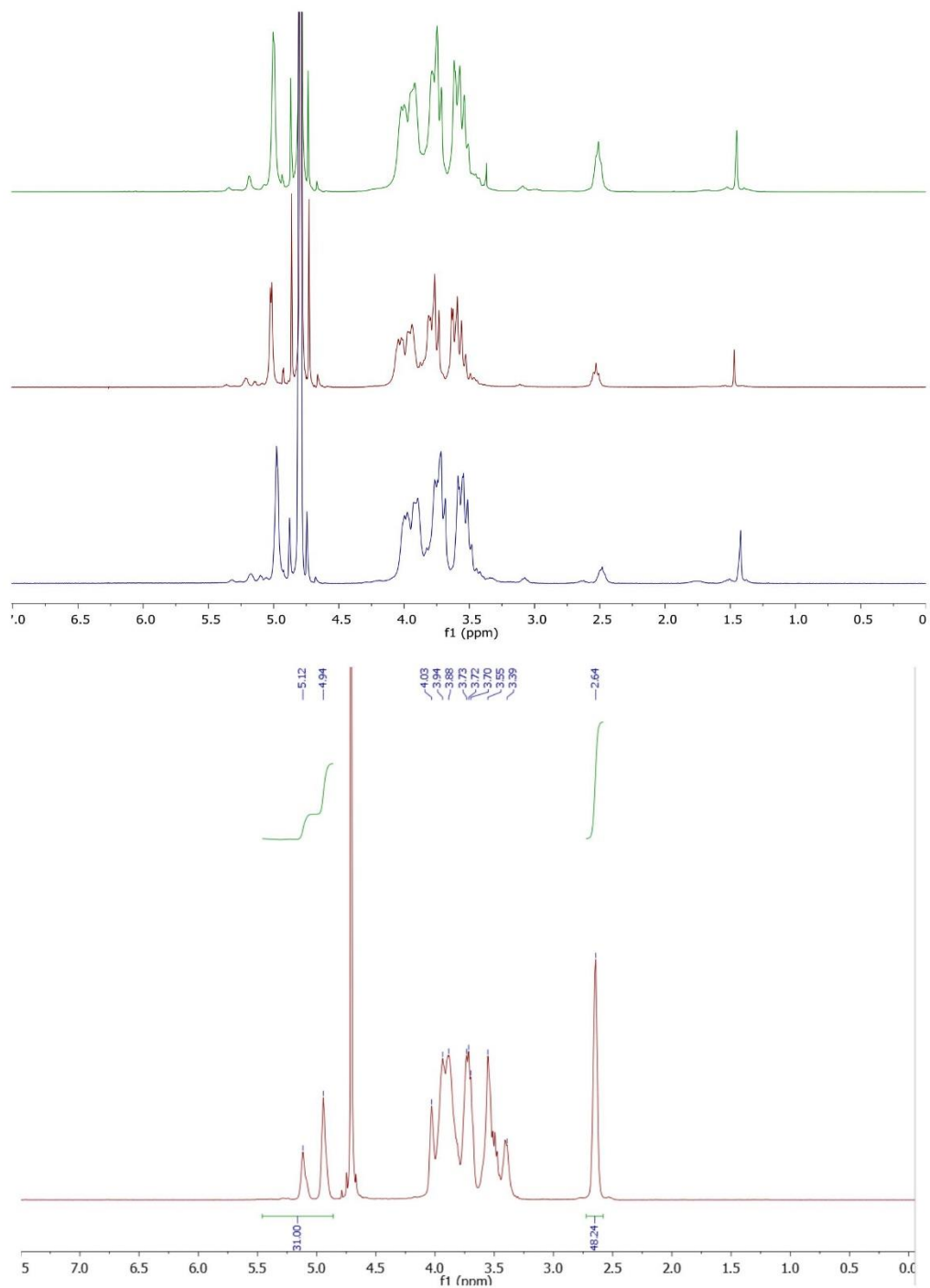


Figure S2: Degree of substitution in 2-CED-*N*-Boc-cadaverine and 2-CED. Upper Figure: Top: 11 CE groups/dextran, compound **6**; middle: 8.5 CE groups/dextran, compound **5**; bottom: 4.5 CE groups/dextran, compound **4**. Lower Figure: 24 CE groups/dextran in dextran (M_w 5000).

1.1.6 Detection of N₃-groups via IR spectroscopy and quantification using NMR spectroscopy

IR spectroscopy was used for the detection of the coupling of azido linker **2** to compounds **4**, **5**, and **6** (Figure S3). The band corresponding to the N₃ group of compound **10**, **11**, and **12** is found at 2120 cm⁻¹ and does not superimpose with any band found in the dextran IR spectra.^[2] Therefore the intensity of this band gives a first evidence for azide modification of dextran. As expected, an increasing intensity of the N₃ band was observed for compounds **10**, **11**, and **12** with increasing numbers of possible conjugation sites (Figure S3).

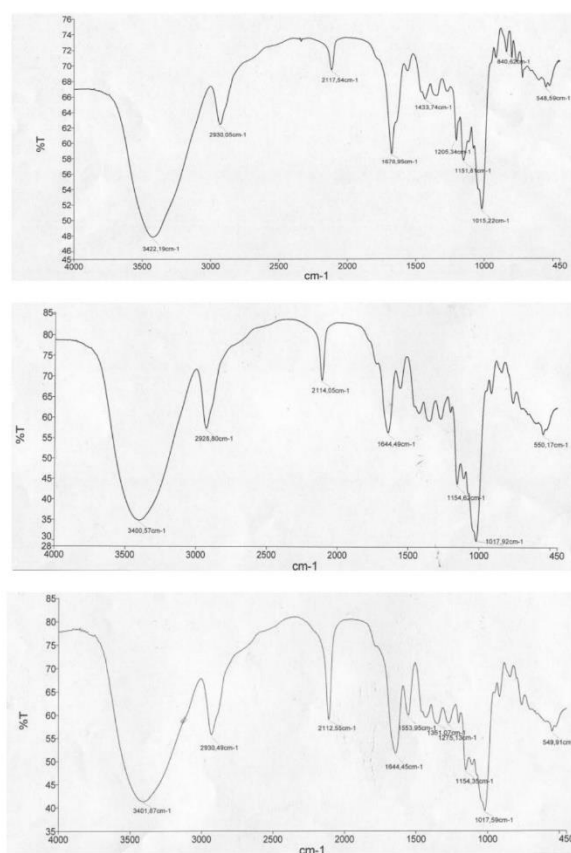


Figure S3: IR spectra of azide modified dextran-cadaverine: Top: 4.5 N₃ groups/dextran, compound **10**; middle: 8.5 N₃ groups/dextran, compound **11**; bottom: 11 N₃ groups/dextran, compound **12**.

Thereupon quantitative determination was performed utilizing ¹H-NMR spectroscopy (Figure S4). Integrals corresponding to the aliphatic protons of azido linker **2** were quantified and compared to the signals corresponding to the C2-protons of the CE group. A quantitative N₃-modification of previously introduced carboxyethyl groups was observed for all compounds (Table 2, for further NMR data see section 1.3.5).

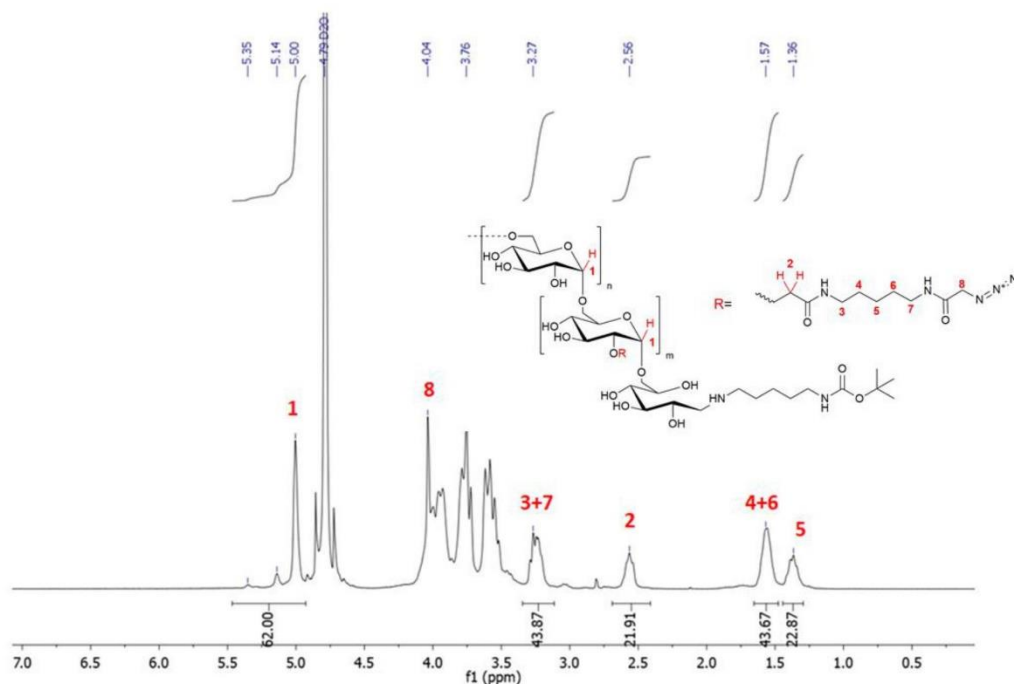


Figure S4: $^1\text{H-NMR}$ spectra of azide-modified dextran-cadaverine **12**: Integrals of corresponding signals give evidence of quantitative azido linker **2** coupling.

Table 2: Quantification of azide-modification.

	7, 10	8, 11	9, 12
N₃-groups/ dextran	4.5	8.5	11

1.1.7 Liquid chromatography

Analytical reversed-phase high-performance liquid chromatography (RP-HPLC) was performed on either an Agilent Infinity 1260 equipped with an *Interchim* (Montluçon, France) *Uptisphere Strategy* (C18-HQ 3 μm , 100 \times 4.6 mm) LC column or on a *Agilent 1100* equipped with a *Agilent Eclipse Plus C18* (100 \times 4.6 mm, 3.5 μm , 95 \AA) LC column at a flow rate of 0.6 mL/min. For isolation of peptides a semi-preparative RP-HPLC *Interchim Puriflash 4250* equipped with a semi-preparative C₁₈ LC column (*Interchim Uptisphere Strategy* (C18-HQ5 μm 250 \times 21.2mm)) was used. At a flow rate of 18 mL/min, 3 min of isocratic flow (starting concentration of eluent B) was followed by 20 min of gradient flow. Eluent A: 0.1% (v/v) aq. trifluoroacetic acid (TFA), eluent B: 90% (v/v) aq. MeCN with 0.1% (v/v) TFA. Absorption was measured by a UV/VIS detector at 220 nm and 280 nm.

1.1.8 Hydrophobic interaction chromatography (HIC)

Analytical hydrophobic interaction chromatography (HIC) was performed on an *Agilent Infinity 1260* equipped with a *Tosoh Bioscience TSKgel Butyl-NPR* (2.5 μ M, 4.6 mm \times 3.5 cm) using a linear gradient 0 to 100% B in 45 min (Eluent A: 1.5 M ammonium sulfate and 25mM TRIS-HCl pH 7.5. Eluent B: 25mM TRIS-HCl pH 7.5). Prior to analysis the constructs were diluted with 3 M ammonium sulfate to a final concentration of 0.75 M ammonium sulfate. Analysis of all generated dextramabs **20 - 23** (and therefore also all azide-modified precursors **14 - 16**) showed that at least 1 dextran was conjugated per trastuzumab, since no signal of unmodified trastuzumab-LLQG **13** was detected (Figure 2).

1.1.9 Cell culture

Cell lines were incubated under standard conditions at 37 °C in a humidified incubator with 5 % CO₂. SK-BR-3 breast cancer cells were grown in DMEM culture medium with 10 % FBS. CHO-KI cells were grown in DMEM F-12 HAM with 10 % FBS. Expi293TM, a non-adherent cell line, was obtained from Thermo Fisher Scientific and was grown in serum-free Expi293TM expression medium on an orbital shaker at 110 rpm.

1.1.10 Protein expression and purification

Trastuzumab LLQG was produced by transient transfection of Expi293TM with the respective pTT5 and pEXPR plasmid using polyethylenimine (PEI). The LLQG mTG recognition tag was added to the C-terminus of the heavy chain using standard PCR procedure. 30 μ g of the corresponding plasmid were mixed with 90 μ g of PEI in serum-free Expi293TM expression medium and added dropwise to 30mL of Expi293TM cells, in a density of 2.5 \times 10⁶ cells/mL, under continuous shaking. After 24 hours the cells were fed with 0.5 % (w/v) tryptone. After 120 h the cell supernatant was purified by protein A affinity chromatography using HiTrap Protein A HP columns (GE Healthcare), A 1:1.5 dilution of antibody production supernatant in running buffer (20 mM sodium phosphate, pH 7) was applied to the column after its equilibration with running buffer. Elution was carried out using 100 mM citrate buffer pH 3. The eluate was dialyzed and concentrated using an Amicon Ultra centrifugation filter.

Inactive pro-microbial transglutaminase was produced as previously described.^[3] Briefly: Inactive pro-mTG was produced in *E. coli* cells using β -D-1-thiogalactopyranoside (IPTG). *E. coli* cells comprising the respective plasmid were grown in dYT+Amp medium (16 g/l tryptone, 10 g/L yeast extract and 5 g/L NaCl supplemented with 100 μ g/mL ampicillin) at 37 °C and 180 rpm to an OD of 0.8-1. Upon induction by IPTG (final concentration 500 μ M) cells were incubated at 24 °C and 180 rpm for 3 h. Cell lysis was accomplished using a Constant Systems Ltd cell disruptor (Daventry, UK). Purification was performed using standard IMAC purification on a HisTrap HP (GE Healthcare) column. Purified pro-mTG was stored in mTG storage buffer (20 μ g dispase/mg pro-mTG; 300 mM NaCl, 50 mM TRIS-HCl pH 8, 5 mM CaCl₂, 1 mM glutathione (reduced)).

1.1.11 Activation of pro-microbial transglutaminase

pro-mTG was activated upon addition of *Bacillus polymyxa* neutral protease (dispace) dissolved in mTG storage buffer. After incubation at 37 °C for 30 min, purification was performed using standard IMAC procedure on a HisTrap HP (GE Healthcare) column. Purified mTG was stored in mTG storage buffer + 10 % glycerol at -80 C.

1.1.12 Thermal shift assay

Thermal shift assays were performed in triplicates on a BioRad96CFX RT-PCR detection system with 0.5 °C/30 s to 99 °C. T_m values were collected from melting curves using the corresponding BioRad analysis software (Figure S5). All reactions were performed in 1 × PBS pH 7.4 at a concentration of 0.1 mg/mL protein upon addition of SYPRO Orange (diluted 1:800).

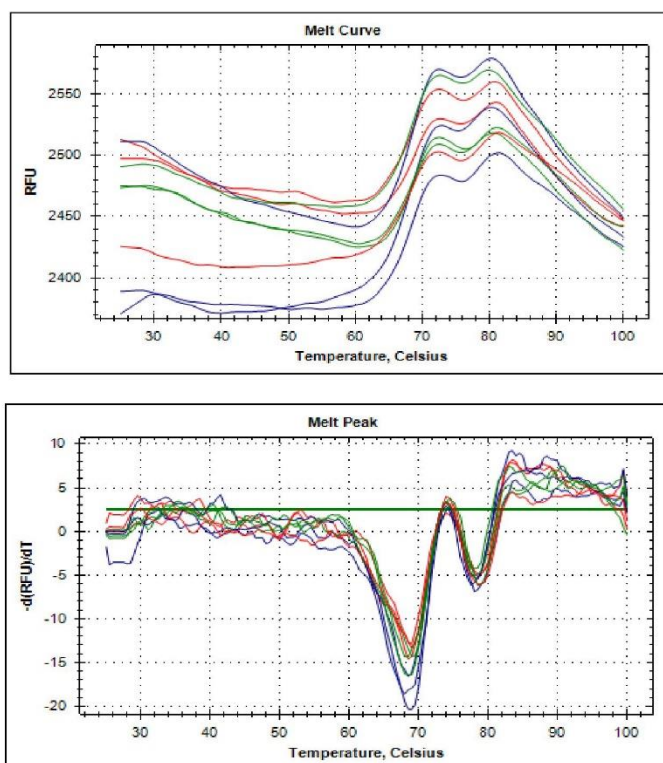


Figure S5: Thermal shift assays of 15, dexamab 22 and trastuzumab-LLQ 13 (triplicates).

1.1.13 Cellular binding

Human cancer SK-BR-3 cells were trypsinized from the culture flask and spun down. Cells (2×10^5) were washed three times with 1 × PBS pH 7.4 containing 1% bovine serum albumin (BSA) followed by incubation

with the respective dextramab-MMAE/Cy5 or the unconjugated trastuzumab-LLQG **13** (100 μ L, 0.1 mg/mL in 1 \times PBS, pH 7.4, 1% BSA) for 10 min on ice. Constructs **22** and **13** were used for cellular binding assays. Subsequently, cells were washed three times with 1 \times PBS, pH 7.4, 1% BSA and incubated with fluorescently labeled secondary antibody goat anti-human IgG Fc, PE-conjugated eBioscience™ (100 μ L, 1/100 dilution) for 10 min on ice. In the case of dextramab-Cy5 **18** no secondary antibody was used. Subsequently, cells were washed three times with 1 \times PBS, pH 7.4, 1% BSA. Cells were analyzed by flow cytometry using a BD Influx cell-sorting device (manufactured by Becton, Dickinson and Company) (Figure S6). Isotype control: Cells only incubated with fluorescently labeled secondary antibody goat anti-human IgG Fc, PE-conjugated eBioscience™.

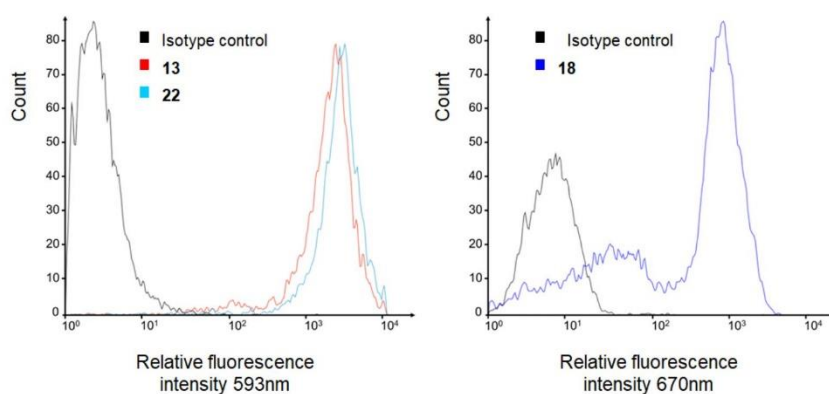


Figure S6: Cellular binding: left: Binding of dextramab **22** and unconjugated trastuzumab **13**, right: Binding of dextramab-Cy5 **18** and unconjugated trastuzumab.

1.1.14 Determination of K_D by flow cytometry

Human cancer SK-BR-3 cells were trypsinized from the culture flask and spun down. Cells were counted and 2×10^5 cells were seeded in a 96-well round-bottom plate. Compound **22** and unmodified trastuzumab-LLQG **13** were used for K_D -determination. Cells were washed three times with 1 \times PBS pH 7.4 containing 1% bovine serum albumin (BSA) followed by incubation with dextramab **22** or trastuzumab-LLQG **13**, in varying concentrations, for 45 min on ice. Subsequently, cells were washed three times with 1 \times PBS pH 7.4 1% BSA and incubated with a 1:100 dilution of α hIgG Fab-Alexa 488 antibody, for 30 min, on ice. Cells were washed three times with 1 \times PBS pH 7.4 1% BSA and diluted in 100 μ L buffer and analyzed with a BD Accuri C6 flow cytometer. Normalized mean fluorescence was plotted against antibody concentration. A single point measurement was executed (Figure S7). The K_D of each compound was determined with graphpad prism software.

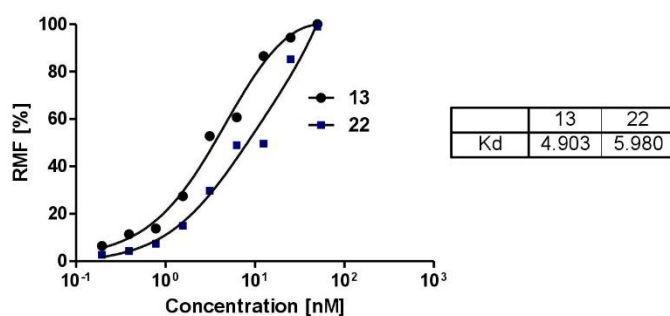


Figure S7: K_D on cells: Determination of K_D on cells of trastuzumab-LLQG **13** and dexamab **22** (Dar 8).

1.1.15 Photometric control of strain-promoted azide-alkyne cycloaddition (SPAAC) and determination of fluorophore-to-antibody ratio (FAR)

The concentration of the Cy5-modified dexamab **18** was determined by standard OD_{280} measurements. A calibration curve for DBCO-Cy5 **17** was measured at 661 nm on a *Shimadzu UVmini-1240 UV-VIS* spectrophotometer (Table S3). For all measurements at least a triple determination was conducted (Figure S8).

Table S3: DBCO-Cy5 calibration curve.

c(dexamab-Cy5 18 , OD_{280}) [μ M]	A(661 nm, average)
31.25	3.389
15.25	1.739
7.83	0.835
5.00	0.501
3.91	0.310
2.50	0.183
1.95	0.100

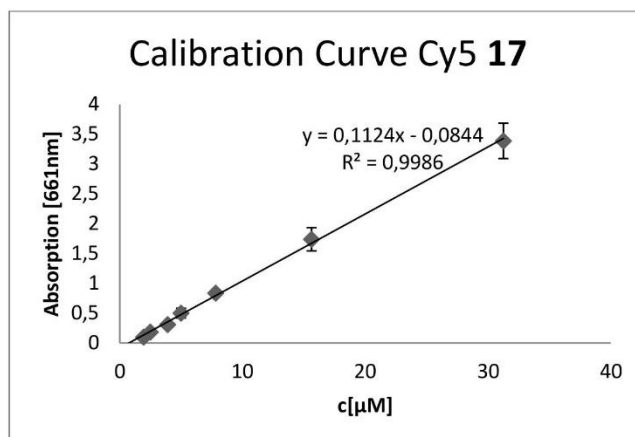


Figure S8: Calibration curve of DBCO-Cy5 17

Three equivalents of DBCO-Cy5 **17** were conjugated to azide modified construct **15** to obtain construct **18**, which was used for the control of quantitative coupling and measured in three different dilutions (Table S4).

Table S4: Ratio of Cy5 per dextramab-Cy5 18.

c(dextramab-Cy5 18, OD ₂₈₀) [µM]	A(661 nm, average)	c (fluorophore)	Fluorophore/dextramab (FAR)
2.10	0.54	5.55	2.63
1.75	0.48	5.02	2.87
0.87	0.26	3.06	3.52
-	-	-	Ø 3.01

The ratio of Cy5/dextramab (FAR) was determined using formula (1).

$$c(\text{dextramab}, \text{Abs. } 661 \text{ nm}) = \frac{(A_{\text{measured}}(661 \text{ nm}) + 0.0844)}{0.1124} \quad (1)$$

A quantitative “click” coupling was preserved for SPAAC of DBCO-Cy5 **18** and construct **15**.

1.1.16 Cytotoxicity assay

HER2 positive breast cancer cells SK-BR-3 and HER2 negative CHO cells were seeded in a 96-well plate in a density of 6.5×10^3 cells/well with addition of pen-strep. After 24h incubation, under standard conditions at 37 °C in a humidified incubator with 5 % CO₂, cells were treated with dextramabs **20** - **23** classical ADC DAR 2 **25** or control azide-modified construct **16** in the respective concentrations and incubated for 72 h at 37 °C, 5 % CO₂ (Figure 2, Figure S9). Cell viability was measured using CellTiter96® AQueous One Solution Cell Proliferation Assay (Promega) following the instructions of the supplier using a Tecan® Infinite F200 Pro.

As comparison a classical DAR 2 ADC **25** was used. Construct **25** showed an IC₅₀ value of 0.218 nm whereas dextramab **22** was found more potent with an IC₅₀ value of 0.10 nm. As non-binding control an antibody

comprising the light chain of matuzumab and the heavy chain of trastuzumab equipped with an mTG recognition tag was used. No toxicity was found for the isotype control (Figure S9).

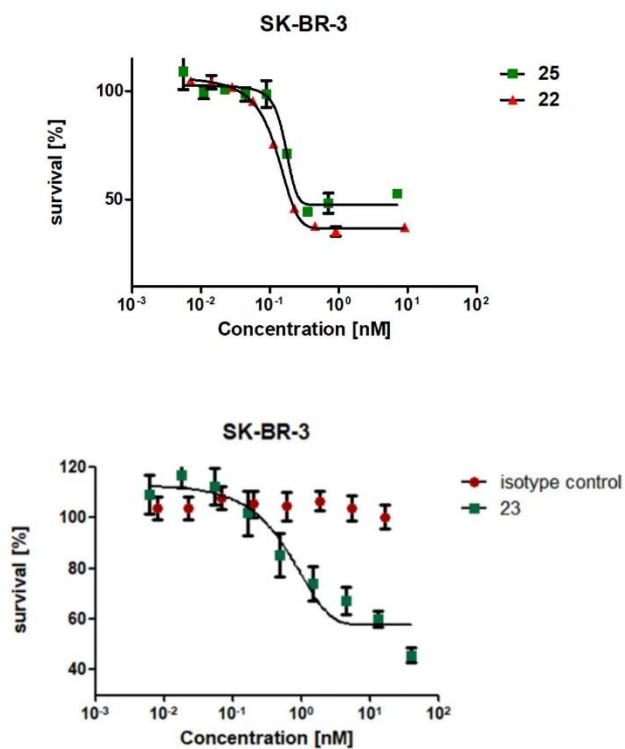


Figure S9: Cell proliferation assays: **Top:** HER 2-positive cells treated with dexamab **22** and classical ADC (DAR 2) **25**. **Bottom:** HER 2-positive cells treated with dexamab **22** and isotype control dexamab (DAR 11). * In these experiment, lower efficiency of Dextran-antibody coupling was observed. It was not further improved.

1.2 Conjugation protocols

1.2.1 Microbial transglutaminase-mediated bioconjugation of trastuzumab

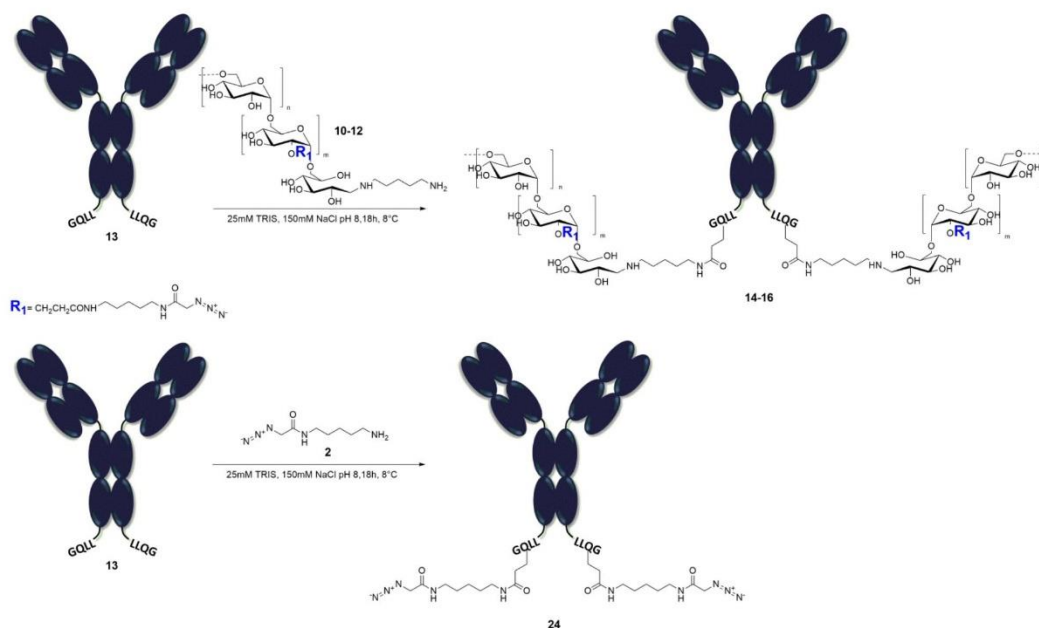


Figure S10: mTG mediated bioconjugation.

Trastuzumab-LLQG **13** was diluted to a concentration of 43.4 μM in 1 \times PBS, pH 7.4, or 250 mM TRIS-HCl, 1.5M NaCl, pH 8, and incubated with 50-100 eq of the respective cadaverine-modified dextran **10**, **11**, **12** or *N*-(5-Aminopentyl)-2-azidoacetamide **2** and 6 U/mL mTG at 8 $^\circ\text{C}$ over-night (Figure S10). The separation of excess cadaverine-modified dextran **10**, **11**, **12** or *N*-(5-aminopentyl)-2-azidoacetamide **2** was performed using a Protein A HP SpinTrap following the instructions of the supplier. After elution, purified azido modified compounds **14**, **15**, and **16**, or *N*-(5-aminopentyl)-2-azidoacetamide modified trastuzumab **24** (N_3 -mAb) were concentrated and buffer-exchanged using Amicon Ultra Centrifugation filters and stored in 1 \times PBS, pH 7.4, at 4 $^\circ\text{C}$ upon usage for SPAAC. As reaction control a SDS-PAGE or a HIC-analysis was performed. An example for SDS-PAGE and HIC-analysis is shown in Figure S11. Constructs **14**, **15** and **16** were generated bearing at least 4.5, 8.5 respectively 11.5 N_3 -groups per antibody (at least one dextran per antibody coupled, see chapter 1.1.8; Figure 1; Figure S11).

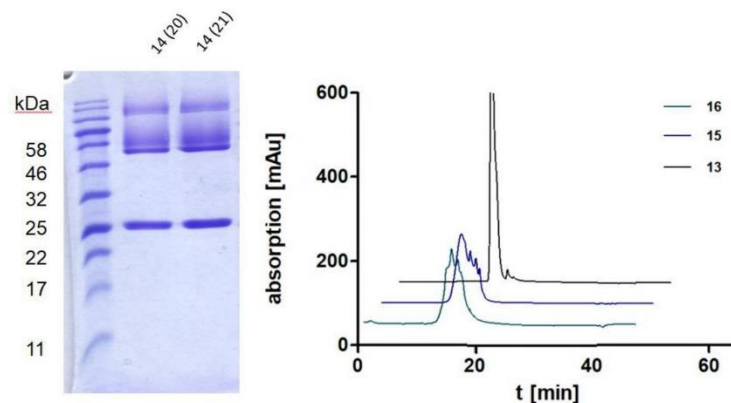


Figure S11: Example for SDS-PAGE and HIC analysis: left: SDS-PAGE of compound **14** generated for further use for the synthesis of compound **20** and **21**. Right: HIC analysis of compound **14** compared to trastuzumab-LLQG **13**.

Construct **24** with only the linker **2** coupled showed no complete consumption of the amine substrate, as three different peaks are visible in HIC analysis (Figure S12). However it was used for “click” reactions. Hence, linker **2** seems to be a poor mTG substrate, trastuzumab-LLQG **13** could neither be modified quantitatively with constructs **14** – **16**, nor directly with linker **2** in this set-up. Since compound **24** was only generated as precursor of MMAE-loaded construct **25**, to get access of HIC data for a DAR 1 and DAR 2 trastuzumab, no further improvements of enzymatic conjugation were carried out.

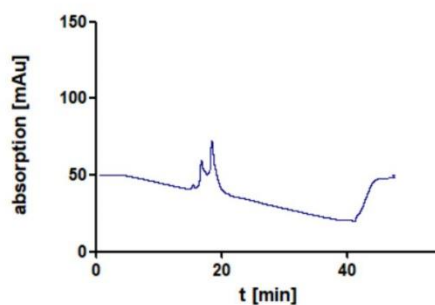


Figure S12: HIC analysis of compound 24.

1.2.2 Strain-promoted azide-alkyne cycloaddition (SPAAC) of dextran-mab or *N*-(5-aminopentyl)-2-azidoacetamide-modified trastuzumab

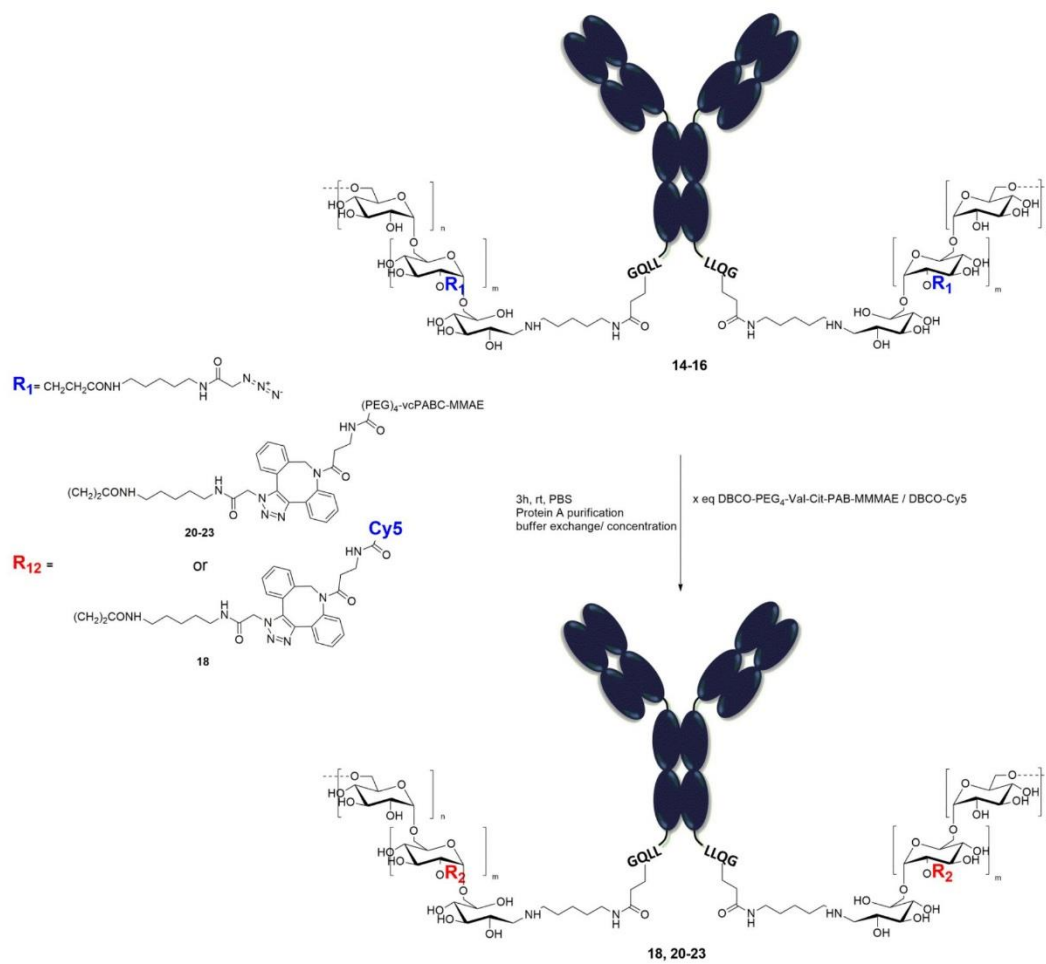


Figure S13: SPAAC of azide-modified compounds 14-16.

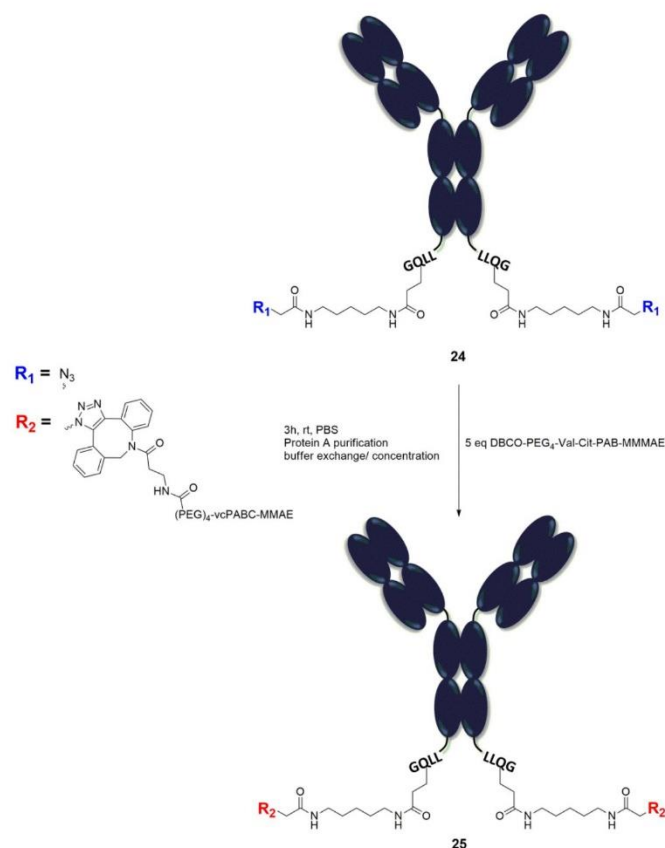


Figure S14: SPAAC of azide-modified compound 24.

For SPAAC the respective compound (**14**, **15**, and **16**) equipped with azide groups or N₃-mAb, **24** was diluted to a final concentration of 2-5 mg/mL in 1×PBS pH 7.4 in the respective equivalents (Table S5) of DBCO-PEG₃-ValCit-PAB-MMAE **19** or DBCO-Cy5 **17** were added and the reaction mixture was incubated at 30 °C and 500 rpm for 3h (Figure S13; S14). The separation of excess DBCO-PEG₃-ValCit-PAB-MMAE **19** or DBCO-Cy5 **17** was performed using a Protein A HP SpinTrap following the instructions of the supplier. After elution, the MMAE modified dextramabs **20**, **21**, **22**, **23**, trastuzumab-MMAE **25** and the Cy5 modified **18** were concentrated and buffer-exchanged using Amicon Ultra Centrifugation filters and stored in 1× PBS pH 7.4 at 4 °C upon usage. As reaction control, SDS-PAGE or a HIC-chromatography was performed (Figure 1, Figure S15). Construct **25** showed a mixture of DAR 1-2 as explained in section 1.2.1 (Figure S15). Both the DAR 1 and the DAR 2 species showed an hydrophobic shift as the retention time on the HIC column shifted to 25.1 respectively 32.3 minutes compared to trastuzumab-LLQG **13** which was found at 16.8 min. In contrast all dextramab compounds (DAR 2-11) **20** - **23** were found at retention times between 12 and 19 minutes. Construct **18** was used for the control of SPAAC (Section 1.1.15)

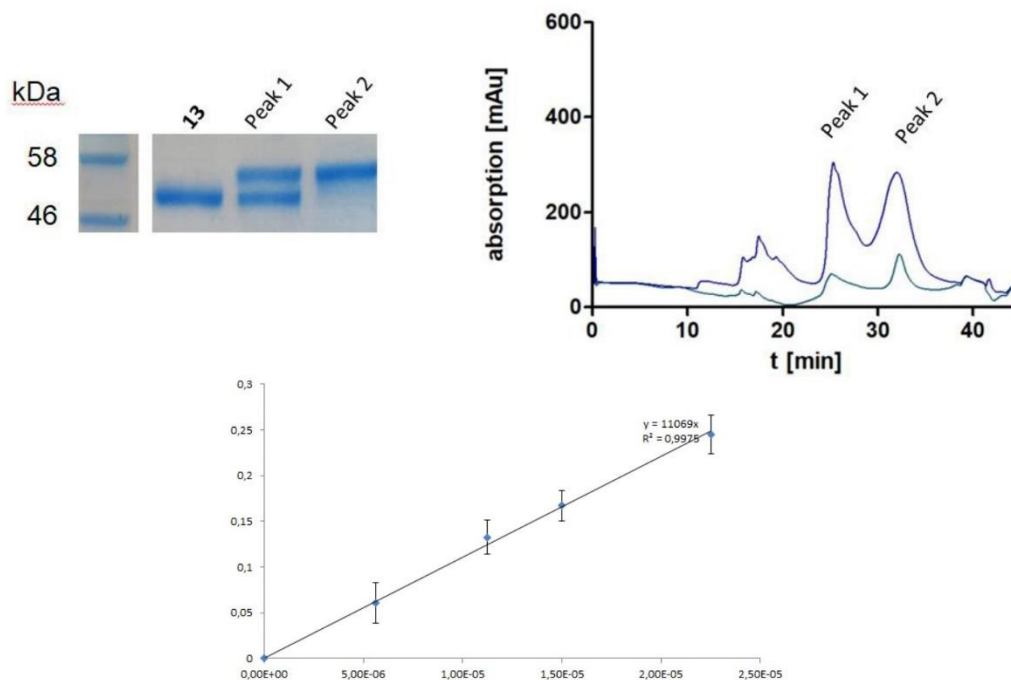


Figure S15: Top: HIC analysis and SDS-PAGE of compound 25: Left: Reducing SDS-PAGE of collected HIC peaks 1 and 2. Right: HIC chromatograms of compound 2: dark blue: 500 μg mAb. Light blue: 30 μg mAb. **Bottom:** Calibration curve for the determination of the extinction coefficient of DBCO-Val-Cit-PAB-MMAE 19. The extinction coefficient of DBCO-Peg4-val-cit-PAB-MMAE at 280nm was determined as 1.107×10^4 L/mol-cm.

Table S5: Reaction conditions for SPAAC of Dextramab or N₃-mAb.

	precursor	dextramab [N ₃ /dextramab]	N ₃ -mAb [N ₃ /mAb]	c [mg/mL]	Equivalents [DBCO-PEG3-vc- PAB-MMAE]	Equivalents [DBCO Cy5]
20	14	4.5	-	3.5	2	-
21	14	4.5	-	3.5	4	-
22	15	8.5	-	3.5	9.5	-
23	16	11	-	3	11.5	-
25	24	--	2	3	5	-
18	15	8.5	-	3.5	-	3

To estimate the concentration of dextramabs *via* photometric analysis the extinction coefficient of DBCO-Val-Cit-PAB-MMAE 19 was determined (Figure S15). The slope of the graph equals the molar extinction coefficient.

1.3 Synthesis of compounds

1.3.1 General remarks

Reactions were performed at room temperature and atmospheric pressure unless mentioned otherwise. Reaction progress was monitored by TLC analysis on *TLC Silica gel 60 F₂₅₄* plates purchased from *Merck KGaA (Darmstadt, Germany)* or by ¹H-NMR. Visualization was carried out with a UV lamp and by staining with potassium permanganate. Purification was obtained either by, RP-HPLC, dialysis or disposable PD10 desalting columns following the instruction of the supplier.

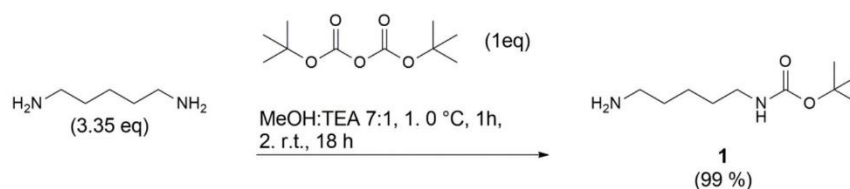


Figure S16: Synthesis of protected amine **1**.

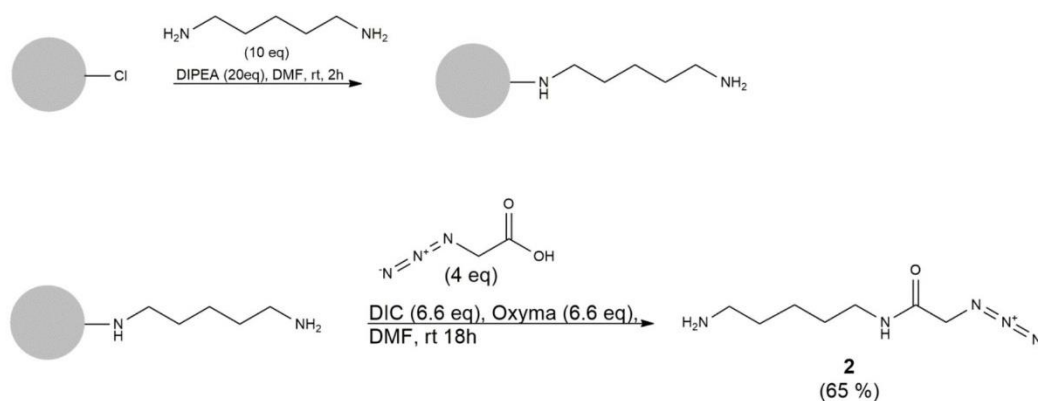


Figure S17: Synthesis of protected azido linker **2** on solid support.

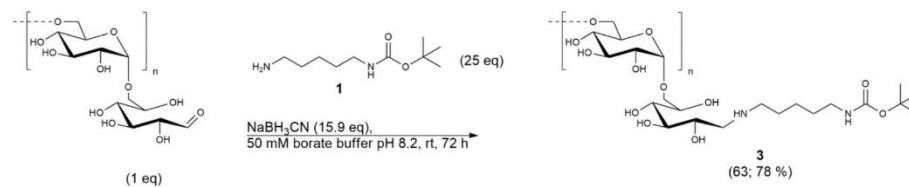


Figure S18: Synthesis of dextran-*N*-Boc-cadaverine **3**

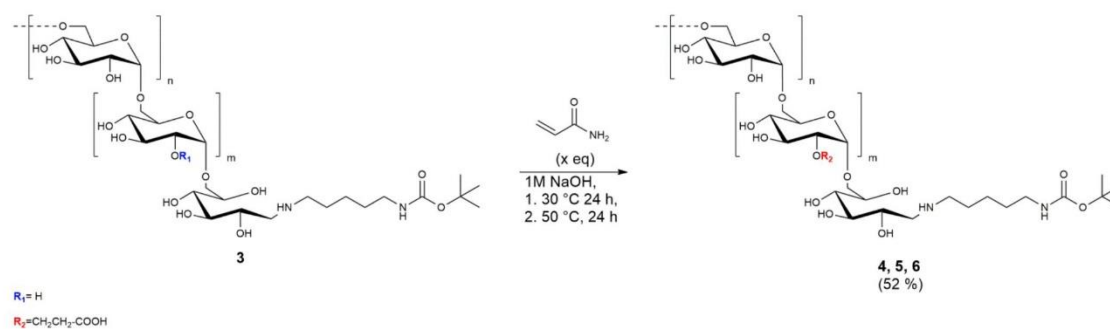


Figure S19: Synthesis of 2-CED-*N*-Boc-cadaverine **4, 5, 6**.

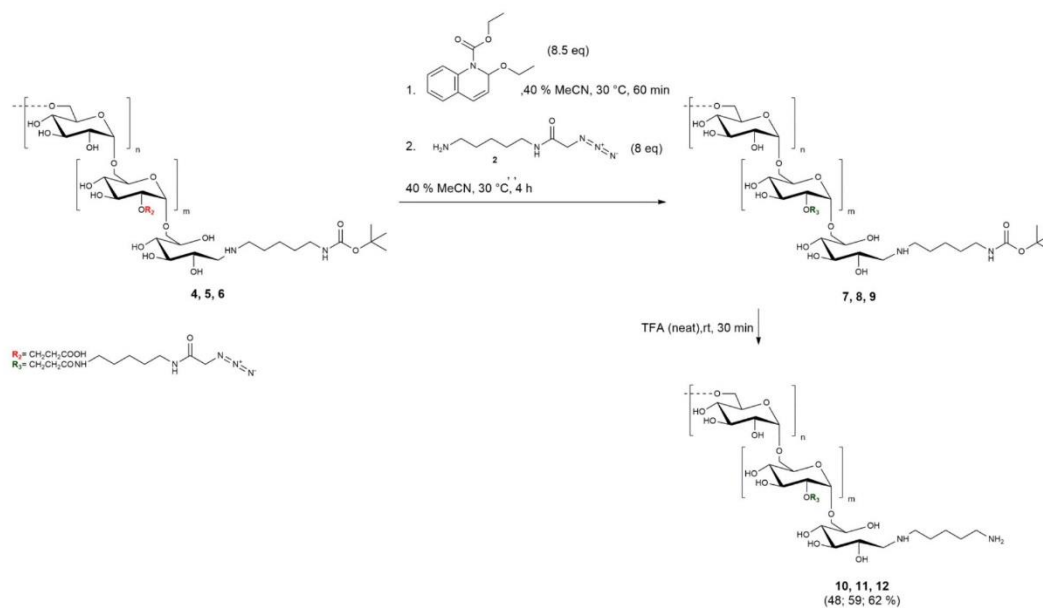
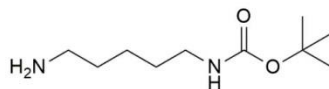


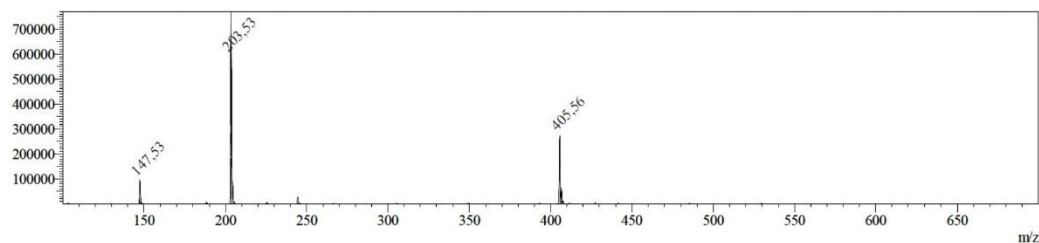
Figure S20: Synthesis of protected **7**, **8**, **9** and deprotected **10**, **11**, **12** azide modified dextran-cadaverine.

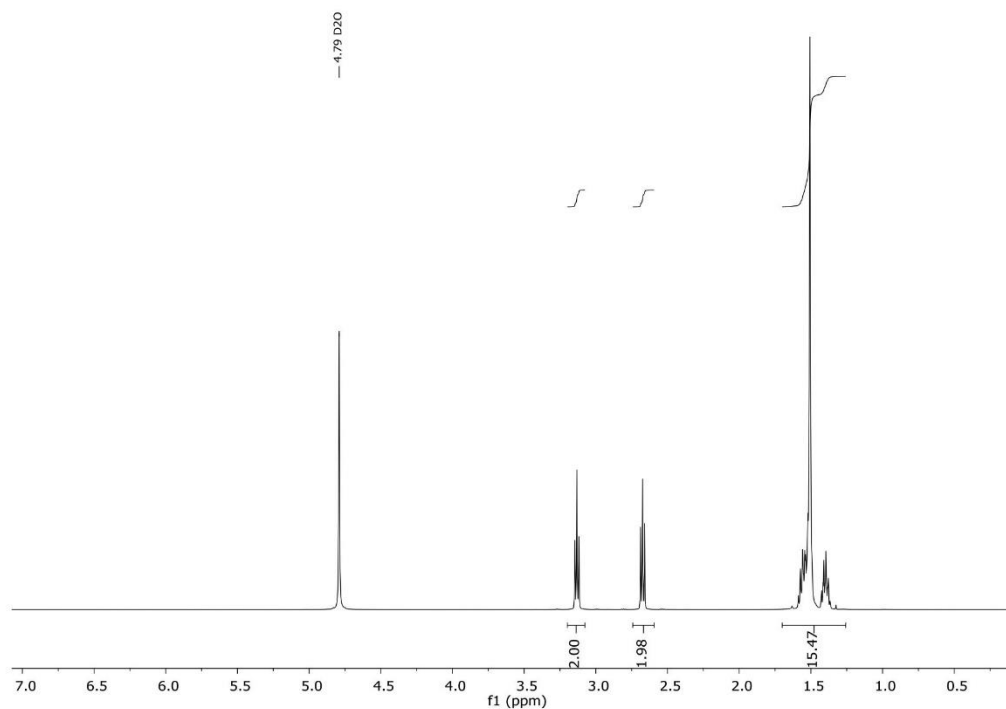
1.3.2 Synthesis of *N*-Boc-cadaverine **1**



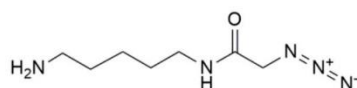
Cadaverine (0.873 g 9.78 mmol, 3.34 eq) was dissolved in MeOH:TEA(triethylamine) (85 mL) (1:7) and stirred at 0 °C for 10 min. Then a solution of Di-*tert*-butyl dicarbonate (0.640 g, 2.9 mmol, 1 eq) in MeOH (30 mL) was added dropwise in over a period of 10 min. The mixture was stirred under Ar-atmosphere for 1h. The reaction mixture was allowed to gradually rise to room temperature (rt) and was stirred over-night. The solvents were removed at the rotary evaporator. The residue was dissolved in dichloromethane (DCM) and extracted 2× with water and 2× with brine. The organic layers were dried over MgSO₄, filtrated and concentrated to give a yellowish oil. m = 0,593g (99 %). MS (ESI) calcd. for C₁₀H₂₂N₂O₂ [M+H]⁺ = 203.29, observed: 203.53

¹H NMR (300 MHz, Deuterium Oxide) δ = 3.10 (t, *J* = 6.7 Hz, 2H, CH₂), 2.66 (t, *J* = 7.0 Hz, 2H, CH₂), 1.62 – 1.29 (overlapped m, 15H, CH₂, CH₂, 3CH₃) ppm

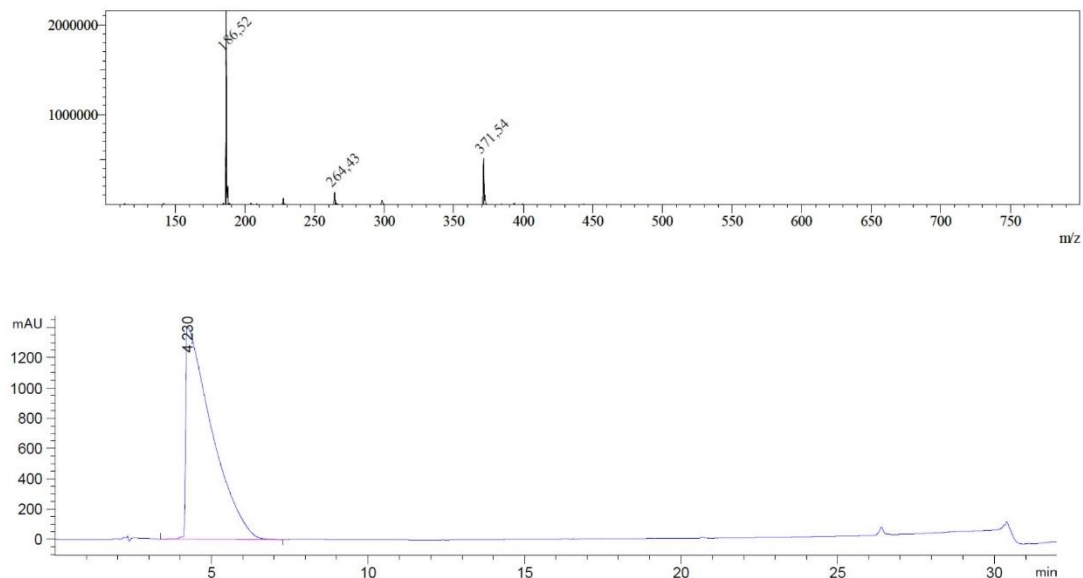




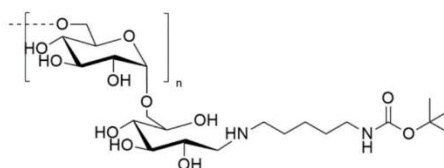
1.3.3 Synthesis of protected azide linker 2



The synthesis was performed on solid support. In a syringe equipped with a frit 2-chlorotrityl chloride resin (1.25 g, equals 2 mmol, loading: 1.6 mmol/g, 1eq) was swollen for 20 min in DCM, washed three times with dimethylformamide (DMF) (10 mL) and again swollen in DMF for 20 min. Subsequently a solution of cadaverine (2.34 mL, 20 mmol, 10 eq) and diisopropylethylamine (DIEA) (6.97 mL, 40 mmol, 20 eq) in DMF (5 mL) was added and the reaction mixture was gently agitated for 2 h at ambient temperature. After washing six times with DMF (10 mL) a mixture of azidoacetic acid (299.5 μ L, 4 mmol, 2 eq), Oxyma (0.938 g, 6.6 mmol, 3.3 eq) and *N,N'*-diisopropylcarbodiimide (DIC) (0.815 g, 6.6 mmol, 3.3 eq) in DMF (10 mL) was added and the reaction mixture was gently agitated for 18 h at ambient temperature. Subsequently the resin was washed 6 \times with DMF (10 mL), DCM (10 mL) and diethyl ether (10 mL) and dried in vacuo over-night. Cleavage from the resin was accomplished by treating the dry resin with a mixture of trifluoroacetic acid: triethylsilane:anisole:H₂O 23:1:1:1 (5 mL) for 3 h and gently agitation at ambient temperature. Product was isolated by precipitation in cold diethyl ether (45 mL) followed by three times washing with diethyl ether. Purification was accomplished by semi-preparative RP-HPLC (220nm, 0to80 % Eluent B). m= 0,390g (65 %). MS (ESI) calcd. for C₇H₁₅N₅O [M+H]⁺ = 186.23, observed: 186.52

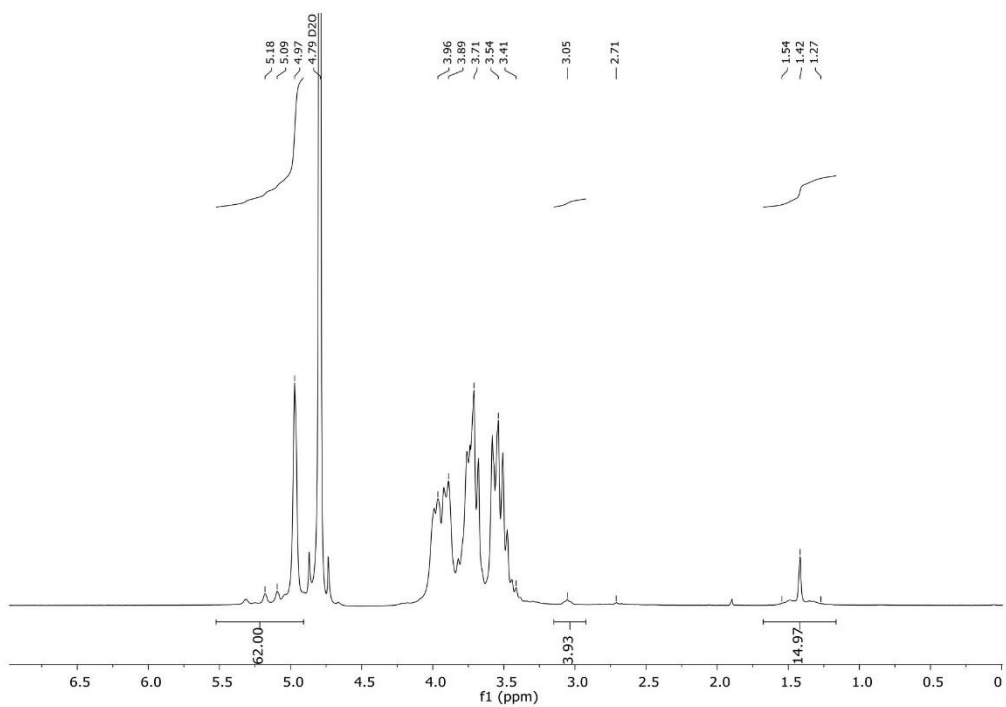
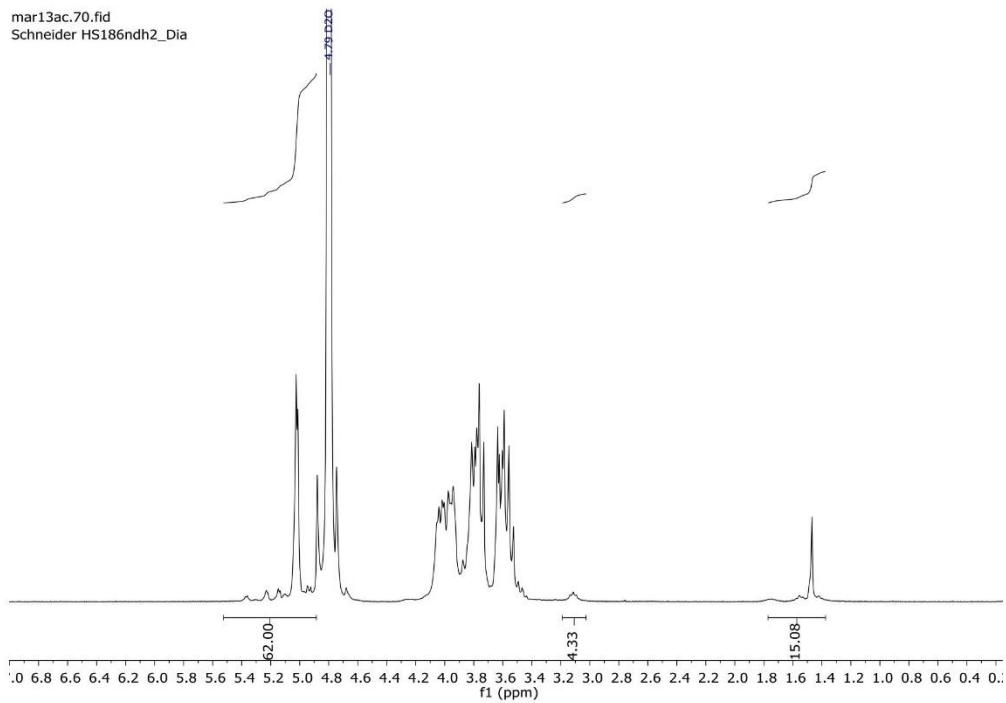


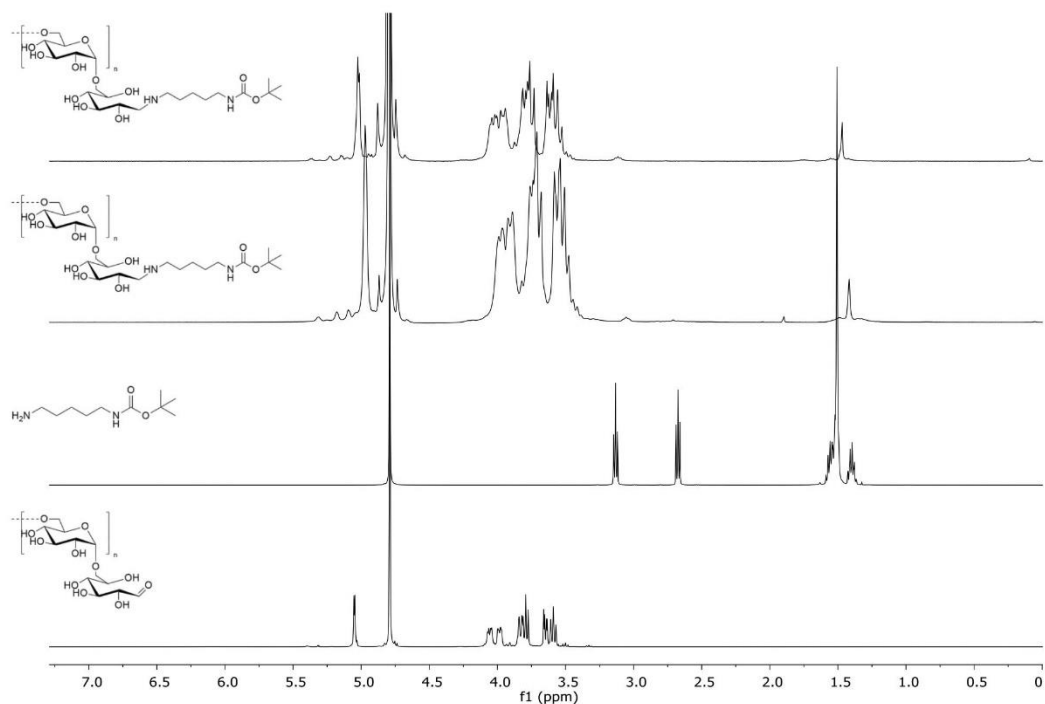
1.3.4 Synthesis of dextran-*N*-Boc-cadaverine 3



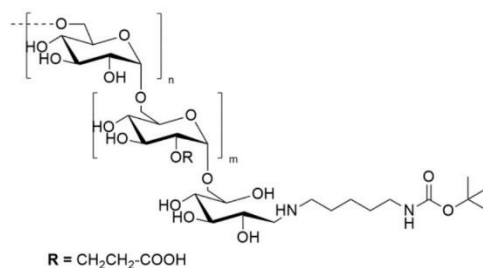
According to the literature in a 15 mL reaction tube dextran (1 eq) was dissolved in 2-5 mL 0.05 M borate buffer pH 8.2, *N*-Boc-cadaverine **1** (25 eq) and NaBH₃CN (15.9 eq) was added.^[4] The reaction mixture was stirred at darkness for 72 h at 30 °. Product was precipitated in cold methanol and washed three times with 30 mL MeOH and dried. The product was dissolved in water and purified, using disposable PD10 desalting columns, following the instruction of the supplier. After freeze-drying a pure white powder was obtained. Quantification of reaction progress was determined by ¹H NMR spectrometry as described in the literature.^[4-5] ¹H NMR (300 MHz, deuterium oxide) δ = 5.43 – 4.83 (m, 1H, C(1)H), 4.18 – 3.21 (m, C (2-6)H (glucose units)), 3.17 – 2.02 (m, 4H, CH₂NH-BOC, CH₂(CH₂)₄NH-Boc), 1.30 – 1.85 (overlapped m, 15H, CH₂(CH₂)₃NH-Boc, CH₂(CH₂)₂NH-Boc, CH₂(CH₂)₁NH-Boc 3CH₃(BOC)) ppm.

	batch 1			batch 2		
	m [g]	n [mmol]	v [mL]	m [g]	n [mmol]	v [mL]
dextran	0.8	0.08	-	1	0.1	-
NaBH₃CN	0.08	1.59	-	0.1	1.59	-
<i>N</i>-Boc-cadaverine	0.404	2.49	-	0.505	2.49	-
0.05 borate buffer pH 8.2	-	-	2	-	-	5





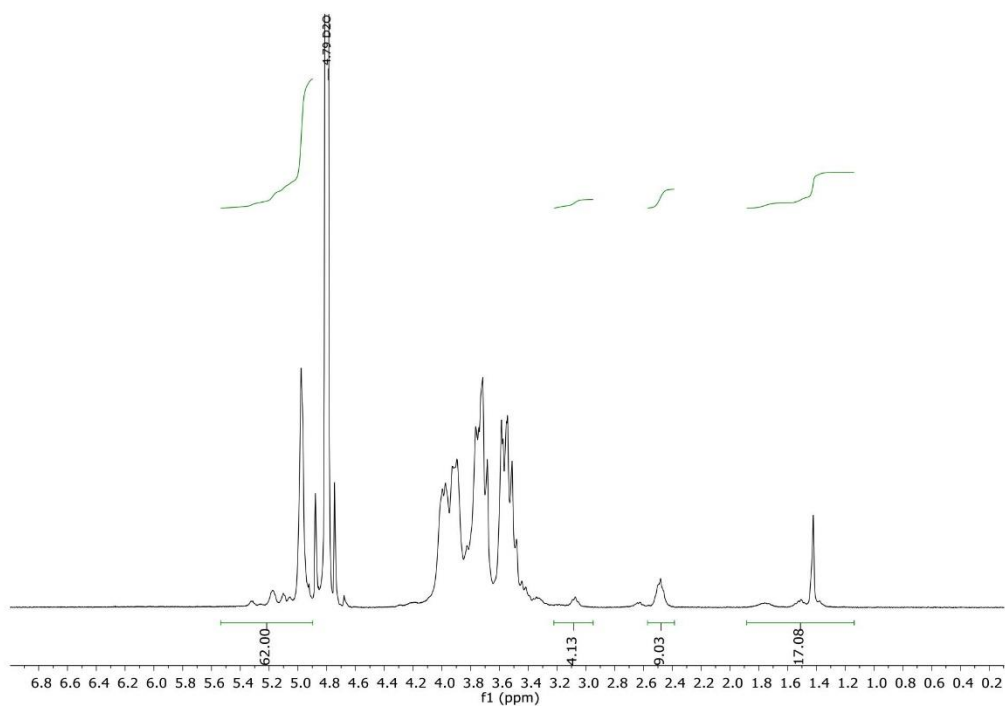
1.3.5 Synthesis of 2-CED-*N*-Boc-cadaverine **4**, **5**, **6**

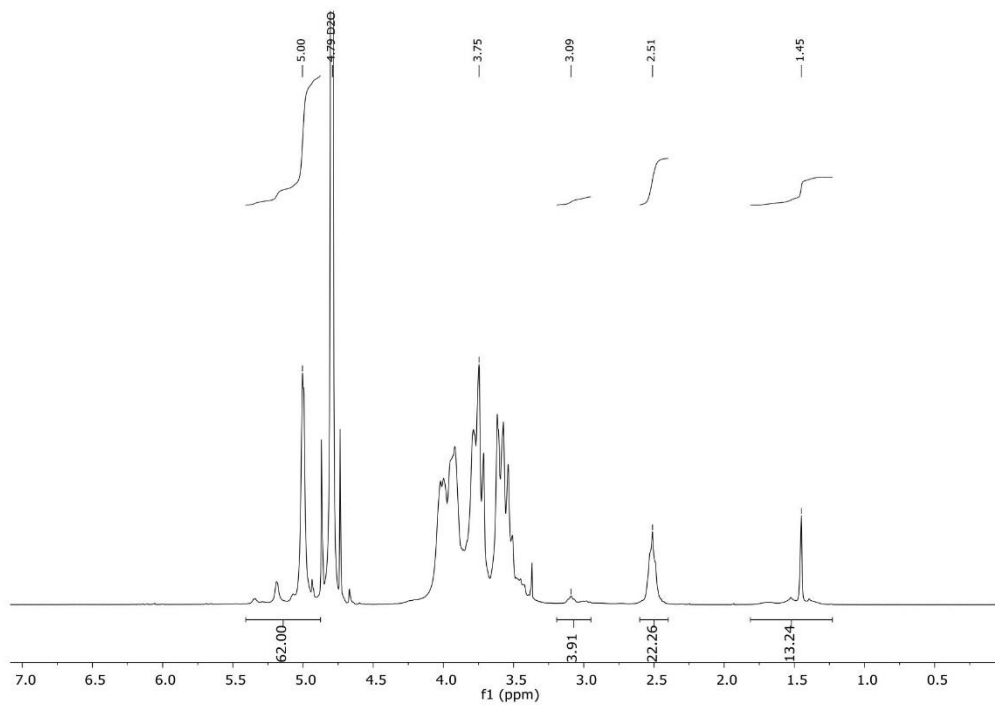
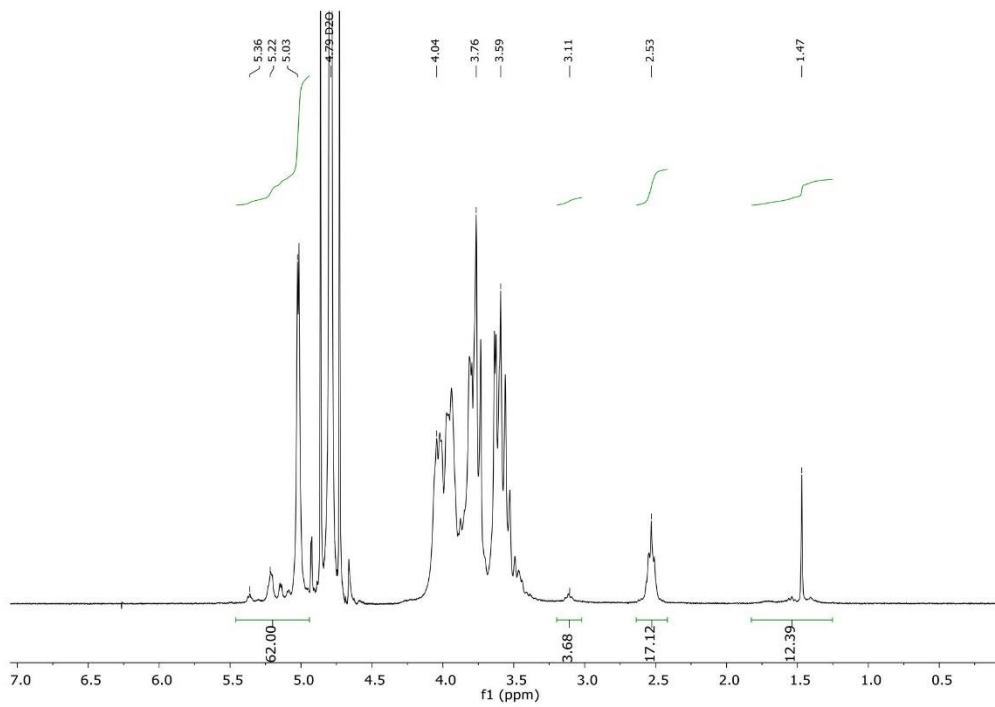


Referring to the literature, synthesis of carboxyethyl-dextran-*N*-Boc-cadaverine **4**, **5**, **6** (2-CED-*N*-Boc-cadaverine, different amounts of CE-groups/dextran) was performed by *O*-carboxyethylation utilizing acrylamide.^[1] **3** was dissolved in 1 M sodium hydroxide (NaOH) solution and acrylamide was added. Solution was stirred at 30 °C for 24 h, subsequently temperature was increased to 50 °C and the reaction mixture was stirred for 24 h. The reaction mixture was neutralized with 0.1 M hydrochloric acid. Product was precipitated in cold methanol and washed three times with 30 mL MeOH and dried. The product was dissolved in water and purified, using disposable PD10 desalting columns, following the instruction of the supplier. After freeze-drying a pure white powder was obtained. Quantification of reaction progress was determined by ¹H-NMR spectrometry as described above (Section 1.1.5). *m* = 408 mg (51 % **4**); 109 mg (26 % **5**); 599 mg (69 % **6**) (¹H NMR (300 MHz, D₂O) δ = 5.58 – 4.95 (m, 1H, C(1)H), 4.19 – 3.30 (m, C (2-

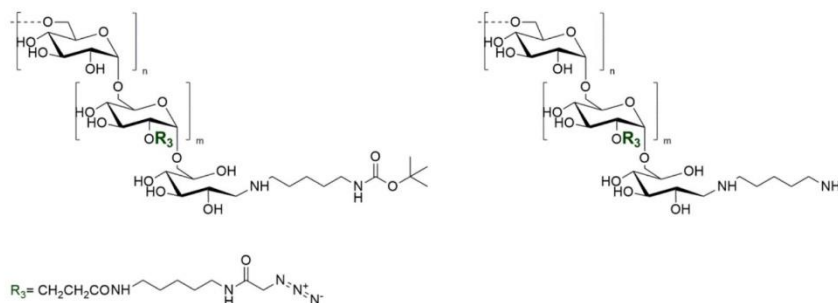
6)H (glucose units); $\text{CH}_2\text{CH}_2\text{COOH}$), 3.04 – 3.16 (m, 4H, $\text{CH}_2\text{NH-Boc}$, $\text{CH}_2(\text{CH}_2)_4\text{NH-Boc}$), 2.68 – 2.38 (t, CH_2COOH), 1.20 – 1.92 (overlapped m, 15H, $\text{CH}_2(\text{CH}_2)_3\text{NH-Boc}$, $\text{CH}_2(\text{CH}_2)_2\text{NH-Boc}$, $\text{CH}_2(\text{CH}_2)_1\text{NH-Boc}$, $3\text{CH}_3(\text{Boc})$) ppm.

	CE-groups/Dextran: 4.5				CE-groups/Dextran: 8.5				CE-groups/Dextran: 11			
	m [g]	n [μmol]	v [mL]	eq	m [g]	n [μmol]	v [mL]	eq	m [g]	n [μmol]	v [mL]	eq
dextran-N-Boc-cadaverine 3	0.779	76.37	-	1	0.389	37.25	-	1	0.801	78.52	-	1
acrylamide	0.069	971.28	-	12.7	54.0	760.13	-	20.4	0.138	1942.57	-	24.7
1 M NaOH	-	-	7.8		-	-	3.9		-	-	8	-



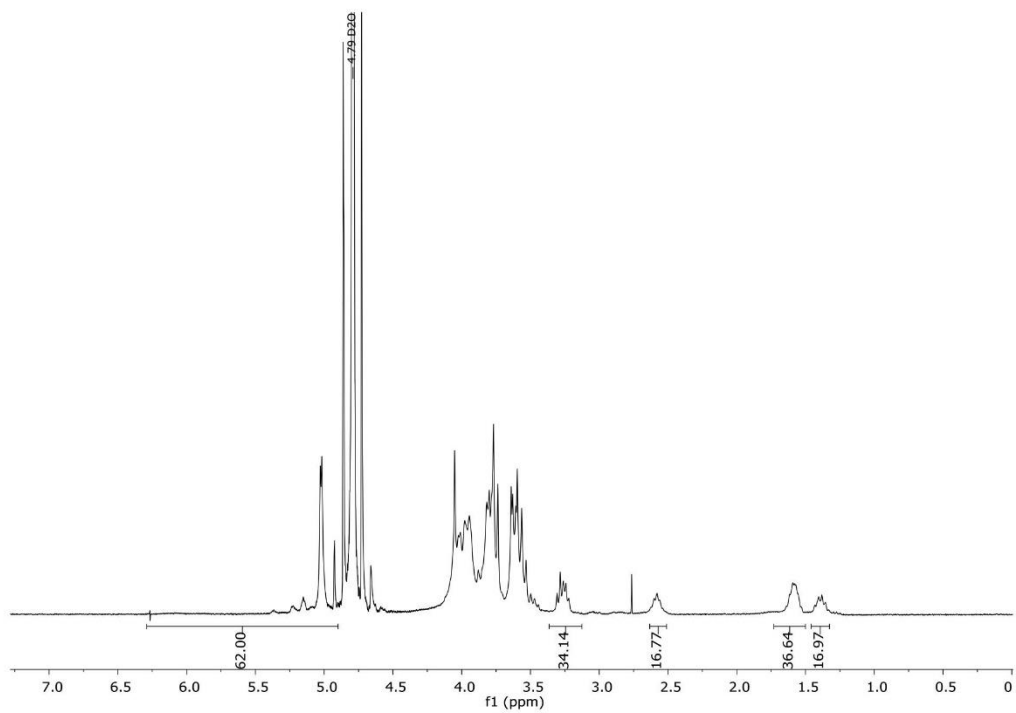
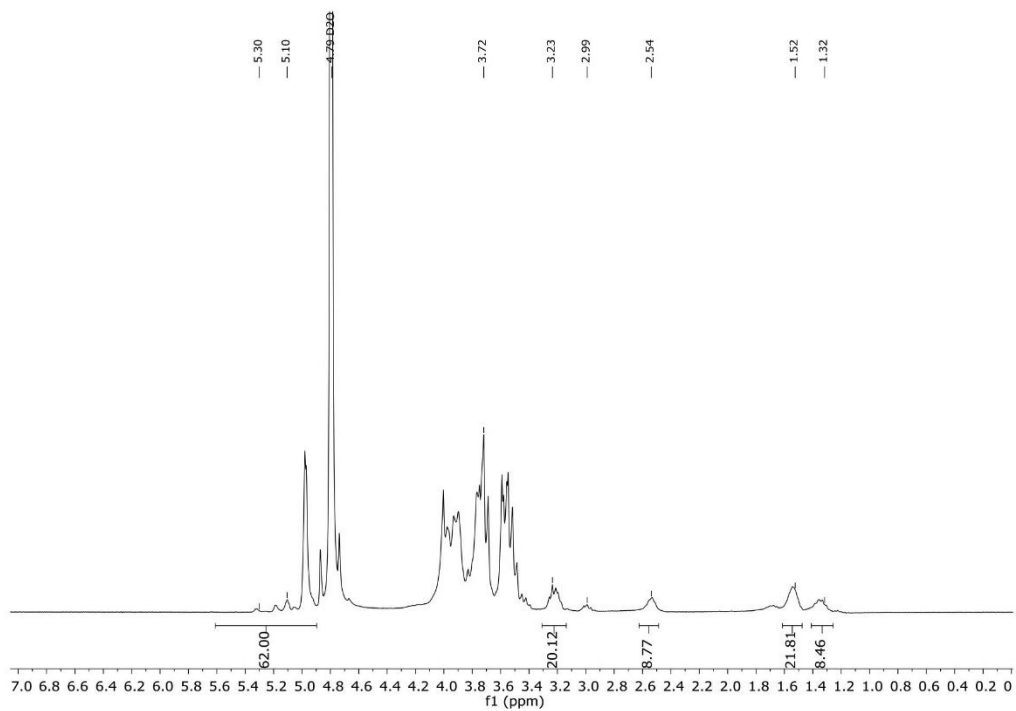


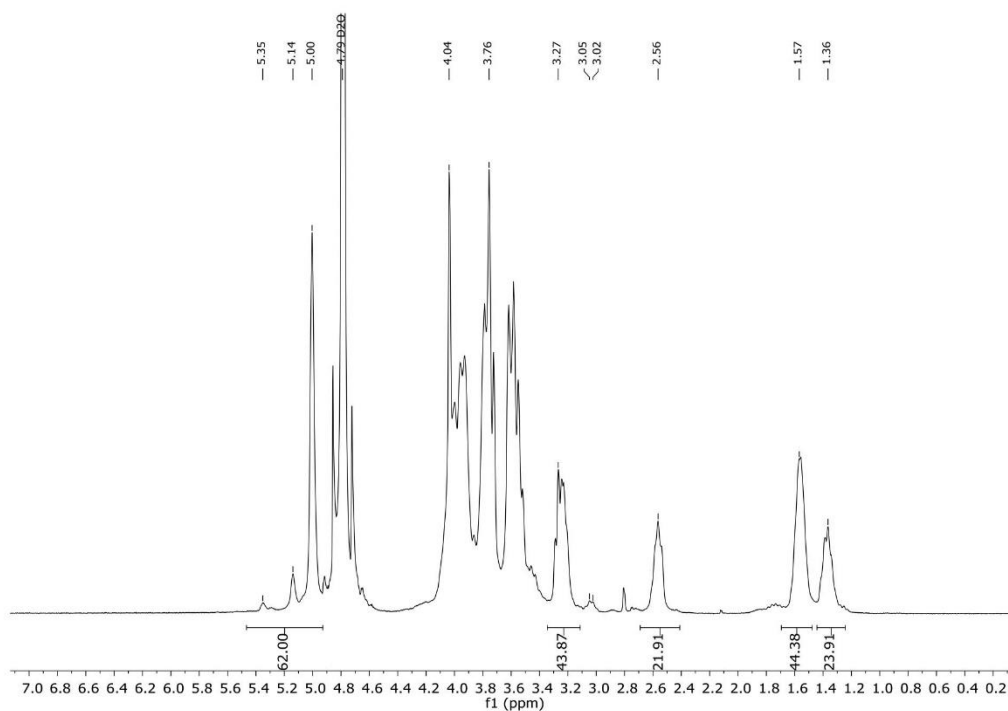
1.3.6 Synthesis of N₃-Dex-N-Boc-cadaverine 7, 8, 9 and N₃-Dex-cadaverine 10, 11, 12



2-CED-N-Boc-Cadaverine **4**, **5** or **6** was dissolved in 40 % acetonitrile (MeCN), and EEDQ dissolved in 40 % MeCN was added. The mixture was stirred at 30 °C for 1 h. Subsequently *N*-(5-aminopentyl)-2-azidoacetamide **2** was added and the mixture was stirred at 30 °C for 4 h. The product was diluted with water and freeze-dried. Purification was conducted using disposable PD10 desalting columns, following the instruction of the supplier. After freeze-drying a pure white powder was obtained. m =29.6 mg (55 % **10**); 14.6 mg (43%, **11**); 46.7 mg (53 %, **12**), ¹H NMR (300 MHz, Deuterium Oxide) δ = 5.58 – 4.95 (m, 1H, C(1)H), 4.19 – 3.30 (m, C (2-6)H (glucose units); CH₂CH₂COOH; CH₂-N₃), 3.12 – 3.34 (m, NHCO-CH₂-N₃; CH₂-(CH₂)₄-NHCO-CH₂-N₃), 3.04 – 3.12 (m, 4H, CH₂NH-BOC, CH₂(CH₂)₄NH-Boc), 2.68 – 2.38 (m, CH₂COOH), 1.20 – 1.92 (overlapped m, 15H, CH₂(CH₂)₃NH-Boc, CH₂(CH₂)₂NH-Boc, CH₂(CH₂)₁NH-Boc 3CH₃(BOC); (1.47-1-66 CH₂-CH₂-NHCO-CH₂-N₃, CH₂-(CH₂)₃-NHCO-CH₂-N₃), 1.29 – 1.44 CH₂-(CH₂)₂-NHCO-CH₂-N₃) ppm.

	batch 1 10				batch 2 11				batch 3 12			
	m [mg]	n [μmol]	v [mL]	eq	m [mg]	n [μmol]	v [mL]	eq	m [mg]	n [μmol]	v [mL]	eq
2-CED-N-Boc-Cadaverine	50	4.78	-	1	30.4	2.81	-	1	75	6.80	-	1
EEDQ	9.45	191.1	-	40	5.4	218.4	-	77.7	181.3	733	-	107.8
azido linker 2	75	202.5	-	42.4	43	232.1	-	82.6	128	691	-	101.6
40 % MeCN	-	-	2		-	-	1	-	-	-	2	-





References

- [1] M. Richter, A. Chakrabarti, I. R. Ruttekkolk, B. Wiesner, M. Beyermann, R. Brock and J. Rademann, *Chem. Eur. J.*, **2012**, 18, 16708-16715.
- [2] M. Hesse and H. Meier, *Spektroskopische Methoden in der organischen Chemie, 8. überarb. Auflage* **2011**, Georg Thieme Verlag, 2014.
- [3] (a) L. Deweid, L. Neureiter, S. Englert, H. Schneider, J. Deweid, D. Yanakieva, J. Sturm, S. Bitsch, A. Christmann and O. Avrutina, *Chem. Eur. J.* **2018**; (b) C. K. Marx, T. C. Hertel and M. Pietzsch, *Enzyme Microb. Technol.*, **2007**, 40, 1543-1550.
- [4] M. S. Verma and F. X. Gu, *Carbohydr. Polym.*, **2012**, 87, 2740-2744.
- [5] Y.-I. Jeong, D.-G. Kim and D.-H. Kang, *J. Chem.*, **2013**, 2013.

4.2. TRAIL-inspired Multivalent Dextran Conjugates Efficiently Induce Apoptosis upon DR5 Receptor Clustering

Title:

TRAIL-inspired multivalent dextran conjugates efficiently induce apoptosis upon DR5 receptor clustering

Authors:

H. Schneider, D. Yanakieva, A. Macarrón, L. Deweid, B. Becker, S. Englert, O. Avrutina, H. Kolmar

Bibliographic data:

ChemBioChem

Volume 20, Issue 24 Pages 3006-3012.

Article first published online: 17th Jun 2019

DOI: <https://doi.org/10.1002/cbic.201900251>

(Marked as Very Important Paper, will be Front Cover in December, Issue 24)

Copyright © 1999-2019 John Wiley & Sons, Inc. Reproduced with permission.

Cover picture

First published online: 29th Nov 2019

DOI: <https://doi.org/10.1002/cbic.201900702> (Cover Picture)

Copyright © 1999-2019 John Wiley & Sons, Inc. Reproduced with permission.

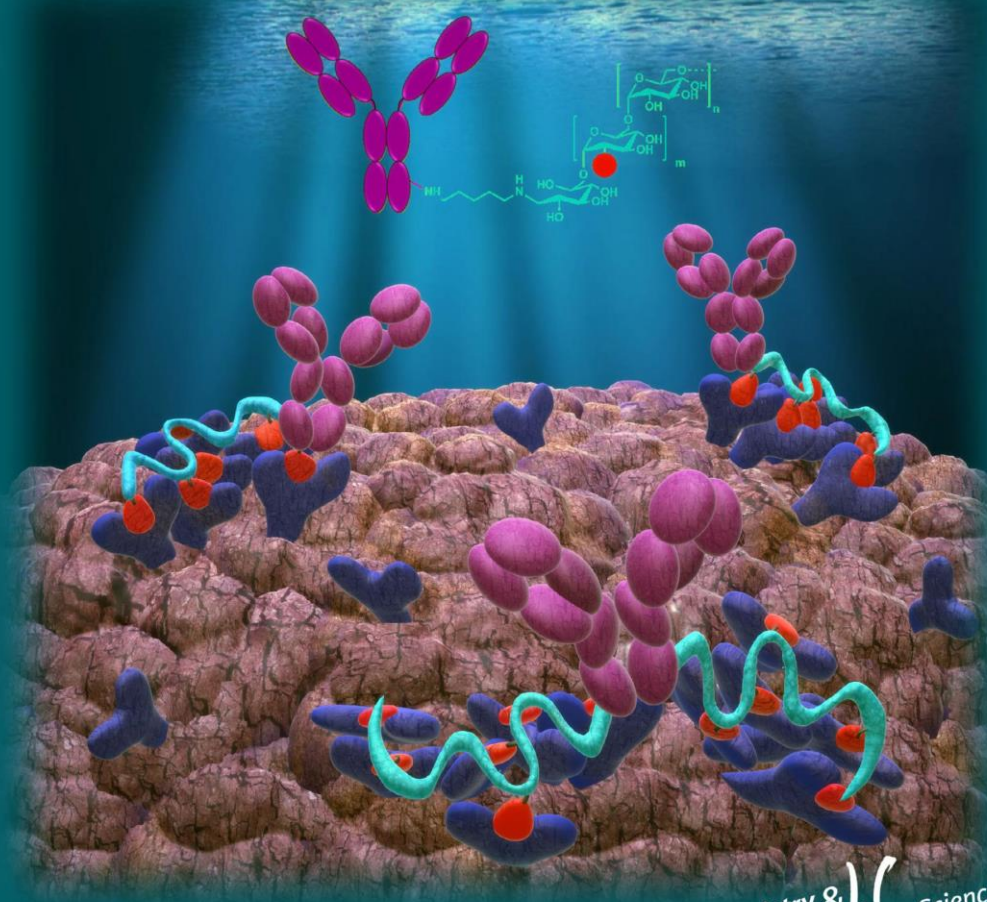
Contributions by Hendrik Schneider:

- Initial idea and project management
- Literature research
- Performed the majority of experiments
- Preparation of the manuscript and all included graphical material
- Revised the manuscript
- Design and preparation of the front cover of ChemBioChem Volume 24 (December)

A EUROPEAN JOURNAL OF CHEMICAL BIOLOGY

CHEMBIOCHEM

SYNTHETIC BIOLOGY & BIO-NANOTECHNOLOGY



24/2019

Chemistry & Life Sciences

Front Cover:

H. Kolmar et al.

TRAIL-Inspired Multivalent Dextran Conjugates Efficiently Induce Apoptosis upon DR5 Receptor Clustering

WILEY-VCH

www.chembiochem.org

A Journal of



COVER PICTURE

H. Schneider, D. Yanakieva, A. Macarrón,
L. Deweid, B. Becker, S. Englert,
O. Avrutina, H. Kolmar*



**TRAIL-Inspired Multivalent Dextran
Conjugates Efficiently Induce
Apoptosis upon DR5 Receptor
Clustering**



Dextran is applied as a hydrophilic modular platform for the covalent multimerization of death receptor-targeting peptides aimed at triggering apoptosis by receptor clustering. The biological activity of the construct is not affected upon conjugation with a human antibody Fc fragment, which may serve as a half-life enhancer *in vivo*. The front cover illustrates the ability of flexible dextran to efficiently cluster death receptors in an antibody-conjugated state leaving antigen-binding fragments (Fabs) unmodified; this opens up avenues for prospective bispecific targeting. More information can be found in the full paper by H. Kolmar et al.

VIP Very Important Paper



TRAIL-Inspired Multivalent Dextran Conjugates Efficiently Induce Apoptosis upon DR5 Receptor Clustering

Hendrik Schneider, Desislava Yanakieva, Arturo Macarrón, Lukas Deweid, Bastian Becker, Simon Englert, Olga Avrutina, and Harald Kolmar*^[a]

Triggering apoptosis of tumor cells has been in focus of cancer-inspired research since decades. As clustering of death receptor 5 (DR5), which is overexpressed on various cancer cells, leads to formation of the death-inducing signaling cascade (DISC), DR5 has recently become a promising target for tumor treatment. Herein, we demonstrate that covalent multimerization of a death receptor targeting peptide (DR5TP) on a dextran scaffold generates potent apoptosis-inducing conjugates ($EC_{50} = 2\text{--}20\text{ nM}$). A higher conformational flexibility compared to reported DR5TP multimerization approaches, intro-

duced by the polysaccharide framework compensates the reported need for the defined ligand orientation that was considered as essential prerequisite for effective receptor clustering and apoptosis induction. Enzyme-catalyzed ligation of a hydrophilic dextran conjugate bearing multiple DR5-targeting sites to a human fragment crystallizable (Fc) receptor did not affect the potency ($EC_{50} = 2\text{--}7\text{ nM}$), providing an option for improved in vivo half-life and prospective conjugation to an antibody of interest in view of bispecific tumor targeting.

Introduction

Killing tumor cells, which often evade apoptosis by disabling the respective pathways, has recently become an ambitious task in cancer research.^[1] Various approaches towards programmed cell death have been taken into consideration, among them classic chemotherapy, novel target-based strategies like toxic antibody–drug conjugates (ADCs), or activation of apoptosis-triggering cascades.^[1,2] In this context the apoptosis-inducing ligand (TRAIL/Apo2L/TNFSF10) is of great interest as the only endogenous protein with the unique capability of inducing death of tumor cells while leaving non-tumor cells intact.^[3] TRAIL is a type II transmembrane protein that possesses a homotrimeric architecture, which allows for the binding of different receptors, namely DcR1, DcR2, osteoprotegerin, and apoptosis-inducing death receptors DR4 and DR5.^[1,3a,b]

Being present as trimer at the surface of immune cells in the native state, TRAIL (contrary to intrinsic stimuli like DNA damage or cell distress) triggers apoptosis by binding and clustering of DR4 and DR5.^[1,3b,4] This apoptotic signal is independent of the p53 tumor-suppressor gene, which makes TRAIL a promising antitumor candidate.^[1,4] Upon binding of TRAIL, oligomerization of death receptors leads to the formation of the death-inducing signaling cascade (DISC) that activates caspase-

8 and -10, thus promoting the death-executing proteolytic cascade resulting in cellular apoptosis.^[3b,c,5]

Numerous approaches towards death receptor targeting have been examined to date, from recombinant TRAIL (rhTRAIL)^[6] to TRAIL-mimicking molecules and antibodies.^[1,3b,7] Thus, monoclonal antibodies (mAbs) like mapatumumab^[8] or conatumumab^[9] combine targeting of DR4 or DR5 with a fragment crystallizable (Fc) receptor function, which result in antibody-dependent cell-mediated cytotoxicity (ADCC) and complement-dependent cytotoxicity (CDC) as well as enhanced in vivo half-life.^[1] Though being well-tolerated, mAbs often share lack of efficacy that may be attributed at least in part to their bivalency compared to the natural trimeric TRAIL.^[1]

Novel TRAIL-inspired approaches rely on multivalent derivatives of antibodies or peptidic binders, among them a DR4-targeting pentavalent IgM^[1] or DR5-targeting tetraivalent scFvs fused to human serum albumin (HAS)^[3c] or the TAS266 nanobody oligomer.^[10] Although TAS266 displays excellent potency on tumor cells, the respective phase I clinical trials were terminated due to unforeseen liver cytotoxicity. This might be caused by a combination of immunogenicity, possible induction of DR5 expression on hepatocytes or by the high potency of the nanobody.^[1,3b,10]

A peptidic mimic of TRAIL called death receptor 5 targeting peptide (DR5TP) was identified upon combinatorial screening.^[3b,11] Possessing a DR5 binding loop stabilized by a disulfide bridge, this construct does not induce apoptosis as a solitary ligand.^[1,3a,b] Although a dimeric DR5TP showed only weak potential in triggering programmed cell death, a trimeric variant based on an adamantane core possessed enhanced inhibition of tumor growth.^[3a]

[a] H. Schneider, D. Yanakieva, A. Macarrón, L. Deweid, B. Becker, S. Englert, Dr. O. Avrutina, Prof. Dr. H. Kolmar
Clemens-Schöpf-Institut für Organische Chemie und Biochemie
Technische Universität Darmstadt
Alarich-Weiss-Strasse 4, 64287 Darmstadt (Germany)
E-mail: kolmar@biochemie-tud.de

Supporting information and the ORCID identification numbers for the authors of this article can be found under <https://doi.org/10.1002/cbic.201900251>.

As spatial orientation of the ligands appeared crucial for the induction of apoptosis, the nature of multimerization scaffold was assumed to play a key role.^[3a,b,11,12] Indeed, a hexameric adamantane-DR5TP conjugate showed weaker biological activity compared to its trimeric counterpart.^[12] Interestingly, different Fc-based bi- or tetravalent DR5TP architectures obtained through enzymatic conjugation revealed improved binding but did not induce apoptosis even in the presence of a cross-linking agent.^[3b] By contrast, a heptameric construct assembled on the scaffold of C4b-binding protein exhibited low-nanomolar EC₅₀ values on DR5-positive COLO205 cells.^[3b]

In the present study, we sought to overcome the mentioned obstacles by inducing steric flexibility of ligands upon their covalent grafting onto a polysaccharide scaffold. Herein, we report non-rigid, apoptosis-inducing hybrid architectures that efficiently cluster DR5 (Scheme 1). We chose dextran ($M_w = 10\,000\text{ g mol}^{-1}$) as a flexible modular multimerization platform, which is known to extend half-life and hydrophilicity when conjugated to a protein of interest.^[13] Dextran is a biocompatible polysaccharide consisting of repeating α -(1-6)-linked oligo-D-glucose units, which is accredited as blood-flow enhancer and plasma expander and is generally regarded as safe (GRAS) by the FDA.^[13c,14] Recently, we reported this polymer as multimerization platform in a conjugation approach towards dextramabs,^[13d] through high drug-to-antibody ratio ADCs with enhanced hydrophilicity. In these potent cytotoxic constructs covalent linkage to dextran could result in some benefits in terms of decreased ADC clearance,^[13a,b] hindered enzymatic degradation,^[15] and reduced immunogenicity *in vivo*, which will be the scope of further investigations.^[13c,d,16]

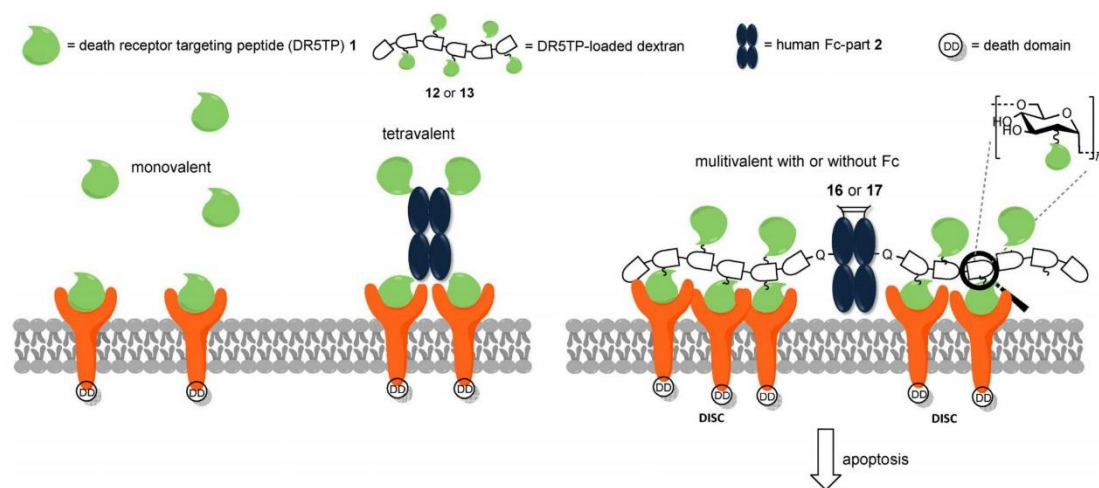
In the present research, we designed a dextran-based multimerization scaffold for efficient DR5 clustering (Scheme 1). Possessing two intrinsic conjugation sites, dextran offers an option for coupling of multiple ligands of different nature. Thus, the hydroxy groups of the glucose repeating units allow for the

decoration with DR5 binders, and the reducing end provides an orthogonally addressable aldehyde for further modification *in view of* enzyme-promoted ligation.^[13d] As a binding ligand we chose the disulfide-bridged peptide DR5TP (1; Schemes 1 and 2), which has been used in recent studies on DR5 clustering.^[3b,11] To combine DR5 targeting with the obvious benefits given by antibodies or their counterparts, dextran was additionally conjugated to the engineered aglycosylated Fc part (N297A) (2) in a transglutaminase-promoted condensation. Microbial transglutaminase (mTG) was chosen as a catalyst for the enzyme-mediated conjugation as it allows for the efficient covalent linkage of a primary amine located at the dextran counterpart with Q295 of an engineered surrogate Fc(N297A) (2). Accessibility of glutamine 295 is ensured by the lack of glycosylation due to mutation N297A (Scheme 1).^[13d,17]

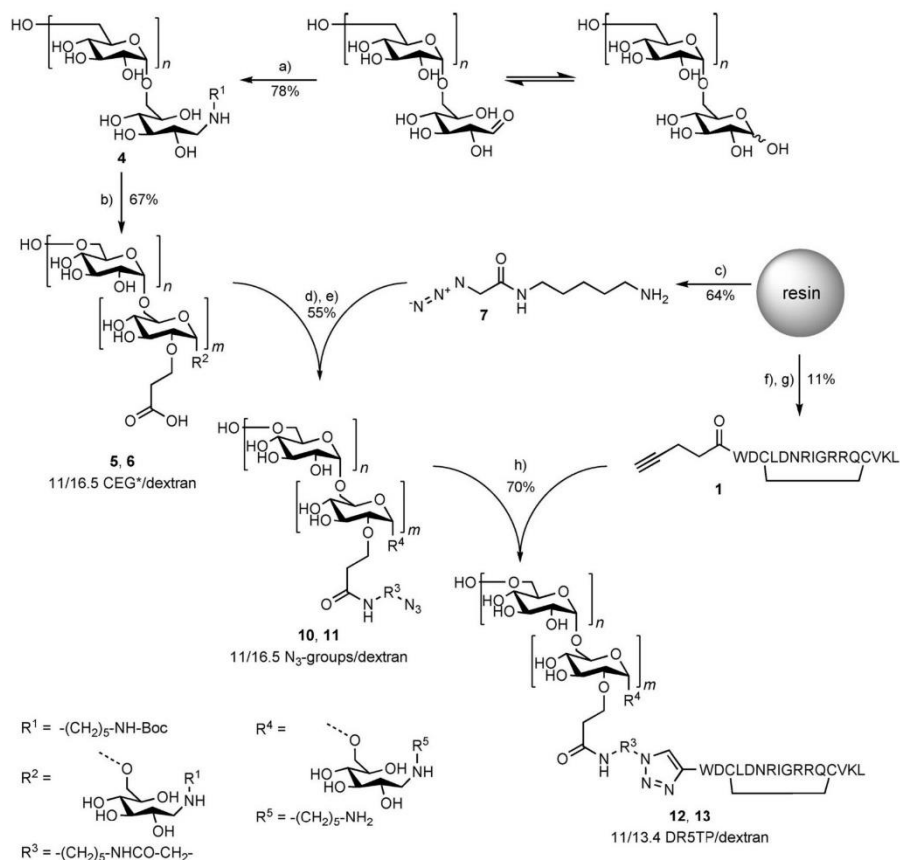
Results and Discussion

Synthesis of compounds

To introduce the required conjugation site at the reducing end of dextran, a protected diamine was incorporated upon reductive amination of an aldehyde with a Boc-masked cadaverine 3 giving compound 4 (Scheme 2). Compound 3 was synthesized by protection of cadaverine with di-*tert*-butyl dicarbonate as previously described.^[13d] Afterwards the modified dextran 4 was equipped with eleven, respectively 16.5, carboxyethyl groups per molecule (compounds 5 and 6, respectively) upon carboxy-ethylation of the C2 hydroxy groups of the glucose repeating units, thus generating amine-reactive moieties (Scheme 2).^[13d,18] Conjugation of the azide linker 7 assembled on solid support, to 5 and 6 yielded the modular scaffolds 8 and 9 equipped with "click"-addressable sites for further conjugation with DR5TP (1) by copper-catalyzed azide-alkyne cycloaddition (Scheme 2). DR5TP bearing an aliphatic alkyne (1),



Scheme 1. Death receptor 5-targeting peptide (DR5TP) binding to DR5 expressed on cell surface. Left: Monovalent solitary DR5TP and middle: tetravalent Fc-DR5TP conjugate not able to cluster DR5.^[3b] Right: Spatially flexible multimeric Fc-dextran-DR5TP conjugates inducing apoptosis.



Scheme 2. Synthetic route to the azide- (repeating units) and amine- (reducing end) functionalized dextrans **10** and **11** for ligand equipment and enzyme-catalyzed conjugation to Fc **2** and synthesis of the DR5TP-equipped dextrans **12** and **13**. a) NH₂-(CH₂)₅-NH-Boc (**3**, Boc = *tert*-butoxycarbonyl), borate buffer pH 8.2; b) acrylamide, 1 M NaOH; c) manual solid-phase peptide synthesis (SPPS); d) *N*-ethoxycarbonyl-2-ethoxy-1,2-dihydroquinoline (EEDQ), 40% MeCN; e) trifluoroacetic acid (TFA) (neat); f) automated SPPS; g) (NH₄)₂CO₃ pH 8.0, 30% DMSO; h) ascorbic acid, CuSO₄·5H₂O. *CEG = carboxethyl groups.

was synthesized by 9-fluorenylmethoxycarbonyl (Fmoc) SPPS followed by oxidative cyclization through a disulfide bridge. Subsequent copper-“click” reaction of dextrans **10** and **11** with **1** gave conjugates **12** and **13** bearing on average 11, or 13.4, DR5 binding ligands (Scheme 1). It should be noted that no quantitative conversion was achieved for compound **13** according to photometric analysis and the respective IR spectrum of the generated conjugate. It could be assumed that lack of space at the applied dextran scaffold (10 kDa) does not permit higher conjugation density due to steric effects (see Section S1.1.4 in the Supporting Information). A repetitive synthesis did not lead to enhanced ligand coupling.

Additionally, mTG-mediated conjugation of **10** and **11** to **2** resulted in compounds **14** and **15**, bearing at least 11, or 16.5, attachment sites per molecule. Consecutive copper-“click” reaction of **14** and **15** immobilized on a protein A spin column with **1** yielded the Fc-dextran conjugates **16** and **17** carrying up to eleven, respectively 13.4, DR5TP ligands attached to each dextran arm (Scheme 1).

Sodium dodecyl sulfate polyacrylamide gel electrophoresis (SDS-PAGE) analysis revealed that every Fc fragment **2** was equipped with at least one dextran **10** or **11** (Section S1.1.5).

Biology

Binding properties of **16** and **17** on DR5-positive cell lines were assessed by flow cytometry. Thus, constructs **16** and **17** demonstrated selective binding on DR5-overexpressing COLO205 colon cells as well as on Jurkat T-lymphocytes (Figure 1). As expected, no binding was observed for Fc(N297A) conjugated with dextran bearing 16.5 azide groups (**15**), lacking binding DR5TP ligands. Thermal shift assays of the Fc conjugate **17** demonstrated no loss in stability compared to the unmodified Fc(N297A) **2**, as identical melting points were observed (Section S1.1.6).

Encouraged by these results, we compared the *in vitro* potency of the solitary DR5TP **1**, the azide-modified dextran **11**, the DR5TP-dextrans **12** and **13**, the N₃-dextran **15** equipped

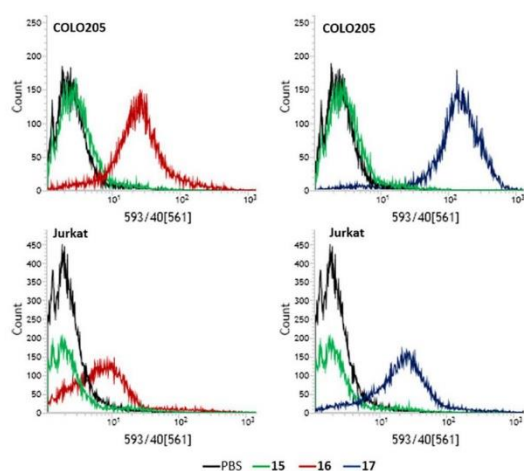


Figure 1. Receptor binding selectivity on two different DR5 overexpressing cell lines of the Fc-dextran conjugates equipped with DR5TP **16** (12.5 nM) and **17** (12.5 nM) compared to the non-ligand bearing Fc-dextran conjugates **15** (400 nM) and phosphate-buffered saline (PBS) as control.

with the highest number of azide groups, and the Fc-conjugated compounds **16** and **17** in cell proliferation assays on two DR5-overexpressing cell lines, namely COLO205 colon cells and Jurkat T-lymphocytes. HEK293 cells, lacking DR5, were utilized as a negative control (Section S1.1.7). Potent cell killing on both DR5-positive cell lines in the range of reported values for spatially restricted scaffolds bearing DR5TP^[3b] were revealed for the DR5TP dextrans **12** and **13** and for the Fc conjugates **16** and **17**, indicating effective receptor clustering (Table 1, Figure 2). The Fc conjugates **16** and **17** revealed a higher potency compared to the DR5TP dextrans **12** and **13**, which may be attributed to a higher number of DR5TP ligands present in these Fc architectures. However, an attribution of enhanced stability introduced by Fc conjugation should also be considered as a potential potency enhancing factor. This issue should be further considered, when finally, a full-length targeting antibody is applied as conjugation scaffold.

These findings indicate that for the dextran-clustered DR5TP a certain spatial positioning of ligands is not a prerequisite for efficient clustering as proposed previously.^[3a,b,11,12] No crosslinking agents were needed, as in the case of death receptor-tar-

Compound	EC ₅₀ [nM] COLO205	EC ₅₀ [nM] Jurkat
biotinylated-DR5TP ^[3b]	> 1 × 10 ⁶ ^[3b]	n.d.
1	— ^[a]	— ^[a]
11	— ^[a]	— ^[a]
12	16.9	20.0
13	15.5	2.2
15	— ^[a]	— ^[a]
16	1.9	4.7
17	2.2	6.7

[a] Determined up to 120 (**1**, **11**) and 400 nM (**15**).

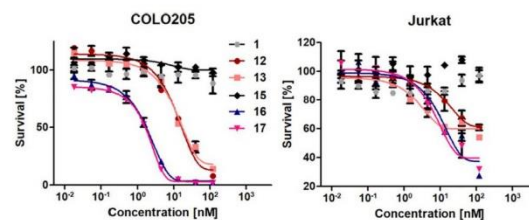


Figure 2. Cell viability assay on DR5-positive cell lines COLO205 and Jurkat.

geting antibodies. Furthermore, being multimerized on a dextran platform, DR5TP retained an efficient DR5 activation upon Fc conjugation (compounds **16** and **17**), whereas tetraivalent fusion to Fc failed (Figure 2).^[3b]

This opens avenues for further investigations in the field of bispecific therapeutics, for example, by combining T-cell recruitment with efficient induction of apoptosis. As expected, no cell death was observed for the solitary DR5TP **1** as well as for the dextran **11** and the dextran-Fc construct **15**, both lacking DR5-binding ligands (Figure 2 and Figure S16 in the Supporting Information). All examined compounds were found innocuous for DR5-negative HEK293 cells, thus displaying a DR5-dependent killing (Figure S17). A discrimination between apoptotic and necrotic cells was not done as multimerized DR5TP is known to solely induce apoptosis.^[3b]

Conclusion

Chemical conjugation of multiple DR5TP (**1**) ligands onto a dextran scaffold paved the way to flexible multivalent building blocks for DR5-induced apoptosis. The dextrans **12** and **13** exhibited efficient killing due to extrinsic stimuli of the caspase cascade mediated by DR5 clustering. These hybrid molecular architectures proved their efficiency on DR5-overexpressing COLO205 colon cells and Jurkat cells, thus delineating a new class of spatially flexible frameworks for DR5 targeting. Remarkably, no secondary antibody was necessary for crosslinking, which is often required for death receptor-addressing antibodies.^[3b] The transglutaminase-mediated conjugation of the azide-bearing dextrans **10** and **11** to a nonglycosylated human Fc (**2**) (compounds **14** and **15**) followed by on-support copper-“click” reaction gave compounds **16** and **17**, each combining a human Fc with multiple ligands of death receptor 5. These constructs showed effective binding. Moreover, conjugation to Fc **2** did not impair potency as compounds **16** and **17** revealed at least the same activity compared to **12** and **13**. It remains to be elucidated by animal studies, whether **16** and **17** display enhanced *in vivo* half-lives due to conjugation to an antibody Fc fragment and whether its effector functions contribute to tumor cell killing.

The attachment of multiple death receptor ligands on a flexible scaffold led to effective receptor clustering without any need for spatial positioning, which is in fact contrarily to numerous reports in the literature.^[3a,b,11,12] Further studies towards engineering of the dextran length and the density of conjugated ligands should be a prospective field for improvements.

Moreover, the discussed synthetic route could be used to equip the modular construct with a second targeting moiety, applying, for example, a full-size antibody for bispecific targeting. Combining and tailoring the selectivity of the two intrinsic targeting domains is a promising approach to improve the safety profile and the antitumor efficacy of bispecifics.^[19] These constructs should combine DR5-mediated cell killing due to a dextran-bound multimeric DR5TP with targeting properties of a respective antibody, like, for example, T-cell recruiting or addressing tumor overexpressed cell markers, for example, HER2, EGFR, or c-MET.

Experimental Section

Materials: All reagents were used as supplied by Iris Biotech, Agilent Technologies, Sigma–Aldrich, Roth, or Fisher Scientific without further purification. Cadaverine, dextran from *Leuconostoc mesenteroides* (average $M_w = 9000\text{--}11\,000\text{ g mol}^{-1}$, minimal branching of about 5%, $M_w = 10\,480\text{ g mol}^{-1}$), *N*-ethoxycarbonyl-2-ethoxy-1,2-dihydroquinoline (EEDQ), SYPRO Orange, and 2-azidoacetic acid were purchased from Sigma–Aldrich. Di-*tert*-butyl dicarbonate was purchased from Carbolutions (St. Ingbert, Germany), and dispase from Cellsystems (Troisdorf, Germany). For immune staining goat anti-human IgG Fc PE eBioscience™ was purchased from Fisher Scientific (Hampton, USA). The used PBS composed of 137 mM NaCl, 2.7 mM KCl, 10 mM Na_2HPO_4 , 1.8 mM KH_2PO_4 (pH 7.4).

Solid-phase peptide synthesis: Peptides were synthesized on AmphiSpheres 40 RAM resin (0.3 mmol g^{-1} , Agilent Technologies) upon automated assembly or on 2-chlorotrityl chloride resin (1.6 mmol g^{-1} , Iris Biotech) upon manual assembly. Automated synthesis was performed at a 0.25 mmol scale by using microwave-assisted Fmoc SPPS with a Liberty blue microwave peptide synthesizer. Manual synthesis was performed as described previously.^[13d]

RP-HPLC: Peptides were analyzed by using either an Agilent Infinity 1260 device equipped with an Interchim (Montluçon, France) Uptisphere Strategy RP column (C18-HQ, $3\ \mu\text{m}$, $100 \times 4.6\text{ mm}^2$) or on an Agilent 1100 device equipped with an Agilent Eclipse Plus RP column (C18, $100 \times 4.6\text{ mm}^2$, $3.5\ \mu\text{m}$, $95\ \text{Å}$) at a flow rate of 0.6 mL min^{-1} . Peptides were isolated on a semi-preparative RP-HPLC Interchim Puriflash 4250 equipped with a semi-preparative C18 RP column (Interchim Uptisphere Strategy (C18-HQ, $5\ \mu\text{m}$, $250 \times 21.2\text{ mm}^2$). At a flow rate of 18 mL min^{-1} , 3 min of isocratic flow (starting concentration of eluent B) was followed by 20 min of gradient flow. Eluent A: 0.1% (v/v) aq. trifluoroacetic acid (TFA), eluent B: 90% (v/v) aq. MeCN with 0.1% (v/v) TFA. Absorption was detected at $\lambda = 220$ and 280 nm .

Mass spectrometry: Electrospray ionization mass spectrometry (ESI-MS) spectra were obtained by using a Shimadzu LCMS-2020 mass spectrometer equipped with a Phenomenex Synergy 4 u Fusion-RP 80 (C-18, $250 \times 4.6\text{ mm}^2$, $2\ \mu\text{m}$, $80\ \text{Å}$). Eluent system: 0.1% (v/v) aq. formic acid (LC-MS grade, Fisher Scientific (Hampton, USA) (eluent A) and acetonitrile containing 0.1% (v/v) formic acid (LC-MS grade, Fisher Scientific (Hampton, USA) (eluent B).

NMR spectroscopy: NMR measurements were recorded on an Avance III or an Avance II NMR Spectrometer at 300 MHz (Bruker BioSpin GmbH, Rheinstetten, Germany). Samples were dissolved in $[\text{D}]\text{chloroform}$ or deuterium oxide from Sigma–Aldrich Chemie GmbH (Munich, Germany, now Merck KGaA, Darmstadt, Germany).

IR spectroscopy: IR measurements were performed by using homogenous potassium bromide pellets on a FTIR-Spectrometer Spectrum Two (Perkin–Elmer, Rodgau, Germany). Spectra were obtained by Perkin–Elmer Spectrum following the instructions of the manufacturer. Wavenumber area $\tilde{\nu} = 8300\text{--}350\text{ cm}^{-1}$, spectral resolution 0.5 cm^{-1} , wavenumber accuracy better than 0.01 cm^{-1} at $\tilde{\nu} = 3000\text{ cm}^{-1}$; wavenumber correctness: 0.1 cm^{-1} at $\tilde{\nu} = 3000\text{ cm}^{-1}$; signal-to-noise ratio: 9300:1 peak-to-peak, 5 s and 32000:1 peak-to-peak, 1 min.

Linker synthesis: Azide linker **7** was synthesized as previously described by manual SPPS on a CTC resin; 390 mg (65%) were obtained.^[13d] Boc-diamine **3** was synthesized as previously described by protection of cadaverine by using di-*tert*-butyl dicarbonate; 593 mg (99%) were obtained.^[13d]

Synthesis of DR5TP alkyne 1: DR5TP was synthesized by automated SPPS by using the standard procedure of the manufacturer with final Fmoc deprotection. Cysteines were coupled at 50°C within 10 min. Following Fmoc deprotection, an N-terminal alkyne moiety was installed on-support manually applying 4-pentynoic acid (2 equiv), *N,N'*-diisopropylcarbodiimide (DIC, 3.3 equiv), and oxyma (3.3 equiv) overnight. Cleavage was performed for 3 h by using a mixture of TFA, tetraethylsilane (TES), anisole, and water (94:2:2:2, v/v/v/v). Following precipitation in cold diethyl ether with subsequent washing (3×), drying, and dilution in 20% MeCN, the solution was freeze-dried. Formation of disulfide bonds was performed in 30% DMSO in 0.1 M $(\text{NH}_4)_2\text{CO}_3$ for 48 h. The oxidized peptide was isolated by semi-preparative RP-HPLC to yield 56.1 mg (11%).

Dextran modification: Dextran-*N*-Boc-cadaverine **4** was synthesized as previously described^[13d] by reductive amination of the reducing end.^[13d,20] Briefly: Dextran (1 equiv) was dissolved in 0.05 M borate buffer (pH 8.2) and *N*-Boc-cadaverine **3** (25 equiv) and NaBH_3CN (15.9 equiv) were added. The reaction mixture was stirred at 30°C for 72 h. The product was precipitated in cold methanol, washed three times, and dried. Afterwards, the product was dissolved in water and isolated by using a disposable PD10 desalting column following the instructions of the supplier. After freeze-drying, product **4** was obtained as white powder (779 mg, 78%).^[13d] Completeness of the reaction was determined by $^1\text{H NMR}$ spectroscopy as described previously.^[13d]

2-CED-*N*-Boc-cadaverine **5** was synthesized as previously described yielding 599 mg (69%).^[13d] Synthesis of 2-CED-*N*-Boc-cadaverine **6** was modified from^[13d,18] Briefly, dextran-*N*-Boc-cadaverine **4** (1 equiv) was dissolved in 1 M NaOH, and acrylamide (35.8 equiv) was added. The solution was stirred at 30°C for 24 h. Afterwards, the temperature was increased to 50°C and the reaction mixture was stirred additionally for 24 h followed by neutralization with 0.1 M HCl. The product was isolated as described for compound **4** giving 809 mg of compound **6** (90%). Quantification of carboxyethyl groups per dextran was determined by $^1\text{H NMR}$ spectroscopy as described previously.^[13d]

N_3 -dextran-cadaverines **10** and **11** were synthesized as reported previously.^[13d] Thus, 2-CED-*N*-Boc-cadaverine **5** or **6** bearing eleven respectively 16.5, CE groups per dextran (1 equiv) was dissolved in 40% MeCN and EEDQ (8.5 equiv per CE group) in 40% MeCN was added. The mixture was stirred at 30°C for 1 h. Subsequently *N*-(5-aminopentyl)-2-azidoacetamide (**7**) (9 equiv per CE group) was added and the mixture was stirred at 30°C for 4 h. The product was isolated as described for compound **4**. Quantification of N_3 groups per dextran was determined by $^1\text{H NMR}$ spectroscopy and IR spectroscopy as described previously.^[13d] Boc deprotection was performed as described previously.^[13d] Briefly, N_3 -dextran-*N*-Boc-ca-

daverine **8** or **9** was dissolved in neat TFA and stirred at ambient temperature for 30 min. Excess TFA was removed under reduced pressure, the oily residue dissolved in water, neutralized with 0.1 M NaOH, and purified as described for compound **4** yielding 46.7 mg (53%) of compound **10**^[13d] and 46.3 mg (65.5%) of compound **11**. Quantification of deprotection was determined by ¹H NMR spectroscopy as described previously.^[13d]

Transglutaminase-mediated bioconjugation: Fc(N297A) (**2**) was diluted to a concentration of 25 μM with either PBS or 250 mM Tris-HCl, 1.5 M NaCl (pH 8) and incubated with the respective N₃-dextran-cadaverine **10** or **11** (50–100 equiv) and 6 U mL⁻¹ mTG at 22 °C overnight, resulting in compounds **14** and **15**. Excess N₃-dextran-cadaverine and mTG were removed by using a Protein A HP Spin Trap. As reaction control an SDS-PAGE was performed.^[13d]

Copper-catalyzed azide-alkyne cycloaddition on dextran: The respective N₃-dextran-cadaverine **10** or **11** (1 equiv) and the DR5TP alkyne **1** (1.6 equiv per N₃) were dissolved in water and a freshly prepared solution of ascorbic acid (3.2 equiv per N₃) and CuSO₄·5H₂O (1.6 equiv per N₃) in water was added. The reaction mixture was stirred at 30 °C for 1 h. The conjugates **12** or **13** were isolated as described for compound **4**. Completeness of the reaction was assessed by IR spectroscopy.

Copper-catalyzed azide-alkyne cycloaddition on Fc-dextran: The respective Prot A (Protein A HP SpinTrap) immobilized Fc-dextran **14** or **15** (1 equiv) was suspended in 200 μL PBS and treated with the DR5TP alkyne **1** (2.5 equiv per N₃) and a freshly prepared solution of ascorbic acid (5 equiv per N₃) and CuSO₄·5H₂O (2.5 equiv per N₃). After incubation under continuous shaking at 30 °C for 3 h the column was washed and the Fc was eluted following the instructions of the supplier. The buffer was exchanged to PBS and the product was concentrated by using Amicon® Ultra centrifugation filters (3 kDa) As reaction control an SDS-PAGE was performed.

Cell culture: Cell lines were incubated under standard conditions at 37 °C in a humidified incubator with 5% CO₂. COLO205 colon adenocarcinoma cells were grown in RPMI 1640 culture medium with 10% fetal bovine serum (FBS). Jurkat T-lymphocytes were grown in RPMI 1640 with 15% FBS. HEK293 kidney cells were grown in DMEM with 10% FBS. Expi293F™, a non-adherent cell line, was obtained from Thermo Fisher Scientific and was grown in serum-free Expi293™ expression medium on an orbital shaker at 110 rpm.

Protein expression and purification: DNA sequence for the aglycosylated (N297A) human IgG1 Fc **1** domain was cloned in standard pEXPR vector for expression in mammals. C-terminal Lys447 was omitted to avoid multimerization. Fc (N297A) **1** was produced by transient transfection of Expi293™ by utilizing polyethyleneimine (PEI). 40 μg of the plasmid was mixed with 120 μg of PEI in serum-free Expi293™ expression medium and added dropwise to 30 mL of Expi293™ cells, in a density of 2.5 × 10⁶ cells mL⁻¹, under perpetual shaking. After 24 h cells were fed with 0.5% (w/v) tryptone. After 120 h the cell supernatant was purified by protein A affinity chromatography by using a HiTrap Protein A HP column (GE Healthcare). Antibody production supernatant was diluted with a half-volume of running buffer (20 mM sodium phosphate, pH 7) and was applied to the column after its equilibration with running buffer. Elution was carried out by using 100 mM citrate buffer pH 3. The eluate was dialyzed against PBS and concentrated by using an Amicon® Ultra centrifugation filters.

Inactive pro-microbial transglutaminase was produced as previously described.^[17b,21] Briefly, inactive pro-mTG was produced in *Escherichia coli* cells by using β-D-1-thiogalactopyranoside (IPTG). *E. coli* cells comprising the plasmid were grown in dYT + Amp medium (16 g L⁻¹ tryptone, 10 g L⁻¹ yeast extract, and 5 g L⁻¹ NaCl supplemented with 100 μg mL⁻¹ ampicillin) at 37 °C and 180 rpm to an OD of 0.7–1. After induction by IPTG (final c = 500 μM) cells were incubated at 24 °C and 180 rpm for 2–3 h. Cells were lysed by using a Constant Systems Ltd cell disruptor (Davenport, UK). Purification was performed by using standard IMAC purification procedure on a HisTrap HP (GE Healthcare) column. Purified pro-mTG was stored in mTG storage buffer (300 mM NaCl, 50 mM Tris-HCl pH 8, 5 mM CaCl₂, 1 mM glutathione (reduced)). pro-mTG was activated as previously described^[17b] upon addition of bacillus polymyxa neutral protease (dispase) 20 μg mL⁻¹ dissolved in mTG storage buffer. After incubation at 37 °C for 30 min, purification was performed by using a standard IMAC procedure on a HisTrap HP (GE Healthcare) column. Purified mTG was stored in mTG storage buffer + 10% glycerol at –80 °C.

Thermal shift assay: Thermal shift assays were performed in triplicate on a BioRad96CFX RT-PCR detection system with 0.5 °C/30 s to 99 °C. T_m values were collected from melting curves by using the corresponding BioRad analysis software. All reactions were performed in PBS at a final concentration of 0.1 mg mL⁻¹ protein upon addition of SYPRO Orange (diluted 1:800).

Cellular binding: Human colon adenocarcinoma cells COLO205 were trypsinized from the culture flask and spun down. Jurkat T-lymphocytes were spun down. Cells (1 × 10⁵ for COLO205 cells, 2.5 × 10⁵ for Jurkat cells) were washed three times with PBS containing 0.1% bovine serum albumin (BSA) followed by incubation with either PBS 0.1% BSA, Fc-dextran-N₃ **15**, or Fc-dextran-DR5TP **16**, **17** (30 μL, 12.5 nM in PBS, 0.1% BSA) for 30 min on ice. Subsequently, the cells were washed three times with PBS, 0.1% BSA and incubated with fluorescently labeled secondary antibody goat anti-human IgG Fc, PE-conjugated eBioscience™ (50 μL, 1/100 dilution) for 40 min on ice. Subsequently, cells were washed three times with PBS, 0.1% BSA. Cells were analyzed by flow cytometry by using a BD Influx cell-sorting device (manufactured by Becton, Dickinson, and Company).

Cell viability assay: Cell viability assay were performed as previously described.^[3b] Briefly, COLO205, Jurkat, and HEK293 cells were seeded in 96-well plates (density: 1 × 10⁴ (COLO205), 0.5 × 10⁴ (Jurkat), and 0.5 × 10⁴ viable cells per well (HEK293)) in a total volume of 90 μL of the respective medium. After 24 h serial dilutions of the constructs in 10 μL (PBS) were added to the cells and incubated for 72 h at 37 °C and 5% CO₂. Cell viability was measured using CellTiter96® AQueous One Solution Cell Proliferation Assay (Promega) following the instructions of the supplier by using a Tecan® Infinite F200 Pro.

Acknowledgements

This work was supported by the Deutsche Forschungsgemeinschaft through grant SPP 1623.

Conflict of Interest

The authors declare no conflict of interest.

Keywords: apoptosis · death receptor 5 · dextrans · oligomerization · TRAIL mimicking peptides

- [1] A. Dubuisson, O. Micheau, *Antibodies* **2017**, *6*, 16.
 [2] J. M. Lambert, A. Berkenblit, *Annu. Rev. Med.* **2018**, *69*, 191.
 [3] a) V. Pavet, J. Beyrath, C. Pardin, A. Morizot, M.-C. Lechner, J.-P. Briand, M. Wendland, W. Maison, S. Fournel, O. Micheau, *J. Cancer Res.* **2010**, *70*, 1101–1110; b) B. Valldorf, H. Fittler, L. Deweid, A. Ebenig, S. Dickgiesser, C. Sellmann, J. Becker, S. Zielonka, M. Empting, O. Avrutina, H. Kolmar, *Angew. Chem. Int. Ed.* **2016**, *55*, 5085–5089; *Angew. Chem.* **2016**, *128*, 5169–5173; c) F. Liu, Y. Si, G. Liu, S. Li, J. Zhang, Y. Ma, *Biomed. Pharmacother.* **2015**, *70*, 41–45.
 [4] S. Wang, W. S. El-Deiry, *Oncogene* **2003**, *22*, 8628.
 [5] A. R. Safa, *J. Clin. Exp. Oncol.* **2012**, *34*, 176–184.
 [6] A. Ashkenazi, R. C. Pai, S. Fong, S. Leung, D. A. Lawrence, S. A. Marsters, C. Blackie, L. Chang, A. E. McMurtrey, A. Hebert, L. DeForge, I. L. Koumenis, D. Lewis, L. Harris, J. Bussiere, H. Koeppen, Z. Shahrokhi, R. H. Schwall, *J. Clin. Invest.* **1999**, *104*, 155–162.
 [7] M. W. den Hollander, J. A. Gietema, S. de Jong, A. M. E. Walenkamp, A. K. L. Reyners, C. N. A. M. Oldenhuis, E. G. E. de Vries, *Cancer Lett.* **2013**, *332*, 194–201.
 [8] L. Pukac, P. Kanakaraj, R. Humphreys, R. Alderson, M. Bloom, C. Sung, T. Riccobene, R. Johnson, M. Fiscella, A. Mahoney, J. Carrell, E. Boyd, X. T. Yao, L. Zhang, L. Zhong, A. von Kerczek, L. Shepard, T. Vaughan, B. Edwards, C. Dobson, T. Salcedo, V. Albert, *Br. J. Cancer* **2005**, *92*, 1430–1441.
 [9] a) R. S. Herbst, R. Kurzrock, D. S. Hong, M. Valdivieso, C.-P. Hsu, L. Goyal, G. Juan, Y. C. Hwang, S. Wong, J. S. Hill, G. Friberg, P. M. LoRusso, *Clin. Cancer Res.* **2010**, *16*, 5883; b) J. D. Graves, J. J. Kordich, T.-H. Huang, J. Piasecki, T. L. Bush, T. Sullivan, I. N. Foltz, W. Chang, H. Douangpanya, T. Dang, J. W. O'Neill, R. Mallari, X. Zhao, D. G. Branstetter, J. M. Rossi, A. M. Long, X. Huang, P. M. Holland, *Cancer Cell* **2014**, *26*, 177–189.
 [10] K. P. Papadopoulos, R. Isaacs, S. Bilic, K. Kentsch, H. A. Huet, M. Hofmann, D. Rasco, N. Kundamal, Z. Tang, J. Cooksey, A. Mahipal, *Cancer Chemother. Pharmacol.* **2015**, *75*, 887–895.
 [11] Y. M. Angell, A. Bhandari, M. N. De Francisco, B. T. Frederick, J. M. Green, K. Leu, K. Leather, R. Sana, P. J. Schatz, E. A. Whitehorn, in *Peptides for Youth*, Springer, **2009**, pp. 101–103.
 [12] G. Lamanna, C. R. Smulski, N. Chekkat, K. Estieu-Gionnet, G. Guichard, S. Fournel, A. Bianco, *Chem. Eur. J.* **2013**, *19*, 1762–1768.
 [13] a) R. P. Lyon, T. D. Bovee, S. O. Doronina, P. J. Burke, J. H. Hunter, H. D. Neff-LaFord, M. Jonas, M. E. Anderson, J. R. Setter, P. D. Senter, *Nat. Biotechnol.* **2015**, *33*, 733; b) A. Valdivia, R. Villalonga, P. Di Pietro, Y. Pérez, L. Mariniello, L. Gómez, R. Porta, *J. Biotechnol.* **2006**, *122*, 326–333; c) S. B. van Witteloostuijn, S. L. Pedersen, K. J. Jensen, *ChemMedChem* **2016**, *11*, 2474–2495; d) H. Schneider, L. Deweid, T. Pirzer, D. Yanakieva, S. Englert, B. Becker, O. Avrutina, H. Kolmar, *ChemistryOpen* **2019**, *8*, 354–357.
 [14] a) H. Maeda, L. W. Seymour, Y. Miyamoto, *Bioconjugate Chem.* **1992**, *3*, 351–362; b) R. Mehvar, *J. Controlled Release* **2000**, *69*, 1–25.
 [15] R. Villalonga, A. Valdivia, Y. Pérez, B. Chongo, *J. Appl. Polym. Sci.* **2006**, *102*, 4573–4576.
 [16] R. Fagnani, M. S. Hagan, R. Bartholomew, *J. Cancer Res.* **1990**, *50*, 3638–3645.
 [17] a) L. Deweid, O. Avrutina, H. Kolmar, *Biol. Chem.* **2019**, *400*, 257–274; b) L. Deweid, L. Neureiter, S. Englert, H. Schneider, J. Deweid, D. Yanakieva, J. Sturm, S. Bitsch, A. Christmann, O. Avrutina, H.-L. Fuchsbaue, H. Kolmar, *Chem. Eur. J.* **2018**, *24*, 15195–15200; c) A. M. Sochaj, K. W. Świdarska, J. J. B. A. Otlewski, *Biotechnol. Adv.* **2015**, *33*, 775–784.
 [18] M. Richter, A. Chakrabarti, I. R. Ruttekkolk, B. Wiesner, M. Beyerermann, R. Brock, J. Rademann, *Chem. Eur. J.* **2012**, *18*, 16708–16715.
 [19] C. Sellmann, A. Doerner, C. Knuehl, N. Rasche, V. Sood, S. Krah, L. Rhiel, A. Messemer, J. Wesolowski, M. Schuette, S. Becker, L. Toleikis, H. Kolmar, B. Hock, *J. Biol. Chem.* **2016**, *291*, 25106–25119.
 [20] a) Y.-I. Jeong, D.-G. Kim, D.-H. Kang, *J. Chem.* **2013**, *2013*, 414185; b) M. S. Verma, F. X. Gu, *Carbohydr. Polym.* **2012**, *87*, 2740–2744.
 [21] C. K. Marx, T. C. Hertel, M. Pietzsch, *Enzyme Microb. Technol.* **2007**, *40*, 1543–1550.

Manuscript received: April 16, 2019

Revised manuscript received: June 5, 2019

Accepted manuscript online: June 17, 2019

Version of record online: September 26, 2019

CHEMBIOCHEM

Supporting Information

TRAIL-Inspired Multivalent Dextran Conjugates Efficiently Induce Apoptosis upon DR5 Receptor Clustering

Hendrik Schneider, Desislava Yanakieva, Arturo Macarrón, Lukas Deweid, Bastian Becker, Simon Englert, Olga Avrutina, and Harald Kolmar^{*[a]}

cbic_201900251_sm_miscellaneous_information.pdf

Electronic Supplemental Information (ESI):

Content

1 Experimental	2
1.1 General	2
1.1.1 Overview of generated compounds	2
1.1.1 Synthesis of 2-CED- <i>N</i> -Boc-cadaverine 6	3
1.1.2 Synthesis of 4-Pentyn-DR5TP 1	4
1.1.3 Synthesis of N ₃ -dextran-cadaverine 11 and quantification of N ₃ -groups per dextran using IR and NMR spectroscopy	7
1.1.4 Copper mediated azide-alkyne cycloaddition 12 and 13 (DR5TP-dextran-cadaverine)	10
1.1.5 Transglutaminase catalyzed Fc conjugation and copper mediated azide-alkyne cycloaddition (Fc-dextran-N ₃)	14
1.1.6 Thermal shift assay	16
1.1.7 Cell viability assay	18
1.1.8 Certificate of analysis for dextran	19

1 Experimental

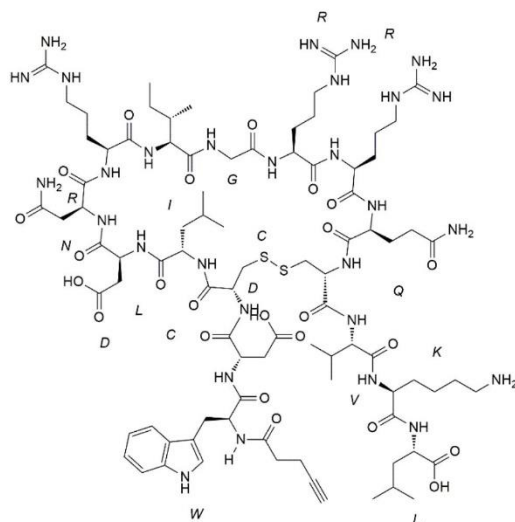
1.1 General

1.1.1 Overview of generated compounds

2 Table 1. Overview of generated compounds.

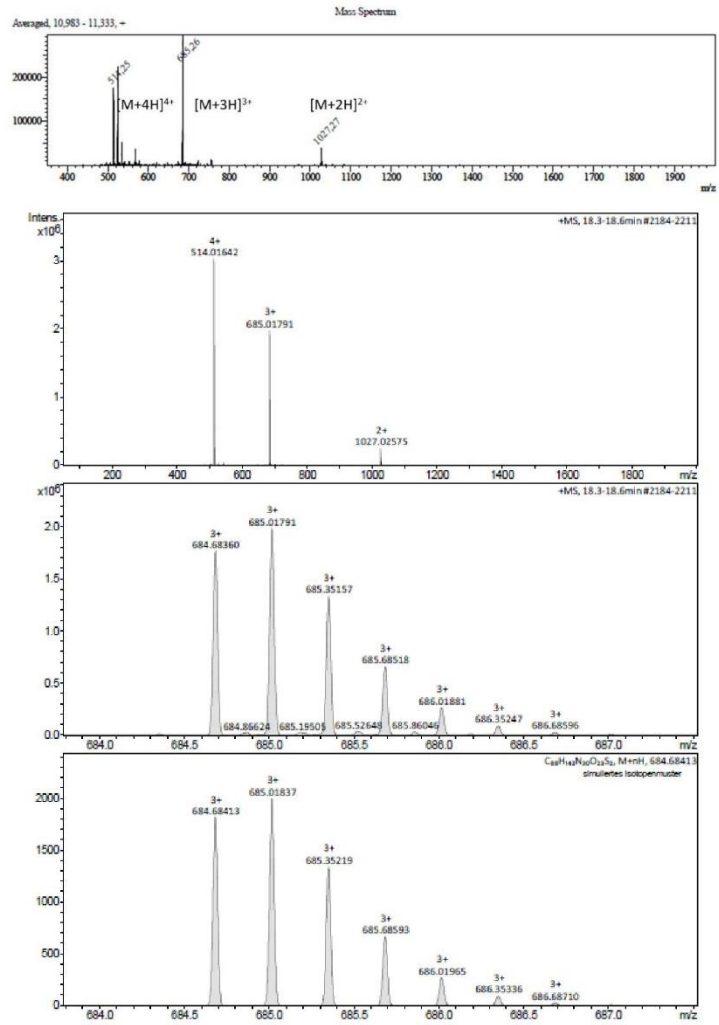
Number	Compound	Description
1	4-Pentyn-DR5TP	DR5TP modified for copper-mediated click reaction
2	Fc(N297A)	Aglycosylated Fc-fragment
3	<i>N</i> -Boc-cadaverine	Protected amine for enzymatic conjugation
4	Dextran- <i>N</i> -Boc-cadaverine	Red-end modified dextran
5	2-CED- <i>N</i> -Boc-cadaverine	11 COOH/dextran
6	2-CED- <i>N</i> -Boc-cadaverine	16.5 COOH/dextran
7	<i>N</i> -(5-aminopentyl)-2-azidoacetamide	Azide linker
8	N ₃ -dextran- <i>N</i> -Boc-cadaverine	11 N ₃ /dextran
9	N ₃ -dextran- <i>N</i> -Boc-cadaverine	16.5 N ₃ /dextran
10	N ₃ -dextran-cadaverine	11 N ₃ /dextran
11	N ₃ -dextran-cadaverine	16.5 N ₃ /dextran
12	DR5TP-dextran-cadaverine	11 DR5TP/dextran
13	DR5TP-dextran-cadaverine	13.4 DR5TP/dextran
14	Fc-dextran-N ₃	11 N ₃ /dextran
15	Fc-dextran-N ₃	13.4 N ₃ /dextran
16	Fc-dextran-DR5TP	11 DR5TP/dextran
17	Fc-dextran-DR5TP	13.4 DR5TP/dextran

1.1.2 Synthesis of 4-Pentyn-DR5TP 1



Chemical Formula: $C_{88}H_{141}N_{29}O_{24}S_2$
Exact Mass: 2052,01
Molecular Weight: 2053,37

Successful synthesis of DR5TP by solid-phase peptide synthesis (SPPS) was analyzed by ESI-MS and RP-HPLC using a C18 column (Figure S2 and S3). 173 mg (67.3 %) of not cyclized DR5TP 1 were obtained by automated peptide synthesis followed by manual coupling of 4-pentynoic acid. After cyclization by disulfide formation and isolation using a C-18 column in a semi-preparative scale 21.1 mg (8.2 %, 0.125 mM scale) were obtained as white powder. A repetitive synthesis gave 56.1 mg (10.9 % 0.25 mM scale) $M_{calc}=2052.39$ gm/mol



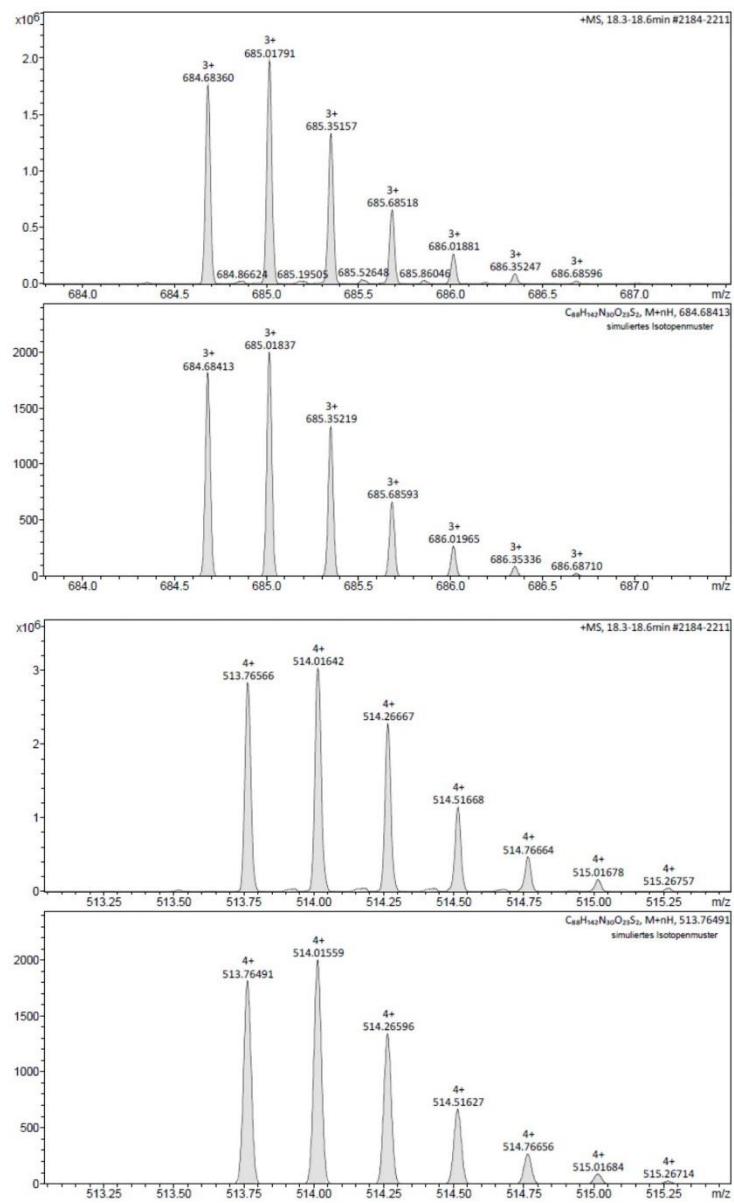


Figure S2. ESI-MS (top) and ESI-HRMS (performed on an Impact II, Fa. Bruker Daltonik) (bottom) analysis of 4-Pentyn-DR5TP 1 revealed the $[M+2H]^{2+}$, $[M+3H]^{3+}$ and $[M+4H]^{4+}$ $M_{\text{calc}} = 2052.39$ g/mol.

ESI-MS and ESI-HRMS analysis revealed a molecule ion series of 3 following signals, that coincided with the predicted isotope distribution.

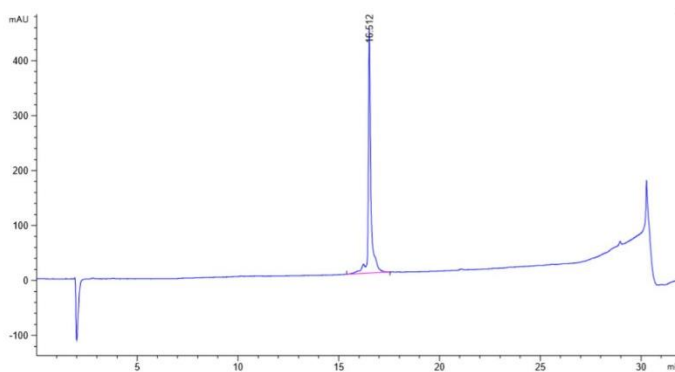
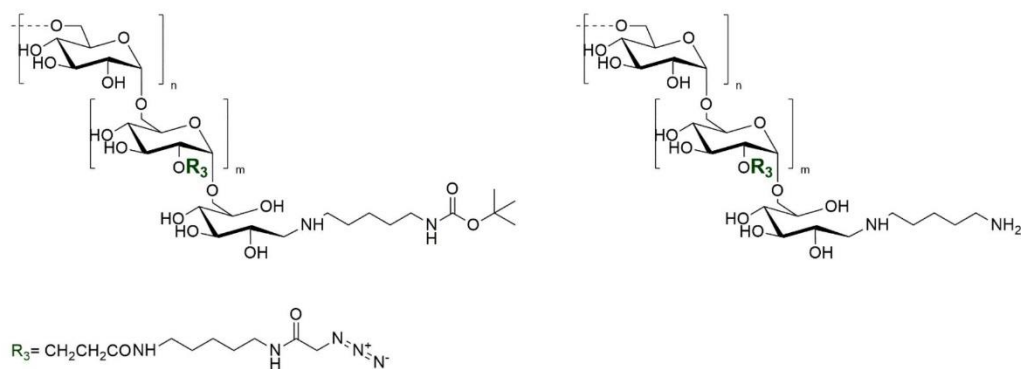


Figure S3. RP-HPLC on *Agilent* Eclipse Plus RP column (C18, 100×4.6 mm, 3.5 μm, 95 Å) at a flow rate of 0.6 ml·min⁻¹ (0 to 80% B) of **1** (0.125 mM scale), Eluent A: 0.1% (v/v) aq. trifluoroacetic acid (TFA), eluent B: 90% (v/v) aq. MeCN with 0.1% (v/v) TFA.

HPLC analysis revealed the purity of isolated peptide **1**.

1.1.3 Synthesis of N₃-dextran-cadaverine **11** and quantification of N₃-groups per dextran using IR and NMR spectroscopy



IR spectroscopy was applied as first hint for azide-modification of **6** generating compound **9/11** as described recently (Figure S4).^[1b] The band found at 2113 cm^{-1} , corresponding to the azide moiety, does not superimpose with any other band found in dextran IR. The intensity of this band gives a first evidence for azide modification.

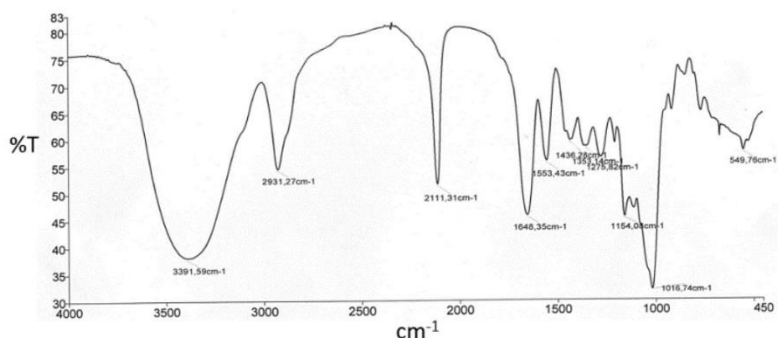


Figure S4. Example IR spectra of compound **11** (16.5 N_3 -groups per dextran)

Quantitative determination was performed by $^1\text{H-NMR}$ spectroscopy (Figure S5). The integrals corresponding to the aliphatic protons of azido linker were quantified and compared to the signals corresponding to the C2-protons of the carboxyethyl group.^[1] Briefly: Signal 1, corresponding to the 62 anomeric protons of the glucose repeating units was used for quantification. Integration of signal 2, corresponding to the two protons of C2 of the introduced carboxyethyl group was used to determine the number of carboxyethyl groups per dextran. Further analysis of the integrals 3+7, 4+6, and 5, corresponding to CH_2 -groups of the introduced azide linker revealed quantitative conjugation.^[1] A quantitative N_3 -modification of the carboxyethyl groups of **5** and **6** was observed. No loss of azide groups was found after deprotection of the Boc-protected reducing end of **9** generating **11**.

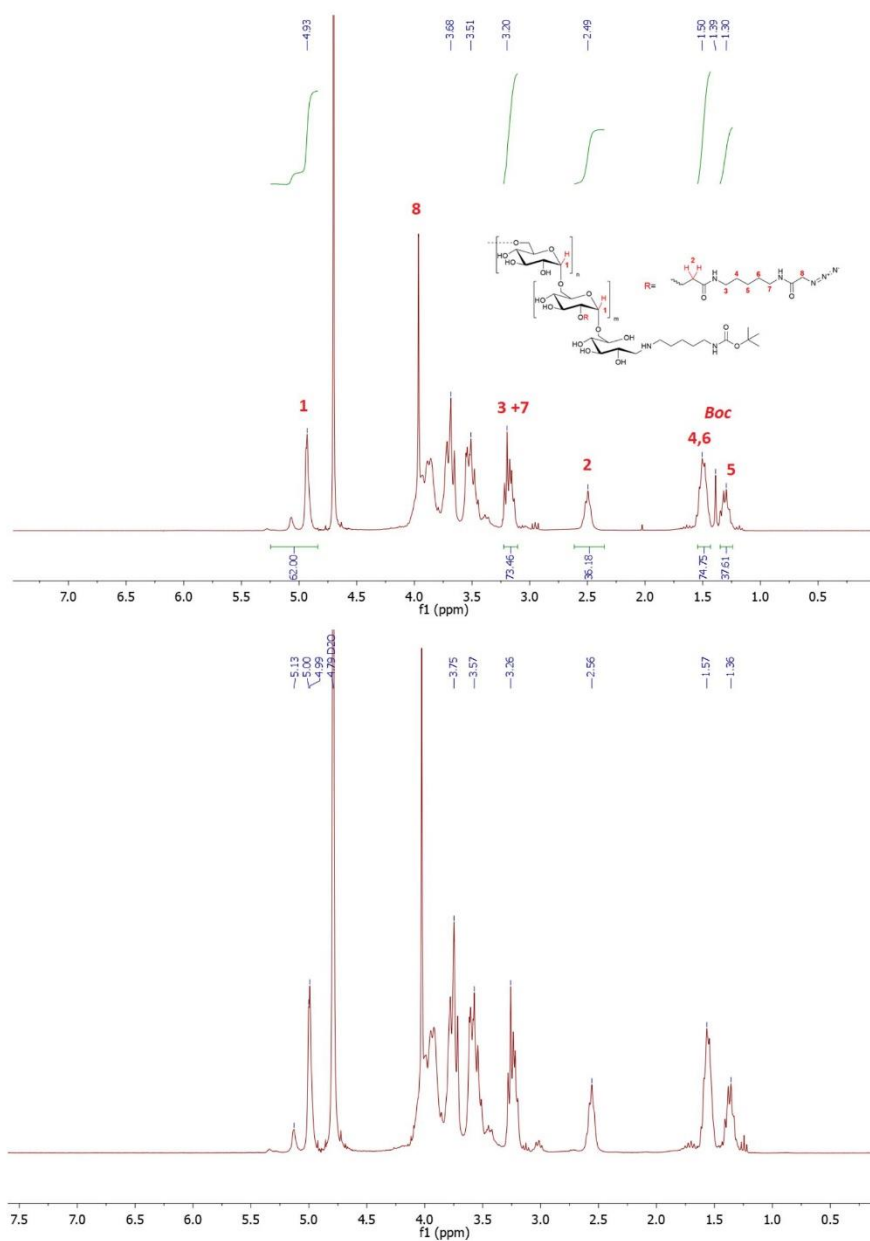


Figure S5. Exemplary ¹H-NMR spectra of azide-modified dextran-*N*-Boc-cadaverine **9** (top) and azide-modified dextran-cadaverine **11** (bottom): The integrals of protons give evidence of quantitative coupling of azide linker **7**.

$m = 46.3$ mg (65.5 % **11**) ^1H NMR (300 MHz, Deuterium Oxide) $\delta = 5.23 - 4.84$ (m, 1H, C(1)H), 4.09 – 3.29 (m, C (2-6)H (glucose units); $\text{CH}_2\text{CH}_2\text{COOH}$; $\text{CH}_2\text{-N}_3$), 3.07 – 3.25 (m, $\text{NHCO-CH}_2\text{-N}_3$), $\text{CH}_2\text{-(CH}_2)_4\text{-NHCO-CH}_2\text{-N}_3$), 2.92 – 3.12 (m, 4H, $\text{CH}_2\text{NH-Boc}$, $\text{CH}_2(\text{CH}_2)_4\text{NH-Boc}$), 2.32 – 2.62 (m, CH_2COOH), 1.23– 1.71 (overlapped m, 15H, $\text{CH}_2(\text{CH}_2)_3\text{NH-Boc}$, $\text{CH}_2(\text{CH}_2)_2\text{NH-Boc}$, $\text{CH}_2(\text{CH}_2)_1\text{NH-Boc}$ 3 $\text{CH}_3(\text{Boc})$ (only for the Boc-protected **9**); (1.47-1.66 $\text{CH}_2\text{-CH}_2\text{-NHCO-CH}_2\text{-N}_3$, $\text{CH}_2\text{-(CH}_2)_3\text{-NHCO-CH}_2\text{-N}_3$), 1.22 – 1.38 $\text{CH}_2\text{-(CH}_2)_2\text{-NHCO-CH}_2\text{-N}_3$) ppm.

1.1.4 Copper mediated azide-alkyne cycloaddition **12** and **13** (DR5TP-dextran-cadaverine)

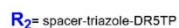
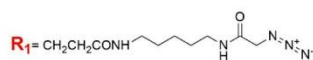
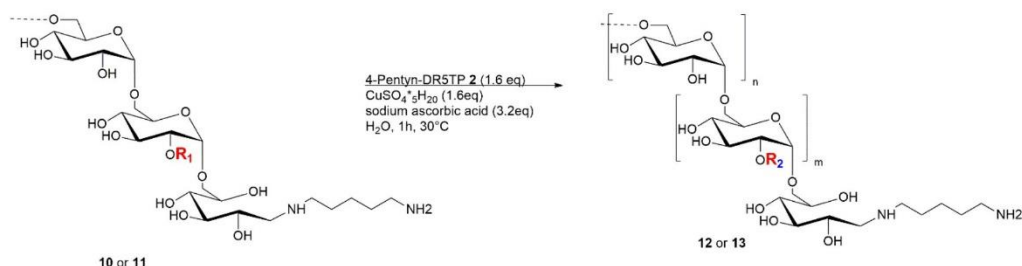


Figure S6. Synthesis of DR5TP-dextran-cadaverine **12** and **13**.

$m = 4.8$ mg (69.5 %, 2 mg approach) **12**; 24.7 mg (93.5 %, 20 mg approach) **13**.

Quantitative ligand conjugation was observed for compound **12** (Figure S7 and S8). For compound **13** no quantitative coupling of ligand **1** was observed (Figure S9 and S10) as a minor band corresponding to N_3 -group was visible in the IR spectra (Figure S10). As comparison a construct bearing only one N_3 -group at the reducing end is shown in Figure S11. A repetitive synthesis did not lead to a further enhancement of coupling.

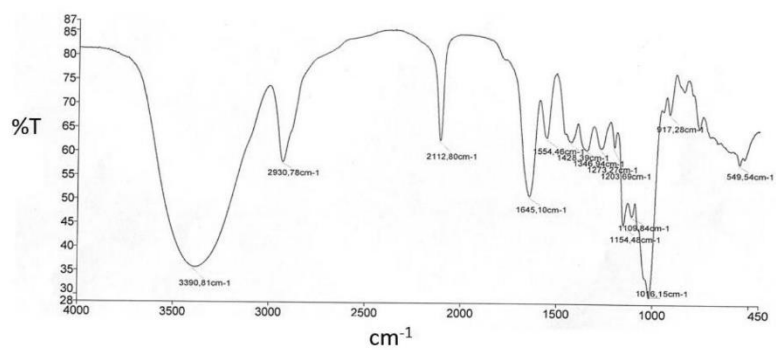


Figure S7. IR spectra of N₃-dextran cadaverine **10** (11 N₃/dextran).

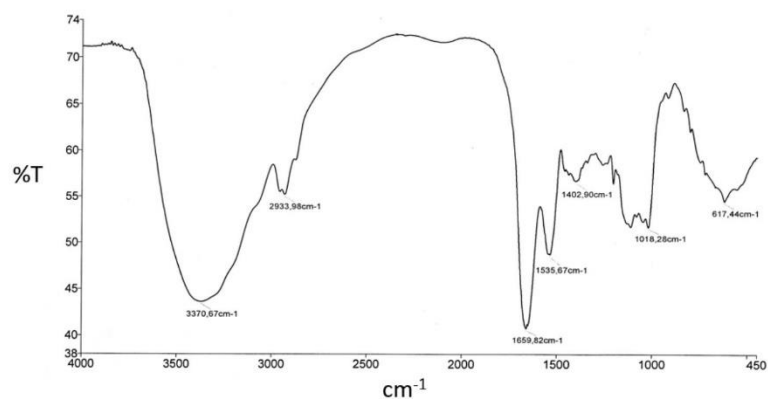


Figure S8. IR spectra DR5TP-dextran-cadaverine **12** (11 DR5TP/dextran).

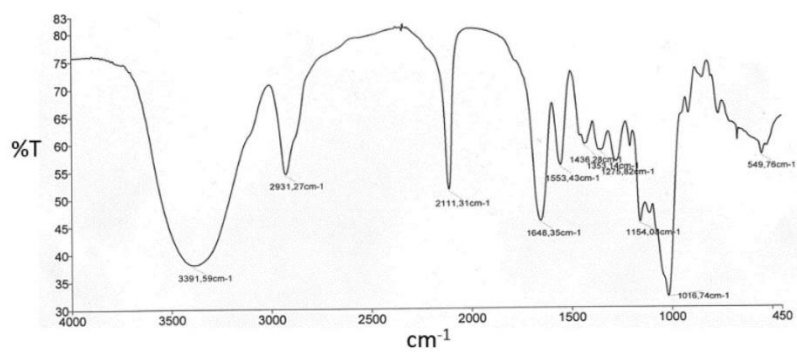


Figure S9. IR spectra of N₃-dextran cadaverine **11** (16.5 N₃/dextran).

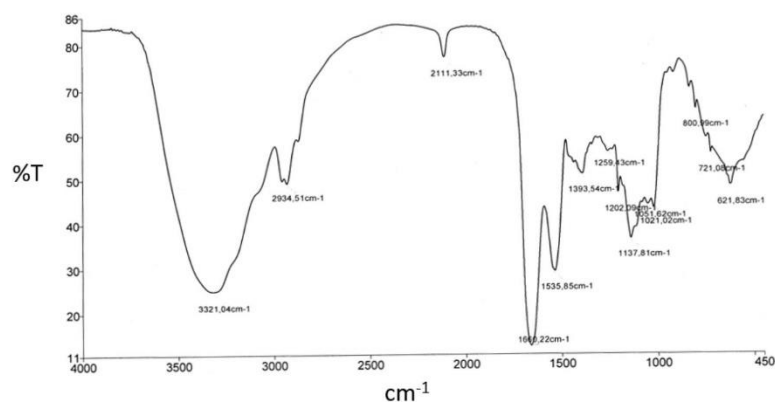


Figure S10. IR spectra DR5TP-dextran-cadaverine **13** (13.4 DR5TP/dextran).

Photometric analysis at 280 nm of DR5TP-dextran-cadaverine **12** and **13** in a concentration of 5 μM revealed 11.2 DR5TP per dextran for **12** and 13.4 DR5TP per dextran for conjugate **13**. Hereby, the calculated molar extinction coefficient was calculated from absorption of tryptophan, tyrosine and cysteine (here as cystine) in the peptide chains at 280 nm following Walker.^[2] An extinction coefficient of 5625 $\text{cm}^{-1} \text{M}^{-1}$ was calculated. The measured absorption of compound **12** and **13** are depicted in table 1. The ratio of DR5TP per dextran was calculated using formula 1 (with ϵ = molar extinction coefficient, d = layer thickness, $c_{\text{applied}} = 5 \mu\text{M}$)

$$\frac{\text{DR5TP}}{\text{dextran}} = \frac{\left(\frac{\text{Absorption}}{\epsilon \cdot d}\right)}{c_{\text{applied}}} \quad (1)$$

Table 1. Determination of the number of DR5TP per Dextran for compound **12** and **13**.

Compound	Absorption	Concentration _{theoretical} [μM]	Concentration _{measured} [μM]	DR5TP/dextran
12	0.315	5	56.00	11.20
13	0.376	5	56.97	13.37

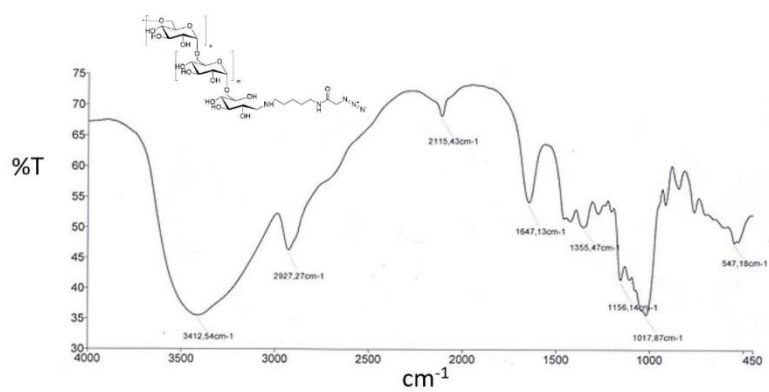


Figure S11. IR spectra of a mono N₃-substituted compound as comparison.

1.1.5 Transglutaminase catalyzed Fc conjugation and copper mediated azide-alkyne cycloaddition (Fc-dextran-N₃)

Conjugation was performed as described recently (Figure S12).^[1b]

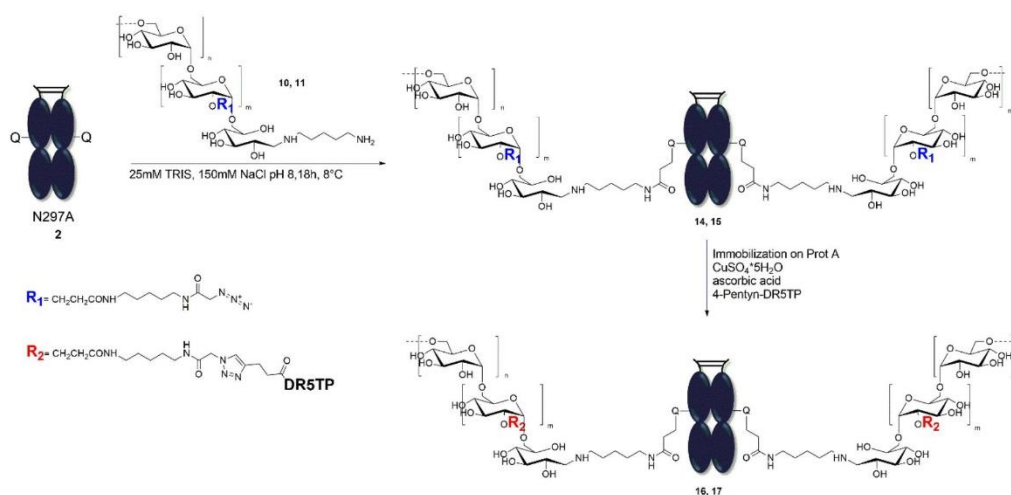


Figure S12. Transglutaminase catalysed conjugation of azide modified-dextran -cadaverine **10** or **11** to Fc(N297A) **2** generating **14** and **15** followed by copper mediated azide-alkyne cycloaddition giving compound **16** and **17**.

Interestingly, no visible reduction of size of the Fc-fragment was observed under reducing conditions in SDS-PAGE, presumably due to the formation of covalent bond between the lysines of the hinge region of Fc-fragment **2** and one of its multiple glutamines upon incubation with mTG (Figure S13). The same phenomenon was detected for the conjugation of azide-dextran-cadaverine **10** or **11** to **2** generating **14** and **15** (Figure S14). Additionally, The SDS PAGE analysis of DR5TP-dextran-cadaverine **12** revealed a smear over the whole lane, even though 11 DR5TP ligands are present in this compound, demonstrating that dextran scaffold does not behave as a protein of the same size in SDS PAGE.

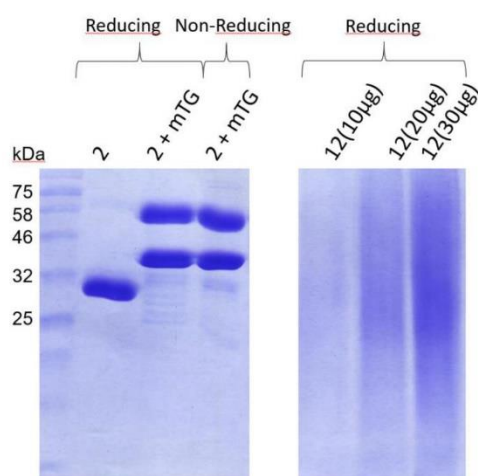


Figure S13. Left. Reducing SDS-PAGE of Fc(N297A) **2**, and reducing and non-reducing of FC(N297A) **2** after addition of mTG and incubation over-night (mTG 39 kDa; Fc 53.2 kDa), **Right.** Reducing SDS-PAGE of DR5TP-dextran-cadaverine (11.5DR5TP per dextran)

SDS-PAGE analysis of compounds **14** and **15** revealed, that at least 1 dextran was conjugated to the Fc(N297A) **2** as the band corresponding to native Fc(N297A) **2** nearly vanished in the lane corresponding to Fc-dex-N₃(11) **14** and Fc-dex-N₃(16.5) **15** (Figure S14). As expected a smeary band was found for the Fc(N297A)-dextran conjugates **14** and **15**,^[1b] that as expected further expanded when DR5TP **1** was coupled (Figure S14, lane 2 and 5). Copper-“click” of **1** to **14** showed an expected increase of the smeary part of the band as the size of the conjugate increased.

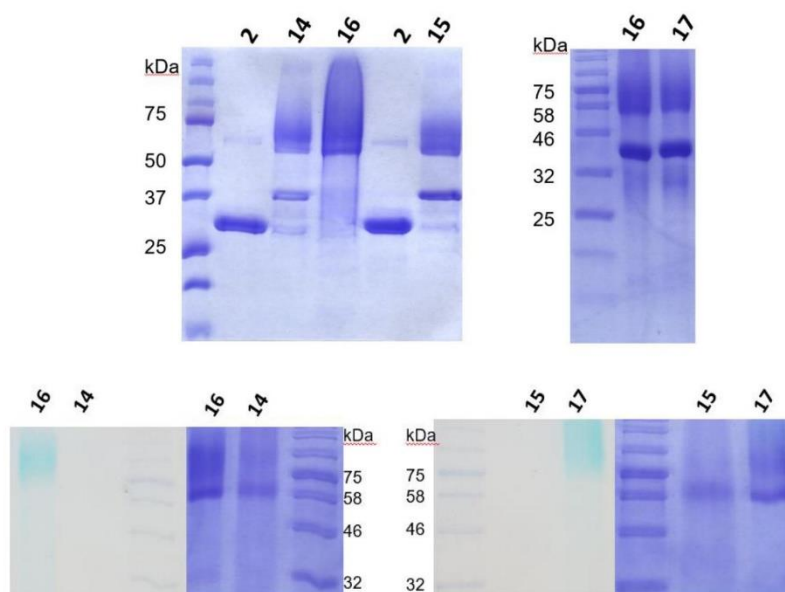


Figure S14. Top. Exemplary SDS-PAGE of Fc(N297A) **2**, Fc-dex-N₃(11) **14**, Fc-dex-N₃(16.5) **15**, Fc-dex-DR5TP(11) **16** and Fc-dex-DR5TP(13.4) **17**. **Bottom.** SDS PAGE of compound **14** – **17** after incubation with DBCO-Cy5 (mTG 39 kDa; Fc 53.2 kDa).

1.1.6 Thermal shift assay

Thermal shift assays were performed in triplicates on a BioRad96CFX RT-PCR detection system with 0.5 °C/30 s to 99 °C (Figure S15). All reactions were performed in 1 × PBS pH 7.4 at a concentration of 0.1 mg·ml⁻¹ protein and upon addition of SYPRO Orange (diluted 1:800). For comparison of stability melting curves of Fc(N297A) **2** and Fc-dextran-DR5TP **15** (11 DR5TP/dextran) were measured. As expected, equal melting curves for **2** and **15** were observed.

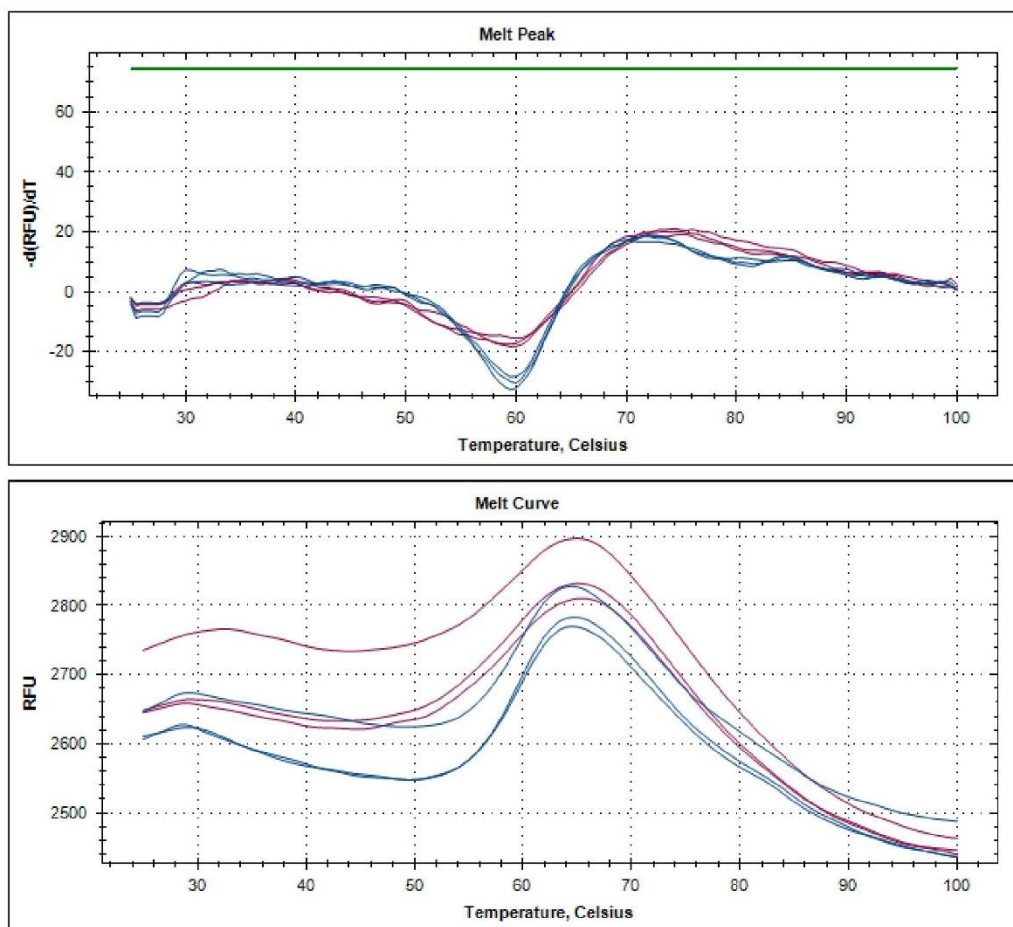


Figure S15. Thermal shift assays of Fc(N978) **2** (blue), and Fc-dextran-DR5TP conjugates **15** (red) (triplicates).

1.1.7 Cell viability assay

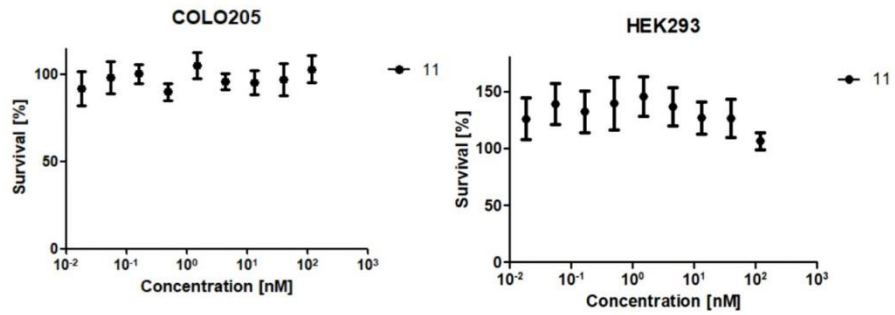


Figure S16. Cell viability assay of DR5-positive cell line COLO205 and DR5-negative cell line HEK293 of construct 11.

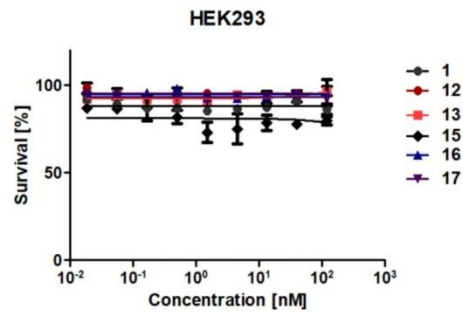


Figure S17. Cell viability assay on DR5-negative cell line HEK293.

1.1.8 Certificate of analysis for dextran

Certificate of Analysis

Product Name: DEXTRAN LEUCONOSTOC MESENTEROIDES
average mol wt 9,000-11,000
Product Number: D9260
Batch Number: BCBD9965V
Brand: Sigma
CAS Number: 9004-54-0
Formula:
Formula Weight:
Storage Temperature: 2-8 C
Quality Release Date: 09 FEB 2011
Date retested: 07 SEP 2018
Recommended Retest Date: AUG 2021

TEST	SPECIFICATION	RESULT
APPEARANCE (COLOR)	WHITE TO OFF WHITE	WHITE
APPEARANCE (FORM)	POWDER	POWDER
MOLECULAR WEIGHT DETERMINATION	9000 - 11000	10480
SOLUBILITY (COLOR)	COLORLESS TO FAINT YELLOW	COLORLESS
SOLUBILITY (TURBIDITY)	CLEAR TO VERY SLIGHTLY HAZY	CLEAR
SOLUBILITY (METHOD)	0.1G/ML WATER	0.1G/ML WATER
INFRARED SPECTRUM	CONFORMS TO STRUCTURE	CONFORMS

Figure S18. Certificate of analysis of dextran from *Leuconstoc mesenteroides* (average Mol. Wt. 9000-11000), obtained from the supplier.

References

- [1] a) M. Richter, A. Chakrabarti, I. R. Ruttekolk, B. Wiesner, M. Beyermann, R. Brock, J. Rademann, *Chem. Eur. J.* **2012**, *18*, 16708-16715; b) H. Schneider, L. Deweid, T. Pirzer, D. Yanakieva, S. Englert, B. Becker, O. Avrutina, H. Kolmar, *ChemistryOpen* **2019**, *8*, 354-357.
- [2] J. M. Walker, *The proteomics protocols handbook*, Springer, **2005**.

4.3. Recent Progress in Transglutaminase-mediated Assembly of Antibody-Drug Conjugates.

Title:

Recent Progress in Transglutaminase-mediated Assembly of Antibody-Drug Conjugates.

Authors:

H. Schneider*, L. Deweid*, O. Avrutina and H. Kolmar

*These authors contributed equally to this work

Bibliographic data:

Analytical Biochemistry

Volume 595, 113615

Article first published online: 5th Feb 2020

DOI: <https://doi.org/10.1016/j.ab.2020.113615>

Copyright © 2020 Elsevier Inc. All rights reserved. Reproduced with permission.

Contributions by Hendrik Schneider:

- Initial idea and literature research together with L. Deweid
- Preparation of the manuscript and included graphical material together with L. Deweid



Recent progress in transglutaminase-mediated assembly of antibody-drug conjugates

Hendrik Schneider¹, Lukas Deweid¹, Olga Avrutina, Harald Kolmar*

Institute for Organic Chemistry and Biochemistry, Technische Universität Darmstadt, Alarich-Weiss-Straße 4, D-64287, Darmstadt, Germany



ARTICLE INFO

Keywords:

Transglutaminase
Bioconjugation
Protein labeling
Antibody-drug conjugates
Site-specific conjugation
Antibodies

ABSTRACT

Antibody-drug conjugates (ADCs) are hybrid molecules intended to overcome the drawbacks of conventional small molecule chemotherapy and therapeutic antibodies by merging beneficial characteristics of both molecule classes to develop more efficient and patient-friendly options for cancer treatment. During the last decades a versatile bioconjugation toolbox that comprises numerous chemical and enzymatic technologies have been developed to covalently attach a cytotoxic cargo to a tumor-targeting antibody. Microbial transglutaminase (mTG) that catalyzes isopeptide bond formation between proteinaceous or peptidic glutamines and lysines, provides many favorable properties that are beneficial for the manufacturing of these conjugates. However, to efficiently utilize the enzyme for the constructions of ADCs, different drawbacks had to be overcome that originate from the enzyme's insufficiently understood substrate specificity. Within this review, pioneering methodologies, recent achievements and remaining limitations of mTG-assisted assembly of ADCs will be highlighted.

1. Introduction

Despite obvious scientific and therapeutic progress, treatment of cancer is still a major challenge. Indeed, malignant tumors represent the second leading cause of death in the United States with over 1.7 million new cases and 600,000 cancer-related deaths predicted for 2019, which corresponds to nearly 1,700 deaths per day [1]. In the twentieth century, chemotherapy alone or in combination with radiotherapy was the predominant approach for tumor treatment [2–4]. For decades, every effort was exerted by oncologists to develop chemotherapeutics with enhanced anticancer efficacy, which do not affect healthy tissues [4,5]. The combination of different anticancer agents possessing diverse modes of action and toxicity profiles led to synergistic effects that positively influenced anti-tumor activity [2,5,6]. Thus, multidrug treatment became a standard therapy to fight most tumor types [2,4]. Further, highly potent cytotoxins, e.g. tubulin inhibitors (dolastatin 10, dolastatin 15, maytansine, cryptophycins), DNA alkylators (pyrrolobenzodiazepine, CC-1065, adozelesin) were employed as chemotherapeutics [2,5]. However, their clinical efficacy was rather limited due to the lack of a sufficient therapeutic window, conditioned by the inability to kill tumor cells without causing systemic toxicity to the healthy ones [2,5].

In addition to commonly known chemotherapeutic approaches,

numerous therapeutic antibodies have been developed that act as tailor-made drugs to specifically address tumor-associated antigens. Upon intravenous administration, these engineered macromolecules accumulate at the tumor and activate the patient's immune defense to neutralize the degenerated cells [7]. The impressive number of FDA-approved therapeutic antibodies highlights the success of this class of drugs [8]. Though their potency has been demonstrated in hundreds of clinical trials, full cancer remission through antibody treatment is challenging as antibodies often possess limited anti-tumor activity [2,9]. To address this issue, combination of the cytotoxic potency of small-molecule cytotoxins and the remarkable targeting properties of an antibody yielded a novel class of tumor therapeutics referred to as antibody-drug conjugates (ADCs). In these constructs, a monoclonal antibody is equipped with a potent antitumor toxin via a cleavable or non-cleavable covalent linker. After entering the tumor tissue from the vasculature, the antibody part of the ADC is capable of recognizing and binding specifically to the target antigen overexpressed on the cell surface. Following internalization through the endosome-lysosome pathway either the linker is cleaved and/or the antibody is degraded to release the payload, which then diffuses into the cytoplasm to interact with its target: e.g. tubulin, DNA (Fig. 1) [5].

This strategy was envisioned to overcome the shortcomings of both conjugation partners, e.g. the small therapeutic window of the highly

* Corresponding author.

E-mail address: Kolmar@Biochemie-TUD.de (H. Kolmar).

¹ These authors contributed equally to this work.

<https://doi.org/10.1016/j.ab.2020.113615>

Received 29 October 2019; Received in revised form 17 January 2020; Accepted 4 February 2020

Available online 05 February 2020

0003-2697/ © 2020 Elsevier Inc. All rights reserved.

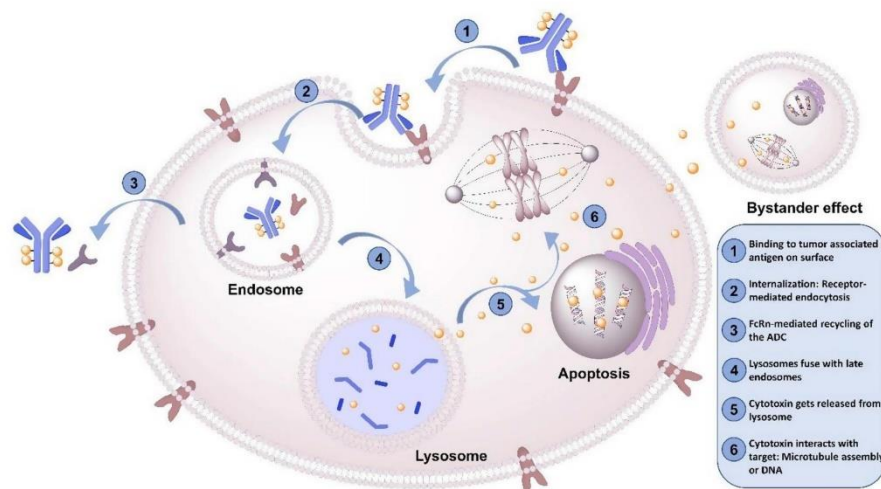


Fig. 1. Mechanism of action of antibody-drug conjugates: ADC are internalized through receptor-mediated endocytosis.

toxic payload and the rather low efficacy of antitumor antibodies, possibly resulting in synergistic benefits [9]. Recently, different ADCs have reached the market, namely brentuximab vedotin (Adcetris®) [10,11] from Seattle Genetics, gemtuzumab ozogamicin (Mylotarg®) [12,13] and inotuzumab ozogamicin (Besponsa®) [14,15] from Pfizer, as well as ado-trastuzumab emtansin (Kadcyla®) [16,17] from Roche, all targeting hematologic malignancies or solid tumors [5,18]. Furthermore, more than 60 ADCs are in clinical trials [19]. In most of them, the cytotoxic payload is either an antimetabolic microtubule inhibitor (auristatin [20] or maytansine derivatives [21]) or a DNA-damaging agent (pyrrolbenzodiazepine dimers [22], duocarmycin [23], calicheamicin [24], indolino benzodiazepine dimers [25]), which alkylates, crosslinks, or breaks the DNA double strands [5].

Most ADCs that are currently in clinical trials or are marketed rely on the stoichiometrically controlled chemical conjugation of the toxin moiety to endogenous thiols exposed by reduction of interchain disulfides, or to primary amines in lysine side chains [4,5]. However, ADCs obtained by conventional conjugation yielded heterogeneous mixtures of products, representing several species with different pharmacokinetics [18]. Therefore, a drug-to-antibody ratio (DAR) in the range of 3.5–4.0 was chosen for most ADCs, aimed at minimizing the fraction of non-conjugated antibodies and also avoiding species with high DAR [5]. However, FDA-approved ADC Kadcyla®, for example, is assembled from HER2 (human epidermal growth factor receptor 2)-targeting monoclonal antibody trastuzumab that contains 88 lysine residues, from which 70 were shown to be accessible to conjugation with tubulin inhibitor DM1 [26]. As a consequence, despite maintaining the DAR at a

relatively low value, a vast spectrum of variants is generated due to random conjugation to different attachment sites that results in an increased heterogeneity, which is disadvantageous in terms of the pharmacokinetic profile of the drug [27]. To overcome these deficiencies, numerous site-specific conjugation methods have been introduced, and different studies demonstrated improved therapeutic indices (TI) of the resulting constructs compared to their statistically conjugated counterparts [28]. Addressable moieties for site-specific conjugation have been introduced upon glycoengineering [29–34], incorporation of additional cysteines (Thiomab®) [35–38], selenocysteines [39], and non-natural amino acids [40–42]. In addition, re-bridging of natural thiols [43,44], metalloproteinase-based catalysis [45], redox-based methionine bioconjugation [46] as well as auto-catalytic attachment of the toxin to a reactive antibody lysine were applied [47]. In addition, various enzyme-mediated approaches, among them tubulin tyrosine ligase (TTL) [27,48], formylglycine-generating enzyme (FGE) [49–51], SpyLigase [52], phosphopantetheinyl transferase [53], sortase A [54–56], and mushroom tyrosinase [57] as well as microbial transglutaminase [58] were successfully utilized for the generation of site-specific ADCs.

Transglutaminases belong to a class of protein γ -glutamyl-transferases found in microorganisms, plants, invertebrates, amphibians, fish, and birds [59]. These bond-forming enzymes catalyze the attachment of primary amines to γ -carboxamides via release of ammonia, whereof both counterparts could be located in either a protein or a peptide [59]. In nature, transamidation occurs between the glutamine side chain as acyl donor and the ϵ -amino group of lysine as acyl acceptor, generating either intramolecularly cross-linked proteins or

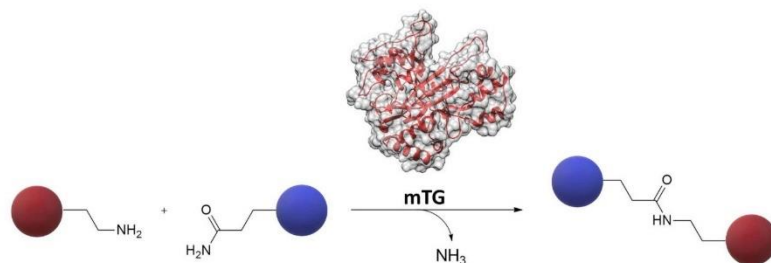


Fig. 2. Reaction catalyzed by mTG. Protein- or peptide-bound glutamine side-chains are covalently crosslinked to lysine residues or primary amines. An isopeptide bond is formed under the release of ammonia.

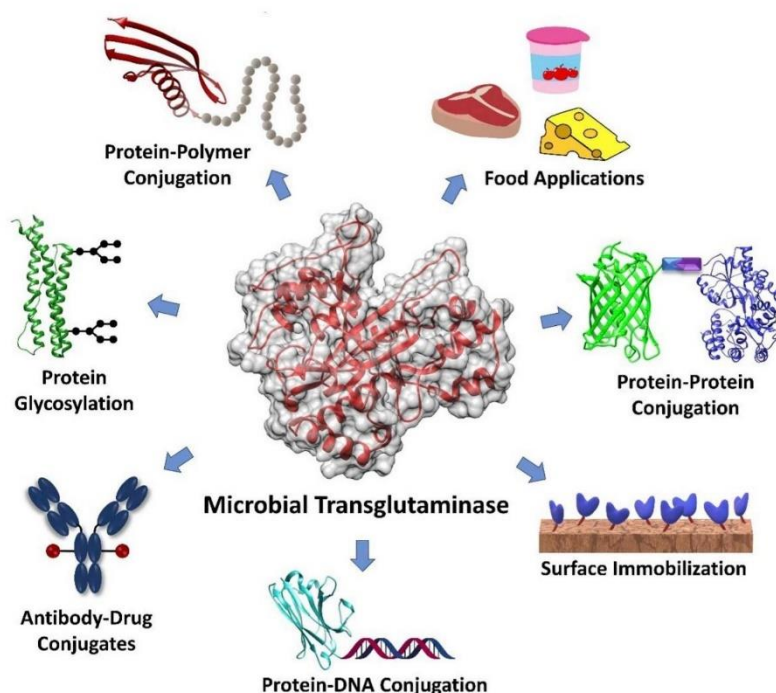


Fig. 3. Overview of biotechnological and industrial applications of microbial transglutaminase.

intermolecular isopeptide linkages (Fig. 2) [59,60]. While transglutaminases possess a certain specificity towards glutamine residues, their promiscuity regarding amine-containing acyl-acceptors provides room for modifications [61].

The demand for homogeneity of ADCs for cancer treatment has put site-specific transglutaminase-catalyzed conjugation with cytotoxic payloads into the focus of research. This review will highlight recent achievements in the field of transglutaminase-mediated antibody modification and discuss the limitations of different strategies as well as unsolved challenges that need to be addressed in future work.

Despite the fact that transglutaminases are widely distributed in multiple phylogenetic species, not all of them are suitable for biotechnological applications [62]. mTG derived from the Gram-positive actinobacterium *Streptomyces mobaraensis* has emerged as the most employed transglutaminase for industrial purposes due to its high stability and pH tolerance combined with an excellent activity [62]. The enzyme is intensively used for food processing in order to texture meat and dairy products (Fig. 3). Its remarkable properties made it a versatile tool for the posttranslational modification of various proteins [62]. PEGylation of small proteinaceous drugs to elevate their half-life *in vivo*, immobilization of aggregation-prone biocatalysts to increase their overall stability or the covalent attachment of nucleic acids to proteins to combine the beneficial properties of both biomolecules, are only a few examples of the diverse applications of the enzyme (Fig. 3) [60].

The following paragraphs will introduce key methodologies that allow for the mTG-mediated modification of antibodies. Based on each of the three strategies, multiple studies that demonstrate recent achievements will be described. Moreover, their advantages and disadvantages will be compared and general remaining limitations of the mTG-technology will be discussed to provide a comprehensive overview to the reader.

2. ADCs generated from deglycosylated and aglycosylated antibodies

At the beginning of the 21st century, Josten and colleagues were the first to report on the conjugation of a monoclonal IgG antibody mediated by microbial transglutaminase [63]. They used amine derivatives of biotin to label an anti-2,4-dichlorophenoxyacetic acid (2-4D) antibody with up to 1.9 biotin moieties per antibody and demonstrated by ELISA that enzymatic modification did not interfere with the target-binding properties of the immunoglobulin. However, further studies did not confirm these results [58]. In 2008, researchers of the Schibli group investigated the reactivity of mTG at intrinsic lysine and glutamine sites of different antibodies [64]. Their studies showed only minor modification of lysine residues with glutamine-containing peptides with an average antibody/label ratio of 0.3–0.5. Almost no labeling of native anti-L1Cam antibody chCE7 and a bovine IgG was observed when glutamine sites were addressed (antibody/label ratio: 0.1) with a fluorophore equipped with cadaverine. Interestingly, a significantly improved labelling was observed when a genetically aglycosylated variant of chCE7 (Asn297 replaced by Gln) was applied [64]. This phenomenon was studied in the following work and MALDI-TOF analysis proved that stoichiometric labelling of aglycosylated chCE7 in a ratio of 4:1 at positions Gln295 and Gln297 was achieved (see Table 1 for an overview of conjugation sites employed in mTG-assisted assembly of ADCs) [65]. Furthermore, enzymatic deglycosylation by PNGase F was applied to native chCE7 and commercially available anti-CD20 antibody rituximab, followed by mTG-promoted ligation of different acyl-acceptor substrates. Again, specific modification of the heavy chain at position Gln295 was confirmed by mass spectrometry and the authors concluded that an increased flexibility of the C/E loop (Q295–T299) of the antibodies Fc region upon deglycosylation renders glutamine residues within this loop amenable to mTG-mediated isopeptide formation [65]. These results gave access to a powerful

Table 1
Conjugation sites applied for mTG-generated ADCs.

Author	Year	Conjugation motif(s)	Native Glycosylation removal	Targeted antigen	Ref.
Steffen et al.	2017	HC C-terminal LLQGA, HC C-terminal GGGSYRQGGG	–	TSH	[89]
Dennler et al.	2014	Q295, Q297	PNGase F, N297Q	HER2/NEU	[66]
Lhospice et al.	2015	Q295, Q297	N297Q	CD30	[67]
Spidel et al.	2017	K447, engineered lysines	–	n.D.	[98]
Josten et al.	2000	Native lysines	–	2,4-D	[63]
Mindt et al.	2008	native Lysines(failed), Q295	N297Q	L1CAM	[64]
Jeger et al.	2010	Q295, Q297	PNGase F, N297Q	L1CAM	[65]
Grünberg et al.	2013	Q295, Q297	N297Q, N297A	L1CAM	[68]
Spycher et al.	2017	Q295, Q297, K288/290, K340	N297A, N297Q	CD30	[97]
Anami et al.	2017	Q295	N297A	HER2/NEU	[72]
Anami et al.	2018	Q295	N297A	HER2/NEU	[74]
Schneider et al.	2019	Q295	N297A	DR5	[96]
Schneider et al.	2019	HC C-terminal LLQG	–	HER2/NEU	[93]
Siegmund et al.	2016	GEN-, GEC-tag C-Terminus HC	–	EGFR/HER1	[52]
Ebenig et al.	2019	HC C-terminal (SPI7G) DIPIGQGMTG	–	HER2/NEU	[91]
Strop et al.	2013	12 sites (terminal or internal)	–	EGFR/HER1, HER2/NEU, TROP-2	[76]
Strop et al.	2015	LLQG inserted 135 HC, Q295, Q297, LC C-terminal GLLQGA, HC C-terminal LLQGA	–	Trop-2/M1S1	[28]
Strop et al.	2016	HC C-terminal LLQGA	–	Trop-2/M1S1	[83]
Wong et al.	2018	LC C-terminal GLLQGPP	N297Q, N297A	EGFR/HER1	[84]
Costa et al.	2019	LLQG inserted 135 HC, HC C-terminal LLQGA, LC C-terminal GLLQGPP, Q295, Q297	N297A, N297Q	CXCR4	[82]
DeVay et al.	2017	LC C-terminal GLLQGPP, Q295, Q297	N297Q	Trop-2/M1S1	[85]
Dorywalska et al.	2015	9 sites (terminal or internal)	N297A, N297Q	Trop-2/M1S1	[78]
Dorywalska et al.	2015	9 sites (terminal or internal)	N297A, N297Q	Trop-2/M1S1	[79]
Dorywalska et al.	2016	9 sites (terminal or internal)	N297A, N297Q	Trop-2/M1S1	[73]
Farias et al.	2013	LC C-terminal GLLQGA, HC C-terminal LLQGA	natural observed aglycosylated, N297A	Trop-2/M1S1	[77]
Ratnayake et al.	2018	LC C-terminal GLLQGA, Q295	–	HER2/NEU	[86]
Puthenvetil et al.	2016	Q295	PNGase F	HER2/NEU	[69]
Beck et al.	2019	Q295	PNGase F	DEC205/CD205/LY75	[71]
Thornlow et al.	2019	Q295	PNGase F	HER2/NEU	[70]

Abbreviations: 2,4-D, 2,4-dichlorophenoxyacetic; TSH, thyrotropin receptor; HER2/Neu, human epidermal growth factor receptor 2; CD30 cluster of differentiation 30; DR5, death receptor 5; CXCR4, chemokine receptor type 4; EGFR, epidermal growth factor receptor; Trop-2 also known as TACSTD2, Tumor-associated calcium signal transducer 2; CD205, cluster of differentiation 205; LY75, Lymphocyte antigen 75.

methodology for the mTG-assisted construction of homogeneous ADCs with a defined DAR and outlined a key technology for various follow-up studies (Fig. 4).

Dennler and colleagues reported a chemoenzymatic approach using deglycosylated HER2-targeting antibody trastuzumab yielding homogeneous ADC in a two-step procedure [66]. Thus, PNGase F treatment, followed by enzymatic conjugation of different chemical handles suitable for maleimide-thiol coupling or strain-promoted azide-alkyne cycloaddition (SPAAC) by mTG was conducted. Subsequent conjugation of monomethyl auristatin F (MMAF) via a protease-cleavable linker gave rise to potent homogeneous ADCs comprising DARs ranging from 1.8 to 2 (the different warheads, linker chemistries and click compounds applied for the construction of ADC under mTG catalysis are overviewed in Table 2). Within this study, the authors took advantage of the remarkable selectivity and kinetics of bioorthogonal conjugation by “click-chemistry” or thiol-maleimide coupling. Ready-to-use building blocks are available from commercial suppliers and can be applied for mTG catalysis at low cost. Subsequent installation of a pricey payload is achieved in a quantitative manner by adding only a slight excess of the respective molecule. Consequently, the authors achieved their DARs employing only a 2.5-fold excess of the corresponding toxin, which represents a major advantage in terms of cost-effective ADC manufacturing [66]. When employing a two-step chemoenzymatic approach, it should be considered that removal of non-coupled compounds is necessary to enable specific labelling of the desired target in the following reaction. Additional purification steps however, might diminish the yield of the overall process.

In 2015, Lhospice and co-workers further investigated the applicability of this approach and reported superior pharmacokinetic properties of an mTG generated drug conjugate of the anti-CD30 antibody

brentuximab in rodent lymphoma models compared to state-of-the-art ADC Adcetris® [67]. A genetically mutated version of brentuximab (N297Q) comprising two distinct addressable glutamines (Q295 and Q297) was functionalized with derivatives of monomethyl auristatin E (MMAE) under mTG catalysis. Employing different linker chemistries, four different ADCs were assembled by either direct enzymatic coupling of the warhead or in a two-step approach using SPAAC. Biodistribution experiments in mice revealed better tumor uptake and lower non-targeted liver and spleen uptake of the chemo-enzymatically conjugated ADC compared to Adcetris®. Moreover, pharmacokinetic studies in rats demonstrated an elevated maximal tolerated dose and decelerated clearance of the homogeneously labeled ADCs. The authors attribute these observations to the absence of species with DAR > 4, which suffer from faster catabolism and reduced binding to Fcγ receptors (FcγRs) and surface mannose receptors [67].

In further research, Grünberg and co-workers applied different aglycosylated variants of anti-L1CAM antibody chCE7 and the chelator 1,4,7,10-tetraazacyclododecane-1,4,7,10-tetraacetic acid (DOTA) for the generation of radioimmunoconjugates (RIC) [68]. Decalysines bearing 1, 3 or 5 DOTA pendants were site-specifically conjugated to each heavy chain of the genetically aglycosylated antibodies (N297D, N297Q) by mTG catalysis to generate uniform conjugates with high DOTA loading. Moreover, preferred biodistribution compared to heterogeneous, chemically modified constructs was demonstrated in mice bearing ovarian tumor xenografts. Interestingly, aglycosylated antibody chCE7agl (N297Q) with two accessible glutamines was conjugated with only one DOTA-polylysine per heavy chain as conjugation occurred at two lysine residues of the same polylysine chain simultaneously. The site-specific RIC generated by mTG catalysis with the highest DOTA/antibody ratio revealed the best tumor-to-liver ratios. Based on their

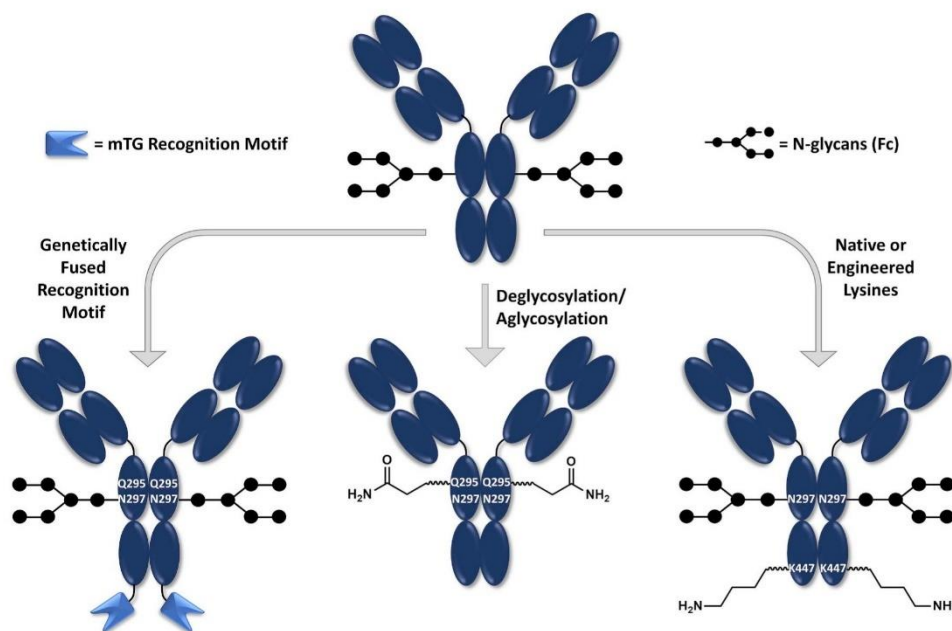


Fig. 4. Harnessing transglutaminase activity for site-specific ADC generation. (top) Native, fully glycosylated antibodies are no substrate for mTG. The following strategies allow for its transamidation: (left) genetic incorporation of specific peptidyl linker sequences; (middle) genetic or enzymatic truncation of the CH2 glycan moiety to expose Gln295; (right) engineering of reactive lysines or additional C-terminal residues to prevent Lys447 from intracellular processing.

results, the authors hypothesized that other properties - polarity, pI of the immunoconjugate, but not the antibody-to-ligand ratio alone - stipulate its biodistribution [68].

As outlined above, removal of the CH2 polysaccharide moiety makes Gln295 accessible for mTG-mediated modification. This straightforward strategy was further adopted by different research groups. Thus, Puthenveetil and co-workers reported a site-specific conjugation strategy for dual antibody labeling on solid support based on the above-mentioned chemoenzymatic procedure [69]. An engineered variant of trastuzumab (KK183c) bearing an additional cysteine in the light chain was deglycosylated using PNGase F and captured on solid support via binding to immobilized protein A. Subsequent mTG-catalyzed conjugation of NH₂-PEG₂-bicyclo[6.1.0]nonyne (NH₂-PEG₂-BCN), reduction and mild reoxidation generated an antibody bearing two orthogonal reaction handles, namely a strained alkyne (BCN) at each heavy and a thiol at each light chain. Subsequent labeling of these moieties with different fluorophores gave rise to a dual-labeled antibody, confirmed by in-gel fluorescence of a reduced antibody-fluorophore conjugate [69]. This procedure paves the way for the high-throughput generation of site-specific ADCs on solid support, utilizing mTG-mediated conjugation in a two-step procedure.

Recently, a chemoenzymatic strategy for the one-pot dual labeling of antibodies that relies on the orthogonal reactivities of microbial transglutaminase and lipoic acid ligase (LplA) was envisioned [70]. LplA is capable of ligating different derivatives of valeric acid site-specifically to a lysine residue within the 13 amino acids long amino acid motif GFEIDKVWYDLDA (LAP-tag). In the first place, a LAP-tag was engineered to the C-terminus of the heavy and light chains of trastuzumab and picolyl-azide (pAz) or trans-cyclooctene (TCO) substrates were attached under LplA-catalyzed. Light chain (LC) modification proceeded with 86% with pAz and 88% with TCO while modification of the heavy chain (HC) proceeded with 82% with pAz and 69% with TCO, respectively. Following “click”-reactions using either dibenzocyclooctyne-amine (DBCO)- or methyl-tetrazine (MeTz)-

modified PEG5000 resulted in a significant shift to higher masses of the corresponding protein band in SDS-PAGE analysis. Further, a dual-labelling approach for spatially controlled cargo release in the tumor environment was investigated. TCO-modified valeric acid was conjugated to the engineered LAP-tag by LplA and NH₂-PEG₃-N₃ to Q295 of PNGase F-deglycosylated trastuzumab by mTG. The two different click chemistry handles were subsequently modified with MeTz-PEG₄-Valine-Citrulline(VC)-PAB-PEG₂-fluorescein and DBCO-PEG₄-PVGLIG-PEG₂-Rhodamine to yield dual labeled antibodies. The peptidic sequences PVGLIG and VC allowed for the controlled payload release in SK-BR-3 breast cancer cells mediated by extracellularly overexpressed matrix metalloproteinase II (MMP-2) and intracellular lysosomal cysteine protease cathepsin B (CatB), as demonstrated by *in vitro* cleavage assays and confocal laser scanning microscopy [70].

In a proof-of-concept study, researchers of the Zentel group used mTG-mediated conjugation combined with SPAAC to attach anti-DEC205 antibodies, specific for dendritic immune cells, to an azide-modified block copolymer P(Lys)-*b*-P(HPMA) aimed at the delivery of tumor antigen-encoding plasmid DNA (pDNA) to dendritic cells for the generation of pDNA vaccines [71]. After PNGase F-mediated deglycosylation, a DBCO reaction handle bearing an ϵ -amino group of lysine was introduced to Q295 of DEC205 antibody by mTG catalysis. Subsequent reaction of DEC205 with a polyplex consisting of pDNA and a stochastically azide-modified P(Lys)-*b*-P(HPMA) led to successful conjugation. It should be mentioned that a large excess of DEC205-DBCO was crucial for conjugation, presumably due to the low diffusivity of two macromolecular reaction partners and the low DBCO-loading of the DEC205-DBCO compound (1–2) [71].

In 2017, researchers of the Tsuchikama group employed branched PEG linkers to attach multiple payloads to antibodies [72]. Different formats of these linkers, containing one primary amine and two azide moieties for SPAAC, were synthesized and enzymatically conjugated to Q295 (N297A) or Q295 and Q297 (N297Q) of a mutated non-glycosylated HER2-targeting antibody, respectively. A comparison of

Table 2
Cytotoxic payloads and linkers published for ADCs generated via mTG.

Mode of Action	Applied Toxins	References
DNA intercalator	NPBIDs: SW163D Luzopectin A Sandramycin	[86]
Tubulin Inhibitor	MMAD MMAE MMAF Aur0131 Aur0101 Aur337 Auristatin F PF-06380101	[28,73,76–79,85] [66,67,91,93] [72,74] [82] [73,78,79,82] [79] [98] [83,84]
Acyl donor side	Chemistry	References
PEGylated		[28,63,66–70,72,74,76,77,79,82,85,91]
Non-PEGylated		[63,65–67,71,73,76,78,82–84,86,93,96]
Applied Linker	Chemistry	References
stable		[28,76,77,79,82,85]
cleavable	Cathepsin B (X)VC-PABC MMP-2 PVGLIG	[66,67,72–74,76,78,82–84,86,91,93,96] [70]
Chemoenzymatic Mechanism	Reaction handles	References
SPAAC Michael-Addition	N ₃ ; BCN; DBCO thiol; Maleimide	[66,67,69–72,74,91,93,96] [66]

Abbreviations: BCN, Bicyclononyne; DBCO, dibenzocyclooctyne; MMAD/E/F, monomethyl auristatin D/E/F; MMP-2, matrix metallo-proteinase II; NPBIDs, Natural Product Bis-Intercalator Depsipeptides; PABC, *p*-amino-benzyloxy-carbonyl; PEG, polyethyleneglycol; VC, valine-citrulline; XVC, different R-groups on C2 position of valine-citrulline linker.

cleavable linear and branched linkers was conducted. Förster resonance energy transfer (FRET) assays for cathepsin-mediated cleavage were exploited for different linear and branched spacers. A branched, PEG-containing linker revealed a release rate comparable to a linear reference, while negligible release was observed for the branched, non-PEG bearing counterpart. For the construction of an ADC, a chemoenzymatic approach based on mTG-catalyzed linker conjugation and SPAAC for payload equipment was applied. As payload, the relatively hydrophilic tubulin inhibitor MMAF was utilized generating homogeneous ADCs with an average DAR of 3.9 (N297A) and 7.4 (N297Q), respectively. The target-binding properties of these homogeneous ADCs were not affected and enhanced *in vitro* cytotoxicity on HER2-expressing breast cancer cell lines was shown for the DAR 3.9 (N297A) in comparison to its linear DAR 1.9 counterpart [72]. This approach opens avenues for the generation of homogeneous high-DAR ADCs. Interestingly, the potency of the DAR 7.4 ADC has not been demonstrated yet and, according to the authors, further investigations are currently ongoing. The fine-tuning of their hydrophilic branched linkers is a crucial step for further conjugation of more hydrophobic payloads e.g. MMAE, as high-DAR ADCs containing hydrophobic payloads suffer from protein aggregation and rapid clearance [72].

Branched PEG linkers were further applied to discover cathepsin cleavable linkers with enhanced stability in mouse plasma aimed at improving efficacy and accuracy in mouse models (see also work of Dorywalska et al. [73] below) [74]. Different hydrophilic amino acids were introduced at the N-terminus of conventional L-valyl-L-citrulline dipeptide linker (VC), as modification of this position is known to affect

its plasma stability [73]. Addition of glutamic acid to the linker sequence (EVC-PABC) inhibited hydrolysis catalyzed by murine carboxylesterase 1c (Ces1c), which is reported for VC-PABC linkers applied in commonly used cleavable ADCs [73]. Furthermore, faster cathepsin-mediated cleavage as well as enhanced hydrophilicity was observed for the EVC-PABC bearing DAR 3.9 ADCs [74].

As collectively described above, the utility of de- or aglycosylated antibodies providing Gln295 as a suitable site for transamidation was consistently reported by various groups. Nevertheless, the contribution of the glycan moiety to the antibody's stability should also be considered. Lhospice et al. demonstrated that ADCs assembled from aglycosylated cAC10Q antibody remained stable for at least one week in human, cynomolgus monkey and rat serum [67]. Interestingly, constructs with longer linker moieties suffered from premature drug loss upon incubation in mouse plasma [67]. Though stability of their anti-CD30 ADCs was clearly proven, careful case-to-case evaluation is necessary since some studies reported aglycosylated antibodies to be more sensitive to heat and prone to aggregation [75].

3. ADCs by generated applying engineered mTG recognition motifs

Besides truncation of the antibody's native glycosylation pattern, incorporation of specific recognition tags is a common strategy to achieve efficient modification by mTG (Fig. 4). One major benefit of this approach is the high flexibility in comparison to other conjugation enzymes. While the reactivity of conventional catalysts like Sortase A is

limited to terminal sites, mTG also recognizes internal positions [76]. In 2013, Strop and co-workers took advantage of this capability and introduced a novel "glutamine tag" for transglutaminase-mediated conjugation that can be engineered at desired positions within the antibody [76]. This pioneering approach not only resulted in highly homogeneous and reproducible ADCs but also allowed investigating the role of conjugation-site, linker and payload to optimize the drug's TI. Their engineered recognition sequence LLQG was introduced at approximately 90 surface-exposed sites of an epidermal growth factor receptor (EGFR)-targeting IgG1 antibody and screened for efficient conjugation. Twelve of the investigated positions revealed suitable biophysical properties combined with a high degree of payload loading. Further, these results were confirmed using an anti-M1S1 antibody (C16), an anti-HER2 antibody and other IgG subtypes. mTG conjugation of different amine-bearing payloads, e.g. cadaverine-Alexa488 or AcLys-VC-MMAD (monomethyl auristatin D) led to DARs between 1.2 and 2.0, depending on the utilized conjugation site. Two distinct conjugation sites (C16 HC: C-terminal lysine replaced by LLQGA tag and C16 LC: GLLQGA after C-terminal cysteine) were further examined; DARs approaching quantitative conjugation (1.9 and 1.8, respectively) were gained. Both generated ADCs were found to be highly potent *in vitro* on different M1S1-positive cell lines as well as *in vivo* upon single-dose intravenous administration in mice implanted with M1S1-positive BxPC3 pancreatic cancer cells. Interestingly, results comparable to those of a cysteine conjugate (DAR 3.6) were obtained. Moreover, these rodent models revealed that the choice of conjugation site strongly influenced the pharmacokinetic properties of an ADC. While C16-LC-AcLys-VC-MMAD remained stable in mice and rats, C16-HC-AcLys-VC-MMAD significantly suffered from premature drug loss in circulation of Sprague Dawley rats [76].

In 2015, the same group investigated the impact of site-specific and homogeneous payload attachment on the TI of ADCs with high DARs [28]. To that end, ADCs with a DAR of 2, 4, 6 or 8 were generated by site-specific conjugation of a non-cleavable MMAD on anti-M1S1 antibody C16 via mTG (N297Q, LLQG inserted at position 135 HC, LC C-terminus GLLQGA; HC C-terminus LLQGA) and compared to cysteine-maleimide conjugates possessing comparable toxin loading (DAR4-8). *In vitro* experiments showed no significant difference in potency on BxPC3 (M1S1 + + +) and Colo205 (M1S1 +) cells between site-specific and conventional maleimide-cysteine conjugates. However, divergence in tumor growth inhibition was obtained from *in vivo* Colo205 xenograft models with low target expression, as the conventional DAR 8 conjugate showed only minor inhibition, whereas site-selective conjugates with DAR 6 and 8 induced long-term tumor growth inhibition. Follow-up pharmacokinetic (PK) studies revealed increased exposure of the homogeneous high DAR ADCs in mice (up to DAR 8) and rat (up to DAR 6). Additionally, comparable safety and tolerability was observed, widening the TI and opening avenues for addressing tumor targets with low target expression, slow internalization or intracellular processing by high DAR ADC [28].

Likewise, Farias and co-workers investigated the site-specificity of their mTG approach by HR-MS analysis [77]. C16 anti-M1S1 antibody with the LLQGA-tag at the C-terminus of either heavy or light chain (or both) were site-specifically linked to NH₂-PEG₆-MMAD. The generated ADCs were characterized by intact mass, high resolution peptide mapping and in-source fragmentation analysis, revealing site-specific payload attachment. However, a small amount of off-target conjugation of approximately 1.3% was observed, corresponding to a small fraction of aglycosylated antibody present in the produced material. A generated C16 HC Q295 N mutant lacking the off-target conjugation site, yielded highly homogeneous conjugates that were more than 99.8% site-specific [77].

Further, Dorywalska and co-workers investigated the effect of the attachment site on the stability of ADCs equipped with a cleavable linker and MMAD in rodent serum [78]. To that end, a series of different ADCs was generated by coupling of cleavable aminocaproyl-VC-

PABC-MMAD to an engineered LLQG recognition site or Q295 of anti-M1S1 antibody C16 using mTG. While nearly no loss of payload was observed in rat, cynomolgus monkey, and human, a different linker stability was observed in mice serum, depending on the respective conjugation site. Due to steric hindrance, varying extent of enzymatic cleavage of the natural cathepsin B site was found at each investigated position. *In vitro* cytotoxicity assays upon plasma treatment of the different ADCs and *in vivo* xenograft models in mice implanted with BxPC3 cells revealed the importance of linker stability for cytotoxic potency. Interestingly, this cleavage was found to be CatB-independent. These results suggest that the conjugation site plays a key role for the stability and potency of cleavable auristatin based ADCs. Therefore, site-directed conjugation via mTG generating homogeneous ADCs is an advantageous procedure for the production of potent ADCs for preclinical trials [78]. Additionally, homogeneous non-cleavable ADCs bearing PEG₆-propionyl(C2)-MMAD as a payload were investigated for stability in rodent plasma applying the same conjugation sites [79]. A position-dependent degradation of the C-terminus of MMAD was observed, which had a detrimental effect on ADC potency. Notably, an ADC bearing MMAF analog Aur3377 as a payload and the same linker did not show detectable degradation or a loss of potency [79]. In 2016, the same group identified murine serum protease carboxylesterase 1C (Ces1C) to be responsible for premature extracellular hydrolysis of the cleavable aminocaproyl-VC-PABC linker moiety of ADCs [73]. To overcome this limitation, 10 different chemical functionalities were considered at the C2 position of the C6-VC-PABC-Aur0101 linker-payload to protect it from enzymatic degradation. Upon mTG-assisted conjugation, plasma stability assays of the resulting ADCs revealed a significant impact of the utilized linker derivatives on extracellular drug loss. Depending on the addressed glutamine site, some substitutions even accelerated Ces1C-mediated degradation while others successfully protected the linker from undesired enzymatic cleavage. Successive xenograft models demonstrated improved antitumor efficacy as a result of elevated systemic ADCs stability, originating from the superior stability of a protected linker (Anami et al. [74] further investigated these effects, see above) [73].

The therapeutic index of an antibody-drug conjugate is influenced by a plethora of physiological and pharmaceutical parameters including the location of the tumor, linker stability, the toxic warhead's mode of action and the choice of the targeted antigen [5,18,19,80,81]. Antigens that are highly overexpressed on malignant cells but almost absent in healthy tissue are usually favored to avoid undesired side-effects during treatment of the patient. However, several promising tumor markers are present on both degenerated and healthy cells differing only in the extent of antigen expression. To address these molecules, engineering antibodies with mediocre affinities that accumulate only at elevated antigen levels, is a suitable approach to improve the TI of an ADC. A group from Rinat-Pfizer applied this approach in combination with their well-established transglutaminase labelling strategy to develop homogeneous ADCs with balanced efficacy and toxicity, hence enriched TI [82-84].

In 2016 Strop and co-workers investigated a medium-affinity ADC against type I transmembrane cell-surface glycoprotein Trop-2 (trophoblast cell-surface antigen 2; also known as M1S1, TACSTD2, EGP-1, GA733-1), which is highly expressed in most human carcinomas [83]. Despite the fact that its biological role is still a matter of discussion, Trop-2 overexpression is associated with cancer growth, aggressiveness, metastasis and poor prognosis in carcinomas [83]. Unfortunately, Trop-2 is also expressed on normal epithelial cells, thus an adjustment between efficacy and safety is needed. The C-terminal lysine on the heavy chain of a humanized anti-Trop-2 hIgG1 antibody was replaced with the LLQGA motif to allow for mTG-mediated modification. Subsequent conjugation with cleavable AcLys-VC-PABC-PF-06380101, a potent microtubule inhibitor (MTI), yielded a DAR 1.9 ADC (RN927C). The applied linker was assessed as stable in BxPC3 tumor-bearing animals and highly efficient in multiple pancreatic tumor xenograft models

including cell line BxPC3 and PDX models Pan0123 (pancreatic ductal carcinoma from peritoneal biopsy), Pan0135 (pancreatic adenocarcinoma), and Pan0146 (metastatic pancreatic carcinoma from liver biopsy) (0.75–1.5 mg/kg), whereas a non-binding control antibody showed no effect (up to 3 mg/kg). *In vivo* ovarian, lung and triple-negative breast cancer PDX xenograft models further showed potent inhibition of tumor growth, which was superior to standard chemotherapeutic treatment with paclitaxel or gemcitabine. It should be noted that only partial tumor growth inhibition was achieved in lung PDX model with RN927C, but RN927C was superior to paclitaxel (20 mg/kg) in a comparing study. The combination of medium-affinity binding and site-specific stable isopeptide linkage of the payload led to reduced off-target toxicity in preclinical exploratory safety studies in non-human primates, as only fully recoverable on-target epithelial toxicity was detected with minimal, non-dose limiting off-target toxicity [83].

The above-mentioned strategy was further applied for the preparation of a safety-enhanced ADC targeting EGFR [84]. A low-affinity parental antibody was chosen to reduce off-target toxicity and to enhance tumor penetration, which was further humanized and equipped with a transglutaminase recognition motif at the C-terminus of the light chain constant domain by addition of the sequence GLLQGPP. Upon transglutaminase-catalyzed conjugation of AcLys-VC-PABC-PF-06380101, the generated ADC RN765C comprised a DAR of 1.93–2.0 and revealed potent cell-killing properties *in vitro* on EGFR-overexpressing HCC827 cells, and even on cells insensitive to the clinically approved anti-EGFR antibody cetuximab. Additionally, RN765C was found to be less effective in killing normal human keratinocytes that express low levels of the targeted receptor. *In vivo* xenograft models based on BxPC3 cells and PDX models of colorectal and lung cancer using 1.5–3 mg/kg of RN965C resulted in persistent tumor growth inhibition regardless of their KRAS mutation. Notably, potent tumor growth inhibition was found in non-small cell lung cancer PDX LG1049 carrying the EGFR exon 19 deletion and T790 M mutation, known to drive resistance for tyrosine kinase inhibitors [84].

In 2019 Costa and co-workers designed efficacy- and tolerability-enhanced ADCs targeting the CXC motif chemokine receptor 4 (CXCR4) [82]. CXCR4 has multiple functions in hematopoietic progenitor cells, e.g. maintenance of quiescence, protection against oxidative stress in adult tissues, and retention of granulocytes and neutrophils in bone marrow. Though first approaches applying small molecules have advanced into clinical trials, these compounds often comprise unfavorable PK profiles and require combinatorial treatment to achieve therapeutic benefit [82]. Thus, the first anti-CXCR4 ADC effective in xenograft models of haemopoietic cancers resistant to standard of care and anti-CXCR4 antibodies was developed. Different types of linker-payloads, DARs, affinities and Fc formats were investigated to carefully evaluate the TI of the resulting drugs. Twenty-two ADCs were generated upon site-specific mTG-mediated conjugation to engineered antibodies with different mTG-recognition motifs. Auristatins were chosen as cytotoxic payloads, as these cell division-blocking tubulin polymerization inhibitors mediated significant loss of viability in tumor cells (Ramos and OPM2) and left peripheral blood mononuclear cells (PBMCs, CXCR4-positive) untouched. The lead ADC 713 comprised a low-affinity antibody with reduced Fc-effector functions armed with 4 non-cleavable auristatin payloads conjugated to an LLQG tag at position 135 in the CH1 and to the accessible Q295 of N297A-mutated CH2. It was found active in hematological and solid tumors presenting a favorable TI and therefore demonstrating the possibility to generate an ADC with improved TI through empiric studies for targets with broad normal-tissue expression [82].

The incorporation of genetically encoded mTG recognition motifs was further employed for the generation of non-cleavable ADCs with improved lysosomal trafficking [85]. ADCs bearing non-cleavable toxic payloads are hypothesized to possess enhanced stability in circulation and release their payloads upon ADC degradation in the lysosome. To investigate whether the intracellular trafficking pathway can modulate

potency of an ADC, two different constructs were generated targeting two different tumor markers with comparable internalization rates: Amyloid Precursor Like Protein 2 (APLP2), which is known to efficiently deliver its interacting partners to lysosomes, and Trop-2, whose expression is often associated with poor prognosis of diseases, but is less effective in lysosomal trafficking compared to APLP2. Trop-2- and APLP2-targeting antibodies were conjugated with NH₂-PEG₆-MMAD via transglutaminase to generate ADCs with DAR 2 (C-terminal GLLQGPP transglutaminase tag of the light chain) or 4 (N297Q mutation for conjugation to Q295 and Q297 in the heavy chain). *In vitro* potency was determined on SKOV3 and Colo205 cells that expressed different ratios of APLP2 to Trop-2 of 1:2 and 1:13, respectively. The lysosomally targeted APLP2-binding ADC induced cell killing more effectively than the one directed against Trop-2; Colo205 xenograft models further demonstrated superior *in vivo* efficacy [85]. HER2 is a prominent tumor target that is overexpressed on different types of ovarian and breast cancers but suffers from rapid recycling back to the cell surface upon endocytosis [85]. In a following approach, HER2/APLP2-targeting bispecific ADCs were investigated to merge the advantages of elevated HER2 expression and the lysosome-directing properties of APLP2. In these constructs, one Fab arm of the antibody mediates binding to the HER2 receptor, while the other arm binds APLP2. Potent growth inhibition of low HER2-expressing MCF7 cells was achieved while a bivalent anti-HER2 ADC lacking APLP2 binding showed no effect. On cell lines expressing medium (JIMT-1) and high (N87) levels of HER2, similar IC₅₀ values were determined, but the HER2/APLP2-addressing molecule exhibited improved maximal cell killing compared to its monospecific counterpart. Unfortunately, this effect was not observed *in vivo* as JIMT-1 orthotopic breast cancer models revealed a lower anti-tumor efficacy of the bispecific ADC than the monospecific reference at two different investigated doses. The authors suggested that multiple factors influence the potency of non-cleavable ADC, among them receptor copy number, DAR, internalization and lysosomal trafficking. Therefore, further studies in the field are needed, but nevertheless this bispecific approach redirecting intracellular trafficking is promising for targeted tumor therapy [85].

In 2018, the group of Graziani introduced DNA-intercalating natural product bis-intercalator depsipeptides (NPBIDs) as a novel class of ADC payloads leading to highly efficient anti-HER2 ADCs [86]. NPBIDs are head-to-tail dimeric C₂-symmetrical polypeptides primarily isolated from *Streptomyces*, which bear a bicyclic heteroaromatic chromophore on each monomer. Their intercalation into the minor groove of DNA occurs via hydrogen bonding between the polypeptide core of the NPBID and the nucleobases of the DNA. These (in principle reversible) binding properties may result in a bystander effect upon cell lysis that could be beneficial for the treatment of solid tumors. A set of nine different NPBIDs was analyzed for their *in vitro* potency in a number of human cancer cell lines (N87, MDA-MB361, HT29; IC₅₀ < 0.1–20 nM). Furthermore, generation of seven different ADCs either by standard maleimide coupling or mTG-catalyzed conjugation applying different PEGylated and non-PEGylated linkers resulted in the lead ADC PF-06888667, consisting of the bis-intercalator, SW-163D conjugated with *N*-acetyl-lysine-valine-citrulline-*p*-aminobenzylalcohol-*N,N*-dimethylethylenediamine linker to an engineered variant of trastuzumab (LC C-terminus tag GLLQGA and mutation N297A for conjugation on Q295). PF-06888667 exhibited complete regression in a N87 tumor xenograft model in mice at 1 mg/kg and a cytostatic effect at 0.3 mg/kg. Interestingly, a previous study applying the same mouse model reported complete tumor regression only at a dose of 10 mg/kg of commercially available ADC T-DM1. Optimization of the employed linker and the attachment site as well as the conjugation method were revealed to be key factors for the success of their work. Thus, an SW-163 based ADC obtained by maleimide coupling to engineered cysteines C183/290, bearing a PEG spacer showed significantly lower efficacy compared to the mTG generated ADC comprising an *N*-acetyl-lysine linker [86].

According to calculations, 75–80% of the human proteome are

considered to be undruggable by small molecules or biotherapeutics due to a lack of suitable hydrophobic pockets or their absence from the cell surface [87]. Nucleic acid therapeutics (NAT) bear great potential to address these challenging targets that are involved in multiple kinds of cancers and genetic disorders. By binding of antisense oligonucleotides or siRNAs to the mRNA of the “undruggable” protein, its translation by the ribosome is inhibited and its total concentration is downregulated. Unfortunately, unfavorable pharmacokinetics, short half-life and target-indiscrimination strongly limits the application of NAT in therapy. Through coupling of NATs to monoclonal antibodies, Huggins et al. intended to overcome these limitations. To that end, a chemoenzymatic approach was developed that employed mTG for the attachment of a SPAAC-reactive acyl-acceptor peptide K-PEG₆-SG-K-N₃ to an engineered LLQGA motif at the C-terminus of an anti-CD33 mAb. Subsequently, a 5' DBCO-modified siRNA was synthesized and coupled to the mAb-linker conjugate to form an antibody-siRNA conjugate with a DAR of approximately 2 and unaltered binding properties. The authors report on a straight-forward approach that allows for the assembly of antibody-nucleic acid conjugates by applying mTG catalysis and SPAAC without undesired off-target conjugation. Modification of their approach towards construction of higher or lower DAR conjugates are discussed as well as a potential application in drug-delivery of therapeutic oligonucleotides. However, cell killing experiments and *in vivo* data to further demonstrate the impact of their approach are missing [88].

Transglutaminases are present in a vast number of different microorganisms, but besides the most prominent one from *Streptomyces mobaraensis* only a few of them have been applied for biotechnological purposes even though homologs bearing novel properties would be of great value. A promising example is the newly described KalbTG from Gram-positive actinobacterium *Kutzneria albida*. In 2017, researchers from Roche identified the enzyme that comprises 32% sequence identity and conserved active site residues by sequence alignments using the *S. mobaraensis* enzyme as a query [89]. The hypothetical gene coded for the smallest transglutaminase known to date (26.4 kDa) and a strategy for the recombinant expression in *E. coli* cells was established that employed ammonia, the inhibitory byproduct of the catalyzed transamidation, to suppress the enzyme's cytotoxic intracellular crosslinking activity. KalbTG exhibited no cross-reactivity with known mTG substrates and ultra-high throughput screening of 1.4 million different 5-mer peptides using the NimbleGen peptide array technology revealed YRYRQ and RYESK as favored glutamine and lysine sequences. Interestingly, KalbTG was found orthogonal to mTG, making dual labeling of a 7-kDa substrate bearing a YRYRQ KalbTG site and a DYALQ mTG recognition sequence possible. Antibody conjugates were generated via mTG or KalbTG catalysis applying recognition motifs YRYRQ and LLQGA that are C-terminally fused to the heavy chain of a mouse, monoclonal anti-TSH (thyroid stimulating hormone) antibody. Site-specific conjugation by both transglutaminases was found with no labelling of mTG recognition sequence LLQGA by KalbTG. In the scope of that work, no antibody-drug conjugates were presented, but the demonstrated results provided a powerful tool for the dual-labelling of antibody employing orthogonal transglutaminases [89].

Among others, the coupling efficiency of the used ligation strategy is a key factor for the generation of ADCs since inefficient conjugation results in heterogeneous product formation. In our group, we are interested in developing novel recognition motifs for microbial transglutaminase that facilitate highly efficient labelling of therapeutic antibodies. In 2015, we unveiled a rationally designed sequence GECTYFQAYGCTE (GEC) that was derived from a natural mTG substrate disperse-autolysis inducing protein (DAIP) [90]. The motif comprised the amino acids that surround reactive Q298 of DAIP, which is located within a type II β -turn connecting two beta strands, and lacks similarity with known linear recognition motifs. To precisely mimic the native structure of the loop region, an intramolecular disulfide bridge was introduced that locked both termini at 4 Å distance. On a peptide

level, the conformationally constrained molecule outperformed a linear control in terms of mTG-catalyzed labelling. Fused to the heavy chain of EGFR-targeting antibody cetuximab, both sequences mediated site-specific biotinylation of the immunoglobulin as revealed by Western blot and MALDI TOF-MS analysis. Microscopic studies and flow cytometry using EGFR positive EBC-1 cells demonstrated that target binding of biotinylated constructs was not impaired upon bioconjugation by mTG [90].

In recent research, we further employed the demonstrated approach based on deriving efficient bioconjugation tags from native mTG substrates and revealed the sequence DIPIGQGMTG (SPI7G) from *Streptomyces papain inhibitor* (SPI_p) [91]. SPI_p is a 12 kDa protein that is secreted by *S. mobaraensis* and previous studies showed that substitution of Lys7 massively influenced transamidation of the only mTG-reactive glutamine Gln6 by mTG [92]. A small set of peptides that mimicked the N-terminus of SPI_p and different regions of DAIP was synthesized and investigated towards their reactivity under mTG catalysis. Interestingly, SPI7G in which the native Lys7 was replaced by glycine, outperformed previously identified sequence GEC. A similar trend was observed in a biotinylation experiment that addressed a C-terminally fused tag at the heavy chain of trastuzumab. To further demonstrate the practical applicability of the approach, HER2-targeting ADCs were assembled from SPI7G- and LLQG-decorated trastuzumab in a chemoenzymatic two-step procedure. NH₂-PEG₂-BCN was coupled to the heavy chains of the immunoglobulins under mTG catalysis and further modified using SPAAC to arm the respective antibody with N₃-PEG₃-VC-PAB-MMAE for targeted cancer therapy. Within a strictly contracted reaction time of 1 h, the ADC assembled from the novel tag SPI7G revealed a 4-fold increased DAR of 1.81 compared to its counterpart synthesized from conventional sequence LLQG (DAR: 0.48). Consequently, the former ADC exhibited 12.6-fold more potent killing on HER2-overexpressing SK-BR-3 cells. These studies demonstrated that mimicking the native pattern of intrinsic mTG substrates is a powerful strategy to isolate potent recognition tags for the site-specific labelling of antibodies [91].

Besides the development of novel bioconjugation tags, mTG was also used for the generation of hydrophilic high-DAR ADCs to overcome the challenge of maintaining hydrophilicity of a conjugate equipped with numerous hydrophobic toxins [93]. To compensate the hydrophobicity of most commonly applied cytotoxins, which may negatively affect formulation, manufacturing and the biophysical properties of an ADC, 10 kDa dextran, a clinically and FDA-approved biocompatible polysaccharide consisting of repeating α -(1-6)-linked oligo-D-glucose units, was applied as a modular multimerization scaffold [5,93-95]. Dextran equipped with a single amine moiety at the reducing end and numerous azides at the glucose repeating units, was conjugated to the HER2-targeting antibody trastuzumab bearing the C-terminal mTG-recognition motif LLQG. Subsequent SPAAC of hydrophobic DBCO-PEG₃-VC-PAB-MMAE yielded novel hybrid molecules, dextramabs, comprising DARs of 2-11. Compared to the unmodified parent antibody, the hybrid ADCs revealed similar binding to its target and potent target-dependent killing (IC₅₀ = 0.1 nM) on SK-BR-3 (HER2 + +) cells *in vitro*. HER2-negative CHO-K1 cells were not affected by all dextramabs indicating a HER2-dependent cellular uptake. Hydrophobic interaction chromatography demonstrated that dextramabs were at least as hydrophilic as the unmodified parental antibody trastuzumab, indicating that the hydrophilicity of the conjugated toxins was compensated by the introduced hydrophilic polysaccharide scaffold. This approach may open avenues towards the application of milder toxins in higher density; follow-up animal studies will reveal if the enriched hydrophilicity could assure longer half-life and less immunogenicity *in vivo* [93].

The versatility of the mTG-mediated site-specific conjugation in combination with the multivalent dextran scaffold was further used in another approach, where dextran bearing different amounts of addressable azides on the repeating glucose units and a single amine at the reducing end was conjugated with death receptor 5 targeting peptide

(DR5TP) by copper(I)-catalyzed azide alkyne cycloaddition (CuAAC) [96]. Death receptor 5 (DR5) which is overexpressed on various cancer cells has recently become a promising target in tumor therapy. Clustering of DR5 leads to the formation of the death-inducing signal cascade (DISC) triggering apoptosis of the targeted cell. A flexible multivalent compound was assembled that effectively triggered apoptosis upon receptor clustering on DR5-positive COLO205 and Jurkat cells *in vitro*. mTG-catalyzed conjugation of the azide-modified polysaccharide to an aglycosylated human Fc fragment (N297A) bearing Q295 as a conjugation site resulted in a protein-sugar hybrid compound bearing multiple addressable azide moieties, which were further equipped with DR5TP in different copies. Conjugation of the scaffold to the Fc fragment did not impair potency. Furthermore, no toxicity was found for all constructs on DR5-negative HEK293 cells, revealing a DR5-dependent toxicity. Interestingly, in these constructs targeting is not mediated by the antibody part, but rather by the multivalent dextran-DR5TP scaffold. This may allow for the prospective attachment of a second targeting moiety, e.g. a full-size antibody, for bispecific targeting of overexpressed tumor markers, among them HER2/ErbB2, Trop-2 or EGFR, which may result in synergistic effects [96].

4. ADCs addressing natural or engineered lysines

All previously envisioned approaches exclusively employed the addressed antibody as the acyl-donor substrate for the catalyzed transamidation. This arrangement takes advantage of the enzyme's remarkable acyl-acceptor promiscuity that allows it to handle numerous aminated toxins. However, some studies reported the reverse procedure that targets lysine side chains of the respective antibody for payload attachment by mTG catalysis (Fig. 4). mTG that was non-covalently immobilized onto glass microbeads was able to modify K288/290 and K340 of aglycosylated cAC10 antibody with azide-decorated heptapeptide FGLQRPY in >70% yield, as shown by Spycher and co-workers [97]. Subsequent bioorthogonal SPAAC using DBCO-PEG₄-5/6-carboxyfluorescein (5/6-FAM) resulted in quantitative fluorescent labelling of the immunoglobulin. After establishing lysine conjugation by immobilized mTG, a dual-labeling strategy was developed. In the first step, NH₂-PEG₃-*trans*-cyclooctene (TCO) was coupled to Q295 of the aglycosylated antibody (>95% yield) followed by the attachment of FGLQRPYK-(N₃) to the side chain of K340 (38% yield). Again, SPAAC was applied to functionalize the antibody with tetrazine(Tz)-PEG₄-DOTAGA and DBCO-PEG₄-5/6-FAM in a straightforward one-pot reaction; the success was confirmed by SDS-PAGE and LC-MS [97].

In a different approach, researchers from Morphotek Inc./Eisai Inc. investigated varying antibodies including human-mouse chimeric, humanized, and fully human variants comprising either κ or λ light chains towards their reactivity in mTG-catalyzed reactions [98]. Since none of the approximately 80 present lysine sites reacted with biotin-modified standard substrate carboxybenzyl group-Gln-Gly (ZQG), they engineered a K-tag GGSTKHKIPGGS at the C-terminus of a heavy or a light chain, respectively. While the light chain was dually labeled with ZQG as expected, ESI-MS analysis revealed triple modification of the heavy chain. The authors concluded that cleavage of Lys447 by carboxypeptidase B during recombinant expression in HEK293 cells is prevented by additional C-terminal amino acids facilitating mTG-mediated transamidation. Engineering of dipeptides or single amino acids at the C-terminus (position 448) confirmed their hypothesis as efficient conjugation to Lys447 was demonstrated for all non-acidic and non-proline amino acids. Of note, positively charged amino acids arginine and lysine failed to prevent cleavage of Lys447 since they are substrate of carboxypeptidase B themselves. Moreover, the authors screened IgG1 antibodies for solitary residues that allowed for transamidation upon substitution against lysine and provided a detailed protocol therefore [99]. This approach applying minimal transglutaminase recognition tags would reduce the risk of perturbing the immunoglobulin's native structure and causing an undesired response by the patient immune

system [98,100]. To that end, multiple different sites within the light chain, heavy chain and hinge region were identified and their reactivity in mTG catalysis was investigated employing different acyl-donor substrates (ZQG-biotin, ZQG-N₃, ZQG-PEG₂-BCN, ZQG-PEG₂-auristatin F). Interestingly, the choice of the acyl-donor, as well as the conjugation site strongly influenced the degree of transamidation. Further, the identified sites were combined and reacted with previously employed acyl-donor substrates. However, a defined and homogeneous DAR of 4, 6 or 8 was not achieved as combination of otherwise efficiently modified sites resulted in suboptimal overall conjugation [98].

5. Conclusions and outlook

The concept of targeted therapeutics bears the potential to improve the TI of tumor treatment compared to classical chemotherapy. Hence, ADCs that combine the targeting properties of an antibody with the cytotoxic potential of a payload are widely studied in a still growing number of clinical trials and publications. Besides drugs, linkers and target selection the homogeneity of ADCs has become a promising field for ADC refinement. Site-specific conjugation is a widely distributed strategy to post-translationally customize the properties of target proteins towards different applications in pharmaceutical and biotechnological research e.g. arming tumor-specific antibodies with cytotoxic small molecules to yield antibody-drug conjugates. Numerous studies demonstrated the considerable impact of mTG from *Streptomyces mobaraensis* for the site-specific construction of homogeneous ADCs. In comparison to traditional conjugation methodologies, mTG-assisted catalysis bears certain advantages. The reactivity of other frequently employed conjugation enzymes is often limited to terminal sites (e.g. Sortase A) [54] or requires incorporation of >10 amino acids-long motifs that might interfere with mAb stability (e.g. lipoic acid ligase) [70]. Comparably short mTG-recognitions tags though, provide high flexibility since they can be inserted into various regions of a mAb to efficiently mediate its labelling [76]. Additionally, the remarkable stability of the formed isopeptide bond prevents premature drug loss in circulation and therefore minimizes systemic toxicity, an issue that is often observed when payloads are installed at cysteine residues via maleimide-chemistry [101,102]. Unfortunately, native human immunoglobulins do not serve as a substrate for mTG-mediated ligation. Thus, additional genetic engineering or glycosidase treatment are still necessary to achieve efficient modification and are accompanied by distinct advantages and disadvantages. Enzymatic deglycosylation to expose Gln295 can be applied to virtually any antibody in a straightforward manner. However, glycan truncation increases the antibody's hydrophobicity and its tendency to pH- and temperature-induced aggregation [75]. Incorporation of peptidyl-linker sequences into varying sites of the antibody allows for the careful fine-tuning of ADC pharmacokinetics but presupposes genetic modification and might interfere with the stability and overall polarity of the mAb. Engineering of a solitary lysine residue (acyl-acceptor) minimizes the risk of impairing the intrinsic stability and polarity of the mAb. However, laborious organic synthesis of the corresponding reaction partner is required because the commercial selection of pharmaceutically relevant acyl-donor substrates is limited. To overcome these limitations, efforts are currently ongoing to engineer mTG towards altered properties and fruitful results were obtained in terms of thermostability [103], catalytic activity [104,105] and substrate specificity [106]. Moreover, functionally homologous enzymes from alternative hosts beyond *Streptomyces mobaraensis* are being investigated as tools for site-specific antibody modification [89,107]. Notwithstanding, cytotoxin-armed antibodies that were generated via mTG conjugation showed very promising results in preclinical studies as illustrated in this review.

Declaration of competing interest

Authors declare that they have no conflict of interest.

Acknowledgments

This work was supported by the Deutsche Forschungsgemeinschaft through grant SPP 1623 and by the NANOKAT II grant from the BMBF (Bundesministerium für Bildung und Forschung).

References

- [1] R.L. Siegel, K.D. Miller, A. Jemal, Cancer statistics, 2019, CA: A Cancer J. Clin. 69 (2019) 7–34, <https://doi.org/10.3322/caac.21551>.
- [2] R.V. Chari, M.L. Miller, W.C. Widdison, Antibody–drug conjugates: an emerging concept in cancer therapy, *Angew. Chem. Int. Ed.* 53 (2014) 3796–3827, <https://doi.org/10.1002/anie.201307628>.
- [3] V.T. DeVita, E. Chu, A history of cancer chemotherapy, *Canc. Res.* 68 (2008) 8643, <https://doi.org/10.1158/0008-5472.CAN-07-6611>.
- [4] J.M. Lambert, C.Q. Morris, Antibody–drug conjugates (ADCs) for personalized treatment of solid tumors: a review, *Adv. Ther.* 34 (2017) 1015–1035, <https://doi.org/10.1007/s12325-017-0519-6>.
- [5] J.M. Lambert, A. Berkenblit, Antibody–drug conjugates for cancer treatment, *Annu. Rev. Med.* 69 (2018), <https://doi.org/10.1146/annurev-med-061516-121357>.
- [6] E. Frei, Combination cancer therapy: presidential address, *Canc. Res.* 32 (1972) 2593.
- [7] R.A. Beckman, L.M. Weiner, H.M. Davis, Antibody constructs in cancer therapy, *Cancer* 109 (2007) 170–179, <https://doi.org/10.1002/cncr.22402>.
- [8] J.M. Reichert, Marketed therapeutic antibodies compendium, *mAbs* 4 (2012) 413–415, <https://doi.org/10.4161/mabs.19931>.
- [9] K.C. Nicolaou, S. Rigol, The role of organic synthesis in the emergence and development of antibody–drug conjugates as targeted cancer therapies, *Angew. Chem. Int. Ed.* (2019), <https://doi.org/10.1002/anie.201903498>.
- [10] J.H. Yi, S.J. Kim, W.S. Kim, Brentuximab vedotin: clinical updates and practical guidance, *Blood Res* 52 (2017) 243–253, <https://doi.org/10.5045/br.2017.52.4.243>.
- [11] P.D. Senter, E.L. Sievers, The discovery and development of brentuximab vedotin for use in relapsed Hodgkin lymphoma and systemic anaplastic large cell lymphoma, *Nat. Biotechnol.* 30 (2012) 631, <https://doi.org/10.1038/nbt.2289>.
- [12] J.K. Lamba, L. Chauhan, M. Shin, M.R. Loken, J.A. Pollard, Y.-C. Wang, R.E. Ries, R. Aplenc, B.A. Hirsch, S.C. Raimondi, R.B. Walter, I.D. Bernstein, A.S. Gamis, T.A. Alonzo, S. Meshinchi, CD33 splicing polymorphism determines gemtuzumab ozogamicin response in de novo acute myeloid leukemia: report from randomized phase III children's oncology group trial AAML0531, *J. Clin. Oncol. : official journal of the American Society of Clinical Oncology* 35 (2017) 2674–2682, <https://doi.org/10.1200/JCO.2016.71.2513>.
- [13] F.R. Appelbaum, I.D. Bernstein, Gemtuzumab ozogamicin for acute myeloid leukemia, *Blood* 130 (2017) 2373, <https://doi.org/10.1182/blood-2017-09-797712>.
- [14] B. Shor, H.-P. Gerber, P. Sapra, Preclinical and clinical development of inotuzumab-ozogamicin in hematological malignancies, *Mol. Immunol.* 67 (2015) 107–116, <https://doi.org/10.1016/j.molimm.2014.09.014>.
- [15] Y.N. Lamb, Inotuzumab ozogamicin: first global approval, *Drugs* 77 (2017) 1603–1610, <https://doi.org/10.1007/s40265-017-0802-5>.
- [16] I. Niculescu-Duvaz, Trastuzumab emtansine, an antibody–drug conjugate for the treatment of HER2+ metastatic breast cancer, *Curr. Opin. Mol. Therapeut.* 12 (2010) 350–360.
- [17] P.M. LoRusso, D. Weiss, E. Guardino, S. Girish, M.X. Sliwkowski, Trastuzumab emtansine: a unique antibody–drug conjugate in development for human epidermal growth factor receptor 2–positive cancer, *Clin. Canc. Res.* 17 (2011) 6437, <https://doi.org/10.1158/1078-0432.CCR-11-0762>.
- [18] T. Kline, A.R. Steiner, K. Penta, A.K. Sato, T.J. Hallam, G. Yin, Methods to make homogenous antibody drug conjugates, *Pharmaceut. Res.* 32 (2015) 3480–3493, <https://doi.org/10.1007/s11095-014-1596-8>.
- [19] A. Beck, L. Goetsch, C. Dumontet, N. Corvaia, Strategies and challenges for the next generation of antibody–drug conjugates, *Nat. Rev. Drug Discov.* 16 (2017) 315, <https://doi.org/10.1038/nrd.2016.268>.
- [20] S.O. Doronina, B.E. Toki, M.Y. Torgov, B.A. Mendelsohn, C.G. Cerveny, D.F. Chace, R.L. DeBlanc, R.P. Gearing, T.D. Bovee, C.B. Siegall, J.A. Francisco, A.F. Wahl, D.L. Meyer, P.D. Senter, Development of potent monoclonal antibody auristatin conjugates for cancer therapy, *Nat. Biotechnol.* 21 (2003) 778–784, <https://doi.org/10.1038/nbt832>.
- [21] W.C. Widdison, S.D. Wilhelm, E.E. Cavanagh, K.R. Whiteman, B.A. Leece, Y. Kovtun, V.S. Goldmacher, H. Xie, R.M. Steeves, R.J. Lutz, R. Zhao, L. Wang, W.A. Blättler, R.V.J. Chari, Semisynthetic maytansine analogues for the targeted treatment of cancer, *J. Med. Chem.* 49 (2006) 4392–4408, <https://doi.org/10.1021/jm060319f>.
- [22] M.S. Kung Sutherland, R.B. Walter, S.C. Jeffrey, P.J. Burke, C. Yu, H. Kostner, I. Stone, M.C. Ryan, D. Sussman, R.P. Lyon, W. Zeng, K.H. Harrington, K. Klussman, L. Westendorf, D. Meyer, I.D. Bernstein, P.D. Senter, D.R. Benjamin, J.G. Drachman, J.A. McEarchern, SGN-CD33A: a novel CD33-targeting antibody–drug conjugate using a pyrrolbenzodiazepine dimer is active in models of drug-resistant AML, *Blood* 122 (2013) 1455, <https://doi.org/10.1182/blood-2013-03-491506>.
- [23] R.C. Elgersma, R.G.E. Coumans, T. Huijbregts, W.M.P.B. Menge, J.A.F. Joosten, H.J. Spijker, F.M.H. de Groot, M.M.C. van der Lee, R. Ubink, D.J. van den Dobbelaer, D.F. Egging, W.H.A. Dokter, G.F.M. Verheijden, J.M. Lemmens, C.M. Timmers, P.H. Beusker, Design, synthesis, and evaluation of linker-duo-carmycin payloads: toward selection of HER2-targeting antibody–drug conjugate SYD985, *Mol. Pharm.* 12 (2015) 1813–1835, <https://doi.org/10.1021/mp500781a>.
- [24] A.L. Smith, K.C. Nicolaou, The enediyne antibiotics, *J. Med. Chem.* 39 (1996) 2103–2117, <https://doi.org/10.1021/jm9600398>.
- [25] M.L. Miller, N.E. Fishkin, W. Li, K.R. Whiteman, Y. Kovtun, E.E. Reid, K.E. Archer, E.K. Maloney, C.A. Audette, M.F. Mayo, A. Wilhelm, H.A. Modafferi, R. Singh, J. Pinkas, V. Goldmacher, J.M. Lambert, R.V.J. Chari, A new class of antibody–drug conjugates with potent DNA alkylating activity, *Mol. Canc. Therapeut.* 15 (2016) 1870, <https://doi.org/10.1158/1535-7163.MCT-16-0184>.
- [26] M.T. Kim, Y. Chen, J. Marhouf, F. Jacobson, Statistical modeling of the drug load distribution on trastuzumab emtansine (Kadcyla), a lysine-linked antibody drug conjugate, *Bioconjugate Chem.* 25 (2014) 1223–1232, <https://doi.org/10.1021/bc5000109>.
- [27] D. Schumacher, C.P.R. Hackenberger, H. Leonhardt, J. Helma, Current status: site-specific antibody drug conjugates, *J. Clin. Immunol.* 36 (2016) 100–107, <https://doi.org/10.1007/s10875-016-0265-6>.
- [28] P. Strop, K. Delaria, D. Foletti, J.M. Witt, A. Hasa-Moreno, K. Poulsen, M.G. Casas, M. Dorywalska, S. Farias, A. Pios, V. Lui, R. Dushin, D. Zhou, T. Navaratnam, T.-T. Tran, J. Sutton, K.C. Lindquist, B. Han, S.-H. Liu, D.L. Shelton, J. Pons, A. Rajpal, Site-specific conjugation improves therapeutic index of antibody drug conjugates with high drug loading, *Nat. Biotechnol.* 33 (2015) 694, <https://doi.org/10.1038/nbt.3274>.
- [29] X. Li, T. Fang, G.-J. Boons, Preparation of well-defined antibody–drug conjugates through glycan remodeling and strain-promoted azide–alkyne cycloadditions, *Angew. Chem. Int. Ed.* 53 (2014) 7179–7182, <https://doi.org/10.1002/anie.201402606>.
- [30] Z. Zhu, B. Ramakrishnan, J. Li, Y. Wang, Y. Feng, P. Prabakaran, S. Colantonio, M.A. Dyba, P.K. Qasba, D.S. Dimitrov, Site-specific antibody–drug conjugation through an engineered glycotransferase and a chemically reactive sugar, *mAbs* 6 (2014) 1190–1200, <https://doi.org/10.4161/mabs.29889>.
- [31] B. Ramakrishnan, E. Boeggeman, P.K. Qasba, Applications of glycosyltransferases in the site-specific conjugation of biomolecules and the development of a targeted drug delivery system and contrast agents for MRI, *Expet Opin. Drug Deliv.* 5 (2008) 149–153, <https://doi.org/10.1517/17425247.5.2.149>.
- [32] P.K. Qasba, Glycans of antibodies as a specific site for drug conjugation using glycosyltransferases, *Bioconjugate Chem.* 26 (2015) 2170–2175, <https://doi.org/10.1021/acs.bioconjchem.5b00173>.
- [33] Q. Zhou, J.E. Stefano, C. Manning, J. Kyazike, B. Chen, D.A. Gianolio, A. Park, M. Busch, J. Bird, X. Zheng, H. Simonds-Mannes, J. Kim, R.C. Gregory, R.J. Miller, W.H. Brondyk, P.K. Dhal, C.Q. Pan, Site-specific antibody–drug conjugation through glycoengineering, *Bioconjugate Chem.* 25 (2014) 510–520, <https://doi.org/10.1021/bc400505q>.
- [34] R. van Geel, M.A. Wijdeven, R. Heesbeen, J.M.M. Verkade, A.A. Wasie, S.S. van Berkel, F.L. van Delft, Chemoenzymatic conjugation of toxic payloads to the globally conserved N-glycan of native mAbs provides homogeneous and highly efficacious antibody–drug conjugates, *Bioconjugate Chem.* 26 (2015) 2233–2242, <https://doi.org/10.1021/acs.bioconjchem.5b00224>.
- [35] D. Shinmi, E. Taguchi, J. Iwano, T. Yamaguchi, K. Masuda, J. Enokizono, Y. Shiraiishi, One-step conjugation method for site-specific antibody–drug conjugates through reactive cysteine-engineered antibodies, *Bioconjugate Chem.* 27 (2016) 1324–1331, <https://doi.org/10.1021/acs.bioconjchem.6b00133>.
- [36] N. Dimasi, R. Fleming, H. Zhong, B. Bezabeh, K. Kinneer, R.J. Christie, C. Fazanbaker, H. Wu, C. Gao, Efficient preparation of site-specific antibody–drug conjugates using cysteine insertion, *Mol. Pharm.* 14 (2017) 1501–1516, <https://doi.org/10.1021/acs.molpharmaceut.6b00995>.
- [37] B.-Q. Shen, K. Xu, L. Liu, H. Raab, S. Bhakta, M. Kenrick, K.L. Parsons-Reponte, J. Tien, S.-F. Yu, E. Mai, D. Li, J. Tibbitts, J. Baudys, O.M. Saad, S.J. Scales, P.J. McDonald, P.E. Hass, C. Eigenbrot, T. Nguyen, W.A. Solis, R.N. Fujii, K.M. Flagella, D. Patel, S.D. Spencer, L.A. Khawli, A. Ebens, W.L. Wong, R. Vandlen, S. Kaur, M.X. Sliwkowski, R.H. Scheller, P. Polakis, J.R. Junutula, Conjugation site modulates the in vivo stability and therapeutic activity of antibody–drug conjugates, *Nat. Biotechnol.* 30 (2012) 184, <https://doi.org/10.1038/nbt.2108>.
- [38] J.R. Junutula, H. Raab, S. Clark, S. Bhakta, D.D. Leipold, S. Weir, Y. Chen, M. Simpson, S.P. Tsai, M.S. Dennis, Y. Lu, Y.G. Meng, C. Ng, J. Yang, C.C. Lee, E. Duenas, J. Gorrell, V. Katta, A. Kim, K. McDorman, K. Flagella, R. Venook, S. Ross, S.D. Spencer, W. Lee Wong, H.B. Lowman, R. Vandlen, M.X. Sliwkowski, R.H. Scheller, P. Polakis, W. Mallet, Site-specific conjugation of a cytotoxic drug to an antibody improves the therapeutic index, *Nat. Biotechnol.* 26 (2008) 925, <https://doi.org/10.1038/nbt.1480>.
- [39] X. Li, C.G. Nelson, R.R. Nair, L. Hazlehurst, T. Moroni, P. Martinez-Acedo, A.R. Nanna, D. Hymel, T.R. Burke, C. Rader, Stable and potent selenomab–drug conjugates, *Cell Chem. Biol.* 24 (2017) 433–442, <https://doi.org/10.1016/j.chembiol.2017.02.012> e436.
- [40] M.P. VanBrunt, K. Shanebeck, Z. Caldwell, J. Johnson, P. Thompson, T. Martin, H. Dong, G. Li, H. Xu, F. D'Hooge, L. Masterson, P. Bariola, A. Tiberghien, E. Ezeadi, D.G. Williams, J.A. Hartley, P.W. Howard, K.H. Grabstein, M.A. Bowen, M. Marelli, Genetically encoded azide containing amino acid in mammalian cells enables site-specific antibody–drug conjugates using click cycloaddition chemistry, *Bioconjugate Chem.* 26 (2015) 2249–2260, <https://doi.org/10.1021/acs.bioconjchem.5b00359>.
- [41] E.S. Zimmerman, T.H. Heibeck, A. Gill, X. Li, C.J. Murray, M.R. Madlansacay, C. Tran, N.T. Uter, G. Yin, P.J. Rivers, A.Y. Yam, W.D. Wang, A.R. Steiner, S.U. Bajad, K. Penta, W. Yang, T.J. Hallam, C.D. Thanos, A.K. Sato, Production of

- site-specific antibody–drug conjugates using optimized non-natural amino acids in a cell-free expression system, *Bioconjugate Chem.* 25 (2014) 351–361, <https://doi.org/10.1021/bc400490z>.
- [42] J.Y. Axup, K.M. Bajjuri, M. Ritland, B.M. Hutchins, C.H. Kim, S.A. Kazane, R. Halder, J.S. Forsyth, A.F. Santidrian, K. Stafin, Y. Lu, H. Tran, A.J. Seller, S.L. Biroc, A. Szydluk, J.K. Pinkstaff, F. Tian, S.C. Sinha, B. Felding-Habermann, V.V. Smider, P.G. Schultz, Synthesis of site-specific antibody–drug conjugates using unnatural amino acids, *Proc. Natl. Acad. Sci. Unit. States Am.* 109 (2012) 16101, <https://doi.org/10.1073/pnas.1211023109>.
- [43] P. Bryant, M. Pabst, G. Badescu, M. Bird, W. McDowell, E. Jamieson, J. Swierkosz, K. Jurlewicz, R. Tommasi, K. Henseleit, X. Sheng, N. Camper, A. Manin, K. Kozakowska, K. Peciak, E. Laurine, R. Grygorash, A. Kyle, D. Morris, V. Parekh, A. Abhilash, J.-w. Choi, J. Edwards, M. Frigerio, M.P. Baker, A. Godwin, In vitro and in vivo evaluation of cysteine rebridged trastuzumab–MMAE antibody drug conjugates with defined drug-to-antibody ratios, *Mol. Pharm.* 12 (2015) 1872–1879, <https://doi.org/10.1021/acs.molpharmaceut.5b00116>.
- [44] C.R. Behrens, E.H. Ha, L.L. Chinn, S. Bowers, G. Probst, M. Fitch-Bruhns, J. Monteon, A. Valdiosera, A. Bermudez, S. Liao-Chan, T. Wong, J. Melnick, J.-W. Theunissen, M.R. Flory, D. Houser, K. Venstrom, Z. Levashova, P. Sauer, T.-S. Migone, E.H. van der Horst, R.L. Halcomb, D.Y. Jackson, Antibody–drug conjugates (ADCs) derived from interchain cysteine cross-linking demonstrate improved homogeneity and other pharmacological properties over conventional heterogeneous ADCs, *Mol. Pharm.* 12 (2015) 3986–3998, <https://doi.org/10.1021/acs.molpharmaceut.5b00432>.
- [45] J. Ohata, Z.T. Ball, A hexa-rhodium metalloprotein catalyst for site-specific functionalization of natural antibodies, *J. Am. Chem. Soc.* 139 (2017) 12617–12622, <https://doi.org/10.1021/jacs.7b06428>.
- [46] S. Lin, X. Yang, S. Jia, A.M. Weeks, M. Hornsby, P.S. Lee, R.V. Nichiporuk, A.T. Iavarone, J.A. Wells, F.D. Toste, C.J. Chang, Redox-based reagents for chemoselective methionine bioconjugation, *Science* 355 (2017) 597, <https://doi.org/10.1126/science.aal3316>.
- [47] A.R. Nanna, X. Li, E. Walseng, L. Pedzisa, R.S. Goydel, D. Hymel, T.R. Burke Jr., W.R. Roush, C. Rader, Harnessing a catalytic lysine residue for the one-step preparation of homogeneous antibody–drug conjugates, *Nat. Commun.* 8 (2017) 1112, <https://doi.org/10.1038/s41467-017-01257-1>.
- [48] D. Schumacher, J. Helma, F.A. Mann, G. Pichler, F. Natale, E. Krause, M.C. Cardoso, C.P.R. Hackenberger, H. Leonhardt, Versatile and efficient site-specific protein functionalization by tubulin tyrosine ligase, *Angew. Chem. Int. Ed.* 54 (2015) 13787–13791, <https://doi.org/10.1002/anie.201505456>.
- [49] P.M. Drake, A.E. Albers, J. Baker, S. Banas, R.M. Barfield, A.S. Bhat, G.W. de Hart, A.W. Garofalo, P. Holder, L.C. Jones, R. Kudirka, J. McFarland, W. Zmolek, D. Rabuka, Aldehyde tag coupled with HIPS chemistry enables the production of ADCs conjugated site-specifically to different antibody regions with distinct in vivo efficacy and PK outcomes, *Bioconjugate Chem.* 25 (2014) 1331–1341, <https://doi.org/10.1021/bc500189z>.
- [50] T. Krüger, T. Dierks, N.J.B.c. Sewald, Formylglycine-generating Enzymes for Site-specific Bioconjugation, *Biological chemistry*, 2019, pp. 289–297.
- [51] T. Krüger, S. Weiland, G. Falck, M. Gerlach, M. Boschanski, S. Alam, K.M. Müller, T. Dierks, N. Sewald, Two-fold bioorthogonal derivatization by different formylglycine-generating enzymes, *Angew. Chem. Int. Ed.* 57 (2018) 7245–7249, <https://doi.org/10.1002/anie.201803183>.
- [52] V. Siegmund, B. Piater, B. Zakeri, T. Eichhorn, F. Fischer, C. Deutsch, S. Becker, L. Toleikis, B. Hock, U.A.K. Betz, H. Kolmar, Spontaneous isopeptide bond formation as a powerful tool for engineering site-specific antibody–drug conjugates, *Sci. Rep.* 6 (2016) 39291, <https://doi.org/10.1038/srep39291>.
- [53] J. Grünwald, H.E. Klock, S.E. Cellitti, B. Bursulaya, D. McMullan, D.H. Jones, H.-P. Chiu, X. Wang, P. Patterson, H. Zhou, J. Vance, E. Nigoghossian, H. Tong, D. Daniel, W. Mallet, W. Ou, T. Uno, A. Brock, S.A. Lesley, B.H. Geierstanger, Efficient preparation of site-specific antibody–drug conjugates using phosphotriethyl transferases, *Bioconjugate Chem.* 26 (2015) 2554–2562, <https://doi.org/10.1021/acs.bioconjugchem.5b00558>.
- [54] R.R. Beerli, T. Hell, A.S. Merkel, U. Grawunder, Sortase enzyme-mediated generation of site-specifically conjugated antibody drug conjugates with high in vitro and in vivo potency, *PLoS One* 10 (2015) e0131177, <https://doi.org/10.1371/journal.pone.0131177>.
- [55] L. Chen, J. Cohen, X. Song, A. Zhao, Z. Ye, C.J. Feulner, P. Doonan, W. Somers, L. Lin, P.R. Chen, Improved variants of SrtA for site-specific conjugation on antibodies and proteins with high efficiency, *Sci. Rep.* 6 (2016) 31899, <https://doi.org/10.1038/srep31899>.
- [56] Y. Xu, S. Jin, W. Zhao, W. Liu, D. Ding, J. Zhou, S. Chen, A versatile chemo-enzymatic conjugation approach yields homogeneous and highly potent antibody–drug conjugates, *Int. J. Mol. Sci.* 18 (2017), <https://doi.org/10.3390/ijms18112284>.
- [57] J.J. Bruins, A.H. Westphal, B. Albada, K. Wagner, L. Bartels, H. Spits, W.J.H. van Berkel, F.L. van Delft, Inducible, site-specific protein labeling by tyrosine oxidation–strain-promoted (4 + 2) cycloaddition, *Bioconjugate Chem.* 28 (2017) 1189–1193, <https://doi.org/10.1021/acs.bioconjugchem.7b00046>.
- [58] P. Strop, Versatility of microbial transglutaminase, *Bioconjugate Chem.* 25 (2014) 855–862, <https://doi.org/10.1021/bc500099v>.
- [59] M. Griffin, R. Casadio, C.M. Bergamini, Transglutaminases: nature's biological glues, *Biochem. J.* 368 (2002) 377–396, <https://doi.org/10.1042/BJ20021234>.
- [60] L. Deweid, O. Avrutina, H. Kolmar, *Microbial Transglutaminase for Biotechnological and Biomedical Engineering*, Biological Chemistry, (2018).
- [61] G. Falck, M.K. Müller, Enzyme-based labeling strategies for antibody–drug conjugates and antibody mimetics, *Antibodies* 7 (2018), <https://doi.org/10.3390/antib7010004>.
- [62] M.J. Arrizubieta, Transglutaminases, in: J. Polaina, A.P. MacCabe (Eds.), *Industrial Enzymes: Structure, Function and Applications*, Springer Netherlands, Dordrecht, 2007, pp. 567–581.
- [63] A. Josten, L. Haalck, F. Spener, M. Meusel, Use of microbial transglutaminase for the enzymatic biotinylation of antibodies, *J. Immunol. Methods* 240 (2000) 47–54, [https://doi.org/10.1016/S0022-1759\(00\)00172-1](https://doi.org/10.1016/S0022-1759(00)00172-1).
- [64] T.L. Mindt, V. Jungli, S. Wyss, A. Friedli, G. Pla, I. Novak-Hofer, J. Grünberg, R. Schibli, Modification of different IgG1 antibodies via glutamine and lysine using bacterial and human tissue transglutaminase, *Bioconjugate Chem.* 19 (2008) 271–278, <https://doi.org/10.1021/bc700306n>.
- [65] S. Jeger, K. Zimmermann, A. Blanc, J. Grünberg, M. Honer, P. Hunziker, H. Struthers, R. Schibli, Site-specific and stoichiometric modification of antibodies by bacterial transglutaminase, *Angew. Chem. Int. Ed.* 49 (2010) 9995–9997, <https://doi.org/10.1002/anie.201004243>.
- [66] P. Drenler, A. Chiotellis, E. Fischer, D. Brégeon, C. Belmont, L. Gauthier, F. Lhosspice, F. Romagne, R. Schibli, Transglutaminase-based chemo-enzymatic conjugation approach yields homogeneous antibody–drug conjugates, *Bioconjugate Chem.* 25 (2014) 569–578, <https://doi.org/10.1021/bc400574z>.
- [67] F. Lhosspice, D. Brégeon, C. Belmont, P. Drenler, A. Chiotellis, E. Fischer, L. Gauthier, A. Boëdec, H. Rispaud, S. Savard-Chambard, A. Represa, N. Schneider, C. Patrel, M. Sapet, C. Delcambre, S. Ingoure, N. Viaud, C. Bonnafont, R. Schibli, F. Romagné, Site-specific conjugation of monomethyl auristatin E to anti-CD30 antibodies improves their pharmacokinetics and therapeutic index in rodent models, *Mol. Pharm.* 12 (2015) 1863–1871, <https://doi.org/10.1021/mp500666j>.
- [68] J. Grünberg, S. Jeger, D. Sarko, P. Drenler, K. Zimmermann, W. Mier, R. Schibli, DOTA-functionalized polylysine: a high number of DOTA chelates positively influences the biodistribution of enzymatic conjugated anti-tumor antibody chCE7ag1, *PLoS One* 8 (2013) e60350, <https://doi.org/10.1371/journal.pone.0060350>.
- [69] S. Puthenveetil, S. Musto, F. Loganzo, L.N. Tumej, C.J. O'Donnell, E. Graziani, Development of solid-phase site-specific conjugation and its application toward generation of dual labeled antibody and Fab drug conjugates, *Bioconjugate Chem.* 27 (2016) 1030–1039, <https://doi.org/10.1021/acs.bioconjugchem.6b00054>.
- [70] D.N. Thornlow, E.C. Cox, J.A. Walker, M. Sorokin, J.B. Plesset, M.P. DeLisa, C.A. Alabi, Dual site-specific antibody conjugates for sequential and orthogonal cargo release, *Bioconjugate Chem.* 30 (2019) 1702–1710, <https://doi.org/10.1021/acs.bioconjugchem.9b00244>.
- [71] S. Beck, J. Schultze, H.-J. Räder, R. Holm, M. Schinnerer, M. Barz, K. Koynov, R. Zentel, Site-specific DBCO modification of DEC205 antibody for polymer conjugation, *Polymers* 10 (2018), <https://doi.org/10.3390/polym10020141>.
- [72] Y. Anami, W. Xiong, X. Gui, M. Deng, C.C. Zhang, N. Zhang, Z. An, K. Tsuchikama, Enzymatic conjugation using branched linkers for constructing homogeneous antibody–drug conjugates with high potency, *Org. Biomol. Chem.* 15 (2017) 5635–5642, <https://doi.org/10.1039/C7OB01027C>.
- [73] M. Dorywalska, R. Dushin, L. Moine, S.E. Farias, D. Zhou, T. Navaratnam, V. Lui, A. Hasa-Moreno, M.G. Casas, T.-T. Tran, K. Delaria, S.-H. Liu, D. Foletti, C.J. Donnell, J. Pons, D.L. Shelton, A. Rajpal, P. Strop, Molecular basis of valine-citrulline-PABC linker instability in site-specific ADCs and its mitigation by linker design, *Mol. Canc. Therapeut.* 15 (2016) 958, <https://doi.org/10.1158/1535-7163.MCT-15-1004>.
- [74] Y. Anami, C.M. Yamazaki, W. Xiong, X. Gui, N. Zhang, Z. An, K. Tsuchikama, Glutamic acid–valine–citrulline linkers ensure stability and efficacy of antibody–drug conjugates in mice, *Nat. Commun.* 9 (2018) 2512, <https://doi.org/10.1038/s41467-018-04982-3>.
- [75] D. Reusch, M.L. Tejada, Fe glycans of therapeutic antibodies as critical quality attributes, *Glycobiology* 25 (2015) 1325–1334, <https://doi.org/10.1093/glycob/cvv065>.
- [76] P. Strop, S.-H. Liu, M. Dorywalska, K. Delaria, Russell G. Dushin, T.-T. Tran, W.-H. Ho, S. Farias, Meritxell G. Casas, Y. Abdiche, D. Zhou, R. Chandrasekaran, C. Samain, C. Loo, A. Rossi, M. Rickert, S. Krimm, T. Wong, Sherman M. Chin, J. Yu, J. Dilley, J. Chaparro-Riggers, Gary F. Filzen, Christopher J. O'Donnell, F. Wang, Jeremy S. Myers, J. Pons, David L. Shelton, A. Rajpal, Location matters: site of conjugation modulates stability and pharmacokinetics of antibody drug conjugates, *Chem. Biol.* 20 (2013) 161–167, <https://doi.org/10.1016/j.chembiol.2013.01.010>.
- [77] S.E. Farias, P. Strop, K. Delaria, M. Galindo Casas, M. Dorywalska, D.L. Shelton, J. Pons, A. Rajpal, Mass spectrometric characterization of transglutaminase based site-specific antibody–drug conjugates, *Bioconjugate Chem.* 25 (2014) 240–250, <https://doi.org/10.1021/bc4003794>.
- [78] M. Dorywalska, P. Strop, J.A. Melton-Witt, A. Hasa-Moreno, S.E. Farias, M. Galindo Casas, K. Delaria, V. Lui, K. Poulsen, C. Loo, S. Krimm, G. Bolton, L. Moine, R. Dushin, T.-T. Tran, S.-H. Liu, M. Rickert, D. Foletti, D.L. Shelton, J. Pons, A. Rajpal, Effect of attachment site on stability of cleavable antibody drug conjugates, *Bioconjugate Chem.* 26 (2015) 650–659, <https://doi.org/10.1021/bc5005747>.
- [79] M. Dorywalska, P. Strop, J.A. Melton-Witt, A. Hasa-Moreno, S.E. Farias, M. Galindo Casas, K. Delaria, V. Lui, K. Poulsen, J. Sutton, G. Bolton, D. Zhou, L. Moine, R. Dushin, T.-T. Tran, S.-H. Liu, M. Rickert, D. Foletti, D.L. Shelton, J. Pons, A. Rajpal, Site-dependent degradation of a non-cleavable auristatin-based linker-payload in rodent plasma and its effect on ADC efficacy, *PLoS One* 10 (2015) e0132282, <https://doi.org/10.1371/journal.pone.0132282>.
- [80] N. Jain, S.W. Smith, S. Ghone, B. Tomczuk, Current ADC linker chemistry, *Pharmaceut. Res.* 32 (2015) 3526–3540, <https://doi.org/10.1007/s11095-015-1657-7>.
- [81] S. Panowski, S. Bhakta, H. Raab, P. Polakis, J.R. Junutula, Site-specific antibody drug conjugates for cancer therapy, *mAbs* 6 (2014) 34–45, <https://doi.org/10.4161/mab.2014.6.1.700000>.

- 4161/mabs.27022.
- [82] M.J. Costa, J. Kudaravalli, J.-T. Ma, W.-H. Ho, K. Delaria, C. Holz, A. Stauffer, A.G. Chunyk, Q. Zong, E. Blasi, B. Bucetow, T.-T. Tran, K. Lindquist, M. Dorywalska, A. Rajpal, D.L. Shelton, P. Strop, S.-H. Liu, Optimal design, anti-tumour efficacy and tolerability of anti-CXCR4 antibody drug conjugates, *Sci. Rep.* 9 (2019) 2443, <https://doi.org/10.1038/s41598-019-38745-x>.
- [83] P. Strop, T.-T. Tran, M. Dorywalska, K. Delaria, R. Dushin, O.K. Wong, W.-H. Ho, D. Zhou, A. Wu, E. Kraynov, L. Aschenbrenner, B. Han, C.J. Donnell, J. Pons, A. Rajpal, D.L. Shelton, S.-H. Liu, RN927C, a site-specific trop-2 antibody–drug conjugate (ADC) with enhanced stability, is highly efficacious in preclinical solid tumor models, *Mol. Canc. Therapeut.* 15 (2016) 2698, <https://doi.org/10.1158/1535-7163.MCT-16-0431>.
- [84] O.K. Wong, T.-T. Tran, W.-H. Ho, M.G. Casas, M. Au, M. Bateman, K.C. Lindquist, A. Rajpal, D.L. Shelton, P. Strop, S.-H. Liu, RN765C, a low affinity EGFR antibody drug conjugate with potent anti-tumor activity in preclinical solid tumor models, *Oncotarget* 9 (2018) 33446–33458, <https://doi.org/10.18632/oncotarget.26002>.
- [85] R.M. DeVay, K. Delaria, G. Zhu, C. Holz, D. Foletti, J. Sutton, G. Bolton, R. Dushin, C. Bee, J. Pons, A. Rajpal, H. Liang, D. Shelton, S.-H. Liu, P. Strop, Improved lysosomal trafficking can modulate the potency of antibody drug conjugates, *Bioconjugate Chem.* 28 (2017) 1102–1114, <https://doi.org/10.1021/acs.bioconjchem.7b00013>.
- [86] A.S. Ratnayake, L.-p. Chang, L.N. Turney, F. Loganzo, J.A. Chemler, M. Wagenaar, S. Musto, F. Li, J.E. Janso, T.E. Ballard, B. Rago, G.L. Steele, W. Ding, X. Feng, C. Hosselet, V. Buklan, J. Lucas, F.E. Koehn, C.J. O'Donnell, E.I. Graziani, Natural product bis-intercalator depsipeptides as a new class of payloads for antibody–drug conjugates, *Bioconjugate Chem.* 30 (2019) 200–209, <https://doi.org/10.1021/acs.bioconjchem.8b00843>.
- [87] G.L. Verdine, L.D. Walensky, The challenge of drugging undruggable targets in cancer: lessons learned from targeting BCL-2 family members, *Clin. Canc. Res.* 13 (2007) 7264, <https://doi.org/10.1158/1078-0432.CCR-07-2184>.
- [88] I.J. Huggins, C.A. Medina, A.D. Springer, A. van den Berg, S. Jadhav, X. Cui, S.F.J.M. Dowdy, Site selective antibody-oligonucleotide conjugation via microbial transglutaminase, *Molecules* 24 (2019) 3287, <https://doi.org/10.3390/molecules24183287>.
- [89] W. Steffen, F.C. Ko, J. Patel, V. Lyamichev, T.J. Albert, J. Benz, M.G. Rudolph, F. Bergmann, T. Streidl, P. Kratzsch, M. Boenitz-Dulat, T. Oelschlaegel, M. Schraemel, Discovery of a microbial transglutaminase enabling highly site-specific labeling of proteins, *J. Biol. Chem.* 292 (2017) 15622–15635, <https://doi.org/10.1074/jbc.M117.797811>.
- [90] V. Siegmund, S. Schmelz, S. Dickgiesser, J. Beck, A. Ebenig, H. Fittler, H. Frauendorf, B. Piater, U.A.K. Betz, O. Avrutina, A. Scrima, H.-L. Fuchsbauer, H. Kolmar, Locked by design: a conformationally constrained transglutaminase tag enables efficient site-specific conjugation, *Angew. Chem. Int. Ed.* 54 (2015) 13420–13424, <https://doi.org/10.1002/anie.201504851>.
- [91] A. Ebenig, N.E. Juettner, L. Deweid, O. Avrutina, H.-L. Fuchsbauer, H. Kolmar, Efficient site-specific antibody–drug conjugation by engineering a nature-derived recognition tag for microbial transglutaminase, *Chembiochem* (2019), <https://doi.org/10.1002/cbic.201900101>.
- [92] N.E. Juettner, S. Schmelz, J.P. Bogen, D. Happel, W.-D. Fessner, F. Pfeifer, H.-L. Fuchsbauer, A. Scrima, Illuminating structure and acyl donor sites of a physiological transglutaminase substrate from *Streptomyces mobaraensis*, *Protein Sci.* 27 (2018) 910–922, <https://doi.org/10.1002/pro.3388>.
- [93] H. Schneider, L. Deweid, T. Pirzer, D. Yanakieva, S. Englert, B. Becker, O. Avrutina, H. Kolmar, Dextramabs: a novel format of antibody–drug conjugates featuring a multivalent polysaccharide scaffold, *ChemistryOpen* 8 (2019) 354–357, <https://doi.org/10.1002/open.201900066>.
- [94] E.E. Hong, H. Erickson, R.J. Lutz, K.R. Whiteman, G. Jones, Y. Kovtun, V. Blanc, J.M. Lambert, Design of coltuximab ravtansine, a CD19-targeting antibody–drug conjugate (ADC) for the treatment of B-cell malignancies: structure–activity relationships and preclinical evaluation, *Mol. Pharm.* 12 (2015) 1703–1716, <https://doi.org/10.1021/acs.molpharmaceut.5b00175>.
- [95] X. Sun, J.F. Ponte, N.C. Yoder, R. Laleau, J. Coccia, L. Lanieri, Q. Qiu, R. Wu, E. Hong, M. Bogalhas, L. Wang, L. Dong, Y. Setiady, E.K. Maloney, O. Ab, X. Zhang, J. Pinkas, T.A. Keating, R. Chari, H.K. Erickson, J.M. Lambert, Effects of drug–antibody ratio on pharmacokinetics, biodistribution, efficacy, and tolerability of antibody–maytansinoid conjugates, *Bioconjugate Chem.* 28 (2017) 1371–1381, <https://doi.org/10.1021/acs.bioconjchem.7b00062>.
- [96] H. Schneider, D. Yanakieva, A. Macarrón, L. Deweid, B. Becker, S. Englert, O. Avrutina, H. Kolmar, TRAIL-inspired multivalent dextran conjugates efficiently induce apoptosis upon DR5 receptor clustering, *Chembiochem* (2019), <https://doi.org/10.1002/cbic.201900251>.
- [97] P.R. Spycher, C.A. Amann, J.E. Wehrmüller, D.R. Hurwitz, O. Kreis, D. Messmer, A. Ritler, A. Küchler, A. Blanc, M. Béhé, P. Walde, R. Schibli, Dual, site-specific modification of antibodies by using solid-phase immobilized microbial transglutaminase, *Chembiochem* 18 (2017) 1923–1927, <https://doi.org/10.1002/cbic.201700188>.
- [98] J.L. Spidel, B. Vaessen, E.F. Albone, X. Cheng, A. Verdi, J.B. Kline, Site-specific conjugation to native and engineered lysines in human immunoglobulins by microbial transglutaminase, *Bioconjugate Chem.* 28 (2017) 2471–2484, <https://doi.org/10.1021/acs.bioconjchem.7b00439>.
- [99] J.L. Spidel, E.F. Albone, Efficient production of homogeneous lysine-based antibody conjugates using microbial transglutaminase, in: S. Massa, N. Devoogdt (Eds.), *Bioconjugation: Methods and Protocols*, Springer New York, New York, NY, 2019, pp. 53–65.
- [100] K. Terpe, Overview of tag protein fusions: from molecular and biochemical fundamentals to commercial systems, *Appl. Microbiol. Biotechnol.* 60 (2003) 523–533, <https://doi.org/10.1007/s00253-002-1158-6>.
- [101] C. Wei, G. Zhang, T. Clark, F. Barletta, L.N. Turney, B. Rago, S. Hansel, X. Han, Where did the linker-payload go? A quantitative investigation on the destination of the released linker-payload from an antibody–drug conjugate with a maleimide linker in plasma, *Anal. Chem.* 88 (2016) 4979–4986, <https://doi.org/10.1021/acs.analchem.6b00976>.
- [102] R.J. Christie, R. Fleming, B. Bezabeh, R. Woods, S. Mao, J. Harper, A. Joseph, Q. Wang, Z.-Q. Xu, H. Wu, C. Gao, N. Dimasi, Stabilization of cysteine-linked antibody drug conjugates with N-aryl maleimides, *J. Contr. Release* 220 (2015) 660–670, <https://doi.org/10.1016/j.jconrel.2015.09.032>.
- [103] B. Böhme, B. Moritz, J. Wendler, T.C. Hertel, C. Ihling, W. Brandt, M. Pietzsch, Enzymatic activity and thermo resistance of improved microbial transglutaminase variants, *Amino Acids* (2019), <https://doi.org/10.1007/s00726-019-02764-9>.
- [104] K. Yokoyama, H. Utsumi, T. Nakamura, D. Ogaya, N. Shimba, E. Suzuki, S. Taguchi, Screening for improved activity of a transglutaminase from *Streptomyces mobaraensis* created by a novel rational mutagenesis and random mutagenesis, *Appl. Microbiol. Biotechnol.* 87 (2010) 2087–2096, <https://doi.org/10.1007/s00253-010-2656-6>.
- [105] L. Deweid, L. Neureiter, S. Englert, H. Schneider, J. Deweid, D. Yanakieva, J. Sturm, S. Bitsch, A. Christmann, O. Avrutina, H.-L. Fuchsbauer, H. Kolmar, Directed evolution of a bond-forming enzyme: ultrahigh-throughput screening of microbial transglutaminase using yeast surface display, *Chem. Eur J.* 24 (2018) 15195–15200, <https://doi.org/10.1002/chem.201803485>.
- [106] X. Zhao, A.C. Shaw, J. Wang, C.-C. Chang, J. Deng, J. Su, A novel high-throughput screening method for microbial transglutaminases with high specificity toward Gln141 of human growth hormone, *J. Biomol. Screen* 15 (2010) 206–212, <https://doi.org/10.1177/1087057109356206>.
- [107] S. Hu, L. Allen, Homogenous Antibody Drug Conjugates via Enzymatic Methods, (2019) US10471037B10471032.

5. Additional Results

To further test the modularity of dextran, we examined it as a carrier for multiple metal chelators. This concept may open space for attachment of a higher number of radioisotopes per targeting protein and improving pharmacokinetic properties of small targeting proteins like affibodies. For that purpose, we applied 1,4,7,10-tetraazacyclododecane-1,4,7,10-tetraacetic acid (DOTA), a well-known chelator for various metal ions. Dextran was equipped with a Boc-protected amine at the reducing end followed by carboxyethylation at the C-2 of the glucose repeating units. Subsequent, conjugation of an azide-bearing amine linker and deprotection of the reducing end to generate a free amine moiety was performed (Figure 19). Dextran was equipped with 4.2 or 7.5 azide moieties which could be easily visualized by NMR analysis as previously described (see cumulative section 1 and 2, Figure 20)

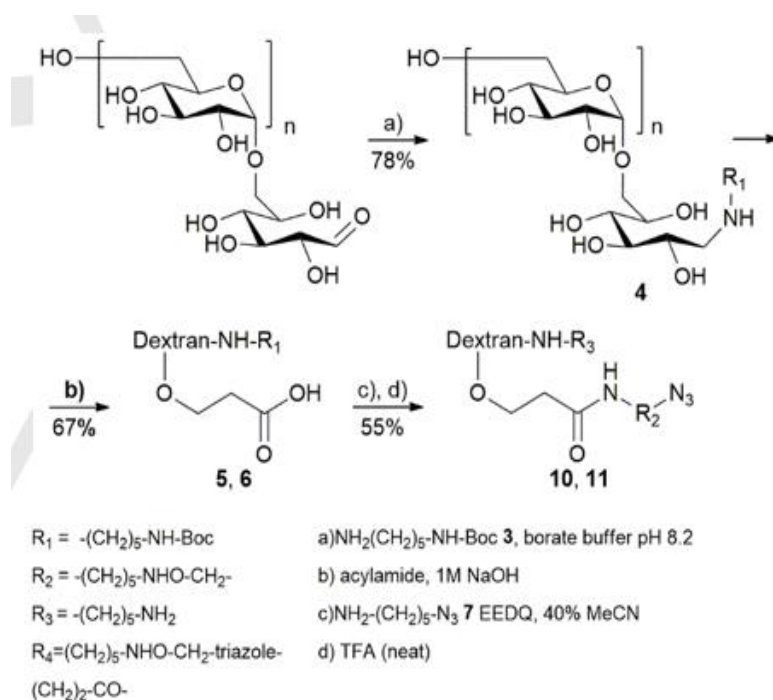


Figure 19. Synthesis scheme for dextran bearing multiple azide moieties on the glucose repeating units and a Boc-protected cadaverine at the reducing end.

Subsequent conjugation with BCN-DOTA purchased from Chematech (Dijon, France) followed by purification applying size-exclusion chromatography led to dextran bearing multiple DOTA (Figure 21). Hereby, SPAAC was performed as reported in the cumulative section regarding dextramabs. Briefly, dextran bearing multiple azide groups was dissolved in 1 × PBS and 2.5 eq of BCN-DOTA per azide moiety was added and the reaction mixture was shaken at 30 °C for 3 h. Pure product was isolated by PD-10 desalting columns and SEC on a BioSep-SEC-s2000, 300 x 7080 mm, 5µM (Phenomenex) applying an isocratic procedure (40 min, water).

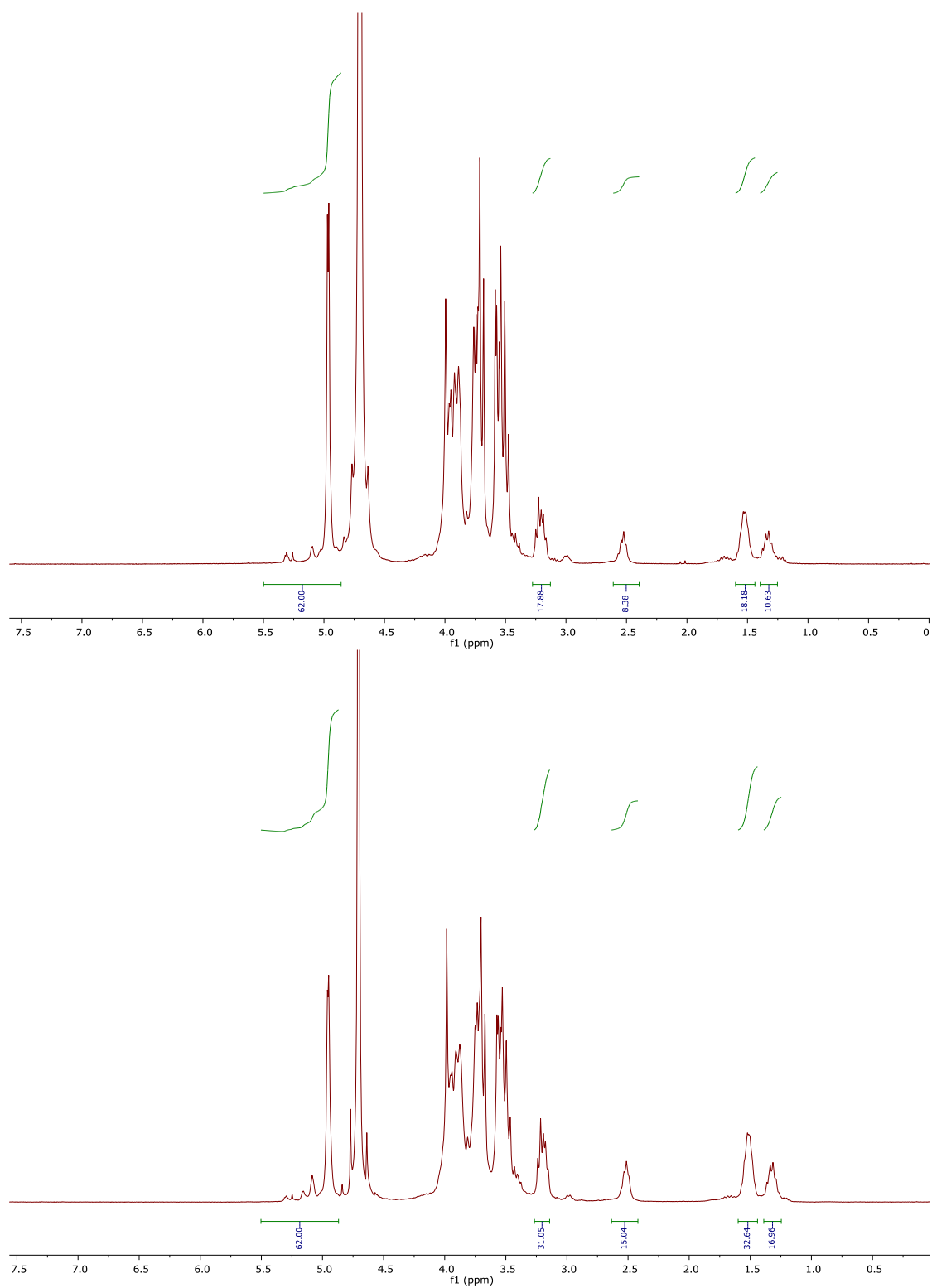


Figure 20. NMR spectra of azido-dextran cadaverine. (top) Dextran equipped with 4.2 azide moieties per dextran and dextran equipped with 7.5 azide moieties(bottom).

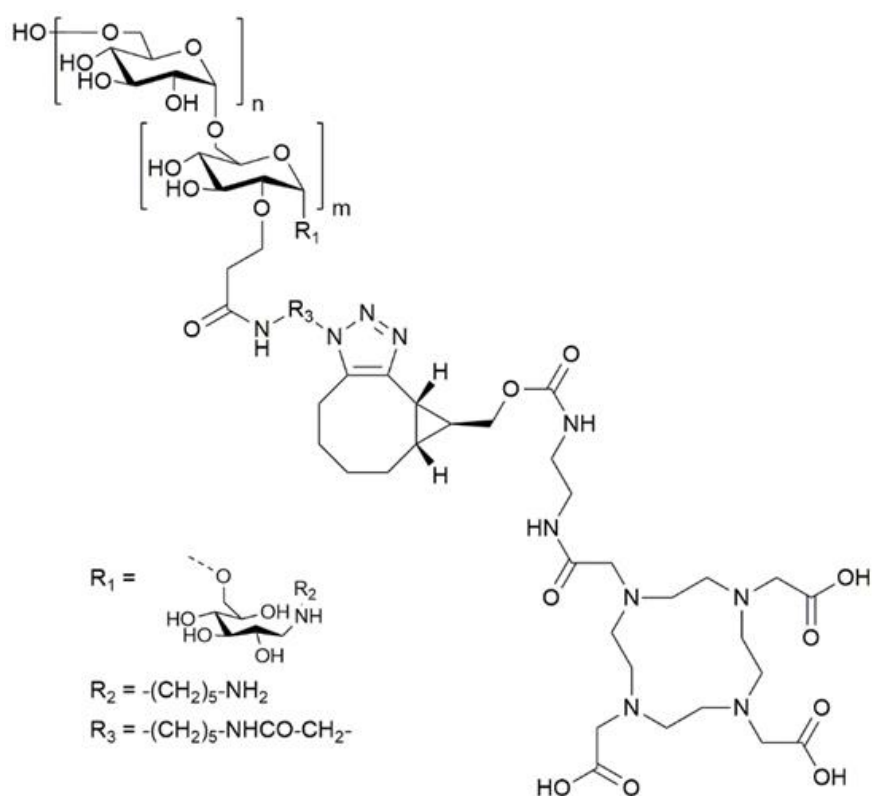


Figure 21. Scheme of dextran quipped with multiple DOTA

The number of conjugated DOTA groups per dextran was assessed by the complexation of Cu^{2+} ions, which results in measurable absorption at 265 nm. In a first step a calibration curve for the Cu^{2+} -complex of DOTA was generated to get access to the molar extinction coefficient of the formed complex. Therefore, a serial dilution bearing BCN-DOTA at different concentrations (0.01-0.2 mM) and $CuSO_4$ (500 mM) was prepared. Photometric analysis revealed the molar extinction coefficient ($4147 L \cdot^{-1} \cdot cm$) that was obtained by linear regression applying Beer–Lambert law. Subsequent, measurement of complexation of Cu^{2+} by DOTA-dextran-cadaverine constructs in three different concentrations indicated that in average 3.2 or 5.3 Cu^{2+} -ions were complexed by DOTA-dextran conjugates, respectively. These measurements were performed in triplicates. To test the biodistribution of the assembled DOTA-dextran conjugates *in vivo* studies in mice are currently ongoing. In a prospective proof-of concept-study, DOTA-dextran conjugates should be linked to commonly applied targeting proteins e.g. affibodies, that suffer from poor solubility, aggregation and precipitation due to their intrinsic hydrophobic properties.

6. Danksagung

In diesem Teil möchte ich mich herzlich bei allen Menschen bedanken, die mich während der Zeit meiner Promotion und während der Niederschrift dieser Arbeit begleitet haben!

Mein aufrichtiger Dank gilt den folgenden Personen:

In erster Linie gilt dieser Dank meinem Doktorvater **Prof. Dr. Harald Kolmar**, der mir nicht nur die Möglichkeit gegeben hat, diese Arbeit anzufertigen, sondern mir auch stets ein erreichbarer Ansprechpartner war und mit Rat und Tat zur Seite gestanden hat. Sein unermüdliches Streben nach neuen Synthesen und Projekten hat meine Arbeit vorangetrieben und mir dennoch den Freiraum gelassen, meine eigenen Ideen zu entwickeln, zu diskutieren und diese auch umzusetzen. Die Zeit in deiner Arbeitsgruppe, sei es im Labor oder im Kleinwalsertal, war einfach spitze - Danke für diese Zeit, Harald!

Prof. Dr. Katja Schmitz, Prof. Dr. Markus Biesalski und **PD Dr. Meckel** danke ich für die Übernahme des Korreferats bzw. für ihre Arbeit als zweiter Fachprüfer.

Meinen Co-Autoren **Lukas Deweid, Thomas Pirzer, Desislava Yanakieva, Simon Englert, Bastian Becker, Arturo Maccarón, Sebastian Bitsch, Dr. Olga Avrutina** gilt mein Dank für die gute Zusammenarbeit in unseren Projekten. Insbesondere danke ich Lukas Deweid, der es geschafft hat, sich auf alle meine Publikationen zu schleichen.

Dr. Olga Avrutina danke ich für das Lektorat meiner verfassten Texte. Du hast mir wirklich geholfen und mir beigebracht, wie man meinen Labortätigkeiten auch einen würdigen schriftlichen Rahmen gibt.

Simon „Schirmon“ Englert und Ata „A-TAU“ Ali gilt mein Dank als meine steten Begleiter, ob zu früher Stunde im Fitnessstudio, Biergarten, Skiurlaub, Billiardschuppen, in der Krone oder auf der besten Hüttentour aller Zeiten. Auf euch kann ich immer zählen. Die Zeit mit euch wird mir stets in Erinnerung bleiben!

Bastian „Spritze“ Becker danke ich für die unermüdliche Hilfe und das Ertragen meiner Fragen zu Synthesen und Berechnungen. Ohne dich als meinen längsten Weggefährten, die unendlichen Tassen an Kaffee, sei es in der Kuhle oder in der Stadtmitte und die gemeinsame Zeit des aktiven Betreuens der Praktikanten wäre es nicht dasselbe gewesen.

Dr. Julius „Jules“ Grzeschik für unsere gemeinsamen Abende auf der unvergessenen Dachterrasse, im Kessel und im Stadion, ob in Darmstadt, Frankfurt oder Hannover. Dank dir habe ich meinen Kaffeekonsum verdreifacht. Danke auch für deine umfassende Hilfe, als sich schließlich das Ende der Zeit anbahnte und alles zu Papier gebracht werden musste.

Steffen „Ehh-Steffen“ Hinz für seine bis ins kleinste Detail ausgearbeiteten Planungen der gemeinsamen Urlaube und das Teilen seines tiefgründigen Wissens über die heimischen Vogelarten. Danke für die Beantwortung meiner biologischen Fragen, auch dank dir kann ich heute einige „Biologenpunkte“ mein Eigen nennen.

Dr. Doreen „Dorn“ Könning und Dr. Andreas Christmann gilt mein besonderer Dank dafür, dass sie stets für mich einstanden, wenn es nötig war. Doreen, ohne dich ist das Mittagessen in der Mensa und der sonntägliche Goldrausch nicht dasselbe.

Arturo „Arturito“ Macarrón für seine positive und spanische Art, die mir jeden Tag Lust auf Fiesta macht. Danke für die schönen Abende bei dir, ob am Lagerfeuer, beim Kickern oder beim Dart-spielen.

Adrian „Adi“ Elter gilt mein Dank für seine belustigenden Versuche, seine „allerbeste“ Beziehung zu einer Kollegin zu verheimlichen und seine großzügige Art als Gastgeber bei jedwedem Anlass.

Desislava Yanakieva und Thomas Pirzer gilt mein Dank für die Vorbereitung unzähliger Platten für Toxassays, Zellen fürs FACS und generell für die Einführung in die Arbeit mit Zellen. Dank euch kann jetzt auch ein Chemiker ein wenig in der Zellkultur arbeiten.

Der gesamten Pizza-Pommes-Crew bestehend aus **Simon Englert, Ata Ali, Steffen C. Hinz, Janna Sturm, Dominic „X-Men“ Happel und Jan Bogen** für die unzähligen Abfahrten und die super Zeit im Zillertal. Ich werde nie vergessen, wie wir nach dem einen Abend am nächsten Tag auf den Skiern gestanden haben.

Dr. Thomas Pirzer, Bastian Becker, Lukas Deweid, Arturo Macarrón, Ata Ali, Jan Habermann, Sebastian Bitsch und allen anderen aus der Tischkicker-Crew danke ich für jedes einzelne Spiel, ohne die einem manchmal der Kopf für die Arbeit nicht frei genug gewesen wäre. Es war und wird mir eine Freude sein, euch in weiteren Matches entgegensetzen. **Arturito**, es war mir eine Ehre dich krabbeln zu sehen.

Barbara Diestelmann für die Unterstützung bei jeder organisatorischen Frage und allen weiteren Wehwehchen im Laufe meiner Promotion. Du hältst den Laden hier zusammen!

An **Cecilia „Cilli“ Gorus** ohne die das Labor kaum existieren würde und für jedes „Guten Morgen Hendrik“.

Dr. Stefan Zielonka, Dr. Heiko Fittler, Dr. Julius Grzeschik und Dr. Stephan Dickgiesser gilt mein besonderer Dank für die wunderschöne musikalische Untermalung meiner Anfangszeit. Emil Schlemihl, Madchild und Wing werden mich mein ganzes Leben begleiten. Stephan dir gilt mein Dank insbesondere, denn ohne dich hätte ich den Dieter niemals erlebt!

Adrian Elter, Dr. David Fiebig, Lara Neureiter, Dana Schmidt, Anja Hofmann, Valentina Hilberg, Jan Bogen, Janine Becker, Dr. Vanessa Siegmund, Dr. Daichi Nasu, Sascha Knauer, Dr. Christina Uth und allen weiteren aktuellen und ehemaligen Mitarbeitern des AK Kolmar für jedwede Unterstützung, ob im Labor oder von organisatorischer Seite. Die Zeit, ob im Labor, auf Radtouren, im Biergarten, in der Mensa, beim Dieter, bei Alexander Markus oder im KWT, war unvergesslich. Vielen Dank für die schöne Zeit!

Ein riesiges Dankeschön gilt **meiner Familie** und meinen Freunden, die mich zeitlebens unterstützt, gefördert und so genommen haben, wie ich bin. Insbesondere gilt dieser Dank meinen Eltern **Jeanette** und **Günter**, meiner Schwester **Kirstin** sowie meinen Großeltern **Erika, Werner** und **Martha**. Danke für die Unterstützung, den Rückhalt, Zuspruch und euren steten Glauben an mich. Ohne euch wäre ich nicht der Mensch, der ich heute bin!

Mein wichtigster Dank gilt meiner Freundin **Julia Ebert** für jeden gemeinsamen Tag, während dieser Promotion. Danke, dass du mich immer unterstützt, mir beistehst und meiner, nicht immer einfachen, Art mit einem Lächeln entgegenstehst. Dein Glaube an mich in schwierigen Phasen und deine Unterstützung, haben mich immer wieder vorangetrieben und mir wieder Zuversicht geschenkt. Ohne dich wäre ich manchmal verzweifelt. Danke, für jeden einzelnen Moment!

7. Affirmations

Hendrik Peter Günter

Darmstadt, 6.12.2019

Gutenbergstraße 45

64289 Darmstadt

Schneider@Biochemie-TUD.de

017647361038

Erklärung

Ich erkläre hiermit, dass ich meine Dissertation selbstständig und nur mit den angegebenen Hilfsmitteln angefertigt habe.

Hendrik Peter Günter Schneider

Hendrik Peter Günter

Darmstadt, 6.12.2019

Gutenbergstraße 45

64289 Darmstadt

Schneider@Biochemie-TUD.de

017647361038

Erklärung

Ich erkläre hiermit, noch keinen Promotionsversuch unternommen zu haben.

Hendrik Peter Günter Schneider

Hendrik Peter Günter

Darmstadt, 6.12.2019

Gutenbergstraße 45

64289 Darmstadt

Schneider@Biochemie-TUD.de

017647361038

Erklärung

Ich erkläre hiermit, dass die elektronische Version der Doktorarbeit mit der schriftlichen Version übereinstimmt. Die elektronische Version liegt dem Prüfungssekretariat vor.

Hendrik Peter Günter Schneider